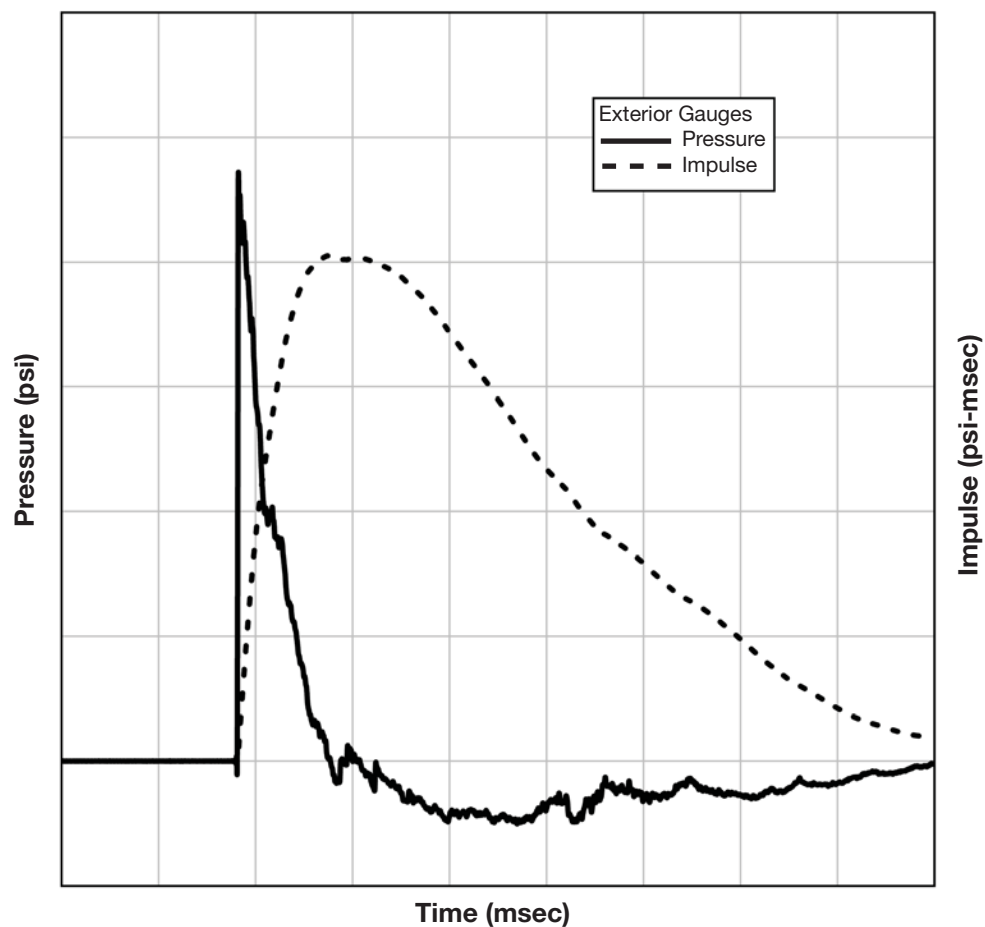# 26

Steel Design Guide

Design of Blast Resistant Structures

Steel Design Guide

26

Design of Blast Resistant Structures

RAMON GILSANZ, Lead Author

Gilsanz Murray Steficek LLP
New York, New York & Los Angeles, California

RONALD HAMBURGER

Simpson Gumpertz & Heger, Inc.
San Francisco, California

DARRELL BARKER

ABS Consulting
San Antonio, Texas

JOSEPH L. SMITH

Applied Research Associates, Inc.
Vicksburg, Mississippi

AHMAD RAHIMIAN

WSP Cantor Seinuk
New York, New York

AMERICAN INSTITUTE OF STEEL CONSTRUCTION

AISC © 2013

by

American Institute of Steel Construction

The information presented in this publication has been prepared in accordance with recognized engineering principles and is for general information only. While it is believed to be accurate, this information should not be used or relied upon for any specific application without competent professional examination and verification of its accuracy, suitability and applicability by a licensed professional engineer, designer or architect. The publication of the material contained herein is not intended as a representation or warranty on the part of the American Institute of Steel Construction or of any other person named herein, that this information is suitable for any general or particular use or of freedom from infringement of any patent or patents. Anyone making use of this information assumes all liability arising from such use.

Caution must be exercised when relying upon other specifications and codes developed by other bodies and incorporated by reference herein since such material may be modified or amended from time to time subsequent to the printing of this edition. The Institute bears no responsibility for such material other than to refer to it and incorporate it by reference at the time of the initial publication of this edition.

Printed in the United States of America

Authors

Ramon Gilsanz, P.E., S.E., is a partner at Gilsanz Murray Steficek LLP. He is a member of AISC Task Committee 3, Loads, Analysis and Systems, and was a member of the AISC Adhoc Task Group on Structural Integrity and of the NCSEA's Ad Hoc Joint Industry Advisory Committee. He also chaired the Department of Buildings panel that wrote the New York City structural integrity code recommendations.

Ronald Hamburger, P.E., S.E., is a senior principal at Simpson Gumpertz & Heger, Inc. He chairs the ASCE 7 Committee and the AISC Connection Prequalification Review Panel, and is a member of AISC Task Committee 9 on Seismic Design. He also chaired the NCSEA Ad Hoc Joint Industry Advisory Committee that developed the structural integrity provisions contained in the *International Building Code*.

Darrell Barker, P.E., is vice president for Extreme Loads and Structural Risk at ABS Consulting. He is a member of ASCE, ACI, ASIS, ASME and PGCI. He contributed to the *Handbook for Blast Resistant Design of Buildings* and to ASCE/SEI 59-11, *Blast Protection of Buildings,* and CSA 850-12, *Design and Assessment of Buildings Subjected to Blast Loads.*

Joseph L. Smith, PSP, is a director and senior vice president of Applied Research Associates, Inc. He is an active member of ASCE, SAME, SARMA, PGCI and the ASIS International participating on several professional committees. He is member of the Department of Homeland Security Explosives Standards Working Group and past Co-Chair of the Explosives Hardening and Mitigation Subgroup, and also contributed to ASCE/SEI 59-11, *Blast Protection of Buildings,* and the *Handbook for Blast Resistant Design of Buildings.*

Ahmad Rahimian, Ph.D., P.E., S.E., is chief executive of WSP Cantor Seinuk in New York. He is an active member of ASCE, AISC and chairs ACI committee 375. He was a member of the Department of Buildings panel that wrote the New York City structural integrity code recommendations.

Acknowledgments

Preface

This Design Guide provides guidance for the design of blast resistant structures and progressive collapse mitigation. Background information and some basic principles are reviewed, as well as the presentation of design examples. The goal of this Design Guide is to provide enough information for a structural engineer to effectively interact with a security or blast consultant.

TABLE OF CONTENTS

Chapter 1
Introduction

The purpose of this guide is to disseminate knowledge of blast resistance and progressive collapse mitigation to the structural engineering community, presenting basic theory with design examples so engineers and architects can achieve simple and effective designs.

Presently, security consultants with the assistance of the owner evaluate the particular vulnerabilities of a given facility and determine the appropriate and acceptable level of security risk. The risk assessment study determines the location and the size of the explosive threat. The blast consultants then calculate the blast pressures and review the design produced by the engineer of record. If the design is found to be insufficient, the blast consultant recommends upgrading the design and these revisions are incorporated into the construction drawings. It is advisable to involve the security consultant and blast consultant as early as possible in the planning and design process.

There is enough information provided in this guide to allow practicing structural engineers with a background in structural dynamics to interact with blast consultants to produce effective designs. The engineer of record can then proceed with the structural design based on the blast pressures given by the blast consultant. As it is with any unusual design, a peer review is a good idea and it is suggested that the final design be reviewed by a qualified blast consultant with experience in the design of blast resistant structures.

This guide is divided into the following chapters:

Chapter 2 addresses external blast explosions and is focused on the shock wave—not on fragment or projectile loading. The chapter does not cover the loads generated by a large blast in close proximity to the structure.

Chapter 3 addresses the evolution of documents related to the design of buildings for blast loading and provides guidance on the relevant factors in protective building design.

Chapter 4 addresses methods of dynamic analysis, simplifying multiple degrees of freedom into single degree of freedom systems, and determining the dynamic response to defined loads. It also explains the use of general structural engineering software to solve simple multiple degree of freedom problems.

Chapter 5 addresses the overall response of a building's structural system to blast loading.

Chapter 6 addresses member design, failure modes and design criteria including breaching, shear failure and bending.

Chapter 7 addresses steel connection design for blast loading.

Chapter 8 addresses basic progressive collapse concepts. Progressive collapse design is independent of blast design because progressive collapse may be caused by other possible events such as fire, accident, impact, etc. Examples demonstrating the determination of the structural response to progressive collapse are included.

The guide addresses only the behavior of structural steel under blast loading. It does not cover doors, windows, or any other structural material.

1.1 HISTORY OF INCIDENTS

In years past, blast resistant design was typically only used for facilities that either housed (or were in close proximity to) explosive material or were known as potential targets for attack. Munitions plants and storage facilities, strategic military and government facilities, and natural gas and petroleum refineries are a few examples of facilities that might have been designed specifically to resist blasts. However, the threat of bombings has increased in recent years. The incidents described in the following are closely associated with the evolution of the different security design criteria described in Chapter 3.

1.1.1 Blast Incidents

While numerous bombing events have occurred throughout the world, a small number of these events over the past three decades has had the largest impact on how the U.S. prepares for, and responds to, such events.

Notable events include:

- April 18, 1983—A suicide car bomber attacked the U.S. Embassy in Beirut, Lebanon, killing 63 people, 17 of whom were Americans.

- October 23, 1983—The U.S. Marine barracks in Beirut, Lebanon, were attacked by a suicide truck bomb killing 241 American military personnel.

- December 1983—Suicide truck bombers attacked the U.S. and French embassies in Kuwait killing 5 and injuring 86.

- September 20, 1984—The annex of the U.S. embassy in Beirut, Lebanon, was attacked with a truck bomb killing 24 and injuring the ambassador.

- December 21, 1988—A terrorist bomb destroyed Pan Am Flight 103 over Lockerbie, Scotland, killing 270 people.

- February 26, 1993—The car bombing of the World Trade Center in New York, NY, resulted in the deaths of six and injuries to over 1,000.
- April 19, 1995—The A.P. Murrah Federal Building in Oklahoma City, OK, was attacked using a truck bomb, killing 168 people and injuring more than 500 others.
- June 25, 1996—Khobar Towers in Dhahran, Saudi Arabia, was truck-bombed, killing 19 airmen.
- July 27, 1996—Pipe bombing of Centennial Olympic Park in Atlanta, GA, during the 1996 Olympic Games.
- January 16, 1997—Double pipe-bombing at the Sandy Springs Professional Building in Atlanta, GA.
- February 21, 1997—Double pipe-bombing at the Otherside Lounge in Atlanta, GA.
- January 29, 1998—Pipe-bombing of the New Woman All Women Health Care Clinic in Birmingham, AL.
- August 7, 1998—Truck bombing of the U.S. Embassies in both Kenya and Tanzania. 224 people were killed in the two events, while nearly 5,000 sustained injuries.
- October 12, 2000—The USS Cole was attacked by a suicide boat while docked in the port of Aden, Yemen.
- September 11, 2001—Attacks on both the Pentagon in Washington, DC, and the World Trade Center in New York, NY, killed thousands and injured many thousands more. While these attacks did not involve the use of explosives, the airplanes involved were used as guided missiles that had explosive effects upon their targets (impact, deflagration and fire).
- May 12, 2003—Suicide bomb attacks on housing killed 34 people in Riyadh, Saudi Arabia.

Similar significant attacks in England, Russia, Spain, the Middle East, and other countries could be added to this list.

1.1.2 Progressive Collapse Incidents

The American Society of Civil Engineers (ASCE) standard ASCE/SEI 7-10 (ASCE, 2010a), Commentary Section C1.4 defines "progressive collapse" as "the spread of an initial local failure from element to element, resulting eventually in the collapse of an entire structure or a disproportionately large part of it." Although some experts may disagree, the following events are generally regarded as progressive collapse failures. Some are also examples of improperly designed or built structures that failed completely.

Notable progressive collapse events include:
- Quebec River Bridge, 1907. Bridge collapsed during construction killing 82 workers; compression members were observed to be distorted by up to 2¼ in., indicating incipient buckling. Improper design of lattice compression braces caused total failure of the partially constructed bridge.
- Ronan Point, 1968, UK. Small kitchen explosion caused partial collapse of 20 stories of a corner of an apartment building.
- Hartford Coliseum, 1978, Hartford, CT. Long-span space frame collapsed under a moderate snow load (less than 20 psf). Compression members had been improperly designed and the failure propagated through the entire arena.
- L'Ambiance Plaza, 1987, Bridgeport, CT. Collapse of two adjoining buildings that were under construction using the lift slab method. Triggered by loss of support of a slab at a column. 28 workers killed. Collapse propagated because final connections had not yet been made.
- Hyatt Regency Walkway, 1981, Kansas City, MO. Revised connection of hanger rods to framing had not been designed by a structural engineer. One connection failed and the lack of redundancy caused the complete collapse of both levels of walkways. Killed 114 people.
- World Trade Center 6, September 11, 2001, New York, NY. Several floors collapsed due to fire. The collapse was arrested by floors that were not on fire.
- World Trade Center 7, September 11, 2001, New York, NY. A fire caused the failure of a key structural member that resulted in the collapse of the entire building.

Progressive collapse failures may be due, in part, to concrete punching shear. Concrete codes now have structural integrity reinforcement that addresses this type of failure. Examples of concrete structures that have collapsed are:
- 200 Commonwealth Avenue, 1971, Boston, MA. A 17-story concrete high-rise under construction. Four workers were killed and 20 injured.
- Skyline Plaza apartment building, 1973, Fairfax County, VA. Collapsed during construction killing 14 workers; 34 others were injured.
- Cocoa Beach Condominium, 1981, FL. Collapsed during construction, killing 11 workers, and injuring 23 others.

1.2   CHARACTERISTICS OF BLAST EFFECTS

An air blast creates a supersonic shock wave, increases the ambient air pressure in the environment, and may generate high velocity fragments due to the destruction of the container that holds the charge. The explosion can happen in an enclosed or open space. In the open there is no confinement of the explosives; therefore, there is no increase of air pressure due to confinement and venting is not relevant. In an enclosed space, venting the explosion byproducts is important.

Blast loads are different from the typical loads familiar to structural engineers due to their large magnitude and short duration. The speed with which a blast load is applied exceeds the loading rate of an earthquake by several orders of magnitude. Blast pressure may exceed hundreds and even thousands of pounds per square inch, but last only a hundredth or even a thousandth of a second. The structure is designed to absorb the energy from the blast. Designers use plastic design with ultimate dynamic strengths without load factors, capacity reduction factors, or safety factors. Due to the nonlinear nature of the response, member failure is characterized by large deformations and/or rotation. Further, the engineer must ensure that failure of members closest to the blast will not cause a failure that propagates to elements outside the area directly affected by the air blast loading. If members outside the area fail, a progressive collapse of the structure may be generated. To prevent progressive collapse, the structure should be sufficiently redundant to allow for load redistribution or members must have sufficient strength to preclude failure.

The patterns of blast damage on a particular structure will vary greatly due to several factors:

- Type/variety of construction, including materials, mass and stiffness
- Type of explosive
- Standoff distance between the charge and the structure
- Orientation of the charge to the structure
- Orientation of other structures surrounding the targeted structure

Structural damage from a blast varies significantly with distance from the charge, robustness of the structure, and characteristics of the material. Blast pressure drops significantly with increased distance and the resulting response is correspondingly decreased. Structural damage also lessens with increased robustness and increased material ductility. An example of these effects is the bombing of the Murrah Federal Building in Oklahoma City, OK, where many nontargeted buildings in the vicinity of the targeted building sustained significant damage from the blast. During the

event, buildings up to 800 ft away from the charge experienced varying levels of structural collapse, largely due to the lack of robustness. Damage varied significantly based on the building construction and the distance from the blast. In addition, windows were broken in many buildings throughout the downtown area within a 1½-mile radius from the charge. The occurrence of breakage decreased, in general, with increased distance from the blast.

There are many different types of explosives, but 1 lb of trinitrotoluene (TNT) is universally used as a standard measure of effectiveness of explosive materials. Homemade explosives such as ammonium nitrate with fuel oil (ANFO) are less powerful than TNT, and thus equivalent weights of other explosive materials would have less effect than TNT. Some military grade explosives, such as C-4 and pentolite, produce more powerful effects using the same weight of material. TNT equivalence is a commonly used metric due to the lack of detailed information available for other materials. TNT weighs about 100 lb/ft^3. This means that the volume of TNT corresponding to 10,000 lb is 100 ft^3, which can be visualized as a 6-ft by 2-ft closet in the average home ≈ (6 ft)(2 ft)(8 ft) = 96 ft^3.

When an explosive device is located very close to a structure, both localized and global damage to the structure may occur. Localized damage may consist of flexural deformation, breaching (e.g., the pulverization of the material), and collapse of primary structural elements and wall systems in the immediate vicinity of the blast. As the distance from the blast increases, localized damage transitions to more widespread damage consisting primarily of broken windows and failure of weaker building components comprising the building envelope.

Varying levels of damage to a structure may also be seen as the orientation of the charge to the structure changes. In a uniformly constructed building, the side of the building directly facing the blast will experience a higher load and more damage than the sides which are not facing the blast. The sides not facing the blast will experience an incidental loading from the blast, which will be lower than the direct reflected loading applied to the side facing the blast.

Structures in the vicinity of the targeted structure may also affect blast patterns but to a lesser extent than the items listed above. A structure located between the explosive charge and the targeted structure will reduce the peak reflected pressure on the target structure. However, it should be noted that only under ideal circumstances will the reduction be significant. In many cases, the shock wave will re-form (almost to its original strength) over the distance between the structures. In certain instances, surrounding structures may even reflect and amplify the loads seen by the targeted structure. In general, however, the first shock loading (not subsequent reflections) will control the level of damage.

1.3 BLAST EFFECTS VERSUS SEISMIC EFFECTS

There are many similarities between the effects of blasts on structures and the effects of earthquakes. Both phenomena are dynamic in nature and as a result, the amount of force and deformation experienced by a structure depends significantly on the dynamic characteristics of the structure. Designs for both blast resistance and seismic resistance usually anticipate that the structure will undergo substantial nonlinear response under design loading and that some structural elements will be damaged, perhaps to the point of failure. Due to the infrequency and magnitude of both types of loading, extensive damage is usually considered acceptable as long as the building response does not result in extensive endangerment of life safety. Because substantial nonlinear response is anticipated for both phenomena, good design practice often entails the use of materials and detailing practices that are capable of developing the yield strength of the structure and experiencing extensive inelastic

deformation without loss of load carrying ability. Since structural steel can withstand large inelastic deformations, it is frequently used in the design of primary structural systems for buildings designed either to resist blast or seismic loads.

Although there are many similarities between design for seismic resistance and design for blast resistance, there are also a number of differences. Earthquake loads are transmitted to the structure via ground shaking and blast loads are transmitted through a pressure wave that hits the envelope of a building first and subsequently is transmitted through load resisting members of the building to the foundation. Seismic response involves a global response of the structural system originating in the foundation and blast begins as a local response of a few structural elements. The response of seismic loads is measured by stresses and displacement, while the response of blast loads is measured by ductility and rotation. The duration of blast loading is much shorter than the duration of seismic loading. Typical pressure waves produced by blasts will have durations on the order of tens of milliseconds, while typical seismic loading of a structure
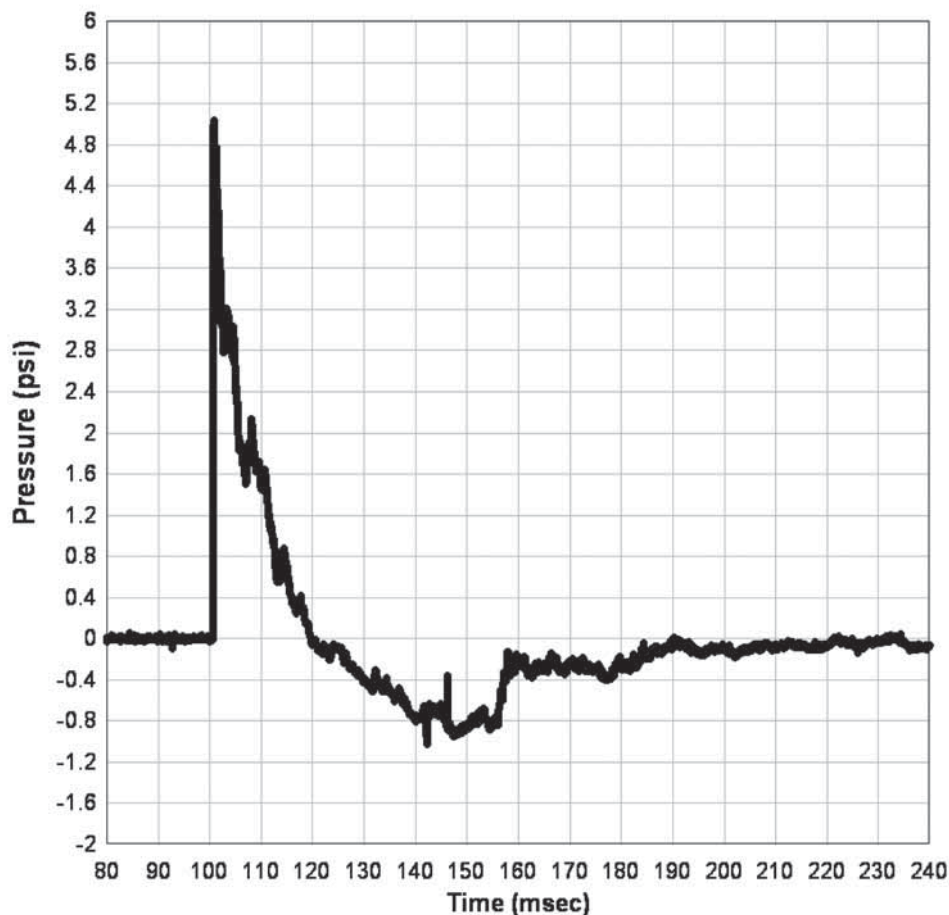
Fig. 1-1. Pressure gauge trace from high-energy explosive detonation.

will have a duration extending from seconds to several minutes. Blast impulses typically produce one phase of significant positive loading and one phase of negative loading that may or may not be significant. Seismic loading will typically include many cycles of loading, making low-cycle fatigue a more significant factor. For comparison, Figure 1-1 and Figure 1-2 illustrate a load history for blast and earthquake effects, respectively. Note the difference in the time scales. Design for seismic loading typically attempts to preclude failure of primary vertical load carrying elements and avoids any type of collapse. Design for blast resistance often anticipates failure of one or more primary vertical load carrying elements and, depending on the design criteria, may permit collapse of limited areas of a building.

Following the blast-induced collapse of the Murrah Federal Building in Oklahoma City in 1995, investigators suggested that if the more ductile detailing practices commonly used in regions of high seismicity had been incorporated in the design the building may have been substantially more resistant to collapse and there may have been fewer fatalities. While this may be true in the case of that particular building, design for seismic resistance alone will not, in general, provide sufficient resistance to arrest progressive collapse or ensure acceptable response under blast loads.
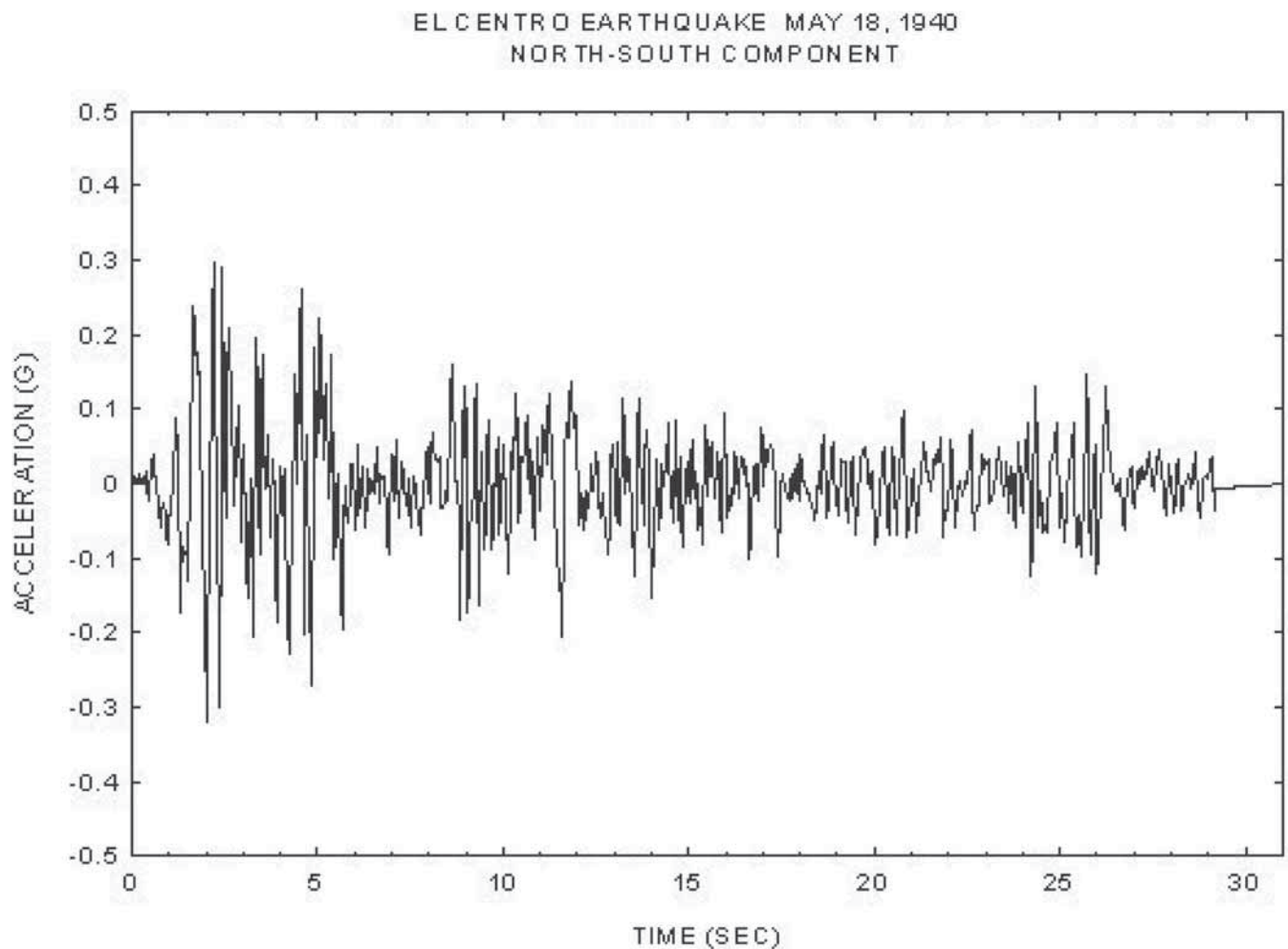
Fig. 1-2. El Centro earthquake ground accelerations.

Chapter 2
Blast Loads

This chapter provides an overview of key characteristics of blast loads, including types of explosion hazards and methods for predicting magnitude and duration. Methodology for load prediction is reviewed along with the types of tools and data typically used. Guidelines are included for application of loads to structures, key parameters required, and limitations. This chapter will give the structural engineer the background necessary to specify blast prediction requirements and apply the results but it is not intended to be a comprehensive methodology for complex problems. Exterior and interior blast loads are addressed as well as leakage pressures into a structure due to openings in or failure of the building envelope. A detailed example problem is included to guide the user through the load prediction process for a simple building.

This chapter provides an overview of the types of explosions that may be encountered by the designer and the methodologies used to define blast loads. Development of design basis loads for blast resistant construction is a key element of the design development phase of a project. The most important factors in blast design are explosive type and size, location of the explosion relative to the building, and the building geometry. Blast loads vary spatially and decrease rapidly with distance, even over the surface of a wall. Loads are influenced by geometric configuration, which provides shielding and reflection. References are provided for more detailed explanations of methods and design aids. Some projects have project-specific predefined blast loads (pressure and impulse).

2.1   EXPLOSION PARAMETERS

Blast loads from high energy explosives may occur due to accidental or intentional detonations. Accidents involving high energy explosives can include explosives processing and handling events. Intentional detonations can include controlled demolition, explosives testing, military weapons and terrorist threats. In the case of intentional detonations, structures may be required to withstand multiple events, such as with a test structure. These events produce supersonic reaction fronts. For convenience in predicting blast pressures, the energy release of a high energy explosive is equated to trinitrotoluene (TNT). TNT equivalence values for peak pressure and impulse are reported for many explosive compounds. TNT equivalencies for many compounds are published in Unified Facilities Criteria 3-340-02, *Structures to Resist the Effects of Accidental Explosions* (DOD, 2008), but in some cases they must be determined

experimentally for the configuration used. The selection of effective charge weights, safety factors on blast loads, and allowable response criteria is discussed in DOD (2008) and Baker (1983).

Fireworks, other pyrotechnics, propellants and blasting agents are broadly classed as low energy explosives due to their relatively low reaction rate and blast pressure output. These materials typically exhibit lower overpressures than high energy explosive materials resulting from a slower energy release rate. The designer should consult an expert for prediction of low energy explosive blast loads. In the far field, the low energy explosive blast loads can be similar to those caused by high energy explosives as the initial and secondary shocks coalesce. In the near field, overpressures are less than those produced by high energy explosives and use of TNT equivalent prediction procedures will overestimate pressure.

Vapor cloud explosions involve the release of a flammable material which, when mixed in the proper proportions with air, forms a combustible material. Vapor cloud explosions typically produce relatively low pressure, long duration blast loads. A burst vessel can produce a short duration blast load. Release of flammable contents from the vessel may result in a follow-on explosion when the contents mix with air.

Charges detonated in a confined area generate gas pressures in addition to the shock waves. The degree of confinement has a pronounced influence on the magnitude of blast loads produced. Confinement promotes buildup of gas pressures due to the rapid heating of air in the confined areas. Confinement can also promote faster reaction fronts in deflagrations, which produce a high blast output.

Elevated gas pressures are typically much longer in duration than shock loads and can be more damaging to structural components. Elevated gas pressure duration may be much longer than the natural period of the key structural components and are effectively a static load. Venting of a confined explosion can be effective in reducing the buildup of gas pressures and minimizing the total effective load. Venting may occur due to material failure or preplanned mechanical vents. Preplanned venting may result from planned weak points or blow-out panels specifically sized and installed in the structure. The weight or mass of the preplanned vent as well as its structural attachment determines the speed at which the vent opens to allow pressure reduction. For terrorist threats, mailrooms and loading docks represent common confined areas for which gas pressures must be considered. As a general rule, spaces adjacent to these areas should be unoccupied, or preferably, these areas should be adjacent to

the outside. This will permit venting into these areas or to the outside, which will reduce the peak gas pressure and resulting demand on the structure.

2.2 EXPLOSIVE THREAT SCENARIOS

Terrorist threats involving explosives can be carried out with a variety of delivery modes and configurations. Perhaps one of the most recognized is a vehicle-borne improvised explosive device (VBIED). Vehicles perform an important function by allowing the terrorist to move a relatively large amount of explosives material close to the target, often without arousing suspicion. The vehicle also produces fragments, many of which generate significant hazard to personnel due to their high velocity impact energy. Hand carried weapons produce much less energy output than larger weapons but are still hazardous due to their proximity to the target.

The most important parameters to define in the initial stages of blast assessment and design are explosive energy and standoff distance. As discussed previously, explosive energy is typically related to an equivalent weight of TNT. Equivalency is determined by comparing the blast pressure and impulse produced by the explosive to loads produced by the equivalent weight of TNT. Because both values are compared, it is evident that the TNT equivalency of a material may be different for pressure and impulse. TNT equivalencies are determined by tests, many of which have been prepared under government research programs. Results are available in Department of Defense technical manuals with limited distribution, such as *The Joint Services Manual for the Design and Analysis of Hardened Structures to Conventional Weapons Effects* that is also distributed as Unified Facilities Criteria 3-340-01, *Design and Analysis of Hardened Structures to Conventional Weapons Effects* (DOD, 2002). Blast loads decrease exponentially with distance, making standoff distance a key parameter for determination of blast loads. Increasing standoff distance is also a key method to mitigating blast damage by reducing peak blast pressure. For close-in blasts, a standoff increase of a few feet significantly changes the loads. Measures that defend facility perimeters are critical for maintaining intended standoff distances and thus reducing blast hazards.

2.3 BLAST PHENOMENA

Blast loads resulting from an explosion are created by a rapid expansion of material creating a pressure disturbance or blast wave which radiates away from the explosion. This blast wave may be termed a shock wave or pressure wave depending on the amplitude and rate of pressure rise. A shock wave, characteristic of a detonation, is an instantaneous rise in pressure which expands in all directions. Pressure waves, characteristic of slower speed deflagrations, have finite rise times and lower peak values than shock waves. As the shock wave travels away from the explosion center, its amplitude

decreases and the duration of the shock increases. Overexpansion at the center of the explosion creates a vacuum which generates a negative pressure. This negative pressure wave, which trails the positive pressure, is lower in magnitude but longer in duration than the positive pulse. A pressure-time history recorded during a high energy explosives detonation is shown in Figure 2-1. Expansion of the explosion causes air particles to move creating a dynamic pressure. This pressure is lower in magnitude than the shock or pressure wave and imparts a drag load on objects in its path, similar to wind loads.

As the shock wave or pressure wave strikes a wall or other object, a reflection occurs which increases the effective pressure on the surface. This reflected pressure may be considerably higher than the incident pressure wave. At the free edges of a reflecting surface, relief of the reflected pressure creates a rarefaction wave which travels across the face of the reflecting surface. This rarefaction wave relieves the positive reflected pressure down to the stagnation pressure (free-field pressure plus dynamic pressure). The time required for the rarefaction wave to travel from the free edge to a particular point on the surface is termed clearing time. If the clearing time exceeds the free-field blast wave duration, clearing does not occur.

2.3.1 Key Parameters

An idealized pressure-time history is shown in Figure 2-2. This figure describes the key parameters of a blast load. U.S. customary units for these parameters are psi for pressure, millisecond (ms) for duration and time of arrival, and psi-ms for impulse. SI units are kPa for pressure, ms for duration and kPa-ms for impulse. Note that the pressures shown are in addition to ambient atmospheric pressure—thus the term "overpressure."

Peak overpressure is the peak pressure value which occurs instantaneously upon arrival of the blast wave or after a short rise time. Positive phase duration is the time for the blast pressure to decay to ambient. Positive impulse is the total pressure-time energy applied during the positive duration and is equal to the area under the pressure-time curve. Negative phase pressure, duration, and impulse follow the positive phase.

Reflected blast loads are produced when a blast wave strikes a surface at an angle of incidence other than parallel to the surface. Blast pressures applied where the shock wave travels parallel to a surface are side-on or incident, also known as free-field. All other blast load impingement involves a reflection. The reflection coefficient, C_r, the ratio of reflected pressure to free-field pressure, is a function of angle of incidence and free-field pressure. Reflected pressure, P_r, is computed by:

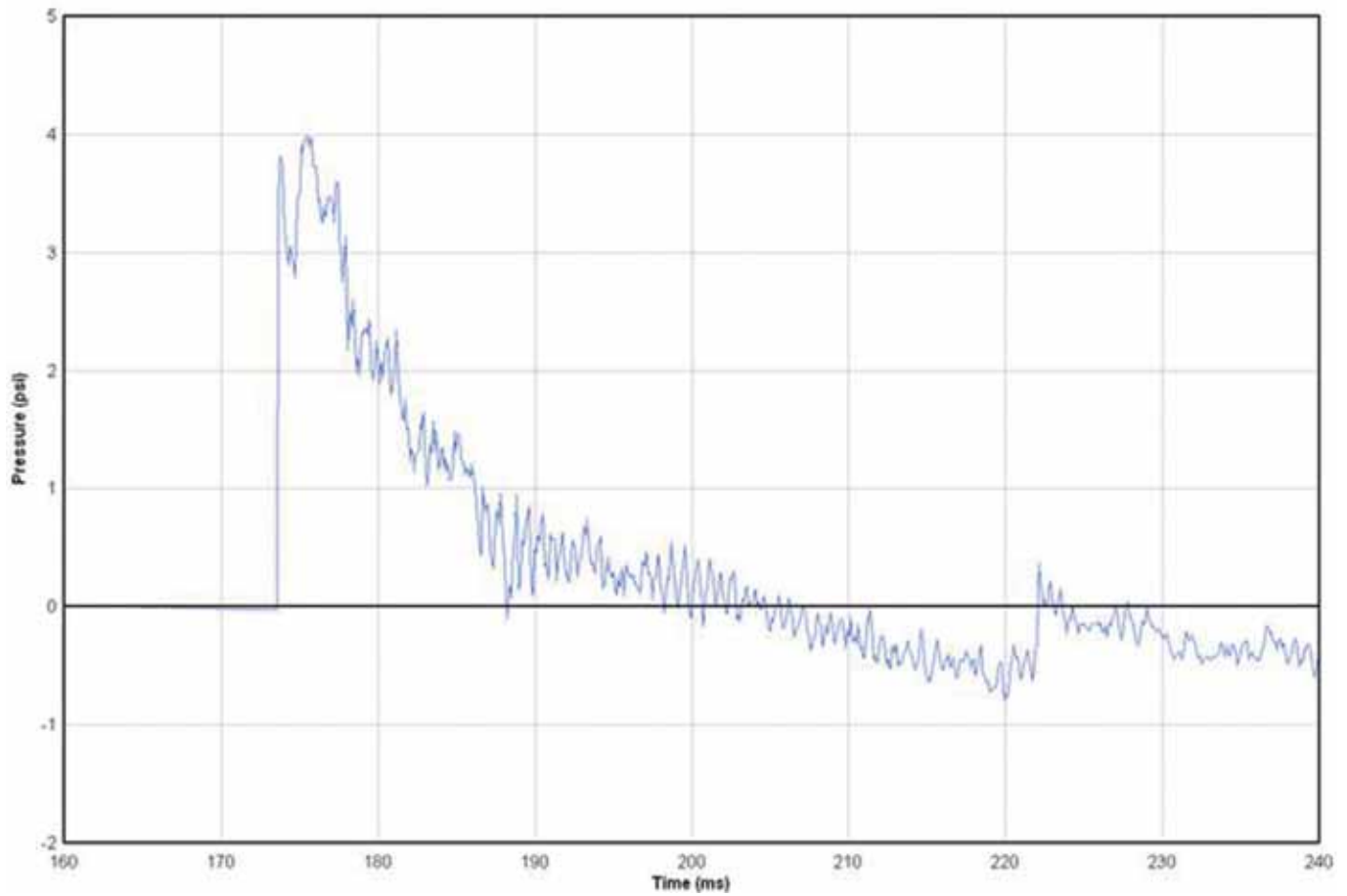$$P_r = C_r P_{so} \qquad (2\text{-}1)$$

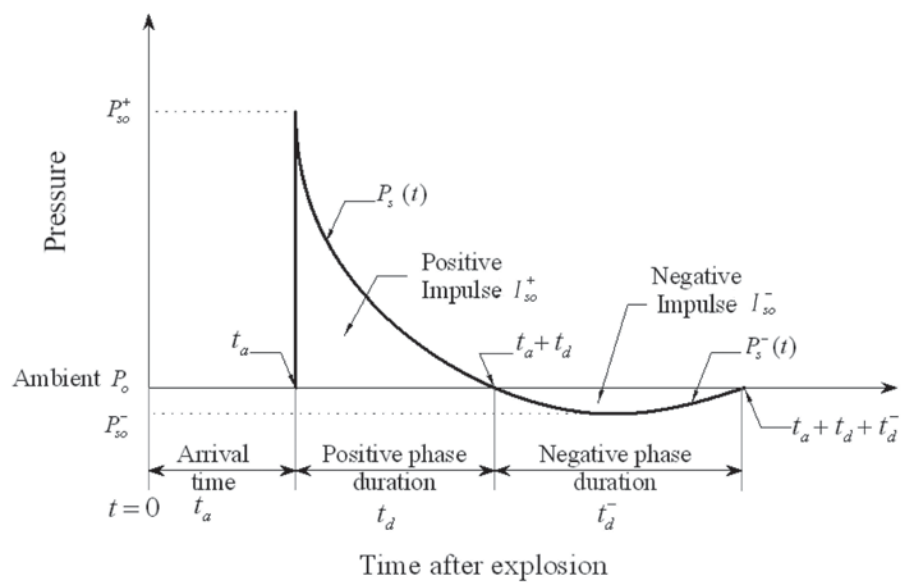Fig. 2-1. Pressure gauge trace from high energy explosives detonation.

Fig. 2-2. Pressure-time history for shock load.

where

P_{so} = free-field pressure, psi

The reflection coefficient ranges from 2 to more than 30. In the range of loads most commonly encountered, the reflection coefficient ranges from 2 to 5. It does not drop below 2 until the angle of incidence is greater than 50°. Reflection coefficient as a function of angle of incidence is shown in Figure 2-3. For a blast wave striking two intersecting surfaces, such as a cornering load, both surfaces will be subjected to reflected loads.

Free-field loads are those produced by a blast wave sweeping over a surface, unimpeded by any objects in its path. This incident load is also referred to as side-on which, as the term implies, traverses a wall, flat roof, or other object parallel to its travel direction. Free-field pressure terms have an "*so*" subscript in the figures in this chapter as well as in most references. Figure 2-4 depicts the relationship between reflected pressure-time histories (indicated by the solid curve) and free-field (incident) pressure-time histories (indicated by the dashed curve).

2.4 BLAST LOAD PREDICTION

Prediction of blast loads on structures typically requires the following basic steps:

1. Threat definition, accounting for charge size, explosive type and charge location

2. Free-field (incident) loads determination

3. Applied loads on structure determination

Determination of appropriate design level threats or explosion energy requires knowledge of both the process and the consequences. Threat levels and locations may be determined from a risk assessment or may be specified by a governing standard such as the *Minimum Antiterrorism Standards for Buildings* (DOD, 2007), the Interagency Security Committee *Security Design Criteria for New Federal Office Buildings and Major Modernization Projects* (ISC, 2004), or the Interagency Security Committee *Physical Security Criteria for Federal Facilities* (ISC, 2010). Chapter 3 of this Design Guide describes these criteria. In some cases, explosive quantities are mandated by government regulations. Vapor cloud explosions require estimation of the quantity of material participating in an explosion which may entail dispersion analysis. Although the blast threat is determined by either specified criteria or project-specific threat assessments, structural engineers should be aware of the factors involved in calculating the explosion energy in order to help guide decisions that are made about structural performance during the structural analysis and design process. Selection of the threat and the response criteria should be consistent.

The basic approach involves predicting free-field loads using empirical or semi-empirical methods. Curves that relate explosion energy, standoff distance, and blast load quantities are typically used in this initial load prediction step. These curves are readily available for high energy explosives and vapor cloud explosions. The free-field loads are then translated into applied loads for the structure or component of interest by consideration of component location and orientation with respect to the detonation. The selection of analysis method and complexity should be based on specific project requirements and type of component being considered. The applied loads are used in a dynamic structural analysis of the building and its components.

2.4.1 Empirical Relationships

A significant amount of data exists that quantifies the relationship between charge weight, standoff distance and blast parameters. Several technical manuals produced by the Department of Defense contain the relationships in the form of scaled distance curves. UFC 3-340-02 (DOD, 2008) and UFC 3-340-01 (DOD, 2002) are perhaps the most well-known sources of this information. Both of these documents are available electronically to aid in the use of figures and tables. Other manuals, charts and calculation tools are used by blast consultants to estimate blast loading.

2.4.2 External Loads

The empirical blast parameter curves are provided in UFC 3-340-02 (DOD, 2008), UFC 3-340-01 (DOD, 2002), and other manuals plot air blast parameters versus scaled distance for both spherical air burst configurations and hemispherical surface burst configurations. A charge detonated on the ground will produce higher blast loads than an air burst due to the reflection of the initial shock by the ground surface. For unyielding surfaces with the charge located on the surface, the effect is equivalent to a doubling of the charge weight since the energy of the blast directed to the ground is fully reflected. For soft soils or charges located above the surface, the reflection factor is less. Guidance for selecting the reflection factor is given in various government technical manuals but it is conservative to assume a fully reflecting surface.

The key to the empirical relationships is the use of Hopkinson scaling (cube-root scaling). Since the shock wave expands as a sphere, scaling of explosive effects is volumetric and leads to the use of cube-root scaling. Cube-root scaling allows a limited number of empirical curves to define airblast parameters for an infinite variety of explosion parameters. To use these empirical curves, one computes the scaled distance by dividing the standoff distance from the charge to the point of interest by the cube root of the charge weight. Standard empirical curves for high energy explosives are based on conditions at sea level. Sachs scaling can be used to account for the effects of altitude.
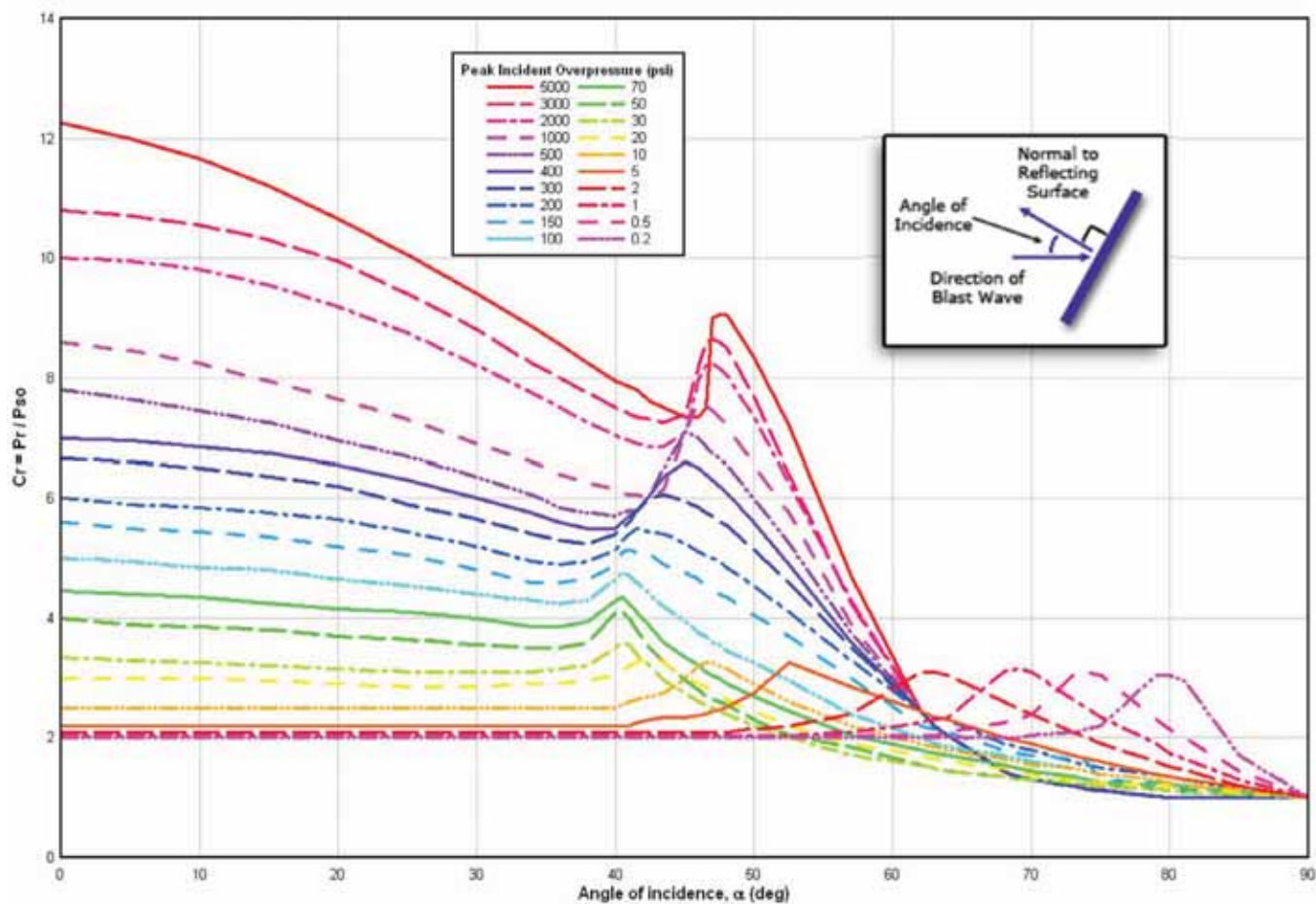
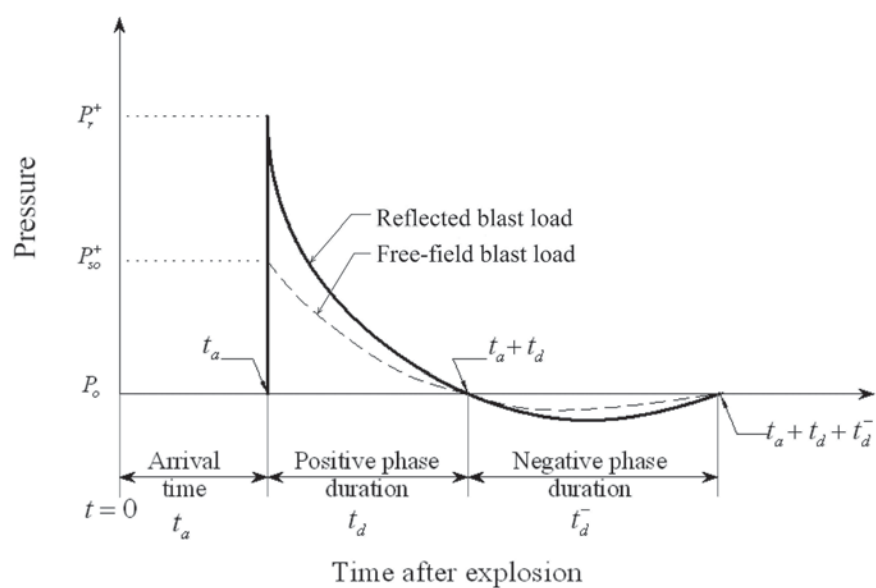*Fig. 2-3. Reflection coefficients (DOD, 2002).*

Fig. 2-4. Relationship of reflected and free-field (side-on) pressure-time histories (P_r = reflected pressure; P_{so} = side-on pressure).

Parameters that are a function of time, such as load duration and impulse, are reported in scaled terms to account for scaling effects. Users are cautioned to read the correct axis and to unscale the parameters prior to application. These curves are based on a unit weight of TNT. Equivalence tables are provided for various materials in UFC 3-340-01 (DOD, 2002) and other technical manuals. One of the more common tools for predicting basic blast loads for bomb threats are the surface burst curves in UFC 3-340-02 (DOD, 2008) and similar documents. These curves are reproduced in Figure 2-5.

2.4.3 Internal Loads

Blast design sometimes involves containment of explosion effects such as for mailrooms and loading docks. Shock waves emanate from the charge surface, strike wall and roof components, and reflect to impact other surfaces. Each surface is subjected to multiple shock waves which combine to form the applied load. Typically the peak pressure of the initial reflected wave is taken for the combined load, and the reflected impulse values are combined to determine the total impulse. Accounting for the reflections requires specialized software to track the response of venting surfaces and the combination of the reflected waves.

Internal explosions also produce gas and heat which cause a pressure increase within the confined space. The peak gas pressure is a function of the charge-weight-to-free-volume ratio in confined areas. Empirical relationships for gas load prediction are covered in UFC 3-340-02 (DOD, 2008) and UFC 3-340-01 (DOD, 2002). This pressure buildup is relatively slow compared with the load duration associated with shock waves. For simplicity, the peak gas pressure or quasi-static pressure is assumed to rise instantaneously to the peak gas pressure but is not additive to shock pressures.

Duration of the gas pressures is a function of the vent area and volume available and the rate at which temperatures decay in the confined area. UFC 3-340-02 (DOD, 2008) contains predictive methods for gas impulses based on vent area and vent weight. Equivalent gas load duration is computed from the peak gas pressure and the predicted impulse assuming a right triangle load shape. Gas pressure loads can be quite important to the response of structural components, especially for very long duration loads. For load durations significantly exceeding the fundamental period, the component blast resistance must be slightly higher than the peak gas pressure to provide adequate response.

Two codes have been developed by the Department of the Navy to compute interior loads. SHOCK computes shock pressures on a wall or roof surface including effects of reflections. FRANG determines gas pressure duration by modeling venting and pressure decay. The Department of the Army and Defense Special Weapons Agency has developed a series of codes for internal load prediction culminating in BLASTX, which is capable of modeling shock and gas pressure propagation through multiple rooms. These codes are not generally available to the public but the calculations can be accomplished in spreadsheets or other math modeling tools using the methods discussed here. Hydrodynamic and computational fluid dynamics (CFD) codes can also be used to develop these loads.

2.4.4 Analytical Methods

Methods have been developed to analytically predict blast loads. These methods fall into two groups: semi-empirical and hydrocode. The semi-empirical approach uses a physics-based model that is tuned to match test data. These models are limited to configurations and charge weight ratios for which data is available but offer the advantage of quick run-times compared with more detailed techniques. BLASTX is an example of this approach. The codes offer limited ability to model shock diffraction, shielding and reflection. Semi-empirical methods have been developed primarily by defense related agencies and are restricted in distribution to government agencies and contractors.

Hydrocodes utilize a grid of computational cells to track shock wave propagation through a medium based on material models, relating kinetics of the combustion to pressure, density and other key parameters. Hydrocodes have been developed by both government agencies and private industries and are available to analysts developing loads for commercial projects. This type of analysis is much more complex and expensive than the use of empirical relationships. Some of the available tools have user interfaces which greatly simplify the analysis, especially for standard materials; however, considerable effort is required to conduct a competent analysis.

2.5 LOADS ON STRUCTURES

Free-field blast parameters obtained from the empirical relationships must be modified to account for interaction with building surfaces before they are used in analysis. Additionally, other parameters which may become important include drag pressures, clearing times, and blast wave length.

Blast loads can change significantly over the surface of a building because of differences in distance from the explosion center and angle of incidence. Multistory buildings will experience substantially smaller loads at upper floors from an explosion near grade. Prediction of the blast load variation over a surface can be computed accurately with complex analysis methodologies; however, simplified approaches may be acceptable, especially for preliminary evaluation or design. Simplified approaches typically involve dividing a surface into a grid and computing the pressure and impulse at the center of the grid point, taking into account the angle of incidence for surfaces with a line of sight to the charge.

Greater accuracy can be achieved by creating a higher resolution grid but even with this approach, loads are averaged over selected areas corresponding to the tributary areas of components of interest. For tall structures, these areas may be the equivalent of one or more floors.

2.5.1 Equivalent Load Shapes

The load time-history from a shock wave is of a shape similar to that shown in Figure 2-2. For design, this time-history is normally simplified to a triangular distribution with an instantaneous rise and a linear decay. This simplified waveform is shown in Figure 2-6. Peak pressure and impulse are preserved from the actual shock parameters and a fictitious duration, t_e, is taken as $t_e = 2(I/P)$. This simplified time-history is readily applied to simple structural models to quickly determine response. A similar approach can be taken with pressure waves which have an increasing-decreasing shape. If pressure and impulse are known, an isosceles triangle may be used with an equivalent duration, t_e, taken as $2(I/P)$ and a rise time to peak pressure, t_r, equal to $t_e/2$.

The negative phase of the blast load is ignored in this equivalent load. This is typical for many blast analysis
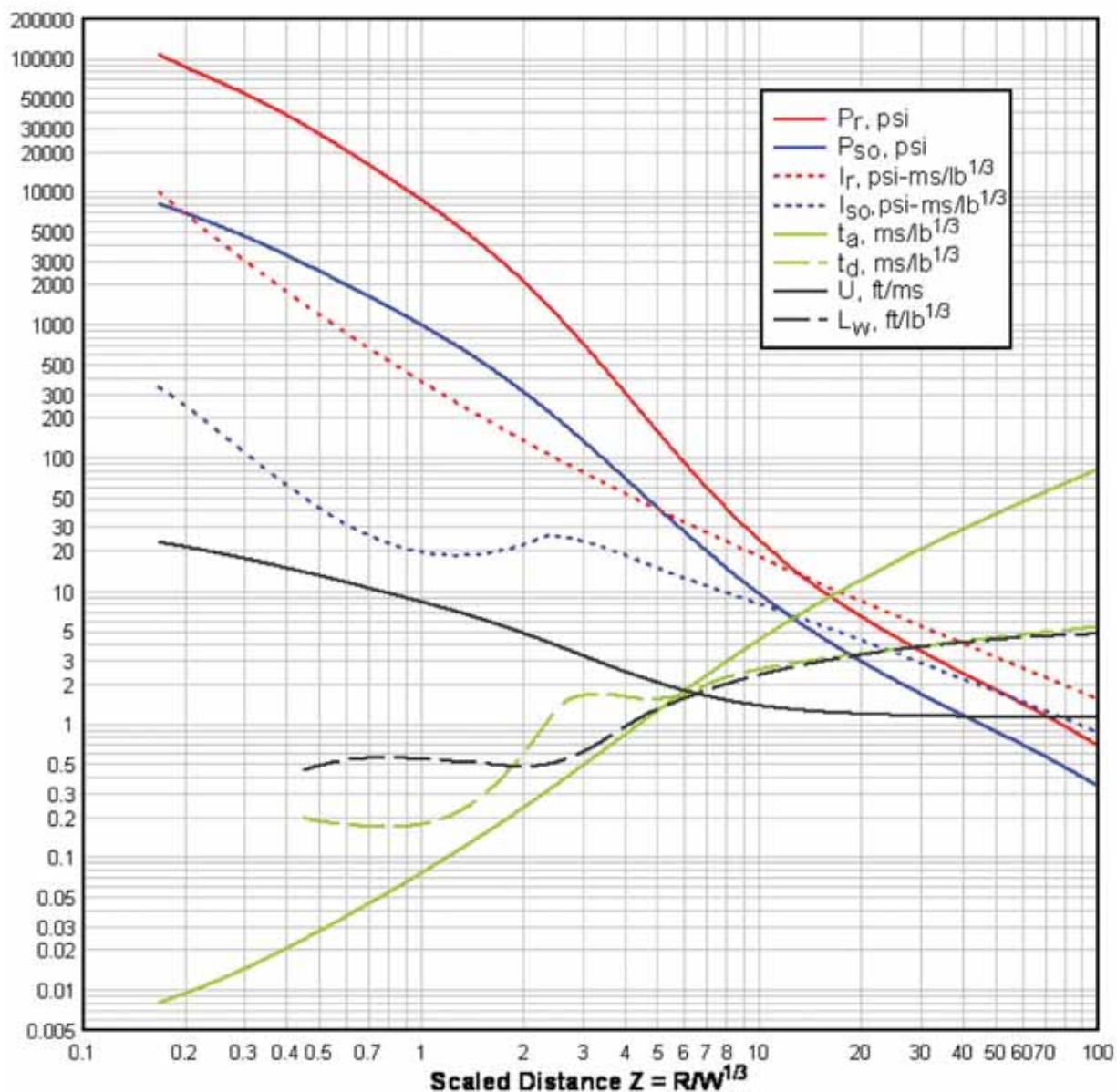

Fig. 2-5. Positive phase parameters for surface burst TNT explosions (DOD, 2008).

problems because the negative phase load often does not significantly affect the response of structural components. Negative phase loads can become important when the components are significantly weaker in the reverse loading direction, especially with high rebound forces.

Clearing effects, which reduce blast loads near the edges, are also often neglected. Clearing typically affects a small portion of the structure and neglecting this effect is conservative. The structural engineer should consider these factors when developing the design loads.

2.5.2 Drag Loads

Air particle movement produces a dynamic pressure which results in a drag load on a structure similar to a wind load. Relationships between free-field pressures and drag loads have been established as shown in Figure 2-7. An equation for dynamic pressure, q_o, was developed by Newmark (1956):

$$q_o = 2.5 P_{so}^2 / (7 P_o + P_{so})$$ (2-2)

where

P_o = atmospheric pressure
P_{so} = free-field pressure

The drag load is a function of dynamic pressure and a drag coefficient. For surfaces facing the blast, the drag coefficient is typically 1.0. For all other surfaces, the drag coefficient is −0.4. For reflected surfaces, drag load contribution is included in the reflection factor data. For side walls, rear walls and roof surfaces, the negative value of the drag coefficient (suction) reduces the applied blast load and is often neglected, but the engineer should be aware of the phenomenon.
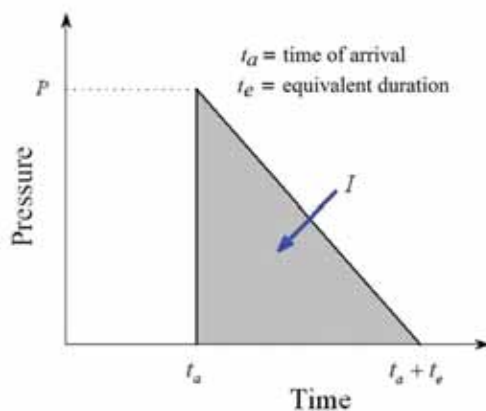
Fig. 2-6. Simplified pressure-time history.

2.5.3 Nonreflected Surface Loads

As a blast wave sweeps across a side or rear wall (not facing the blast) or roof, the surface is subjected to a nonuniform load due to time of arrival of the load and blast pressure decay. Depending on the span and width, all portions of a component may receive the peak load at the same time. If the blast wavelength is long compared with the span, the effective pressure on the component will be high. If the wavelength is short relative to the span, the effect of the load will be small. In design, we typically consider full incident (side-on) pressure for nonreflecting walls and roofs. In some cases, the analyst may use the side-on loads computed at the center of each nonreflected face rather than using the load averaging techniques described in UFC 3-340-02 (DOD, 2008).

2.5.4 Shielding and Reflection

Urban environments with multistory buildings present some unique challenges for blast load prediction, especially when the explosive threat is some distance from the structure being analyzed. Buildings provide shielding to adjacent structures that are not in the line of sight. In many cases, this shielding can be significant, reducing peak blast pressures to a fraction of the loads that would occur without intervening structures. Conversely, adjacent buildings can produce reflections that can amplify loads above those produced by the incident wave acting on the building of interest. Due to the increased travel distance to the reflecting surface, the peak pressure on the target building will not be affected, but the impulse from the reflection will add to the incident wave load. For many practical situations, this additional impulse is low enough to be ignored. However, the engineer should perform some preliminary calculations using an image charge approach to see if the impulse contribution should be included.

Most of the tools available to government agencies and commercial consultants ignore these reflection and shielding effects because they are fast-running tools that rely on empirical relationships between scaled distance and blast loads. Often this assumption is conservative, but the more accurate answers offered by advanced analysis using hydrocode or CFD can result in lower costs for blast resistant construction for large facilities.

2.5.5 Net Lateral Loads

Differences in front and rear wall loads create a net lateral load in the direction of the blast wave travel. Phasing due to delayed blast wave arrival at the rear wall increases the net lateral load. Negative phase loads complicate the net load computation. This phasing can be important for flexible frame-type structures but is less important for shear wall systems. Rear wall loads are often conservatively ignored for net lateral load computation.

2.5.6 Negative Phase

Negative phase loads typically reduce the peak response and in most cases are ignored. However, components with a short fundamental period with respect to the load duration may be rebounding as the negative wave arrives. In this case, ignoring the negative phase is unconservative. This situation is the exception, rather than the rule, but the response of the component should be examined to determine if negative phase loads should be included.

2.5.7 Interior Loads Due to Leakage

Openings in structures may allow blast loads to enter the structure. For large openings, this interior pressure load may reduce the effective net load on the walls. For smaller openings, the reduction in net load is minimal and is typically ignored. Interior loads are most important for evaluation of interior damage and the potential effects of overpressure on personnel. As exterior blast loads are constricted at the opening and then expand into the free volume of the interior, the peak pressure is significantly reduced. Methods are provided in UFC 3-340-02 (DOD, 2008) for predicting leakage loads for simple configurations. More complex situations require hydrocodes to model the propagation of the blast wave in and around the structure.

2.6 RESOURCES

Technical manuals developed for the Department of Defense and other government agencies provide a wealth of information and guidance on prediction of blast loads. These manuals cover a range of threats and hazards including high and low energy explosives as well as bursting vessels. Many of these manuals have electronic versions and supporting
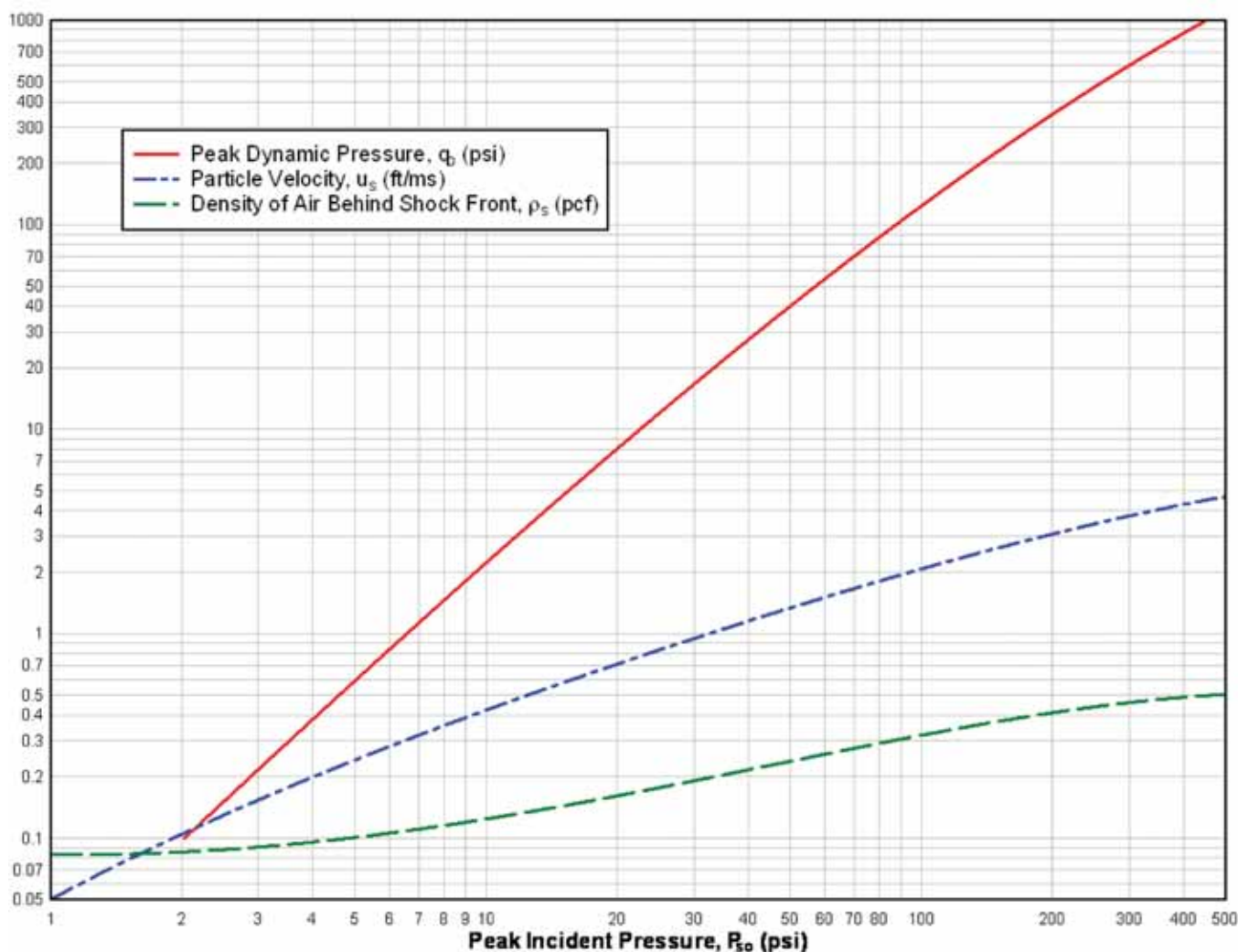
Fig. 2-7. Dynamic pressure (DOD, 2002).

software to aid implementation of the methods; however, they are not readily available to the public.

FEMA 426 (FEMA, 2003a) and FEMA 427 (FEMA, 2003b) provide guidance on predicting and mitigating the effects of terrorist attacks on commercial structures. These two documents provide the most readily available sources of information for selection of threats, prediction of blast loads, response of buildings and components, and structural design to mitigate blast effects.

Prediction methods for vapor cloud explosions and vessel bursts are well documented in proceedings of safety-related industry associations and technical manuals developed by these groups. These documents are widely available and are included in the list of references. Examples include *Guidelines for Evaluating the Characteristics of Vapor Cloud Explosions, Flash Fires, and BLEVEs* (Center for Chemical Process Safety, 1994) and *Understanding Explosions* (Center for Chemical Process Safety, 2003).

Several commercial software codes have been developed for load prediction for solid, liquid and gas explosions. These tools represent the state of the art in blast load prediction for industrial explosions.

2.7   DESIGN EXAMPLE

Example 2.1—Preliminary Evaluation of Blast Resistance of a One-Story Building

Given:

Evaluate the one-story steel building shown in Figure 2-8, Figure 2-9 and Figure 2-10 for a blast caused by a charge with $W = 500$ lb located just above ground level at the location shown in Figure 2-8. The building is 50 ft by 70 ft in plan and has a 15-ft story height. The lateral force resisting system consists of rigid frames in the long dimension and braced frames on the exterior walls in the short dimension. The roof is metal decking over structural steel purlins with a 0% slope.
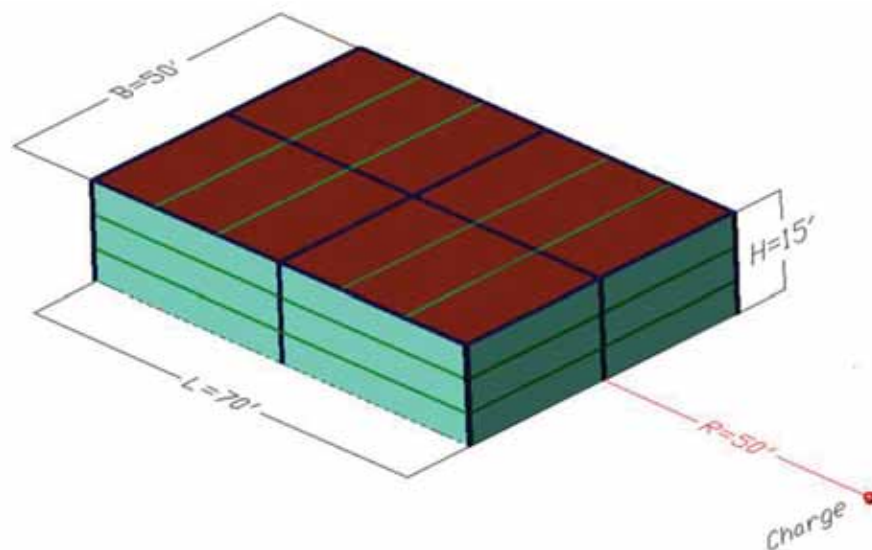
Fig. 2-8. Steel building—isometric view.

Solution:

Scaled Distance

For a stand-off distance of $R = 50$ ft and a TNT equivalent charge weight of 500 lb, the scaled distance is:

$$Z = \frac{R}{W^{1/3}}$$

$$= \frac{50.0\,\text{ft}}{500\,\text{lb}^{1/3}}$$

$$= 6.30\ \text{ft/lb}^{1/3}$$

Since the explosive is located just above ground, the charge is considered to be a hemispherical surface burst explosion.
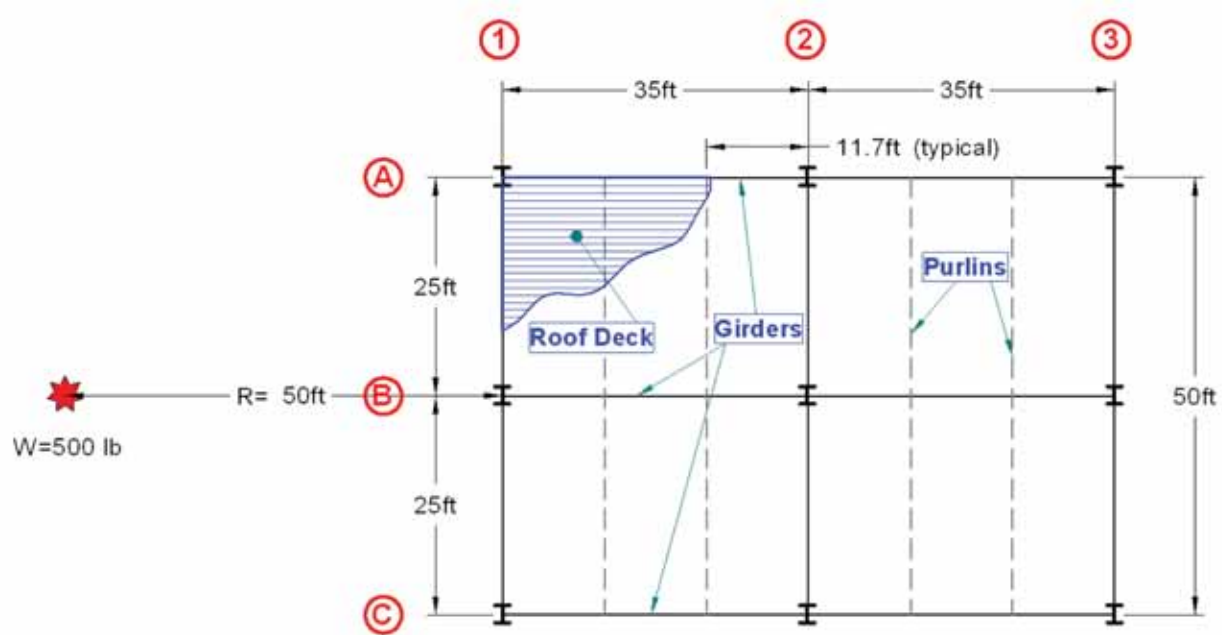
Fig. 2-9. Steel building—plan view.

Fig. 2-10. Steel building—elevation.

Parameters for Blast Loading

From Figure 2-11, using the scaled distance ($Z = 6.30$ ft/lb$^{1/3}$), the following data is obtained for the positive phase:

Blast Loading Parameters	From Figure 2-11	Calculated
Reflected peak pressure (positive phase)	$P_r = 79.5$ psi	–
Side-on peak pressure (positive phase)	$P_{so} = 24.9$ psi	–
Reflected impulse (positive phase)	$I_r = 31.0W^{1/3}$	$I_r = 246$ psi ms
Side-on impulse (positive phase)	$I_{so} = 12.1W^{1/3}$	$I_{so} = 96.0$ psi ms
Time of arrival	$t_a = 1.96W^{1/3}$	$t_a = 15.6$ ms
Exponential load duration (positive phase)	$t_d = 1.77W^{1/3}$	$t_d = 14.0$ ms
Shock front velocity	$U = 1.75$ ft/ms	–
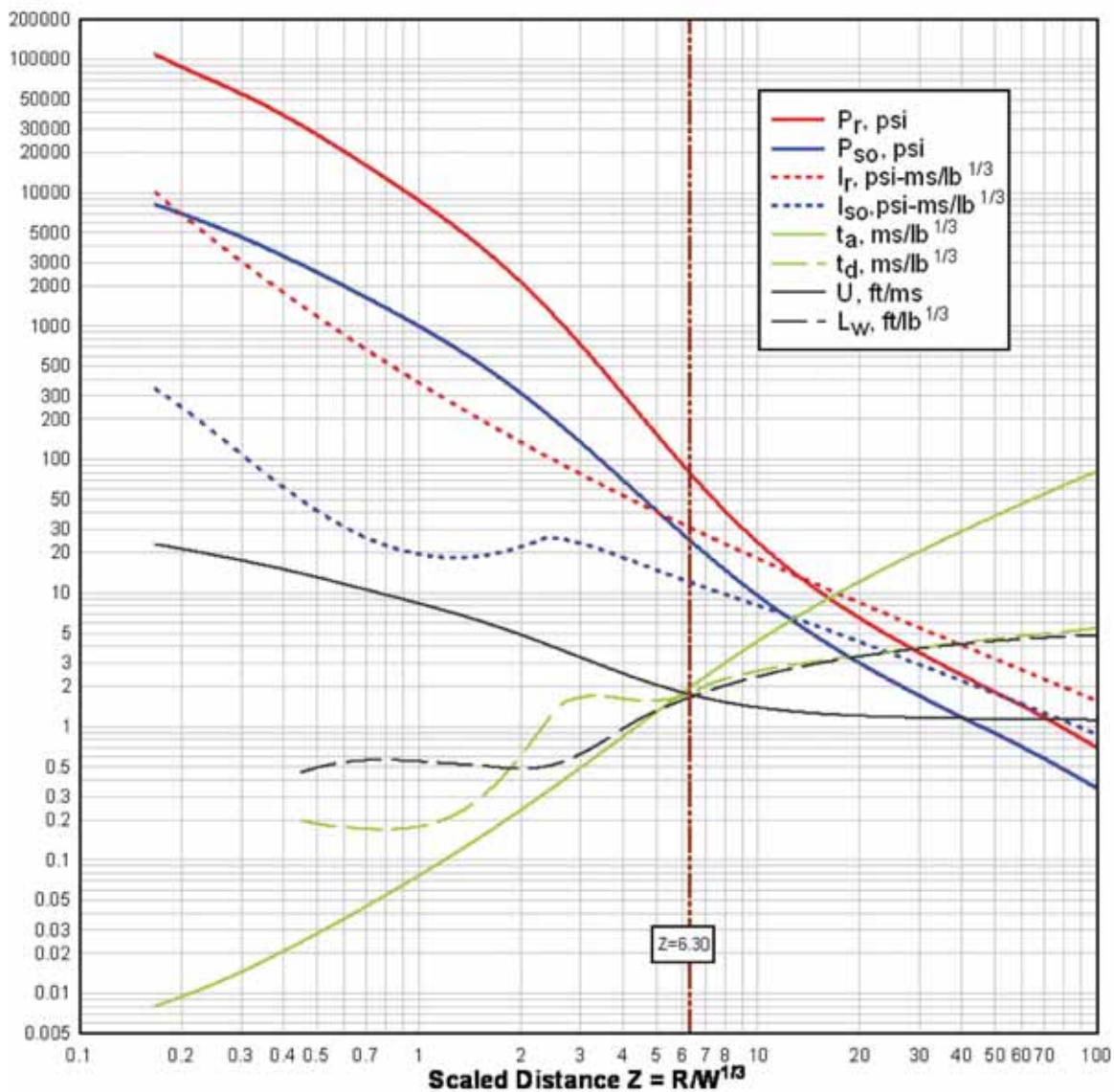
Fig. 2-11. Positive phase shock parameters for hemispherical TNT explosion on the surface at sea level (DOD, 2008).

For design response calculations, the loading function is converted to an equivalent triangular shape in which the peak pressure and impulse of the more complex pressure time-history are preserved and an equivalent load duration is computed. Thus, the equivalent load duration, t_e, is:

$$t_e = \frac{2I}{P}$$

(2-3)

Because the area under the two curves for equivalent reflected pressure in Figure 2-12 and Figure 2-13 must be equal, with the area representing the impulse, the equivalent load duration is always less than the actual duration.
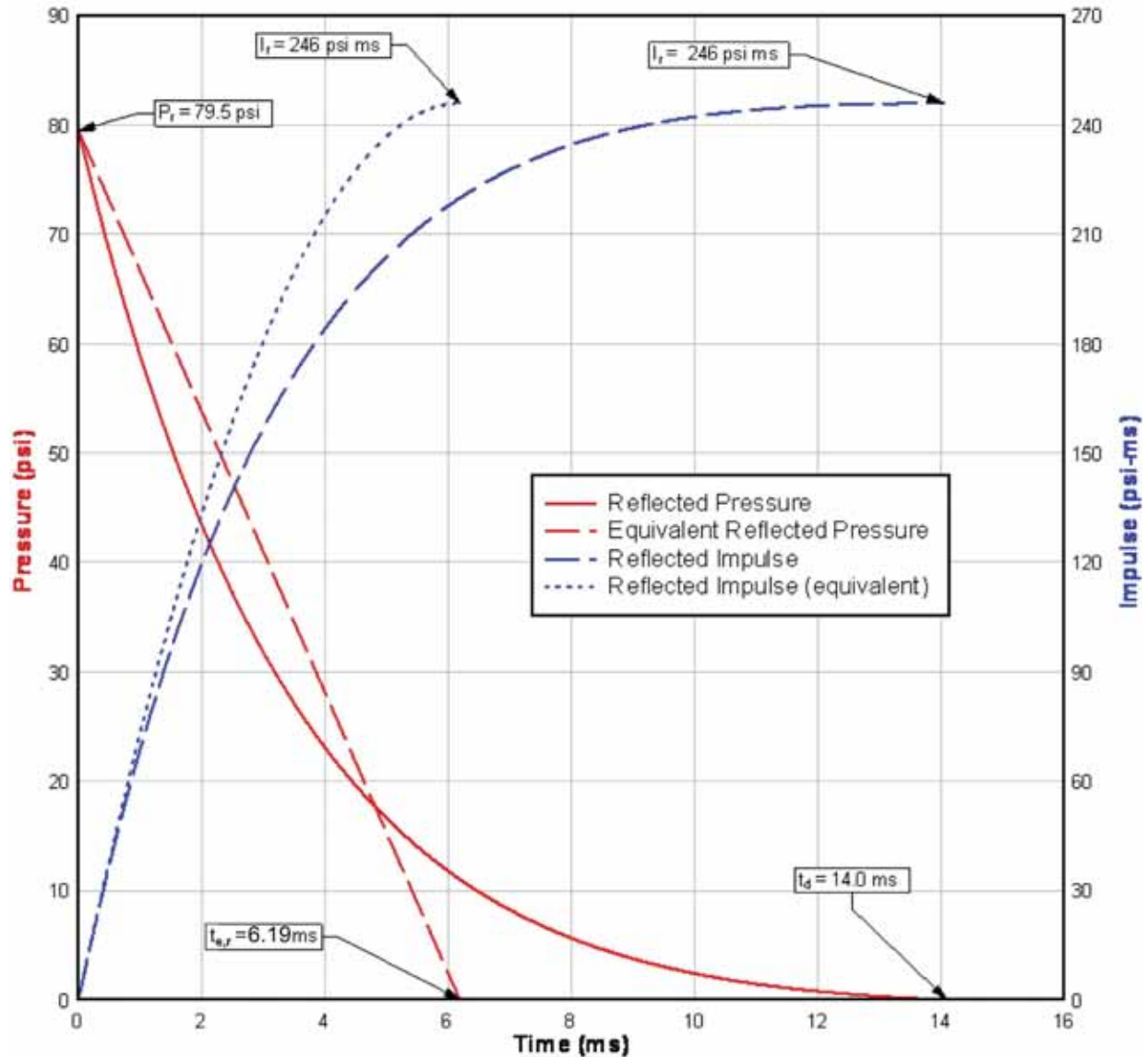
Fig. 2-12. Reflected pressure and impulse.

The equivalent duration of positive phase blast load for reflected pressure is:

$$t_{e,r} = \frac{2\,I_r}{P_r}$$

$$= \frac{2(246 \text{ psi ms})}{79.5 \text{ psi}}$$

$$= 6.19 \text{ ms}$$
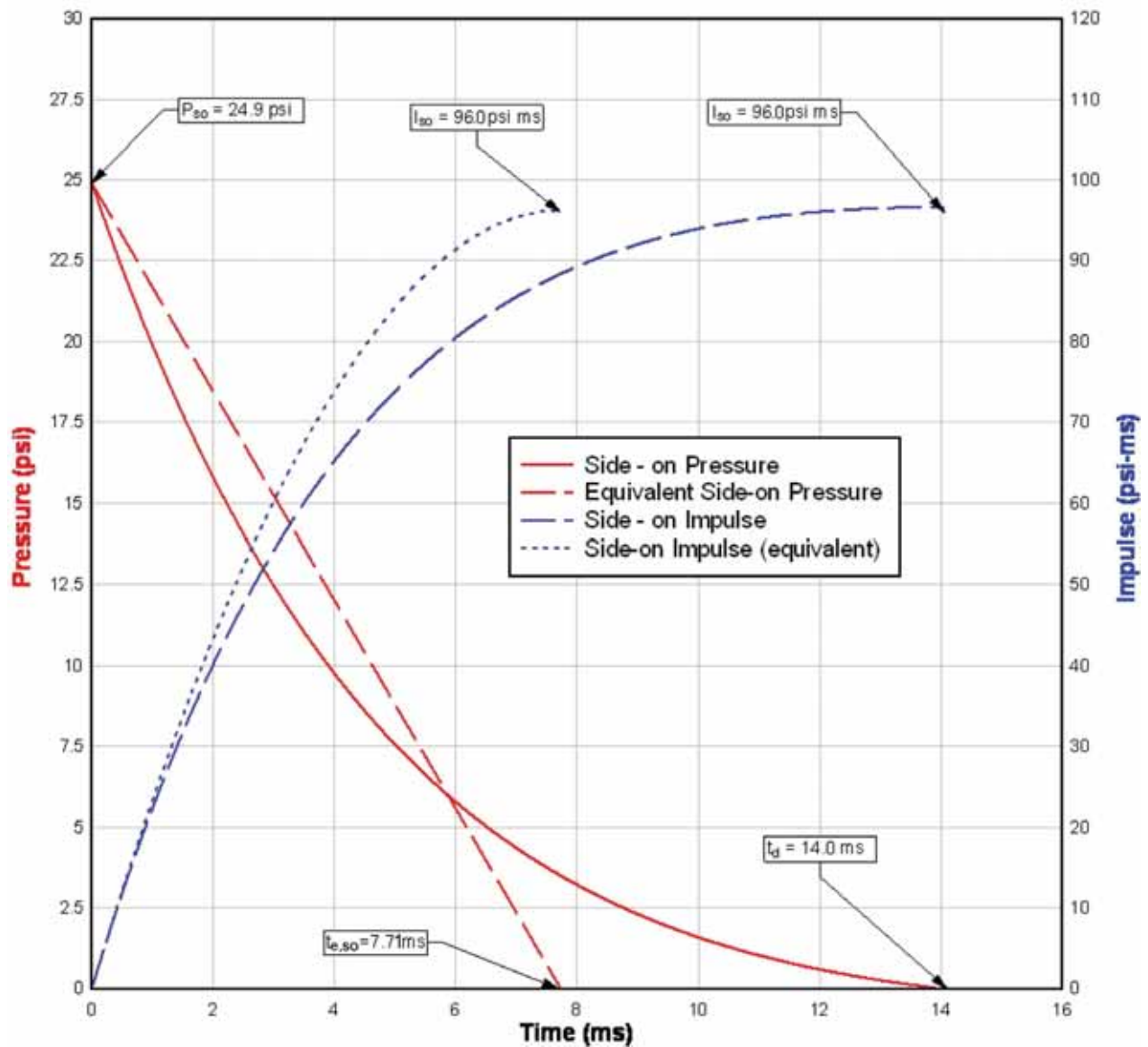
Fig. 2-13. Side-on pressure and impulse.

The equivalent duration of positive phase blast load for side-on pressure is:

$$t_{e,so} = \frac{2\,I_{so}}{P_{so}}$$

$$= \frac{2(96.0 \text{ psi ms})}{24.9 \text{ psi}}$$

$$= 7.71 \text{ ms}$$

Figure 2-12 and Figure 2-13 show the predicted pressure time-history loading function and the equivalent triangular loading function for reflected pressure and side-on pressure.

Front Wall

The typical blast load on a front wall is shown in Figure 2-14.

Determine Blast Load Parameters at the Closest Point to the Charge

The equivalent reflected pressure from Figure 2-12 is used for designing the entire front wall. A more detailed calculation could be used which considers the reduction in pressure and impulse across the wall for overall lateral loading on the building. Figure 2-15 shows the equivalent blast pressure load versus time for the front wall.

Side Walls

The typical blast load on a side wall is shown in Figure 2-16 as a plot of pressure versus time.

The blast load on the side wall is computed near the front corner of the building. For simplicity, the blast parameters (P_{so}, I_{so}, q_o, U) are computed using the scaled distance Z computed at the front wall on the centerline. The sidewall blast parameters are given in Figure 2-13. A more detailed calculation would consider the reduction of blast pressure and impulse over the wall moving toward the rear.

Roof

Similar to the side walls, the blast load on the roof is computed near the corner of the building. For simplicity, the blast parameters (P_{so}, I_{so}, q_o, U) are computed using the scaled distance Z computed at the front wall on the centerline. Thus, the roof parameters are the same as those for the sidewall and shown in Figure 2-13.
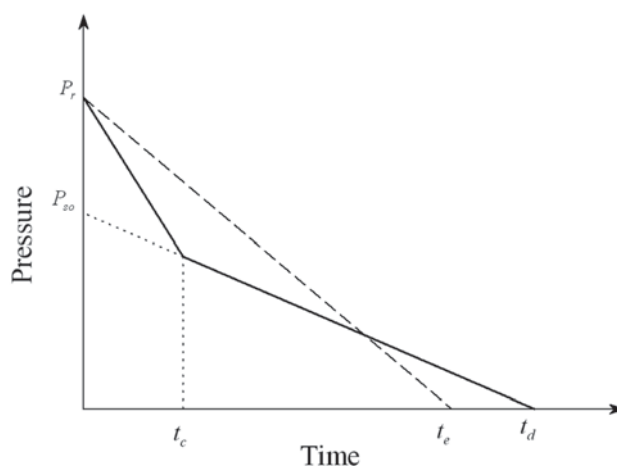
Fig. 2-14. Typical blast load with clearing effect.
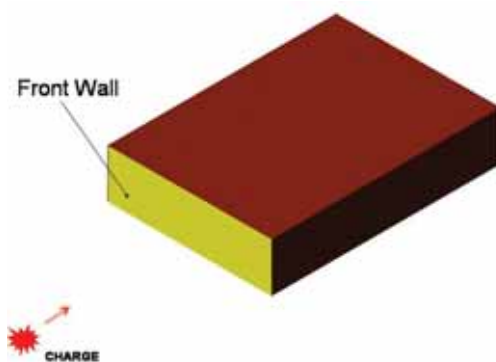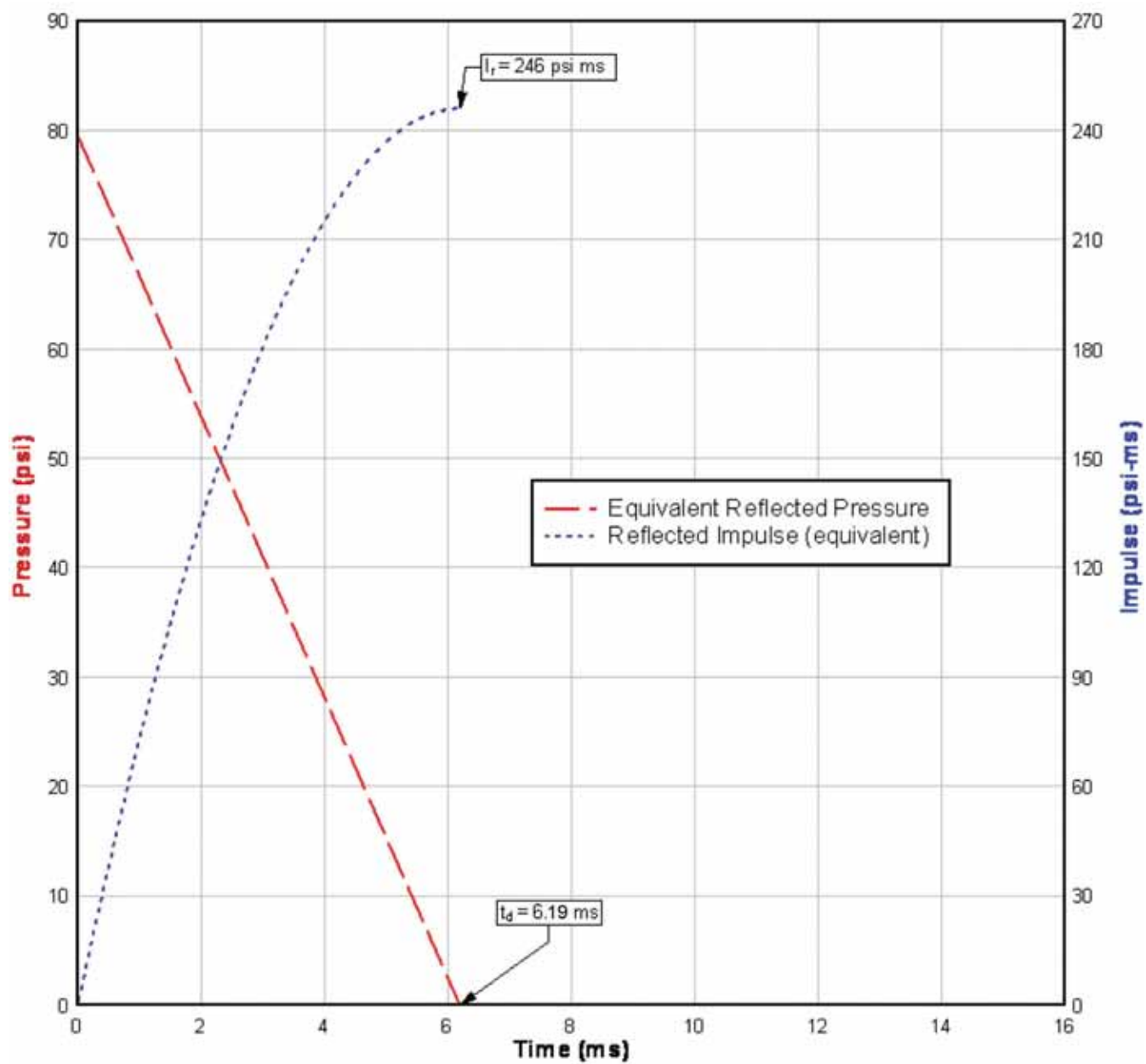
Fig. 2-15. Equivalent blast pressure load for front wall.

Rear Wall

The typical blast load on a rear wall is shown in Figure 2-17 as a plot of pressure versus time.

The blast parameters for the rear wall are computed using the scaled distance to the front and rear of the building as shown in Figure 2-18. The closest distance from the charge to the rear wall is:

$R = 50.0 \text{ ft} + 70.0 \text{ ft}$
$\quad = 120 \text{ ft}$

and the TNT charge weight is again 500 lb. Thus, the scaled distance is:

$$Z = \frac{R}{W^{\frac{1}{3}}}$$
$$\quad = \frac{120 \text{ ft}}{(500 \text{ lb})^{\frac{1}{3}}}$$
$$\quad = 15.1 \text{ ft/lb}^{\frac{1}{3}}$$
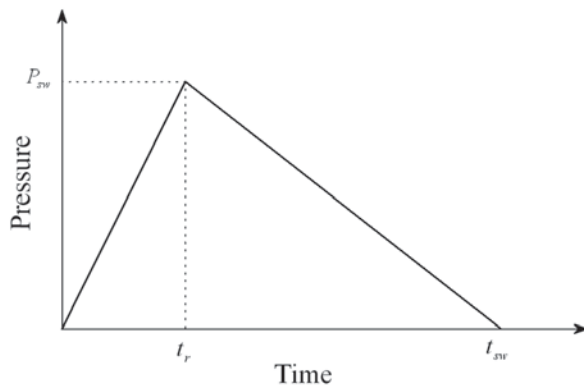
Fig. 2-16. Typical side wall blast loading.
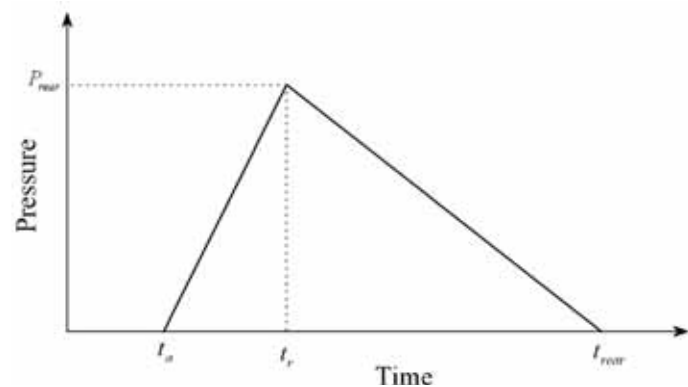
Fig. 2-17. Typical rear wall blast loading.
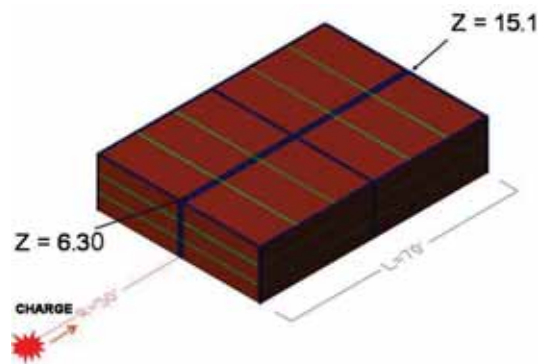
Fig. 2-18. Scaled distances at front and rear walls.

Using Figure 2-11 with a charge weight of 500 lb and the scaled distance, $Z = 15.1$ ft/lb$^{\frac{1}{3}}$, the following values are determined:

Side-on peak pressure (positive phase)	P_{so}	$= 4.60$ psi
Side-on impulse (positive phase)	I_{so}	$= 44.0$ psi ms
Time of arrival	t_a	$= 66.0$ ms
Exponential load duration (positive phase)	t_d	$= 24.7$ ms
Shock front velocity	U	$= 1.26$ ft/ms

Equivalent side-on load duration (positive phase) $\quad t_{e,so} = \dfrac{2 I_{so}}{P_{so}}$

$$= \frac{2 \left(44.0 \text{ psi ms}\right)}{4.60 \text{ psi}}$$

$$= 19.1 \text{ ms}$$

Peak dynamic pressure $\qquad\qquad\qquad\qquad q_o \quad = 2.5 P_{so}^2 / (7 P_o + P_{so})$

$$= 0.500 \text{ psi}$$

$$P_o \quad = 14.7 \text{ psi}$$

Based on these parameters, the side-on blast pressure loads at the top of the rear wall are as shown in Figure 2-19.

Computation of the rear wall load is completed by evaluating the rise time and total duration as the blast wave sweeps down the wall. The combined load is shown in Figure 2-20. In this figure, the equivalent positive phase load duration is used. The negative phase of the load is not shown in this example. The negative phase is often ignored for simplicity and this is typically a conservative approach. The span of the element parallel to the traveling wave is the building height, $L_1 = 15$ ft. The free-field pressure at the top of the wall is 4.60 psi with a time of arrival, $t_a = 66.0$ ms. Thus, the time to peak pressure, t_2, is the rise time plus the time of arrival:

$$t_2 = \frac{L_1}{U} + t_a$$

$$= \frac{15.0 \, \text{ft}}{1.26 \, \text{ft/ms}} + 66.0 \, \text{ms}$$

$$= 77.9 \text{ ms}$$

The time at the end of the blast load (positive phase), t_f, is the time to peak pressure plus the side-on load duration. In the following calculation, the equivalent linear decay duration is used:

$$t_f = t_2 + t_{e,so}$$

$$= 77.9 \, \text{ms} + 19.1 \, \text{ms}$$

$$= 97.0 \text{ ms}$$

Frame Loads

To establish the lateral response of the framing system, blast loads on the front wall and on the rear wall may be computed separately to get the net combined load. The time of arrival of the loads to the walls must be taken into account. The results from the computation of the loading for the frame along gridline B are shown in Figure 2-23.

The positive phase loading on the front (reflected) wall is often conservatively used alone for design for lateral response rather than the net loading calculation results shown in this example.

Front Wall

The pressure load applied to the front wall is the same as previously computed. Figure 2-21 shows the positive phase pressure load incorporating time of arrival and equivalent linear decay load duration computed by dividing the impulse by the peak pressure.

Rear Wall

The pressure load applied to the rear wall is the side-on pressure applied to the rear wall which was shown in Figure 2-19. The interaction of the pressure loading applied in each face of the frame is shown in Figure 2-22. Figure 2-23 shows the superposition to scale of the blast loads for the front and rear walls, accounting for time phasing. Note that positive pressure for the rear wall is shown as a negative value in the graph because this load is in the opposite direction to that applied to the front wall load.
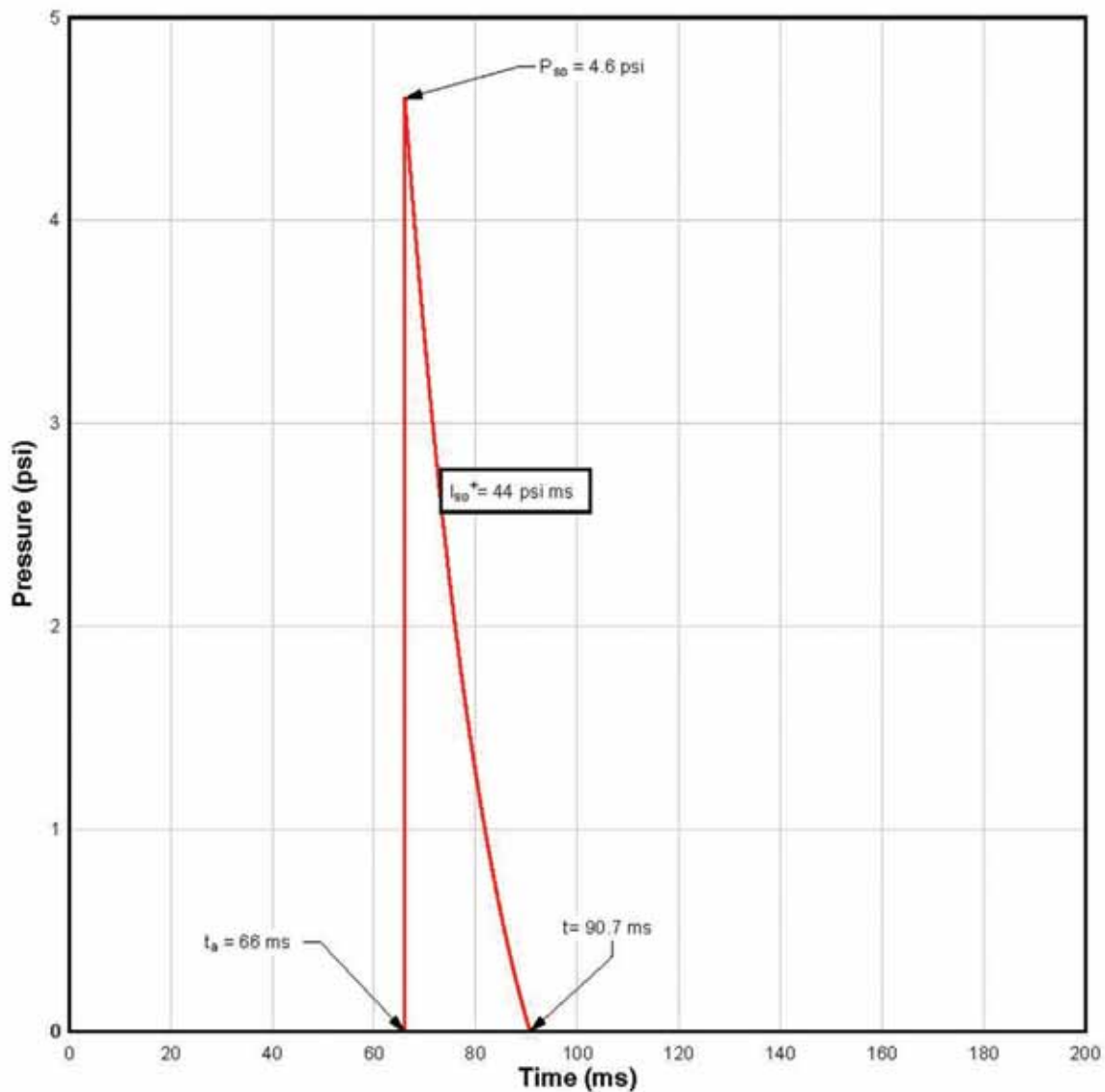
Fig. 2-19. Side-on pressure at top of rear wall.

Summary of Blast Loads

A summary of blast loading ignoring the dynamic pressure and also the negative phase of shock wave is shown in Table 2-1. These positive phase, equivalent loads would typically be used for design. For simplicity, the side load is calculated using the same distance and arrival time as the reflected pressure on the front wall; therefore, the side wall loading shape is similar to the front wall loading shape.

Chapters 5 and 6 will present typical design examples using this information.
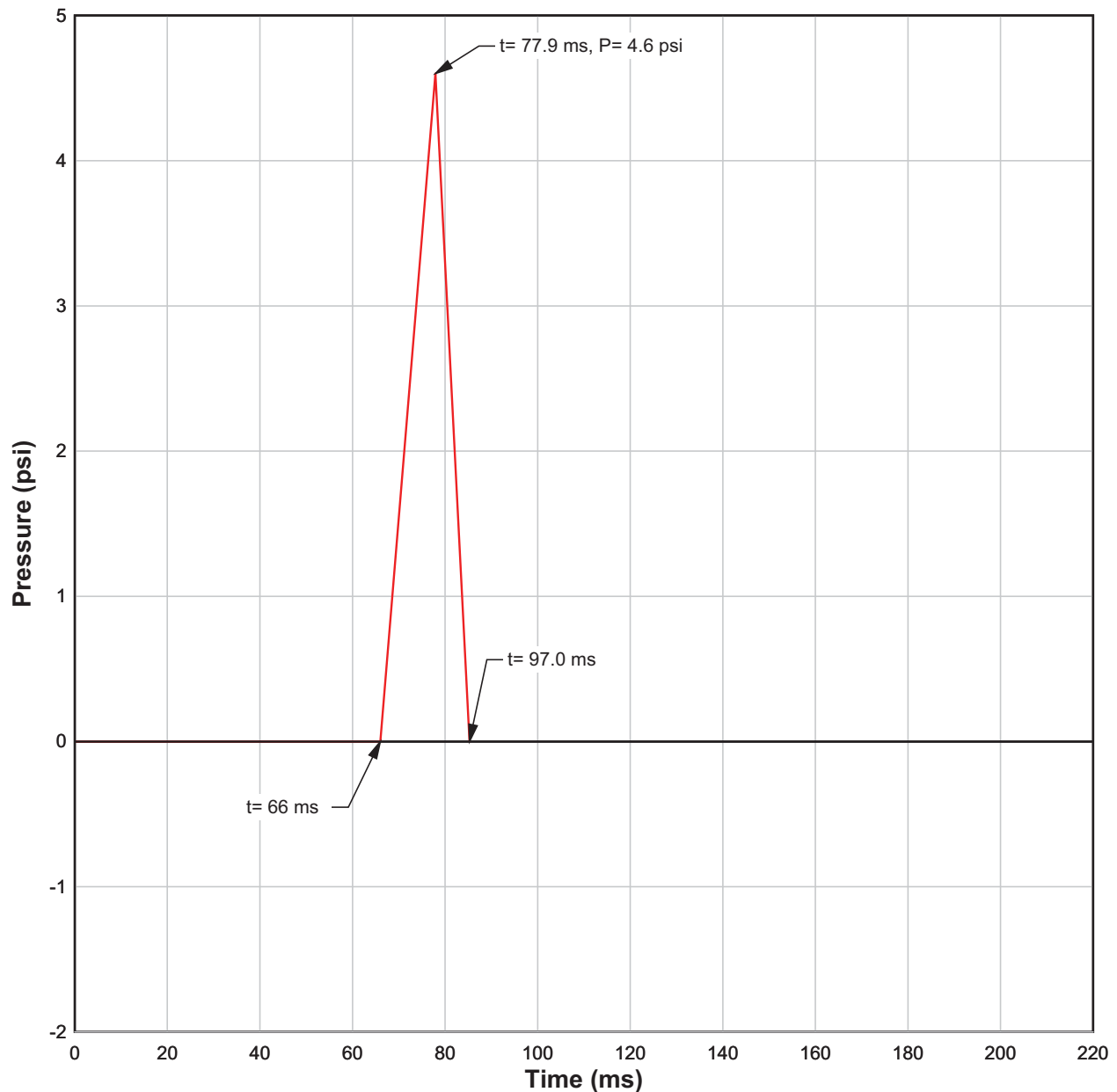
Fig. 2-20. Rear wall load.
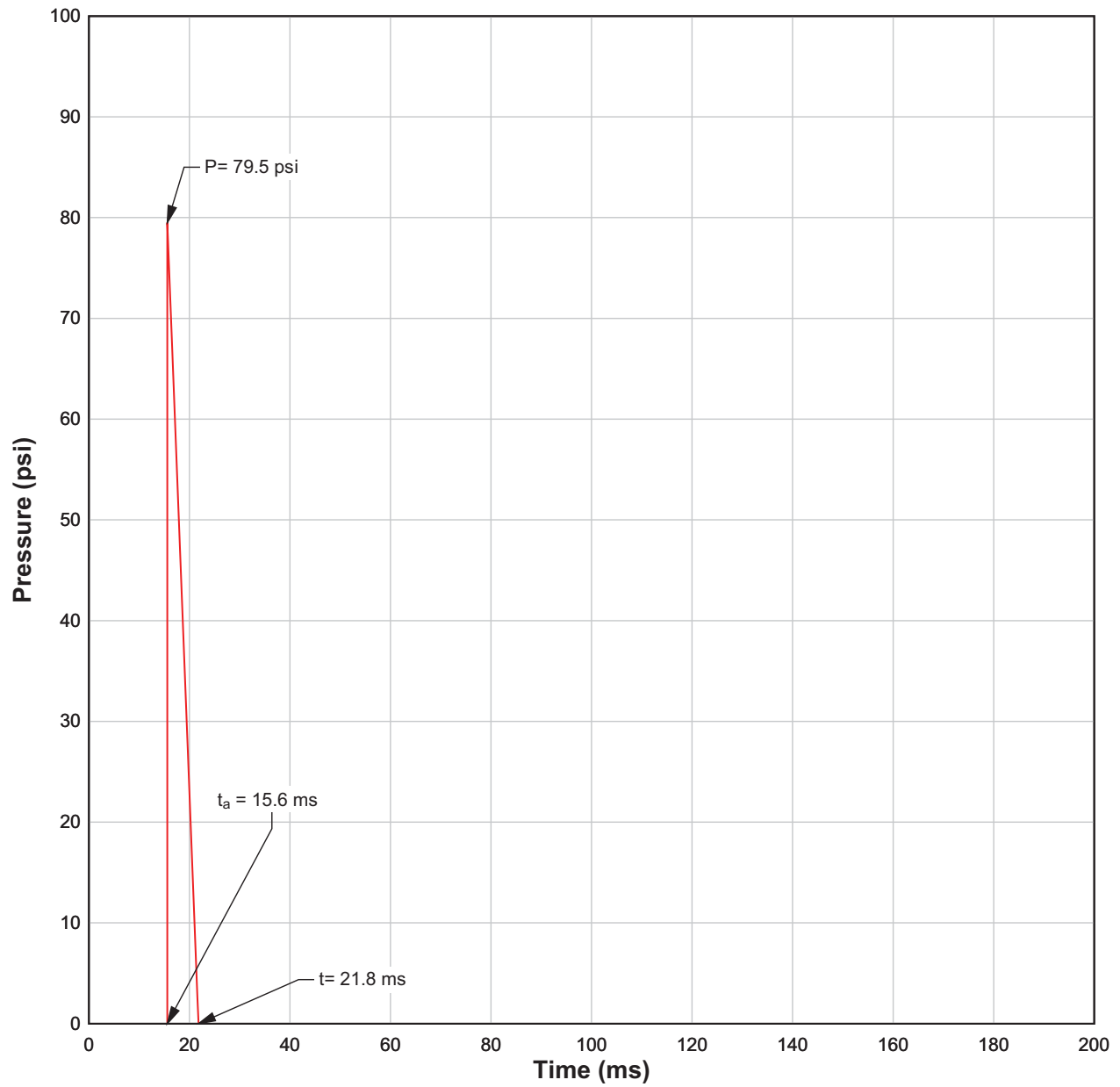
Positive impulse at the front wall:
$I = 246$ psi ms
Negative impulse at the front wall:
$I = 193$ psi ms
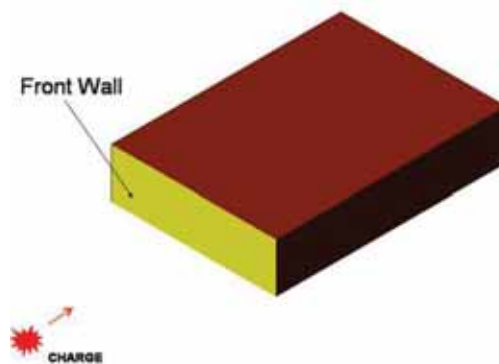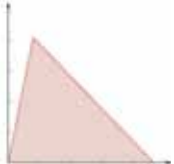
Fig. 2-21. Pressure load for front wall.

Table 2-1. Summary of Blast Loading per Component for W = 500 lb TNT Charge						
Location	Component	Charge Distance, ft	Pressure, P, psi	Impulse, I, psi ms	Equivalent Duration, t_e, ms	Loading Shape
Front wall	Wall panel	50.0	79.5	246	6.19	
Front wall	Girt	50.0	79.5	246	6.19	
Side wall	Wall panel	50.0	24.9	96.0	7.71	
Roof	Purlin	50.0	24.9	96.0	7.71	
Rear wall	Wall panel	120	4.60	44.0	19.1	

Front Wall

Rear Wall

Charge

50ft

70ft

Frame B - Elevation

Direction of pressure applied against wall
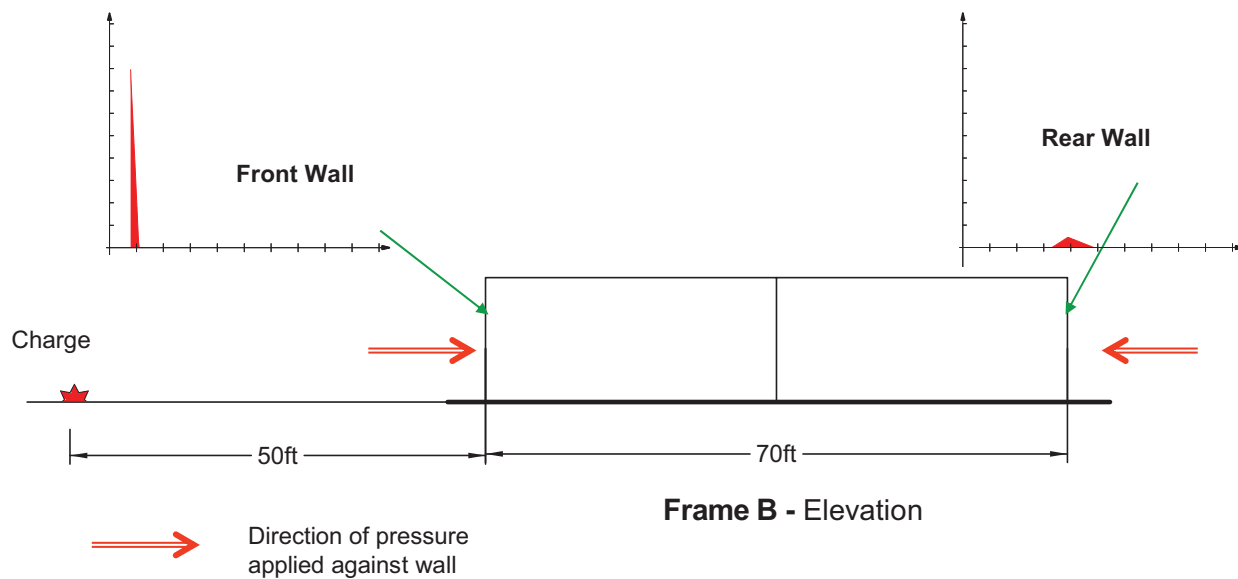
Fig. 2-22. Schematic of loading pressure interaction on Frame B.
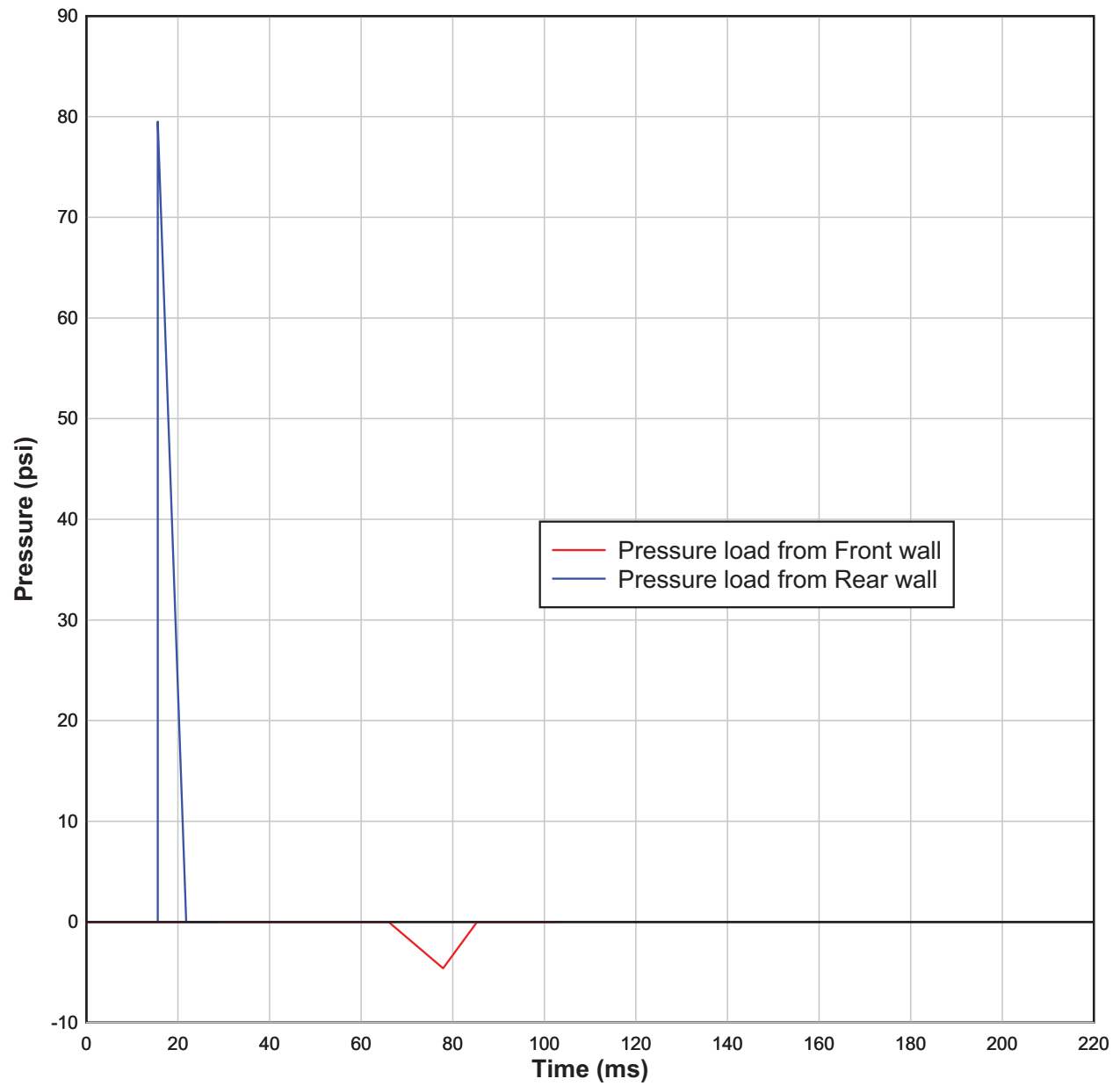
Fig. 2-23. Superposition of pressure loading on Frame B.

Chapter 3
Design Criteria For Buildings

Proper attention to blast design can minimize potential loss from an explosive attack. Protective design can also help to minimize collateral damage stemming from an explosive attack on a nearby building. A number of federal agencies have developed criteria for incorporating protective design into their facilities; there are also a number of general methods that can be used to help protect facilities and their occupants. Attention to the site layout and location of critical building functions can reduce the amount of hardening required. Architects and engineers should be familiar with blast design criteria to minimize the amount of hardening required.

3.1 THREAT ASSESSMENT METHODS

In light of recent terrorist events, much attention has been directed toward protecting the public from explosions. The U.S. Government has been especially active in this area. Several government agencies have conducted research in the areas of blast effects and protective design. A variety of detailed security criteria have been developed and have incorporated much of this research. Several of the most widely used criteria developed for this purpose are described in the following sections.

3.1.1 DOJ Report

In the wake of the 1995 terrorist bombing and progressive collapse of the A.P. Murrah Federal Building in Oklahoma City, the President of the United States responded to the threat of global terrorism by directing the Department of Justice (DOJ) and U.S. Marshals Service to conduct a vulnerability assessment of federal facilities. The resulting report, *Vulnerability Assessment of Federal Facilities,* was issued by the Department of Justice within 60 days of the Oklahoma City bombing (DOJ, 1995). The DOJ Report, as it has become known, was published on June 28, 1995 and consists of classifying federal facilities by five levels of importance which include occupancy and square footage. The DOJ report was the catalyst for development of security criteria in many areas of the federal government. Many refer to the DOJ report as minimum standards; however, they should more appropriately be thought of as general recommendations. In order to actually implement these recommendations, additional criteria are required.

3.1.2 GSA Security Criteria

In response to the DOJ report and subsequent presidential directives (Executive Order 12977 and PDD 39, 62, and 63), and as part of the General Services Administration's (GSA) mission to ensure excellence in development and delivery of public facilities, the GSA developed detailed security criteria (USGSA, 1997). The goal of the GSA criteria was to provide performance-based guidance to designers and to ensure that security became an integral part of the planning, design and construction of new federal facilities and major modernization projects. The *GSA Security Criteria* (USGSA, 1997) covers requirements for blast resistant design and blast hazard mitigation measures in both new construction and the renovation of existing facilities. The *GSA Security Criteria* lists four potential levels of protection: Level A, Level B, Level C and Level D. This document was superseded by the *Security Design Criteria for New Federal Office Buildings and Major Modernization Projects* (ISC, 2004).

3.1.3 ISC Security Design Criteria

The ISC *Security Design Criteria*, developed by the Interagency Security Committee (ISC), was signed and approved by the GSA on May 28, 2001 and was updated on September 29, 2004. The ISC *Security Design Criteria* was developed by revising and updating the *GSA Security Criteria*. The ISC *Security Design Criteria* takes into consideration technology developments, new cost considerations, the experience of practitioners applying the *GSA Security Criteria*, and the need to balance security requirements with public building environments that remain lively, open and accessible. These criteria affect all aspects of security of a facility from operational measures, to site planning, landscaping and exterior approach, to construction types and hardening methods. The intent of the criteria is to reduce (not necessarily eliminate) the potential hazards, recognizing that not all walls and windows will survive a bombing attack, especially in an open public facility.

The ISC document directs users to make security decisions about individual aspects of the design. Tables identifying design issues to be addressed are meant to be completed by a team that includes users, security professionals and budget representation. The ISC states that a "blast engineer must be included as a member of the design team if a blast analysis is required."

The ISC *Security Design Criteria* lists four possible levels of protection: Minimal, Low, Medium and High. These levels correspond to the four levels discussed in the *GSA Security Criteria*. Minimal and Low Levels of Protection are typically used for small facilities with a very low potential for attack. For these two levels of protection, few true requirements are listed, but prudent measures to reduce the risk of injury and death are discussed and encouraged. A Medium Level of Protection is generally provided for larger, more visible facilities and a High Level of Protection is generally applied to facilities that are considered more likely to be targeted or that provide unique services. For federal buildings, the ISC states that the level of protection should be applied to each element and sub-element. Thus the designer may or may not apply a single level of protection to the entire facility for each type of threat discussed (e.g., low ballistic protection with medium blast protection).

A Medium or High Level of Protection requires the facility to have a defended site perimeter capable of stopping a defined moving vehicular threat. In addition, the facility should be hardened to prevent failure of the primary structural members for a defined threat located at the site perimeter and a set of internal threats located in the mailroom, loading dock, parking garage, and any uncontrolled public areas. The threat vehicle size/speed, explosive device size, and maximum design load for a High Level of Protection is larger than that required for a Medium Level of Protection.

The exterior walls and windows for a Medium Level of Protection and the windows for a High Level of Protection should be hardened for the defined threats up to a maximum design load listed in the criteria. This approach allows for hazardous nonstructural damage in areas close to the explosive device, but attempts to limit the amount of collateral damage. The walls and frame for the High Level of Protection should be designed for actual loads.

Balanced design is discussed in the ISC *Security Design Criteria* and considers the load path. The goal is to ensure that each supporting element does not fail due to the reaction of the element it supports. Thus, joists supporting a roof deck would be designed to support the capacity of the deck and the girders would support the capacity of the joists. Balanced design enhances the structural behavior in response to a blast event as it follows the load path through the entire structure.

To achieve a Medium or High Level of Protection, the facility should also be designed to resist progressive collapse depending on factors that include the function of the facility and the value of the construction. The ISC *Security Design Criteria* refers the user to the GSA's *Progressive Collapse Analysis and Design Guidelines for New Federal Office Buildings and Major Modernization Projects* (USGSA, 2003) and *Minimum Design Loads for Buildings and Other Structures* (ASCE, 1995).

In 2008 and 2010, ISC released three new ISC Standards that have replaced the 2004 ISC *Security Design Criteria.* These three documents are *Facility Security Level Determinations*, February 21, 2008 (ISC, 2008); *Design-Basis Threat*, April 2012 (ISC, 2012); and *Physical Security Criteria for Federal Facilities*, April 12, 2010 (ISC, 2010). These new ISC criteria represent a significant evolution of the 2004 ISC *Security Design Criteria*.

3.1.4 Unified Facilities Criteria

The Unified Facilities Criteria (UFC) *Minimum Antiterrorism Standards for Buildings*, UFC 4-010-01, was initially released on October 8, 2003, with an update on January 22, 2007 (DOD, 2007). The intent of these standards is to minimize the possibility of mass casualties in buildings or portions of buildings owned, leased, privatized, or otherwise occupied, managed, or controlled by or for the Department of Defense (DOD). These standards provide appropriate, executable and enforceable measures to establish a level of protection against terrorist attacks for all inhabited DOD buildings where no known threat of terrorist activity currently exists. Facilities with known threats should develop additional site specific requirements. The Unified Facilities Criteria provides a recommended standoff distance for facilities from the site perimeter, from any onsite roadways and parking, and from other facilities. Assuming these standoff distances are met, the criteria allow for standard construction methods with a few prescriptive requirements. This document provides minimum standoff distances and design threats, benefitting from testing performed by the DOD. Clear descriptions of structural behavior are linked to specific rotation criteria. These standards also require the mitigation of progressive collapse which includes minimum uplift requirements on all slabs. UFC 4-010-01 was revised and released on February 9, 2012, with significant changes from the previous version (DOD, 2012).

The DOD establishes progressive collapse criteria in its publication, *Design of Buildings to Resist Progressive Collapse* (DOD, 2010). This document has been released to the public and is available from the National Institute of Building Sciences at www.wbdg.org.

3.1.5 Department of State Criteria

The Department of State (DOS) has also developed a set of requirements for their overseas facilities. These requirements offer a much higher level of protection than is typically used for facilities located in this country. Instead of an approach designed to limit the extent of damage like the GSA, ISC and UFC, the DOS standards call for a facility that has been fully hardened for a large credible device. As a result, these facilities are expensive to build and their exterior appearance is affected by the hardening measures. A facility constructed in

a manner consistent with the DOS criteria should be capable of quick recovery after a design level blast event.

3.1.6 Additional Criteria

Several other organizations have also developed their own independent criteria. While some criteria, such as Federal Aviation Administration (FAA) Order 1600.69B, provide protective design guidelines/criteria for use in FAA facilities, other criteria, such as the Transportation Security Administration's Bomb Incident Protection Plan (BIPP), outline the use of blast envelopes.

A useful starting point for addressing blast and progressive collapse issues is the AISC *Facts for Steel Buildings: Blast and Progressive Collapse* (Marchand and Alfawakhiri, 2005). The development of guides abroad is reflected, among others, in the British Standards (BSI, 1996) and the Eurocodes (CEN, 2006a) and the recently released standard ASCE/SEI 59-11, *Blast Protection of Buildings* (ASCE, 2011).

Additional sources of information can be found on the website of the National Institute of Building Sciences: Whole Building Design Guide (www.wbdg.org), where FEMA, DOD, GSA and other references can be downloaded, and on the website of the Health and Safety Executive (www.hse.gov.uk). The Federal Emergency Management Agency has published a series of documents related to blast and progressive collapse: FEMA 426, *Reference Manual to Mitigate Potential Terrorist Attacks Against Buildings* (FEMA, 2003a); FEMA 427, *Primer for Design of Commercial Buildings to Mitigate Terrorist Attacks* (FEMA, 2003b); and FEMA 452, *Risk Assessment: A How-To Guide to Mitigate Potential Terrorist Attacks* (FEMA, 2005). In blast design, an important reference is the publication of the Department of Defense UFC 3-340-02, *Structures to Resist the Effects of Accidental Explosions* (DOD, 2008), available at www.wbdg.org.

3.2 GOOD PRACTICE

Although a variety of existing criteria are currently used throughout the country, they all share recurring general themes that can be applied to improving the protective design of most any facility. The level of protective design will vary from facility to facility depending upon the uniqueness, function, architectural features, and level of protection selected for each facility.

The general methods of improving site and facility security and survivability can vary greatly depending upon the particular asset, the design criteria applied to that asset category, and the constraints of the project. Improved survivability and protection from blast can be achieved by a variety of means, such as:

- Provide as much standoff distance as practically possible since the effects of an explosion diminish rapidly with distance. Normally, no less than 20 ft should ever be acceptable for vehicular threats. Collapse is likely for a facility this close to a large explosive device.

- Selectively use terrain features to maintain standoff distance and in effect reducing the effect of the blast.

- Ensure good quality construction, which has some inherent resistance to abnormal loadings. For example, details such as structural connection design can greatly affect blast resistance.

- Use structural hardening and ductile detailing to increase the resistance against high levels of load.

- Provide system and location redundancy so that the entire operation is not at risk to an attack on a single critical area.

- Use operational security to enforce the standoff, reduce the risk of an event occurring, or to mitigate the consequences. Operational security can be improved through awareness, response and readiness training. Security and emergency response personnel should have adequate emergency procedures, communication and response equipment with a regular verification program in place.

- Employ full-scale arena explosive testing to qualify performance under blast loads in lieu of blast design calculations. All explosive testing should be performed by a qualified test provider. Qualification is typically recognized as having experience in conducting such tests for the military, U.S. government agencies, or similar experience.

- Design for blast should be done with the help of a qualified blast consultant. Qualification typically is recognized as experience in the design of blast resistant structures, typically for military or government agencies, as there is little guidance in the private sector.

3.2.1 Exterior Considerations

There are a number of exterior considerations that should be addressed. These are focused on explosive threats delivered outside of the building envelope and include:

- Perimeter protection (defended standoff distance, vehicle barriers, and surveillance)

- Structural response (walls, roof, frame and foundation)

- Progressive collapse (local and global)

- Windows (glazing, frames and anchorage)
- Fragments (primary and secondary)

3.2.2 Interior Considerations

Interior considerations are focused on explosive threats delivered inside of the building envelope and include:

- Threat location (mail room, loading dock, underground parking, and uncontrolled areas)

- Structural response (walls, slab and framing adjacent to affected areas)
- Progressive collapse (local and global)
- Proximity to critical systems and occupied space
- Damage due to fragments, fire and smoke

Chapter 4
Structural Response to Blast Loads

This chapter presents a brief introduction to structural dynamics with emphasis on particular strategies currently used in blast resistant design. References of particular note due to their importance in guiding the practices of contemporary blast design are the works of John M. Biggs in *Introduction to Structural Dynamics* (Biggs, 1964) and Charles H. Norris et al. in *Structural Design for Dynamic Loads* (Norris et al., 1959). Several other general references on structural dynamics may be useful, including Chopra (1980), Clough and Penzien (1993), and Hurty and Rubenstein (1964).

A blast creates two important and distinct effects that are important to structures. The first of these is known as *brisance*. Brisance is the shattering effect of an explosion on objects that are in direct proximity to the source of the explosion and can occur only where the energy from the explosion is sufficiently concentrated. The effect of brisance depends on the size of the weapon, type of explosive, distance to the target, geometry of the target, construction quality, and materials. Brisance is the effect relied upon in explosive demolition and can be used to damage critical structural load-carrying elements. Analysis for the brisance effect, frequently referred to as breeching, is most commonly based on experimental data available through U.S. Army publications and other sources. Protection against brisance is generally provided in several forms. These include employing security measures intended to prevent explosive sources from being placed in direct proximity to key load-carrying structural elements, constructing structural elements with sufficient robustness to resist the brisance effects of anticipated charges, and designing structures with sufficient robustness to safely redistribute loads from destroyed elements while resisting the development of unacceptable propagation of collapse. Chapter 8 of this Design Guide addresses the latter of these three design approaches—resistance to progressive collapse.

This chapter addresses the second effect of blasts, the response of structures to blast pressure waves. This second important effect occurs when blasts are at sufficiently large distances from a structure or element making brisance unlikely. Similar to wind loads, these pressure waves produce forces normal to the surface of all exposed structural elements. Depending on the size of the explosion, its distance from the exposed surface, and the presence, position and geometry of reflecting surfaces, the pressures induced by explosions on exposed surfaces of a structure can be several orders of magnitude larger than typical wind loads, and well in excess of typical design loads for most buildings. Because of the magnitude of these forces, most structures subjected to blast loading will experience significant inelastic behavior. The acceptability of structural response is judged based on the flexure and shear induced in the elements. Flexure is generally a ductile mode of behavior, and many elements are capable of exhibiting significant inelastic flexural behavior. Acceptability is measured in terms of rotations induced at supports and other points of hinging and the amount of ductility the element can sustain. Most structures do not generally have the ability to exhibit significant inelastic behavior, and some inelastic failure tends to be brittle, resulting in sudden failure. Generally, structures designed for blast resistance are designed to undergo ductile flexural behavior.

Also, because explosion-induced pressures can cause failure of exterior building elements, these pressures may act on interior building elements as well. Fortunately, except in the case of unvented internal explosions, the duration of these pressure waves tends to be very brief—on the order of a few hundredths to several tenths of a second. As a result, loading on structural elements often dissipates to low levels before the typical structural element can fully respond to the loading so that the effective forces and deformations experienced by the element are much smaller than those that would occur if the pressure loading were applied statically. Analysis of these effects requires consideration of the dynamic characteristics—both of the pressure loading and of the exposed structure itself. Analysis of the pressure loading effects is described in Chapter 2 and the structural response is described in this chapter.

Structural response to short duration loading is a function of the natural period of response of the structural system, which depends on the mass and stiffness of the structure, and the magnitude and duration of the loading function. Generally, if the natural period of vibration of a structural element is much larger than the duration of the load, the response of the structure will be impulse-controlled and the effective forces imparted to the structure will be much less than the peak force. On the other hand, if the natural period of vibration of the structural element is similar to or shorter than the pulse duration, effective forces can approach or exceed the peak force. Since the natural period of vibration of most structural elements tends to be larger than the duration of typical blast loads, the addition of mass to a structure can often be an effective design strategy as it can result in lengthening of the element's natural period of vibration and a reduction in the effective forces experienced by the element. Strengthening and stiffening a structure is often an

unproductive strategy because it can result in a reduction in the element's natural period of vibration, increasing the effective forces the element must resist.

Because most structures must rely on inelastic behavior to resist the large loadings produced by blasts, ductility is an important structural property for blast resistant structures. Ductility is a measure of how far beyond the elastic range of behavior the response of the structural element can be taken before loss of load-carrying capability will occur. It is calculated as the ratio of the maximum deflection, including both elastic and plastic behavior, to the maximum elastic deflection. If an element remains elastic, it will return to its original position once it is unloaded. When deflections exceed the elastic range, residual plastic deformation will remain in the member after unloading. Steel is a ductile material that exhibits a predictable elastic-plastic behavior with a well-defined inelastic range of behavior.

4.1 REPRESENTATION OF BLAST LOADING

Section 2.3 describes the pressure waves generated by a blast. A surface that is exposed to such a pressure wave will first experience a large positive pressure as the zone of increased pressure passes the surface, followed by a negative pressure as the zone of suction behind the wave front passes. The duration of the positive pressure loading against the surface tends to be very short—on the order of a few hundredths of milliseconds to a few tens of milliseconds. The duration of the negative phase tends to be somewhat longer, but generally has greatly reduced intensity. The magnitude of the peak positive and negative pressures experienced and the duration of each phase of loading depends primarily on the energy released by the blast and the distance of the exposed surface from the blast source. Other factors that can significantly affect the characteristics of this pressure loading include the presence of reflecting surfaces in the vicinity of the blast or the surface, and the angle of incidence of the wave front on the surface. Chapter 2 provides information on methods for calculating these pressures, their duration, and their travel velocity as functions of these factors.
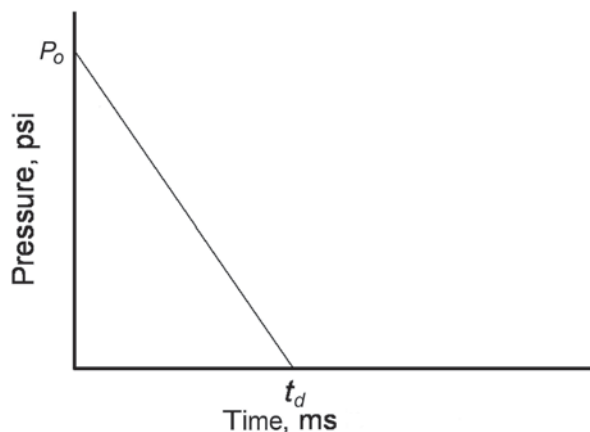
For many applications, it is possible to represent the blast loading on a building in the form of an equivalent triangular load acting normal to the exposed surfaces having a peak pressure, P_o, and a duration, t_d. Figure 4-1 illustrates the time-pressure characteristics of such a load, similar to those shown in Chapter 2. Loading functions of this type are commonly used to evaluate the response of elements that are directly loaded by the blast pressure wave. The loading experienced by secondary elements that are not directly exposed to the blast pressure wave (providing support to elements that are directly exposed to the wave) is more correctly represented by a triangular pulse with separate build-up and tail-down phases, as illustrated in Figure 4-2 and in Chapter 2. The duration and magnitude of the pulse in this type of loading will be a function of the characteristics of the blast pressure wave and of the dynamic properties and strength of the primary elements loaded by the pressure wave.

Regardless of which form of load function is used, the total applied load can be represented as an impulse, I, given by the equation:

$$I = \frac{P_o t_d}{2} A \qquad (4\text{-}1)$$

where

P_o = peak pressure
t_d = load duration
A = surface area exposed to the pressure wave

4.2 SINGLE DEGREE OF FREEDOM SYSTEMS

The response of many structures and elements of structures to blast loading can be adequately evaluated by treating the

Fig. 4-1. Typical triangular loading function used to represent blast pressure loading on structures.
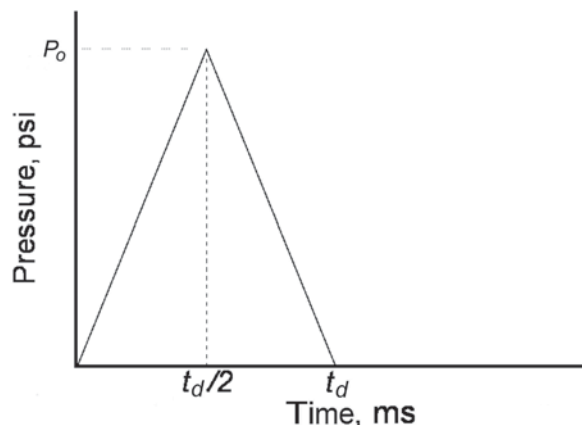
Fig. 4-2. Triangular load function with separate build-up and tail-down phases.

structure as an equivalent single degree of freedom (SDOF) system. SDOF systems are characterized by having all of their mass, m, concentrated at a single point, which is constrained to move along a single axis, x. In classical structural dynamics, resistance to movement of the mass is provided by the stiffness of the structure, K, and by viscous damping, c. A detailed discussion of the dynamic behavior of SDOF systems is beyond the scope of this Design Guide. An extended explanation of the response of single degree of freedom can be found in Biggs (1964) as well as many other texts on structural dynamics.

The equation of motion for an SDOF structure undergoing free vibration is:

$$mx''(t) + cx'(t) + Kx(t) = 0 \qquad (4\text{-}2)$$

where
- $x(t)$ = displacement of the structure, at any time t, relative to its at-rest position
- $x'(t)$ = velocity at time t
- $x''(t)$ = acceleration at time t
- m = mass of the structure
- c = viscous damping
- K = structure stiffness

Solution of this equation for the condition when the structure is displaced to an arbitrary displacement, x_o, and released is given by:

$$x(t) = x_o e^{\frac{-c}{2m}t}\left(\frac{c}{2m\omega_d}\sin\omega_d t + \cos\omega_d t\right) \qquad (4\text{-}3)$$

where
- ω_d = damped natural frequency for the structure, in units of radians per unit of time

$$= \sqrt{\frac{K}{m} - \frac{c^2}{4m^2}} \qquad (4\text{-}4)$$

For most structures, the effect of damping on natural frequency is negligibly small and the damped natural frequency is closely approximated by the undamped natural frequency, given by:

$$\omega = \sqrt{\frac{K}{m}} \qquad (4\text{-}5)$$

This is more commonly expressed in the form of cyclic frequency, f, in units of cycles per second or Hz, where f is given by:

$$f = \frac{1}{2\pi}\sqrt{\frac{K}{m}} \qquad (4\text{-}6)$$

Rather than using natural frequency to characterize dynamic structural behavior, structural engineers often find it more convenient to use the inverse, known as the structural natural period, T. The period represents the time, in seconds, required for a structure in free vibration to undergo one complete cycle of motion and is given by:

$$T = \frac{1}{f} = 2\pi\sqrt{\frac{m}{K}} \qquad (4\text{-}7)$$

Structural damping is often expressed as a fraction of the critical damping of the structure, c_c. The critical damping, c_c, for an SDOF structure is the minimum amount of damping that is sufficient to completely prevent free vibration, when a structure is displaced and then released. It is given by:

$$c_c = \sqrt{4Km} \qquad (4\text{-}8)$$

Most real structures have finite damping that is substantially less than the critical damping. The effects of damping on peak structural response to blast is typically small due to the short duration of the loading and it is generally neglected. However, if damping is used in blast analyses, it should not be taken as greater than 2% of the critical value for the structure.

4.3 BLAST RESPONSE OF ELASTIC SINGLE DEGREE OF FREEDOM SYSTEMS

For design purposes, engineers are usually interested in predicting the peak forces and displacements experienced by a structure when subjected to blast loading. There are three primary methods of estimating the peak blast response of a structure: time-history analysis, graphical methods, and energy techniques. Each of these is described in the following.

4.3.1 Time-History Analysis

The most direct way of determining the response of a structure to a dynamic load function is time-history analysis. Time-history analysis consists of a numerical integration of the equation of motion for the structure, subjected to a time varying forcing function, $f(t)$. In this form, the equation of motion becomes:

$$mx''(t) + cx'(t) + Kx(t) = f(t) \qquad (4\text{-}9)$$

This single degree of freedom equation can be solved by numerical integration, sometimes performed using a spreadsheet program and algorithms available in a number of texts on structural dynamics, such as Wang (1967). More commonly, any of several structural analysis software programs can be used to perform this analysis directly. Regardless, it is important to select an appropriate time increment over which the integration is performed. The time increment needs to be short enough to provide an accurate solution yet long enough

to lead to an efficient solution. As a rule of thumb, the time increment used to solve the equation of motion should not be larger than $^1/_{10}$ of the pulse duration, t_d, or $^1/_{20}$ of the natural period of the structure, T. The key results to be obtained from the analysis are the peak structural displacement and resisting force. The timing of these peak response quantities varies as a function of the structure's natural period, T, and the duration of the positive loading, t_d. If the period of the structure is greater than twice the pulse duration, the analysis need only be continued through a duration equal to one-half the structural period, as this will be sufficient to capture the peak response. When the structural period is shorter than this, the integration should be continued for several cycles (at least one full cycle beyond the load duration) to ensure that the peak response has been determined.

4.3.2 Graphical Solution

Many researchers have developed solutions for the peak response of SDOF structures of varying structural periods to impulsive loading of varying shapes and duration. These solutions have been plotted for reference to obtain a quick relationship between the dynamic characteristics and the peak response quantities of the structure to the load. One of the first publications of plots of this type was in a U.S. Army Corps of Engineers technical manual, *Design of Structures to Resist the Effects of Atomic Weapons* (USACE, 1957). Figure 4-3 is a plot of the elastic response of single degree of freedom structures to the simple triangular loading of Figure 4-1. To use this figure, first compute the ratio of the period of the structure, T, to the load duration, t_d. Enter the figure with this ratio and read across to obtain a dynamic load factor, or *DLF*. The *DLF* is the ratio of the peak displacement experienced by the structure in response to the impulsive loading to the peak displacement that the structure would experience if the peak loading were applied statically. For elastic structures, the *DLF* also provides the ratio of the peak dynamic stress developed in the structure to the static stress. Figure 4-4 is a similar *DLF* diagram plotted for the case of the triangular impulsive loading of Figure 4-2. It should be noted that the maximum dynamic load factor for the load shape in Figure 4-1 is 2.0 and the load factor for the load shape in Figure 4-2 is slightly greater than 1.5.
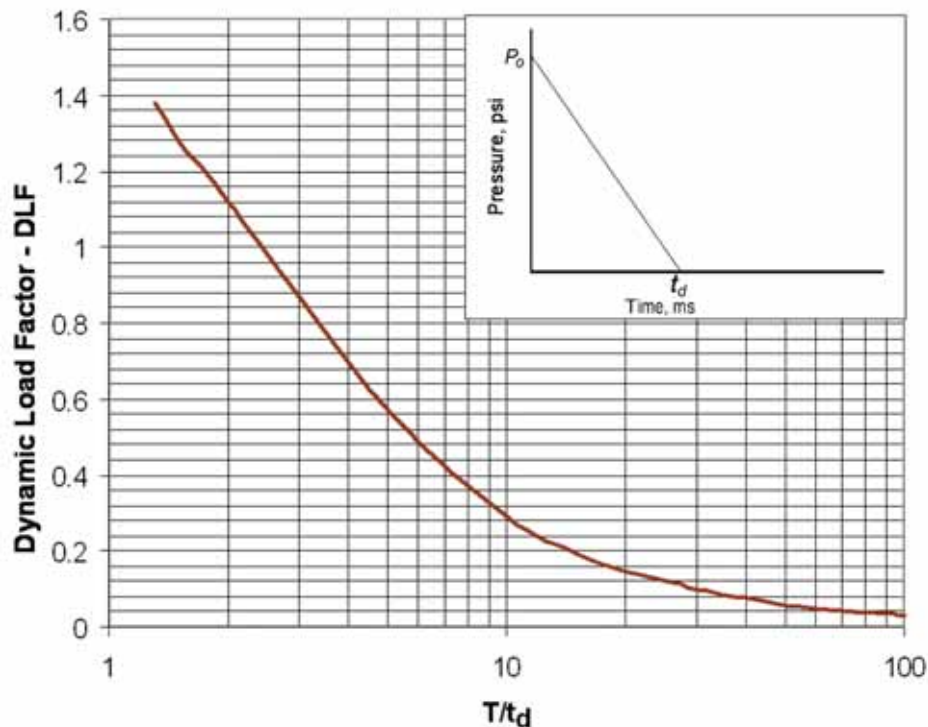
Fig. 4-3. Dynamic load factor and triangular impulse loading for elastic response.

Example 4.1—Determination of the Peak Dynamic Force and Displacement

Given:

Consider a structure with a stiffness of 1,000 kip/in. and a natural period of vibration of 0.5 s. It is subjected to a simple triangular impulsive loading, like that of Figure 4-1, with a peak force on the structure of 10,000 kips and a duration, t_d, of 0.05 s. Using Figure 4-3 or Figure 4-4, as appropriate, determine the peak displacement and force in the structure.

Solution:

Step 1: Compute the force and displacement under statically applied peak loading:

$$F_{static} = 10,000 \text{ kips}$$

$$\Delta_{static} = \frac{F_{static}}{K}$$

$$= \frac{10,000 \text{ kips}}{1,000 \text{ kip/in.}}$$

$$= 10.0 \text{ in.}$$

Step 2: Compute the ratio of structural period, T, to pulse duration, t_d:

$$\frac{T}{t_d} = \frac{0.5 \text{ s}}{0.05 \text{ s}}$$

$$= 10$$

Step 3: Enter Figure 4-3 for the pulse of Figure 4-1 with $T/t_d = 10$, the DLF is:
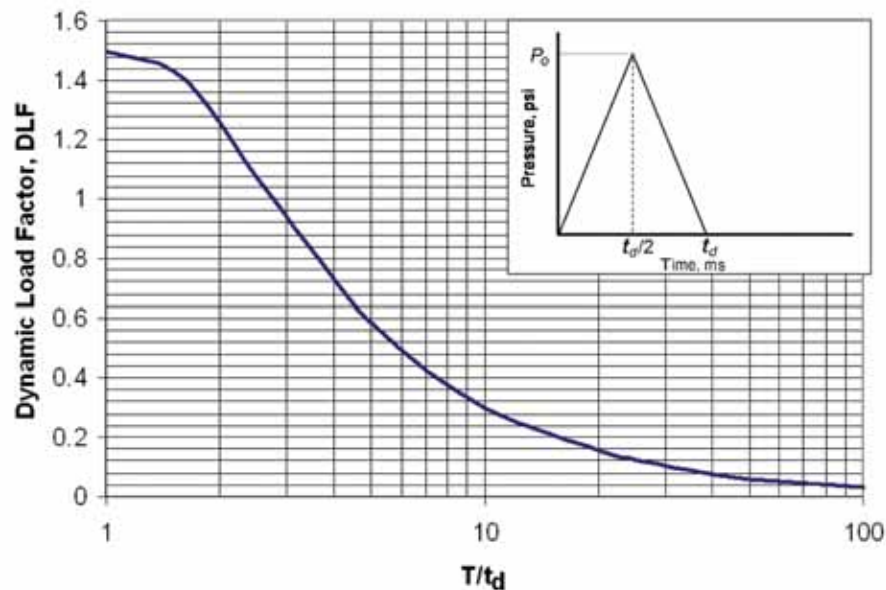
$$DLF = 0.280$$

Fig. 4-4. Dynamic load factor, triangular impulse loading, loading and unloading phases for elastic response.

Step 4: Find the peak dynamic force and displacements:

$$F_{dynamic} = DLF(F_{static})$$
$$= 0.280(10{,}000 \text{ kips})$$
$$= 2{,}800 \text{ kips}$$
$$\Delta_{dynamic} = DLF(\Delta_{static})$$
$$= 0.280(10.0 \text{ in.})$$
$$= 2.80 \text{ in.}$$

4.3.3 Energy Solution

If the duration of the load is short relative to the period of response of the structure, energy methods can be used to approximately determine the peak response of the structure based solely on the impulse of the load.

In this approach, outlined in Biggs (1964), the load is assumed to be essentially instantaneous in nature and to impart an initial velocity to the mass of the structure. The initial velocity, v_i, is given by the impulse momentum law as:

$$v_i = \frac{I}{m} \qquad (4\text{-}10)$$

where

I = impulse, found from Equation 4-1
m = mass of the structure

The velocity imparted to the structure by the impulse provides it with kinetic energy (W_K). As the mass moves away from its at-rest position, it will strain the structure, dissipating the kinetic energy into stored strain energy ($W_{S,el}$). When the stored strain energy identically equals the imparted kinetic energy, the structure will have reached its maximum response. This condition is solved as follows:

$$W_{S,el} = W_K$$
$$\frac{Kx_{max}^2}{2} = \frac{mv_i^2}{2}$$
$$x_{max} = \sqrt{\frac{m}{K}}v_i = \frac{I}{\sqrt{Km}} \qquad (4\text{-}11)$$
$$F_{max} = Kx_{max} = \sqrt{\frac{K}{m}}I \qquad (4\text{-}12)$$

where, x_{max} and F_{max} are, respectively, the peak displacement and resisting force in the structure. This energy solution is not exact, as it neglects the initial movement of the structure while the impulse is being applied. For structures in which the ratio of the structural period to the load duration is greater than about 10, this effect is negligible, and the energy solution is sufficiently accurate.

4.4 ANALYSIS OF NONLINEAR SINGLE DEGREE OF FREEDOM RESPONSE

All of the analysis procedures discussed in Section 4.3 presume that the structure is strong enough to remain elastic. Most real structures are not designed with sufficient strength to behave in this manner. Such structures will yield and experience inelastic straining. The ability of a structure to undergo inelastic straining is typically gauged by the ductility, μ, equal to the ratio of the peak displacement under load, Δ_{max}, to the displacement at yield, Δ_{yield}, given by:

$$\mu = \frac{\Delta_{max}}{\Delta_{yield}} \qquad (4\text{-}13)$$

The effect of inelastic straining is that for a given displacement, Δ, that is greater than the yield displacement, Δ_{yield}, the amount of strain energy stored will be less than if the structure remained elastic. This is illustrated in Figure 4-5, which shows the force-displacement diagram for two structures that are strained to the same deflection, Δ_{max}. Figure 4-5(a) illustrates the force-displacement response of a structure that remains elastic and Figure 4-5(b) illustrates the force-displacement response of a structure that yields at an applied force, F_{yield}, before the maximum displacement is reached.

The strain energy that accumulates in the structure is the area under the force-displacement plot. For an elastic structure, the strain energy is:

$$W_{S,el} = \frac{F_{max}\Delta_{max}}{2} = \frac{K\Delta_{max}^2}{2} \qquad (4\text{-}14)$$

The strain energy that accumulates in the inelastic structure is:

$$W_{S,inelastic} = \frac{F_{yield}\Delta_{yield}}{2} + F_{yield}(\Delta_{max} - \Delta)$$
$$= F_{yield}\Delta_{yield}(\mu - 1/2) \qquad (4\text{-}15)$$

Substituting $F_{yield} = K\Delta_{yield}$ and $K\Delta_{max}^2/2 = W_{S,el}$ into Equation 4-15, and rearranging, it can be shown that at maximum displacement, Δ_{max}, the strain energy stored by the elastic-plastic structure is related to the strain energy stored by the elastic structure as follows:

$$W_{S,elastic\text{-}plastic} = W_{S,el}\frac{2(\mu - 1/2)}{\mu^2} \qquad (4\text{-}16)$$

At a ductility of 2, the elastic-plastic structure will store only 75% of the strain energy stored by the elastic structure. At a ductility of 4, the elastic-plastic structure will store only 44% of the strain energy stored by an elastic structure. Therefore,

in order to arrest the motion imparted to a structure by an impulse, a structure that yields under impulsive loading must move a greater distance than one that does not yield.

As with elastic, single degree of freedom response, there are three methods of solving for the maximum displacement of an inelastic structure subjected to impulsive loading: time-history methods, graphical solutions, and energy solutions. These are described in the following.

4.4.1 Time-History Methods

Time-history methods used for inelastic structures are similar to those previously described for elastic structures. The primary difference is that for inelastic structures, the structural stiffness, K, in the equation of motion, rather than being constant, is a function of the displacement history of the structure. Usually, an elastic-plastic representation of the stiffness is used. As with elastic solutions, either spreadsheets or structural analysis software can be used to solve the equation of motion using numerical integration. Because an inelastic structure will take longer to reach its maximum displacement than an elastic structure, it will be necessary to continue the integration for a longer duration than if the structure remained elastic. When the elastic period of the structure is at least double the pulse duration, the integration

should be carried out for a duration that is at least equal to the elastic period of the structure, T. When the period of the structure is less than twice the pulse duration, the integration should be continued for several cycles (and at least one full cycle after the load dissipates) to verify that the maximum response has been found.

4.4.2 Graphical Solutions

Just as researchers have represented the results of many analyses of elastic structures in graphical form, similar graphs have been developed to represent the results of inelastic behavior on maximum displacement demand. Figure 4-6 presents such a plot. In the figure, the strength ratio, SR, is given by:

$$SR = \frac{F_{max}}{F_{yield}} \qquad (4\text{-}17)$$

where
F_{max} = maximum resisting force the structure would experience if it were capable of remaining elastic, obtained using the DLF of Figure 4-3 or Figure 4-4, kips
F_{yield} = force that would cause the structure to yield, kips

Example 4.2—Determination of Ductility Demand

Given:

Determine the ductility demand for the structure of Example 4.1 if F_{yield} is 1,400 kips. From Example 4.1, the structure has a stiffness of 1,000 kip/in. and a natural period of vibration of 0.5 s. It is subjected to a simple triangular impulsive loading, like that of Figure 4-1, with a peak force on the structure of 10,000 kips and a duration, t_d, of 0.05 s. Find the peak displacement and force in the structure, as well as the strength ratio and ductility demand.

Solution:

Step 1: Find the displacement and force in the structure if it remains elastic. Referring to Example 4.1, the maximum force for elastic response is $F_{max} = 2,800$ kips and the maximum displacement for elastic response is $\Delta_{max} = 2.80$ in.

(a) Elastic   *(b) Elastic-plastic*
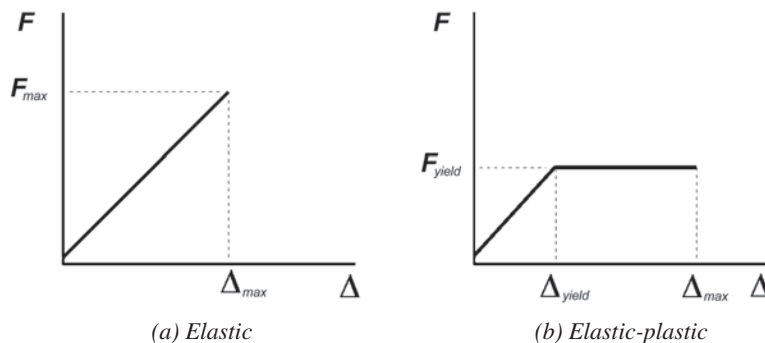
Fig. 4-5. Force-displacement diagram for (a) elastic response and (b) elastic-plastic response.

Step 2: Determine the strength ratio:

$$SR = \frac{F_{max}}{F_{yield}} \tag{4-17}$$

$$= \frac{2,800 \text{ kips}}{1,400 \text{ kips}}$$

$$= 2.00$$

Step 3: Find the ductility demand from Figure 4-6, at a strength ratio of 2.0:

$$\mu \approx 2.50$$

4.4.3 Energy Methods

Energy methods for nonlinear structures are similar to those for linear structures. However, the term for strain energy is modified to account for the nonlinear behavior. Assuming elastic-plastic behavior, the ductility demand, μ, is determined as follows based on previous derivations:

$$W_{S,elastic\text{-}plastic} = W_K$$

$$K\Delta_{yield}^2 \left(\mu - 1/2 \right) = \frac{mv_i^2}{2} = \frac{I^2}{2m}$$

$$\mu = \frac{1}{2}\left(1 + \frac{I^2}{Km\Delta_{yield}^2} \right) \tag{4-18}$$

As with the elastic energy methods, this solution provides sufficient accuracy when the ratio of structural period to impulse duration is 10 or greater.

4.5 MULTIPLE DEGREE OF FREEDOM STRUCTURES

Real structures do not have mass concentrated at a single point, but instead have mass distributed throughout the structure. Such real structures tend to have multiple modes of vibration, each characterized by a unique shape and a unique natural frequency or period. Figure 4-7 illustrates this concept with modes of vibration for a structure with mass concentrated at three points. Such structures are termed multiple degree of freedom (MDOF) structures.
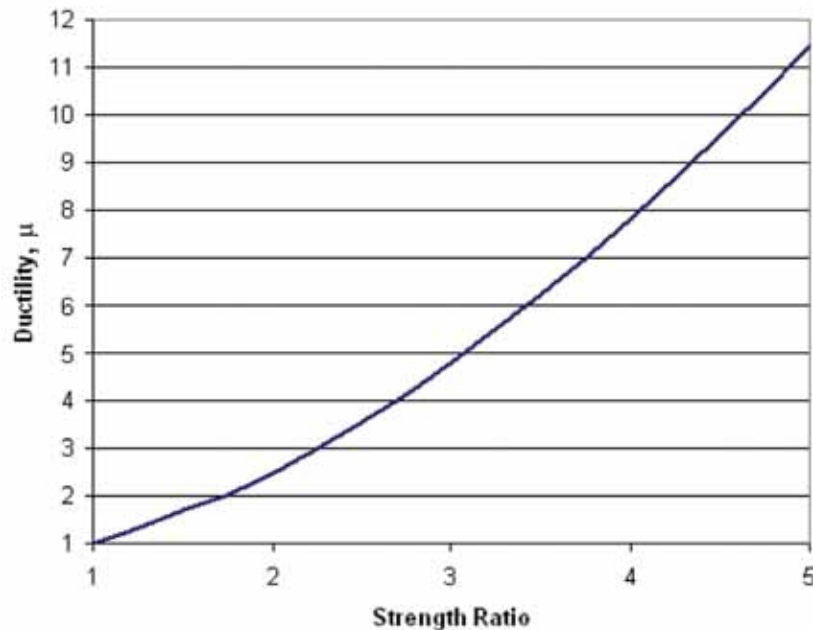
Fig. 4-6. Graphical solution for ductility as a function of strength ratio.

When time-history analysis methods are used to evaluate the response of an MDOF structure to blast response, the distribution of mass and stiffness throughout the structure can be directly modeled and the important response modes for the structure determined. Most structural analysis software used in engineering design offices today provides the capability to do this, as well as the capability to determine the response of such structures through numerical integration of the equation of motion. Section 4.6 summarizes the present capability of common structural analysis software packages in this regard.

It is possible to obtain reasonably accurate solutions of the blast response of many multiple degree of freedom structures by considering the first mode of response only and analyzing the structure as an equivalent single degree of freedom system. This approach is most accurate if the deformed shape of the applied load is similar to the first mode, as explained in Biggs (1964). When this approach is taken, it must be recognized that only a portion of the actual mass of the structure will be mobilized in the first mode, and therefore, transformation factors must be used to relate the response of the idealized single degree of freedom system to that of the real multiple degree of freedom structure.

Table 4-1, obtained from the U.S. Army Corps of Engineers Manual EM 1110-345-415 (USACE, 1957) and replicated by Biggs (1964), provides transformation factors for common single-beam framing systems that can be used to convert real MDOF structures to single degree of freedom (SDOF) systems. In this table, the mass factor, K_M, is the

fraction of the total mass of the structure that is effective in single degree of freedom response; the load factor, K_L, is the fraction of the load and the stiffness on the real structure that is provided by a single degree of freedom solution. The dynamic reactions are the peak forces at the supports. With these tables, it is possible to convert the structure into a simple SDOF equivalent, compute the blast response using the methods of the previous sections, then convert back to the real structure.

Although the SDOF equivalents given in Table 4-1 can be useful, they are only applicable to single span framing with unyielding supports. In real structures, beams and wall panels will often span to other structural elements, such as girders or columns as illustrated in Figure 4-8. Depending on the flexibility and mass distribution along the beams and girders, it may be feasible to evaluate each of the framing elements as an individual SDOF structure, or alternatively, it may be necessary to evaluate the entire system as an MDOF structure, using structural analysis software and time-history methods.

In order to determine if it is possible to evaluate the response of the primary framing (beam in Figure 4-8) and secondary framing (girder in Figure 4-8) as individual SDOF structures, the following procedure should be followed. Determine the period for the primary framing element (beam), assuming it is supported by unyielding supports. Determine the period for the secondary framing element (girder), including the effective mass distributed along the primary element (beam). If the period of the primary element
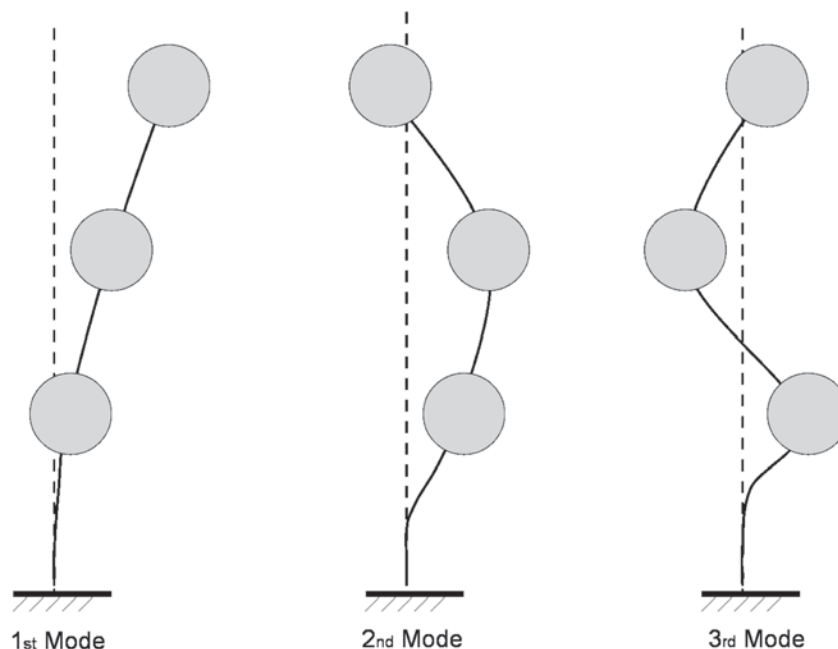
Fig. 4-7. Free vibration modes for three degrees of freedom.

Table 4-1. Conversion Factors for Simply Supported Beams and One-Way Slabs (Biggs, 1964)								

simply-supported
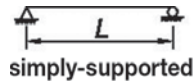
Loading Diagram	Strain Range	Load Factor, K_L	Mass factor, K_M		Load-mass factor, K_{LM}		Maximum Resistance, R_m	Spring Constant, K	Dynamic Reaction, V
			Concentrated Mass*	Uniform Mass	Concentrated Mass*	Uniform Mass			
$F = pL$	Elastic	0.64	—	0.50	—	0.78	$\dfrac{8M_p}{L}$	$\dfrac{384EI}{5L^3}$	$0.39R + 0.11F$
	Plastic	0.50	—	0.33	—	0.66	$\dfrac{8M_p}{L}$	0	$0.38R_m + 0.12F$
F	Elastic	1.0	1.0	0.49	1.0	0.49	$\dfrac{4M_p}{L}$	$\dfrac{48EI}{L^3}$	$0.78R - 0.28F$
	Plastic	1.0	1.0	0.33	1.0	0.33	$\dfrac{4M_p}{L}$	0	$0.75R_m - 0.25F$
$\frac{F}{2}$ $\frac{F}{2}$	Elastic	0.87	0.76	0.52	0.87	0.60	$\dfrac{6M_p}{L}$	$\dfrac{56.4EI}{L^3}$	$0.525R - 0.025F$
	Plastic	1.0	1.0	0.56	1.0	0.56	$\dfrac{6M_p}{L}$	0	$0.52R_m - 0.02F$

*Equal parts of the concentrated mass are lumped at each concentrated load.

Source: *Design of Structures to Resist the Effects of Atomic Weapons,* U.S. Army Corps of Engineers, EM 1110-345-415 (USACE, 1957).
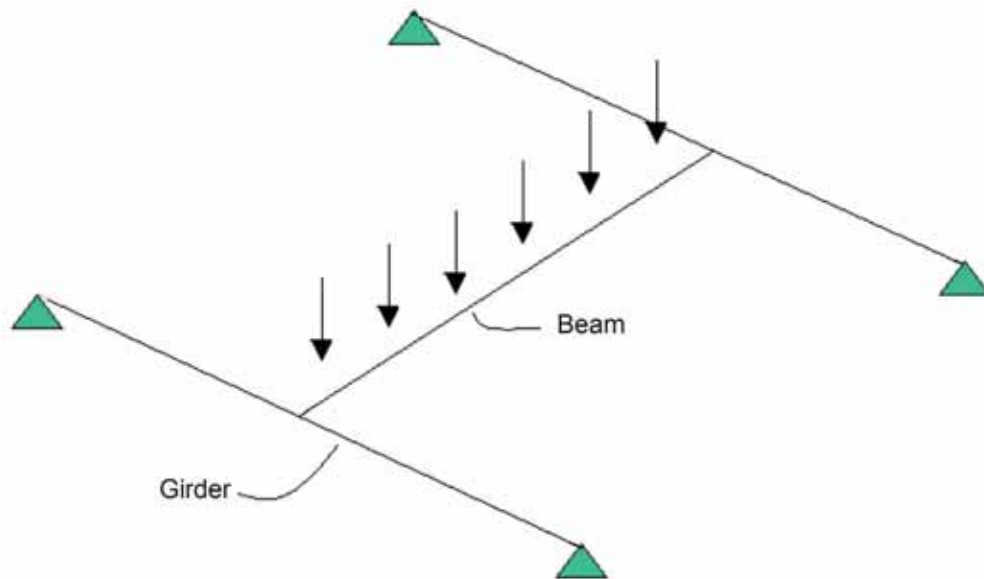
Fig. 4-8. *Complex framing in which one flexural element is supported by other flexural elements.*

TABLE 4-2. Commercially Available Software Packages				
Software	Static Linear Analysis	Modal Analysis	Linear Dynamic Analysis	Nonlinear Dynamic Analysis
ABAQUS	X	X	X	X
ALGOR	X	X	X	X
ANSYS	X	X	X	X
CSI-ETABS	X	X	X	X
CSI-PERFORM	X	X	X	X
CSI-SAP	X	X	X	X
LARSA	X	X	X	X
LARSA 4D	X	X	X	X
LS-DYNA	X	X	X	X
NASTRAN	X	X	X	X
RISA-3D	X	X	X	
STAAD	X	X	X	X

(beam) differs by a factor of 2 from the period of the secondary element (girder), they can be treated as individual SDOF structures. One degree of freedom is the primary element (beam) analyzed with the blast load and unyielding supports and the other degree of freedom is the secondary element (girder) loaded with the reactions from the primary element analysis. If the periods are within a factor of 2 of each other, more exact methods of analysis must be used.

4.6   SOFTWARE

A number of common structural engineering software products can be used to assist in the evaluation of structures and structural elements for blast loads. Table 4-2 lists some of the more popular structural analysis software found in design offices and their ability to perform the various types of analyses described previously, as applicable to blast response evaluation. The types of elements available and the flexibility of each of these software packages vary considerably. Engineers should consult the software documentation, available from the licensors, prior to using the software for specific applications.

Chapter 5
Blast Resistant Design of Structural Systems

The purpose of this chapter is to discuss the implications of blast loading on the design of the lateral load resisting systems of buildings.

In this chapter, simple linear and nonlinear procedures are applied to the design of the lateral load resisting system to support blast loads. The procedures allow blast loads to be compared with wind and earthquake lateral loads, developing an understanding of the magnitude of the blast load and demonstrating why plastic design is desirable in blast design.

Two examples are included in this chapter. The first example is the one-story building defined in Chapter 2 and the second is a three-story building introduced here. Although the examples are different in structural behavior, in both buildings the lateral load resisting systems, as designed for wind, are able to resist the blast loading. Therefore, no additional structure is necessary for blast resistance. For these examples, the general lateral system behavior is checked, columns are modeled as linearly elastic, and beams and bracing are modeled as elastic-plastic. To reduce the extent of failure in a structure, it is good practice to prevent the formation of plastic hinges in columns.

Both lateral design examples illustrate that global lateral response rarely controls building design for blast. Element and connection design will be introduced in Chapters 6 and 7, respectively. Blast loads rarely affect the lateral load resisting system but frequently affect the design of individual loaded elements and their connections.

As discussed in Chapter 2, blast loading produces a shock wave with short duration and elevated peak pressure. For high energy explosives, the blast load duration is usually around 10 to 30 ms, while the fundamental period of buildings is generally on the order of 0.1 to 3.0 s. For a fundamental period greater than 10 times the load duration, the load can be assumed impulsive. Therefore, the global response of most buildings designed for blast can be analyzed under impulsive loads. Impulsive loads are characterized by the area under the load-time curve, independent of the shape of this curve.

The path that the blast load follows through the structure is similar to that for wind loads. From the exterior skin or cladding, the pressure is transferred to girts that transfer the loads to beams or columns, after which it is finally dissipated through the slab to the lateral system and foundations. Generally this path is flexible and behaves plastically, dissipating most of the load energy before it can impact the lateral load resisting system of the building. As will be demonstrated in Chapter 6, the façade can absorb on the order of 80% of the load, depending on its flexibility. In this chapter,

for simplicity, this load path is assumed rigid. This is a conservative approach for checking the lateral system because unless it fails, the lateral system is assumed to absorb all of the energy produced by the impulsive load. A more accurate design would follow the blast load from structural element to structural element until it reached the building's lateral load resisting system, applying the resultant reactions of one element on the next supporting elements. This procedure would consider the energy dissipated within each element through the blast load path. This approach would give a more accurate indication of structural response but it is not necessary in most cases. Design of individual elements to resist blast loading will be introduced in Chapter 6.

Different programming tools and commercial software packages can be used to model and analyze the examples developed in this chapter. Table 4-2 lists many of the commercially available software packages that might be used.

5.1 ENERGY METHOD

Based on the principle of conservation of energy, all of the external work done by the external load is transformed into damping, kinetic and strain energy. This equilibrium is expressed in Equation 5-1. Damping does not play an important role in blast design because most of the damage happens in the first cycle; as a conservative approximation, the energy absorbed by damping is neglected. The following derivation is for a single mass system. Similar results are true for continuous or discrete mass systems.

$$W_P = W_K + W_S \tag{5-1}$$

where

$W_K = \dfrac{m_e V^2}{2} =$ kinetic energy associated with the movement of the system

$W_P =$ energy produced by the load pulse

$W_S =$ strain energy absorbed by the system

$V =$ velocity of the system

$m_e =$ mass of the system

Initially, the system is at rest. Immediately after the impulse load, all of the impulse energy becomes kinetic energy and the strain energy can be neglected. Therefore, the energy produced is:

$$W_P = W_K = \dfrac{m_e V_{max}^2}{2} \tag{5-2}$$

The maximum deflection and support reactions of the system generally appear after the applied load has ended (Figure 5-1). As there are no other external forces acting on the structure, the energy in the system remains constant after the impulse load is finished. Because impulse is defined as the change in momentum, and the system is initially at rest, the impulse can be written as $I = m_e V$. Substituting this impulse into Equation 5-2 yields:

$$W_P = \frac{m_e V_{max}^2}{2} = \frac{I^2}{2m_e} \qquad (5\text{-}3)$$

As the displacement increases, the velocity decreases. As the structure reaches maximum displacement, the velocity becomes zero. At this point, all of the impulse energy has become strain energy in the structure. From the principle of conservation of energy, the strain energy at this time is equal to the initial kinetic energy in the system just after the impulse load and is expressed as follows:

$$W_S = W_P = \frac{I^2}{2m_e} \qquad (5\text{-}4)$$

The strain energy absorbed by a structural system is defined as the area under the force-displacement curve (Figure 5-2).

For linear elastic behavior, the strain energy is:

$$W_{S,el} = \frac{1}{2} K \Delta_{el}^2 = \frac{I^2}{2m_e} \qquad (5\text{-}5)$$
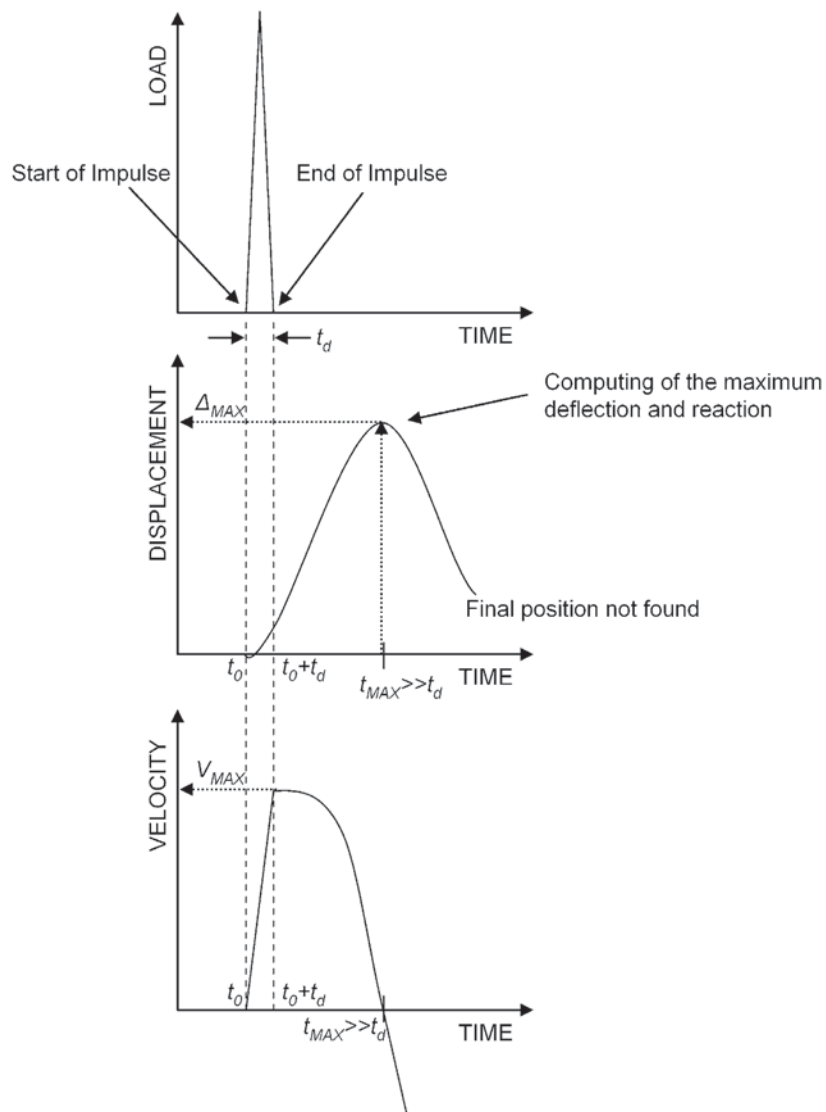
Fig. 5-1. Time-history of impulse loading.

where

K = stiffness of the structure

Δ_{el} = elastic displacement

and the elastic displacement results in the following (see also Section 4.3.3):

$$\Delta_{el} = \frac{I}{\sqrt{m_e K}} \qquad (5\text{-}6)$$

For linear elastic-perfectly plastic behavior (Figure 5-2), the strain energy is:

$$W_{S,pl} = F_{yield} \Delta_{pl} - W_{S,el,max} = \frac{I^2}{2m_e} \qquad (5\text{-}7)$$

The maximum elastic strain energy occurs when the system yields:

$$W_{S,el,max} = \frac{1}{2}K\Delta_{el,max}^2 = \frac{1}{2}F_{yield}\,\Delta_{el,max} \qquad (5\text{-}8)$$

and the plastic displacement can be represented as:

$$\Delta_{pl} = \frac{1}{F_{yield}}\left(\frac{I^2}{2m_e} + W_{S,el,max}\right) \qquad (5\text{-}9)$$

where

F_{yield} = force that would cause the structure to yield

In accordance with UFC 3-340-02 Table 5-8 (DOD, 2008), for blast response designed to avoid imminent collapse, the deflection criteria used for frames limits the interstory drift to $H/25$ (where H is the height between stories), and the maximum member end rotation (measured from the chord
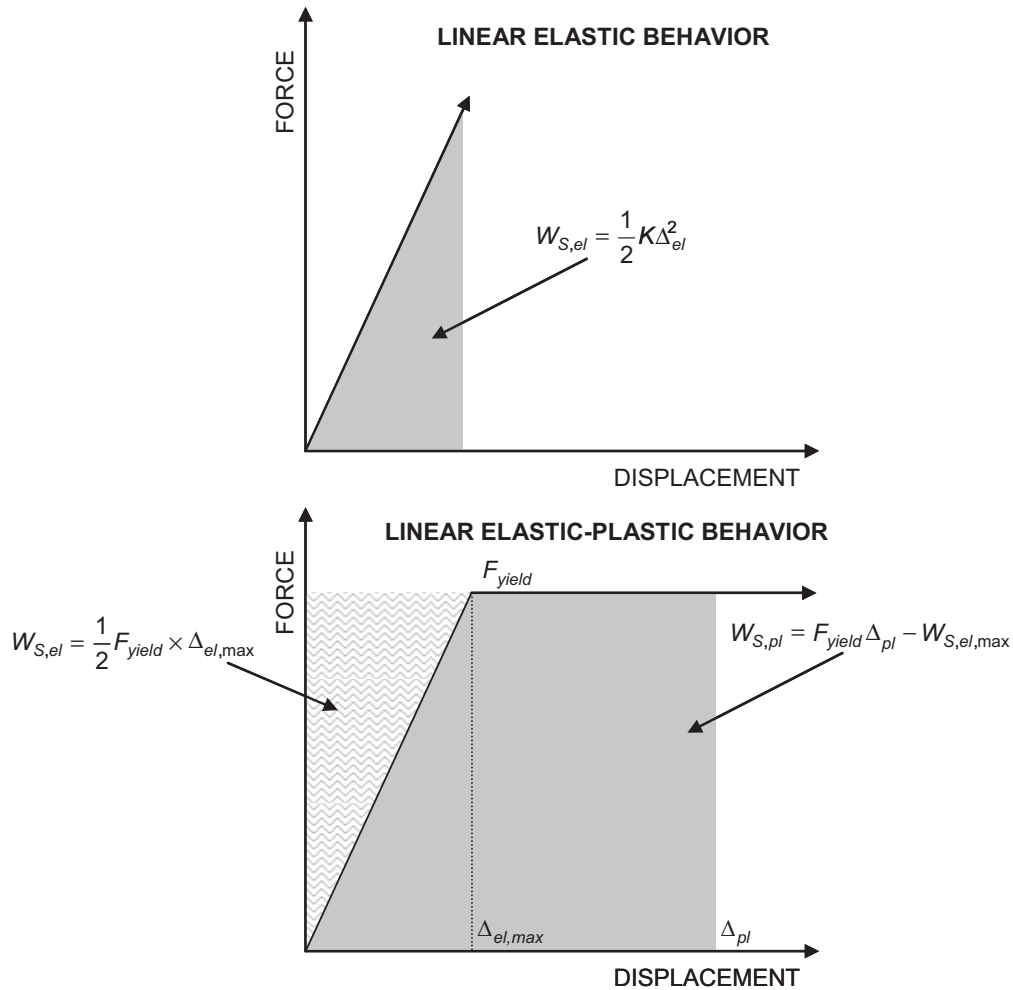
Fig. 5-2. Linear elastic and elastic-plastic strain energy.

joining the member ends) to 2°. These criteria are discussed in Chapter 6, Section 6.2.3, along with criteria for the design of individual elements.

5.2 SIMPLIFICATIONS BASED ON DYNAMIC PARAMETERS

Section 5.1 introduced the energy method used to derive the elastic and elastic-plastic displacement. In this section, those results will be expressed with variables commonly used in structural dynamics.

The period of a structure, previously defined in Chapter 4, is defined as:

$$T = 2\pi \sqrt{\frac{m_e}{K}} \tag{5-10}$$

For a multi-story frame, the fundamental natural period may be determined using Rayleigh's approximation (Biggs, 1964) which is stated as:

$$T = 2\pi \sqrt{\frac{\sum w_i \Delta_i^2}{g \sum f_i \Delta_i}} \tag{5-11}$$

where
f_i = force per floor used to obtain the displacement per floor
g = acceleration due to gravity = 386 in./s^2
w_i = weight per floor
Δ_i = displacement per floor

This approach to calculation of the fundamental period will be used in Example 5.2.

The impulse, defined in Chapter 2, is the area under the time-history curve. Blast loads are commonly simplified to a
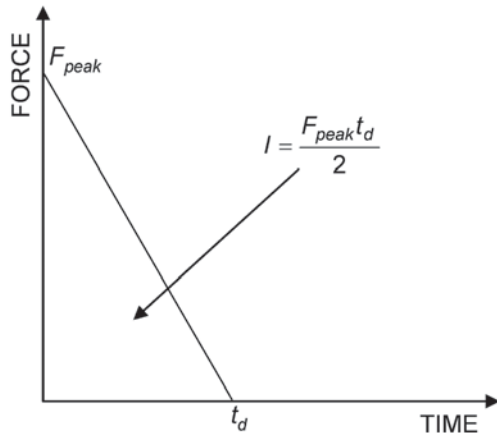
Fig. 5-3. Impulse time-history curve.

triangular impulse. For a triangular time-history curve (Figure 5-3), the impulse is:

$$I = \frac{F_{peak} t_d}{2} \tag{5-12}$$

where
F_{peak} = peak blast load
t_d = load duration

For linear elastic behavior, the displacement was obtained in Equation 5-6 as:

$$\Delta_{el} = \frac{I}{\sqrt{m_e K}} \tag{5-6}$$

Combining the definition of period given by Equation 5-10 with the expression of elastic displacement given by Equation 5-6, the displacement can be expressed as:

$$\Delta_{el} = \frac{2\pi I}{KT} \tag{5-13}$$

Including the definition of impulse from Equation 5-12, the displacement is:

$$\Delta_{el} = \frac{\pi F_{peak}}{KT/t_d} = \frac{\left(\frac{\pi}{T/t_d}\right) F_{peak}}{K} = \frac{k_{DRF} F_{peak}}{K} \tag{5-14}$$

where
k_{DRF} = dynamic reduction factor for impulsive loads where $T > t_d$

$$= \frac{\pi}{T/t_d} \tag{5-15}$$

Based on linear elastic behavior, the relationship between force and displacement is:

$$F = K\Delta \tag{5-16}$$

Therefore, the equivalent force that produces the same elastic displacement is:

$$F_{eq,el} = \frac{\pi F_{peak}}{T/t_d} = k_{DRF} F_{peak} \tag{5-17}$$

To develop an understanding of the magnitude of the blast force, this equivalent force can be compared with the wind and earthquake base shears. The following examples show that although this number can be much greater than the wind load, the lateral system may still have capacity to prevent collapse using its plastic and dynamic properties.

5.3   DESIGN EXAMPLES

Example 5.1—Blast Resistance of a One-Story Building

Given:

In this example, the one-story building from Chapter 2, shown in Figure 5-4, is initially designed to support a 25 psf wind load and to deflect less than H/400 under the design wind load. It is then designed for a 500-lb TNT equivalent blast load located 50 ft away from the short façade. The blast load is assumed uniform on the front façade and any blast pressure on the rear façade is ignored. The W-shapes are ASTM A992 steel and the rod braces are ASTM A572 Grade 50 steel. The gravity loads used in this example are a 30 psf roof dead load and 40 psf façade dead load.

Simplifying assumptions include that the response of the building is predominantly in the first mode of vibration and that the load path from the façade subjected to the blast, back to the lateral force resisting system, is completely rigid. This second assumption is conservative because it implies that there is no energy dissipation along the load path.

Hand calculations are performed to determine the behavior of the system based on the equivalent blast pressure and the lateral capacity of the building. An elastic-perfectly plastic equivalent system is used to obtain the plastic deflection of the system.

Secondly, a computer analysis is used to determine the behavior of the structure under blast load. A nonlinear time-history dynamic analysis is performed for the triangular blast load shown in Figure 5-5 (see Chapter 2 for details). Nonlinear material properties are modeled for the diagonal rods through the use of elastic-plastic axial hinges (see Chapter 6 for details).

For this example, SAP2000 was used. There are many other commercially available software packages that would perform this analysis as well. See Chapter 4 for a discussion of available computer programs; in particular, Table 4-2 shows these packages and their capabilities, including nonlinear dynamic analyses.

The results will show that the system is able to safely withstand the blast load if footings and connections are designed for the overload. Design of columns, beams and connections will be introduced in Chapters 6 and 7.

The building dimensions are shown in Figure 5-4. The load used in the example is shown in Figure 5-5.

Solution:

Design for Lateral Loads

Two lateral braces are located along both long sides of the building. These braces, shown in Figure 5-6, are diagonal rods. The diagonal rods are modeled as tension-only elements with no compression strength. The rods are assumed to be upset rods, not conventional threaded rods where the minimum section is at the thread root, so that the full rod area can be used to resist the
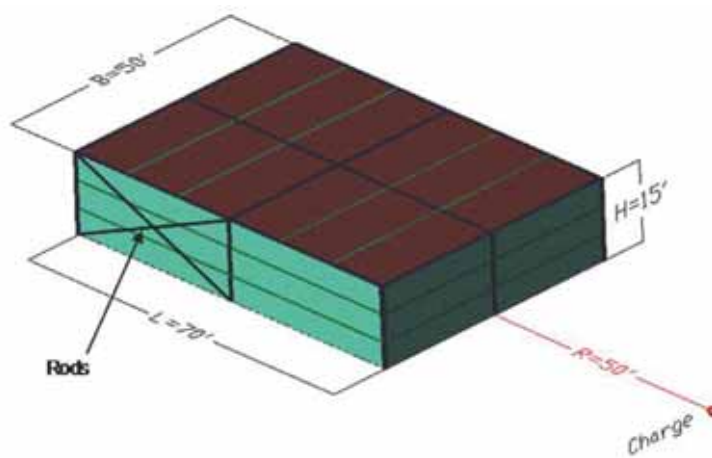
Fig. 5-4. Steel building for Example 5-1—isometric view.

force. It is assumed that the elastic behavior is a result of the tension brace only; the effect of the compression brace is neglected.

The base shear due to wind for a 25 psf wind pressure in the long direction can be computed as:

$$V_{wind} = \text{(wind pressure)(tributary facade area)}$$
$$= \left(25.0 \text{ psf } 1{,}000/\text{lb/kip}\right)\left[(50.0 \text{ ft})(15.0 \text{ ft}/2)\right]$$
$$= 9.40 \text{ kips}$$

Each of the braced frames takes only half of this load, hence the load modeled is 4.70 kips. Figure 5-6 shows the design and the load used for wind design. Beams are modeled as rigid elements to capture the diaphragm behavior. All members are assumed to be pinned at their ends.

Under wind load, the deflection is $H/900 = 0.200$ in. This is less than the $H/400$ limit set in the design statement. This system has a stiffness of 4.70 kips/0.200 in. = 23.5 kip/in. The tension in the rod under wind loading is determined as follows:
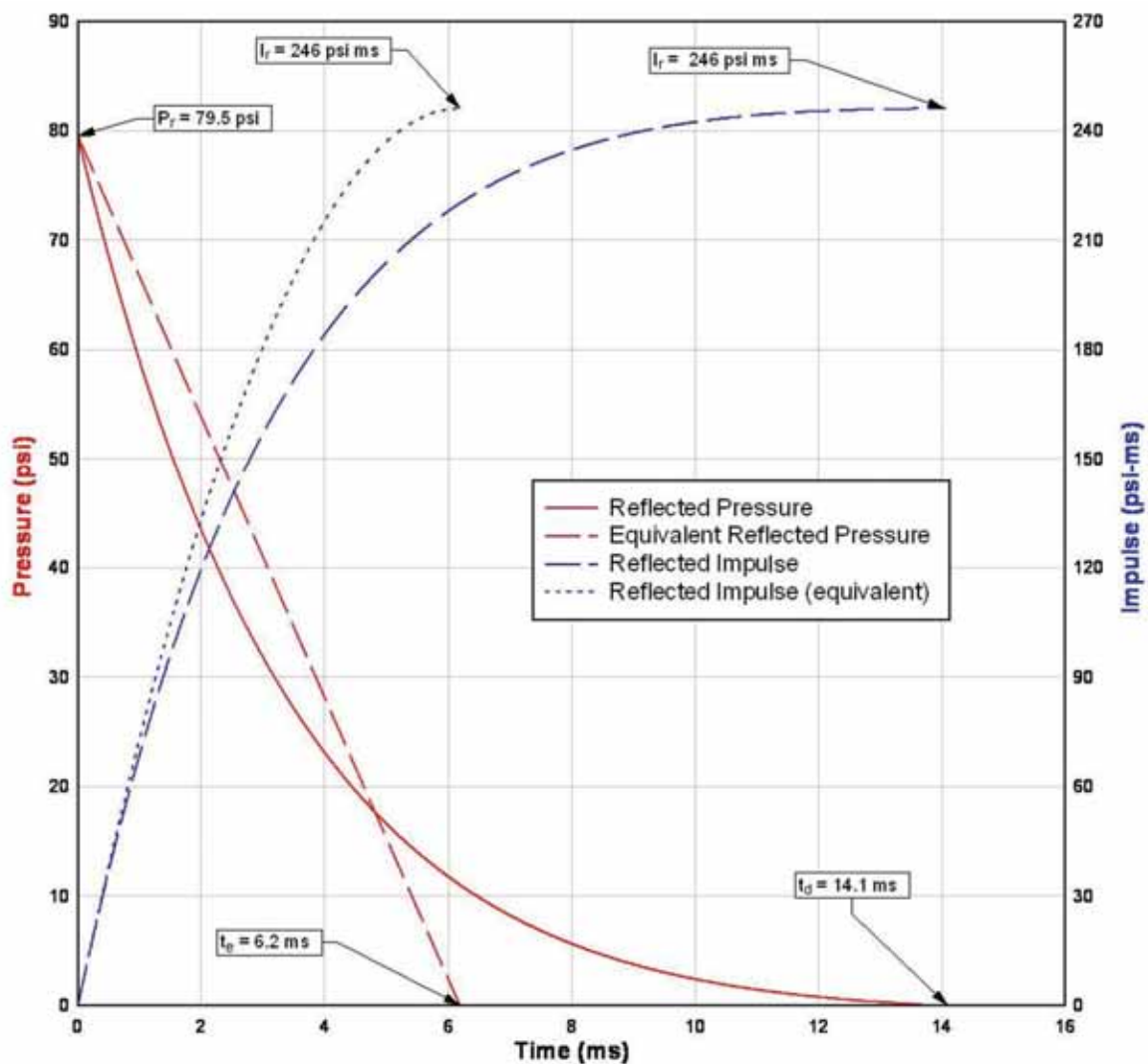
Fig. 5-5. Equivalent reflected pressure and impulse.

$$T_{wind} = \frac{4.70 \text{ kips}}{\cos \alpha}$$

$$= 5.11 \text{ kips}$$

where

$$\alpha = \tan^{-1}\left(15.0 \text{ ft}/35.0 \text{ ft}\right)$$

$$= 23.2°$$

The yield strength should be increased by a factor of 1.30 as discussed in Chapter 6, Equation 6-5. Hence, the available tensile strength of the rod due to yielding is (tensile rupture will not control):

$$T_{max} = 1.30 F_y A_g$$

$$= 1.30(50 \text{ ksi})\left[\pi\left(\frac{3/4 \text{ in.}}{2}\right)^2\right]$$

$$= 28.7 \text{ kips}$$

For this maximum tension, the maximum lateral load that the system can carry is:

$$F_{yield} = \left(\frac{T_{max}}{T_{wind}}\right)(\text{applied wind load})$$

$$= \left(\frac{28.7 \text{ kips}}{5.11 \text{ kips}}\right)(4.70 \text{ kips})$$

$$= 26.4 \text{ kips}$$

The maximum elastic displacement is:

$$\Delta_{el,max} = \left(\frac{T_{max}}{T_{wind}}\right)(\text{wind load deflection})$$

$$= \left(\frac{28.7 \text{ kips}}{5.11 \text{ kips}}\right)(0.200 \text{ in.})$$

$$= 1.12 \text{ in.}$$
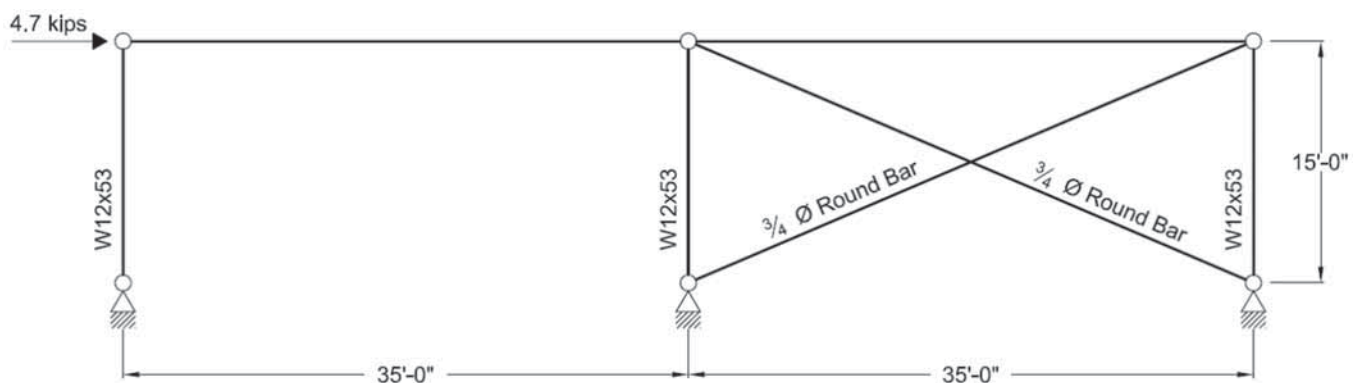
Fig. 5-6. Wind load design.

Equivalent Blast Force and Blast Pressure

Solving for K in Equation 5-16, the lateral stiffness of the structure is:

$$K = \frac{F_{yield}}{\Delta_{el,max}}$$

$$= \frac{26.4 \text{ kips}}{1.12 \text{ in.}}$$

$$= 23.6 \text{ kip/in.}$$

Considering a 30 psf roof dead load and a 40 psf façade dead load using the tributary area of the façade assuming half is carried by the roof, the total weight involved in the movement of the bracing on one side is:

$$w_e = \text{roof dead load} + \text{façade dead load}$$

$$= \frac{(30.0 \text{ psf})(50.0 \text{ ft})(70.0 \text{ ft})/2}{1,000 \text{ ft/kip}} + \frac{(40.0 \text{ psf})(50.0 \text{ ft} + 70.0 \text{ ft})(15.0 \text{ ft}/2)}{1,000 \text{ ft/kip}}$$

$$= 88.5 \text{ kips}$$

According to Equation 5-10, the fundamental period of this single degree of freedom system is:

$$T = 2\pi\sqrt{\frac{m_e}{K}}$$

$$= 2\pi\sqrt{\frac{w_e}{gK}}$$

$$= 2\pi\sqrt{\frac{88.5 \text{ kips}}{(386 \text{ in./s}^2)(23.6 \text{ kip/in.})}}$$

$$= 0.619 \text{ s}$$

The period of 0.619 s is approximately 100 times the duration of the load, $t_e = 0.00620$ s, as given in Figure 5-5; therefore, impulsive behavior is assumed.

The peak blast force applied per brace, F_{peak}, correlating to the peak pressure (P_r from Figure 5-5), is half of the total blast pressure, and is determined as follows:

$$F_{peak} = (\text{peak blast pressure})(\text{tributary facade area})$$

$$= 79.5 \text{ psi} \left[\frac{(50.0 \text{ ft}/2)(12 \text{ in./ft})(15.0 \text{ ft}/2)(12 \text{ in./ft})}{1,000 \text{ lb/kip}} \right]$$

$$= 2,150 \text{ kips}$$

Note that using only half of the story height (15.0 ft/2) is a departure from UFC 3-340-02 (DOD, 2008), which conservatively uses the full façade area in calculating this force. This guide will follow the more conventional method used in wind design.

Based on Equation 5-12, the impulse is:

$$I = \frac{F_{peak} t_d}{2}$$

$$= \frac{(2,150 \text{ kips})(6.20 \times 10^{-3} \text{ s})}{2}$$

$$= 6.67 \text{ kip-s}$$

Using Equation 5-17, the equivalent force results in the following:

$$F_{eq,el} = \frac{\pi F_{peak}}{T/t_d}$$

$$= \frac{\pi(2{,}150 \text{ kips})}{(0.619 \text{ s})/(6.20 \times 10^{-3} \text{ s})}$$

$$= 67.7 \text{ kips}$$

This force is equivalent to a uniform pressure on the façade of:

$$P_{eq} = \frac{F_{eq,el}}{\text{tributary facade area}}$$

$$= \frac{67.7 \text{ kips}(1{,}000 \text{ lb/kip})}{[(50.0 \text{ ft})/2][(15.0 \text{ ft})/2]}$$

$$= 361 \text{ psf} > 25.0 \text{ psf}$$

The equivalent blast pressure is 14 times greater than the wind pressure. The maximum lateral force that the system can carry, determined previously, is $F_{yield} = 26.4$ kips. The equivalent blast load is 67.7 kips, approximately 2.5 times larger than the actual elastic capacity. Hence, the assumption that the structure remains elastic is not appropriate and plastic considerations are necessary for design.

Plastic Deflection

Considering an elastic-plastic behavior of the building with the lateral capacity previously defined, Equation 5-9 gives the plastic displacement as:

$$\Delta_{pl} = \frac{1}{F_{yield}}\left(\frac{I^2}{2m_e} + W_{S,el,max}\right) \tag{5-9}$$

where
I = 6.67 kip-s (as determined previously)
$m_e = w_e/g$

From Equation 4-14, the maximum elastic energy is:

$$W_{S,el,max} = \frac{F_{yield}\,\Delta_{el,max}}{2}$$

$$= \frac{(26.4 \text{ kips})(1.12 \text{ in.})}{2}$$

$$= 14.8 \text{ kip-in.}$$

Therefore, the plastic displacement is:

$$\Delta_{pl} = \frac{1}{F_{yield}}\left(\frac{I^2}{2m_e} + W_{S,el,max}\right) \tag{5-9}$$

$$= \frac{1}{26.4 \text{ kips}}\left[\frac{(6.67 \text{ kip-s})^2}{2(88.5 \text{ kips/386 in./s})} + 14.8 \text{ kip-in.}\right]$$

$$= 4.24 \text{ in.}$$

To avoid imminent collapse, the deflection criterion of $H/25$, as discussed in Section 5.1, gives:

$$\Delta_{pl} = 4.24 \text{ in.}$$
$$< \frac{H}{25} = \frac{15.0 \text{ ft}(12 \text{ in./ft})}{25}$$
$$< 7.20 \text{ in.}$$

Thus, the plastic displacement complies with this criterion.

Based on this deflection, the ductility, Δ_{pl}/Δ_{el}, as discussed in Section 4.4, is:

$$\mu = \frac{\Delta_{pl}}{\Delta_{el}}$$
$$= \frac{4.24 \text{ in.}}{1.12 \text{ in.}}$$
$$= 3.79$$

The structure as designed for wind is able to resist the blast pressure with an acceptable deflection and ductility ratio provided that the connection has enough strength to allow the member to reach its yield strength. Chapter 6 will introduce resistance and ductility criteria to design and check the structural elements.

Computer Analysis

The structure shown in Figure 5-6 is modeled for computer analysis (using SAP 2000) with both rods included to capture the behavior of the structure on rebound. The rods are modeled as tension-only elements with nonlinear axial hinges (see Chapter 6 for further discussion). The beams are modeled as rigid to approximate rigid diaphragm behavior and a rigid path to the lateral system. As discussed earlier, this is a conservative assumption that neglects energy dissipation.

The maximum tensile strength of the rod was computed previously to be 28.7 kips. It is assumed to have no compressive strength. The total weight of the system was computed as 88.5 kips. This weight is distributed linearly over the beams in the frame.

The blast load applied on the structure is given in Figure 5-7. A general material nonlinear time-history analysis was performed. The structure was analyzed for the effect of the blast load alone, excluding dead load. From the computer modal analysis, the period of the first elastic mode is 0.620 s. This is the same as the value obtained by the hand calculations performed previously. However, the period of the blast response ($T \approx 1$ s) is much longer than the calculated elastic period of 0.619 s due to plastic behavior.

Time dependent displacement results are shown in Figure 5-8. The maximum displacement is 4.24 in., which is less than $H/25 = 7.20$ in. This is the same value obtained previously. The structure deforms plastically. The displacement past the maximum elastic displacement is permanent plastic deformation of Rod 1.

The axial forces in the rods are shown in Figure 5-9. Note that Rod 2, which was initially inactive, is activated in the rebound of the structure. The energy absorbed by Rod 1 includes both an elastic and a plastic component. The energy absorbed during the rebound by Rod 2 is elastic and is equal to the elastic energy released by Rod 1 as it unloads. As shown in Figure 5-9, from 0.430 to 0.700 s neither rod is active. Due to the permanent plastic deformation shown in Figure 5-8, both rods are in compression at this time. Rod 2 is compressed because the structure has not reached the original elastic equilibrium point. Rod 1 has been permanently elongated and thus is compressed before reaching the original elastic equilibrium point.

Figure 5-10 shows the axial force in Column 1 and Column 2. Figure 5-11 shows the reactions at the supports. For comparison, the elastic reactions under wind load are ±2 kips. The foundation reaction under blast load is 12 kips, 6 times greater than the wind reaction, but with less than 0.6 s of duration. Note that the foundations are subject to both downward and upward load. In Chapter 6, the columns are designed to remain elastic to avoid the failure of the structure.

The ductility in the system, μ, can be computed as the ratio between the plastic and the elastic yield displacement as determined previously. Chapter 6 defines criteria to classify the blast behavior of the structural system based on ductility ratios.
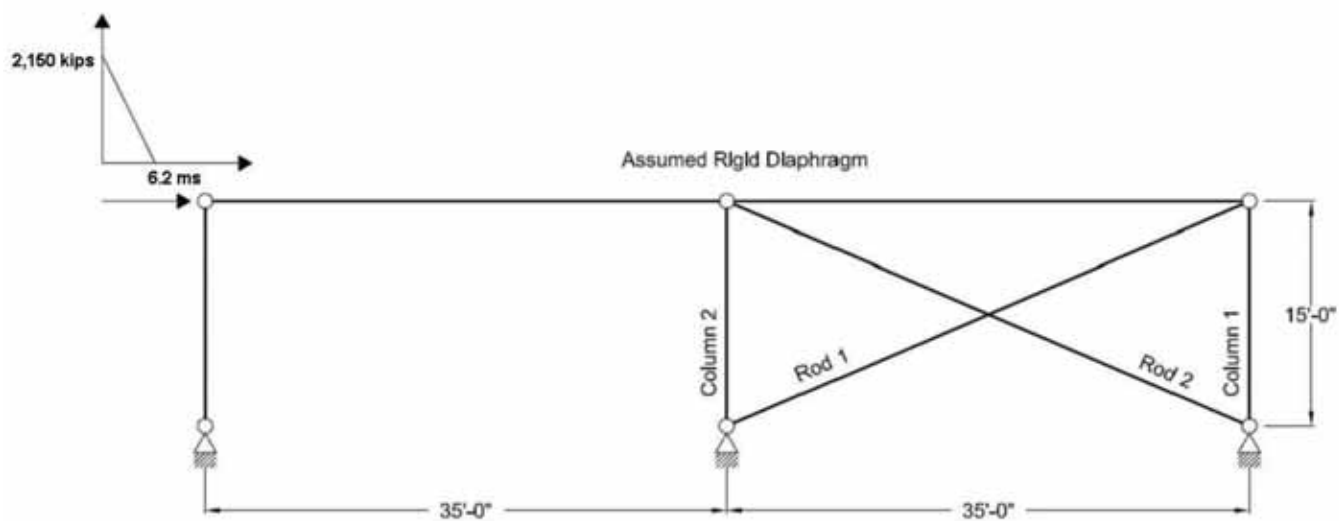
Fig. 5-7. Application of blast load.
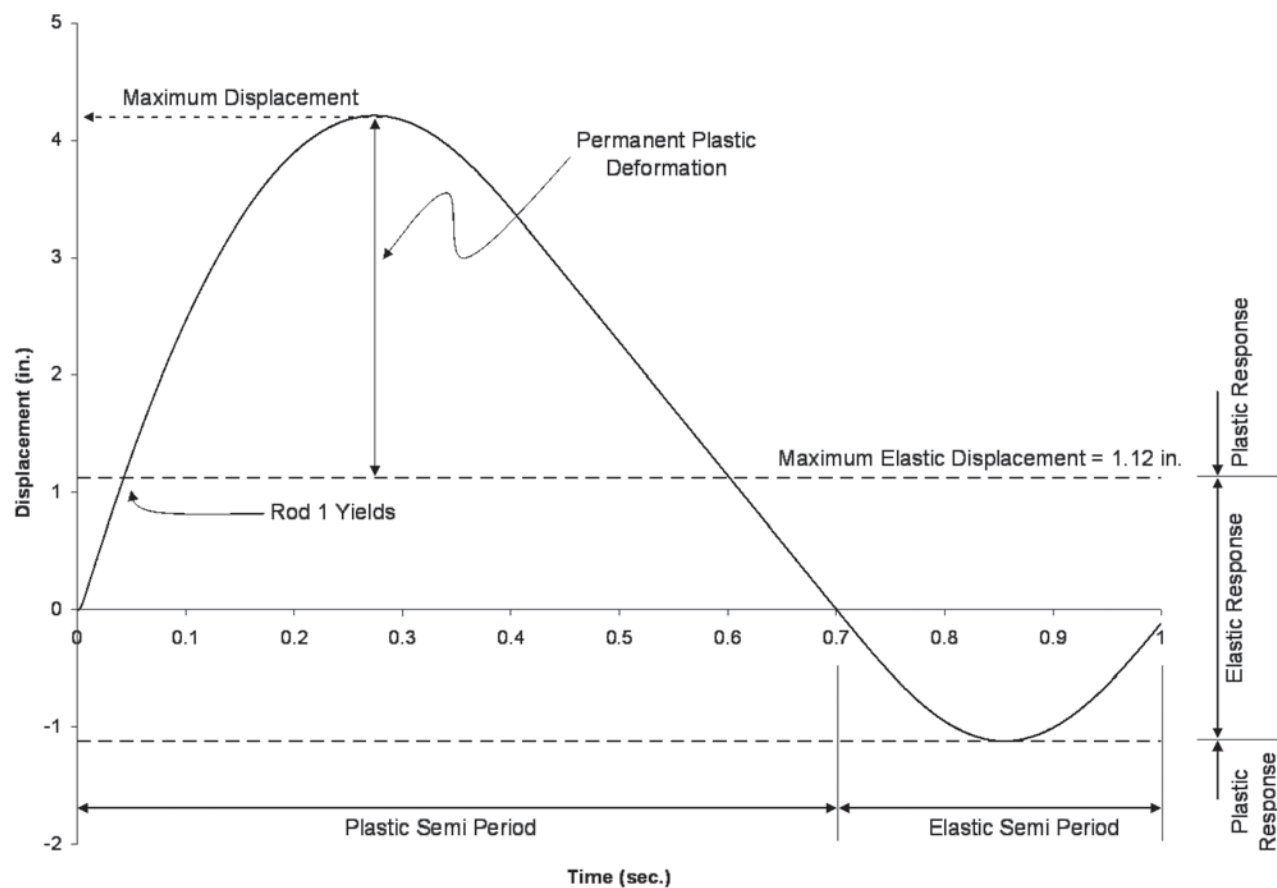
Fig. 5-8. Displacement results for the movement of the roof under blast load.
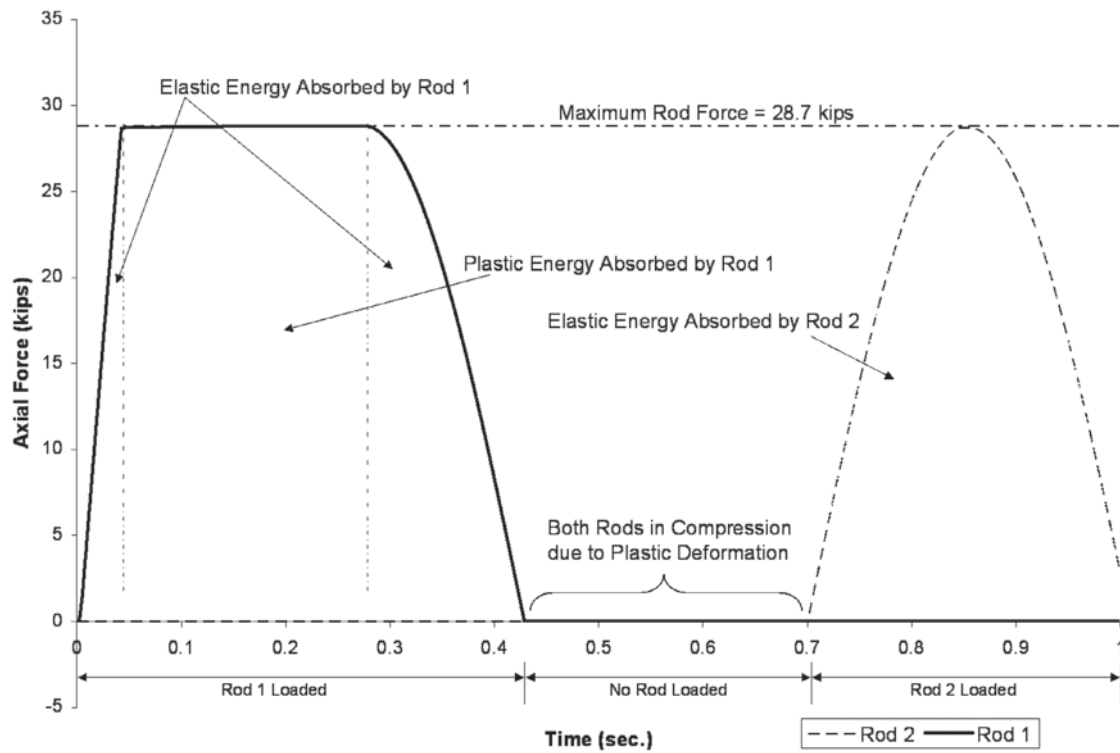
Fig. 5-9. Axial force in rods.
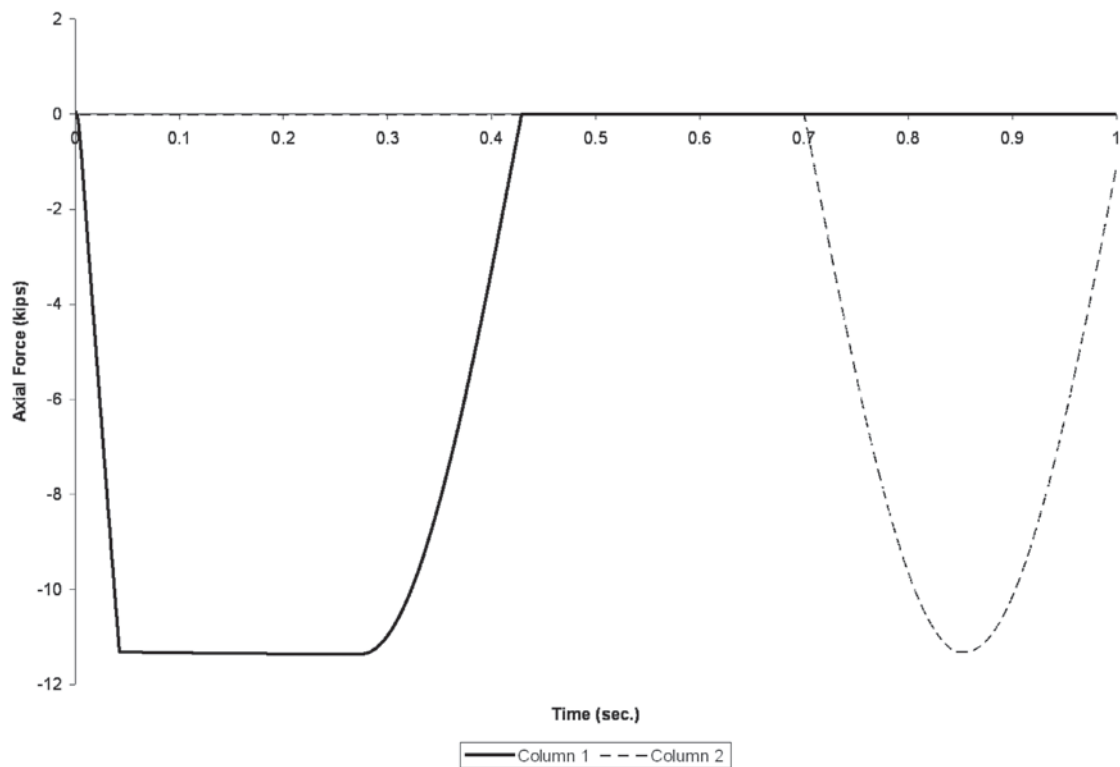
Fig. 5-10. Axial force in columns.

As mentioned at the beginning of this example, the results show that the system is able to safely withstand the blast load if footings and connections are designed for the overload. Due to the simplicity of this example, the computer calculations and the hand calculations yielded the same results. It should be noted that this will not often occur in actual practice. However, even with more complicated structures, these calculations should be within a reasonable margin of each other.

Example 5.2—Blast Resistance of a Three-Story Building

Given:

The three-story building shown in Figure 5-12 is designed for blast loading. The lateral system of the building is formed by a chevron braced frame on each of the 150-ft sides of the building. This building is designed for 25 psf wind load with a deflection limited to $H/400$. The resulting structural design is shown in Figure 5-13. The blast load affects the 120-ft-wide façade and has the same triangular time-history blast pressure used in Example 5.1. The HSS diagonal braces are ASTM A500 Grade C material.

All of the floors are modeled as rigid diaphragms. This neglects the axial load in the beams that can affect the beam design. The façade and the load path to the lateral system are assumed rigid. As described earlier, this is a conservative assumption as it neglects the energy absorbed by the façade and the load path.

Lumping the building's mass at each floor, the mass moving with each frame per floor is:

Roof　　　　 = 450 kips (50 psf)

3rd Floor　 = 900 kips (100 psf)

2nd Floor　 = 900 kips (100 psf)
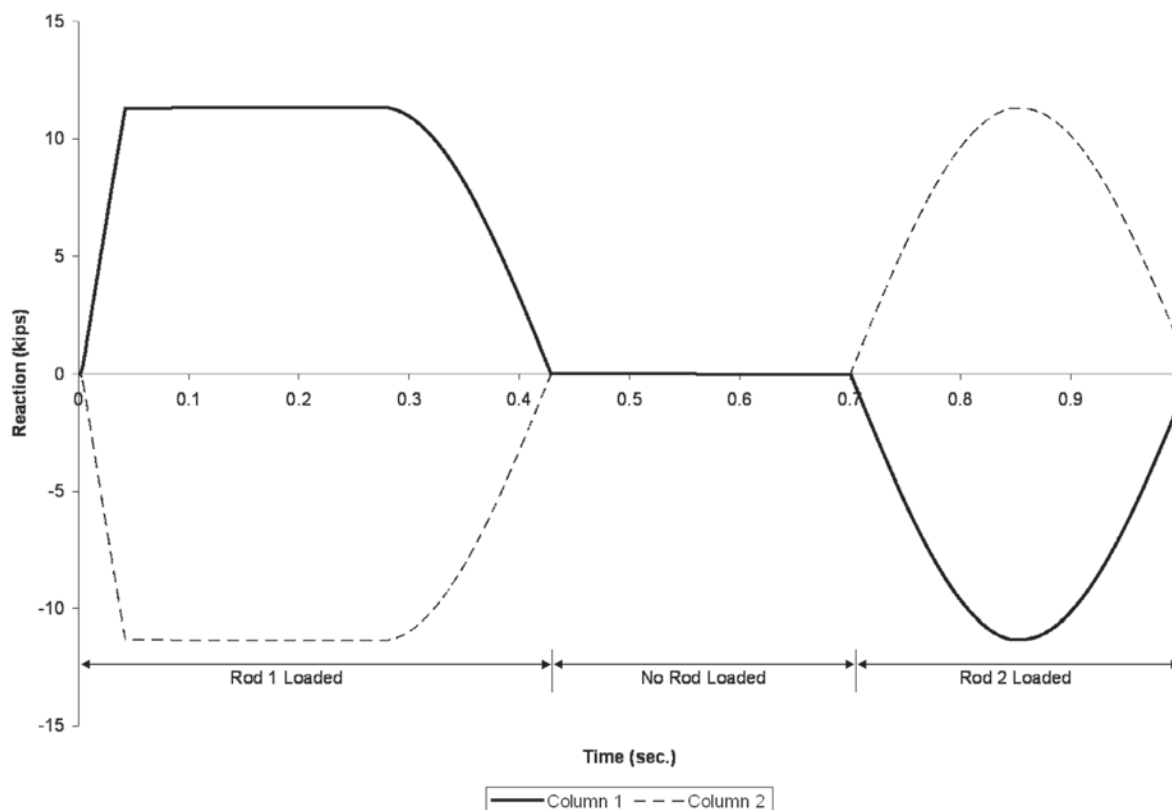
Fig. 5-11. Support reactions.

A linear elastic simplification is used to obtain the equivalent blast load. This equivalent load is used to compare the blast effect with the wind load. Due to sudden failure under buckling, an elastic-perfectly plastic simplification cannot be used in this example. A nonlinear dynamic analysis is carried out by computer analysis. In this particular example, SAP2000 was used.

Solution:

Equivalent Blast Force and Blast Pressure

Based on the masses, wind loads and deflections given, the fundamental period of the building, using Rayleigh's approximation, as provided in Equation 5-11, is:

$$T = 2\pi \sqrt{\frac{\sum w_i \Delta_i^2}{g \sum f_i \Delta_i}}$$

$$= 2\pi \sqrt{\frac{(450 \text{ kips})(0.120 \text{ in.})^2 + (900 \text{ kips})(0.100 \text{ in.})^2 + (900 \text{ kips})(0.0600 \text{ in.})^2}{(386 \text{ in./s})[(9.00 \text{ kips})(0.120 \text{ in.}) + (18.0 \text{ kips})(0.100 \text{ in.}) + (18.0 \text{ kips})(0.0600 \text{ in.})]}}$$

$$= 0.695 \text{ s}$$

Using the same impulse time history function as Example 5.1, using Figure 5-5, the total peak load in this three-story braced frame is:

$$F_{peak} = (\text{peak blast pressure})(\text{tributary façade area})$$

$$= 79.5 \text{ psi} \left[\frac{\left(\frac{120 \text{ ft}}{2}\right)(12 \text{ in./ft})\left(12.0 \text{ ft} + 12.0 \text{ ft} + \frac{12.0 \text{ ft}}{2}\right)(12 \text{ in./ft})}{1,000 \text{ lb/kip}} \right]$$

$$= 20,600 \text{ kips}$$

According to Equation 5-17, the equivalent force is:

$$F_{eq} = \frac{\pi F_{peak}}{T/t_d} \tag{5-17}$$

$$= \frac{\pi (20,600 \text{ kips})}{(0.695 \text{ s})/(6.20 \times 10^{-3} \text{ s})}$$

$$= 577 \text{ kips}$$

This force is equivalent to a uniform pressure on the façade for each braced frame of:

$$\text{Pressure} = \frac{(577 \text{ kips})(1,000 \text{ lb/kip})}{\left(\frac{120 \text{ ft}}{2}\right)(12.0 \text{ ft} + 12.0 \text{ ft} + 12.0 \text{ ft}/2)}$$

$$= 321 \text{ psf} > 25.0 \text{ psf}$$

As with the previous example, the equivalent blast pressure is much greater than the design wind pressure of 25 psf. The elastic yield point is identified as the total load that makes the first diagonal fail in compression. In Figure 5-13, the force in the bottom-most diagonal is 32 kips and the total wind shear is 45 kips. Assuming a blast compressive strength for a 17-ft-long HSS6×6×¼ of 165 kips (see Chapter 6 for discussion of dynamic element strength), the lateral strength is:
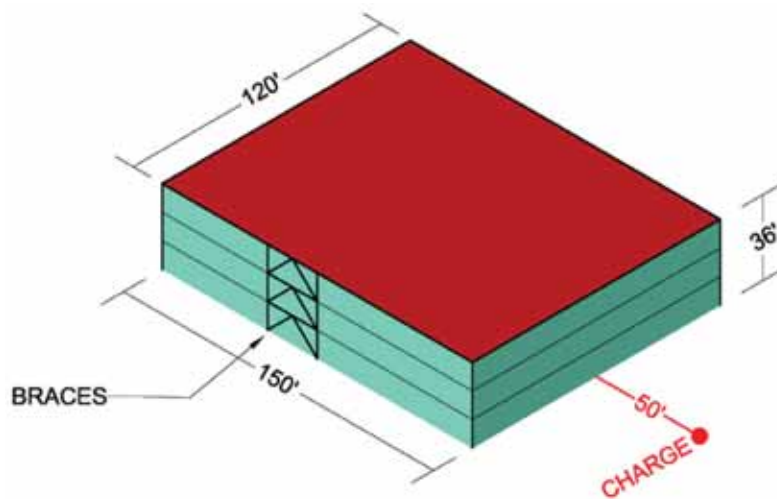
Fig. 5-12. Isometric view of Example 5.2 building.
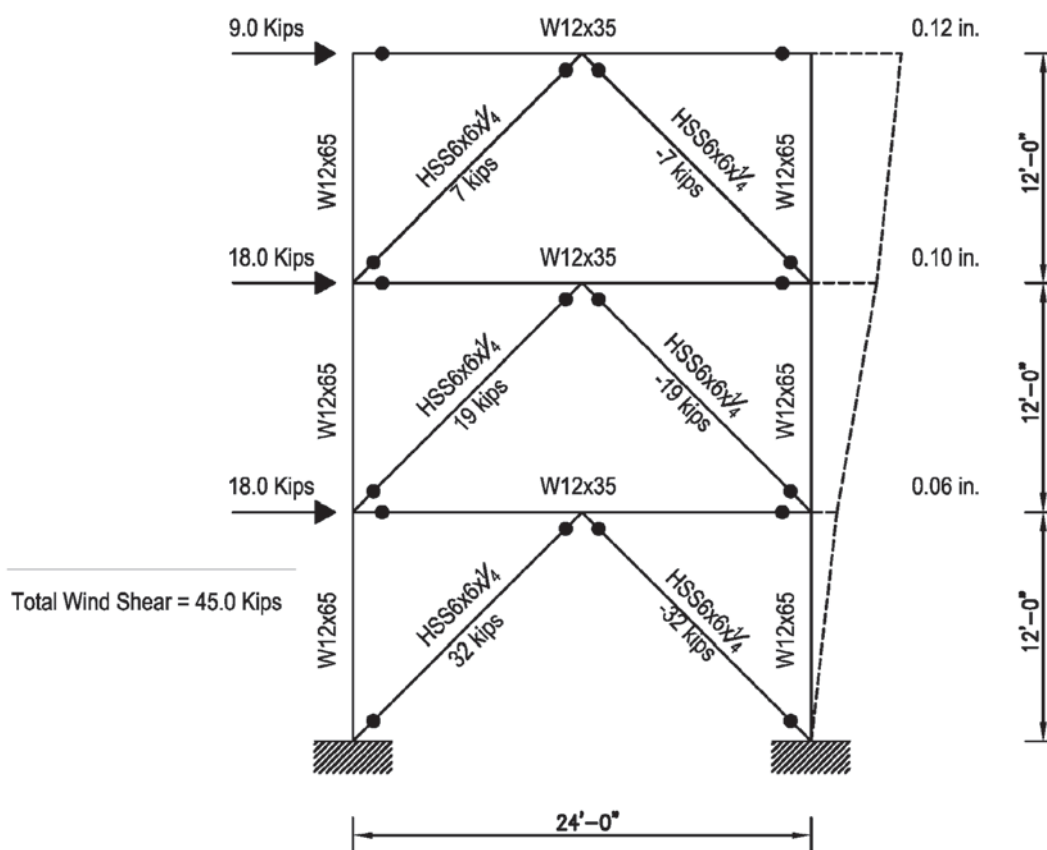
Fig. 5-13. Results of wind analysis and design.

Table 5-1. Maximum Story Deflections			
Story	**Total Drift, Δ**	**Interstory Drift, δ**	**Interstory Drift Angle**
3rd to Roof	3.34 in.	$\delta = 0.24$ in. $= H/600$	$0.09° = 0.002$ rad
2nd to 3rd Floor	3.17 in.	$\delta = 0.36$ in. $= H/400$	$0.14° = 0.002$ rad
Ground to 2nd Floor	3.11 in.	$\delta = 3.11$ in. $= H/46$	$1.24° = 0.022$ rad

$$F_{yield} = \left(\frac{\text{blast compressive strength}}{\text{force due to wind in diagonal member}}\right)(\text{total wind shear})$$

$$= \left(\frac{165 \text{ kips}}{32.0 \text{ kips}}\right)(45.0 \text{ kips})$$

$$= 232 \text{ kips}$$

$$\frac{F_{eq}}{F_{yield}} = \frac{577 \text{ kips}}{232 \text{ kips}}$$

$$= 2.49$$

The equivalent blast force is 2.5 times larger than the actual elastic strength of the system; therefore, a plastic analysis is required. As the braces are behaving plastically, design the system as a special concentrically braced frame (SCBF) as defined in the AISC *Seismic Provisions for Structural Steel Buildings* (AISC, 2010b). Therefore, as an SCBF, the post-buckling and post-yielding strength of the braces is explicitly modeled and considered through the use of nonlinear axial hinges in the next section. Note that, however, the structure is not subject to high seismic loading.

Computer Analysis

The structure shown in Figure 5-13 is modeled as a multiple degree of freedom system in a structural software package (SAP2000) to carry out the nonlinear time-history analysis. The strength and ductility properties for the different elements are calculated in Chapter 6. Columns are assumed to remain elastic and are designed as such in Chapter 6.

Using the dynamic strength of the members to be defined in Chapter 6, the HSS6×6×¼ diagonals have 340 kips of tensile strength and 165 kips of compressive strength (see Example 6.1). The W12×35 beams have 262 kip-ft of flexural strength. The diagonals are modeled in the computer analysis with nonlinear axial hinges at their centers and the beams with nonlinear moment hinges at their midspan. The hinge properties are in accordance with FEMA 356 (FEMA, 2000b). See Example 6.1 for the derivation of these hinge properties. Member ends are assumed pinned.

Figure 5-14 shows the time-history load applied for the nonlinear time-history analysis. The total peak pressure is distributed to the different floors by tributary façade area. For modeling purposes, a leaning column is added to the side of the building and the floor mass is lumped at these nodes, as shown in Figure 5-14. This will prevent high frequency axial modes from developing in the results.

Figure 5-15 shows the nonlinear time-history displacement at each floor of the building. The structure goes from an original elastic period of 0.695 s to an apparent period of roughly 3 s.

The maximum deflections are shown in Table 5-1, where Δ is the total deflection, δ is the interstory deflection, and H is the story-to-story height. The deflection between the 1st (ground) floor and 2nd floor is the most critical. With $\delta = H/46 < H/25$ and a maximum end rotation of $\theta = 1.2° < 2.0°$ (based on a maximum beam deflection of 3 in.), it meets the deflection and rotation criteria, as stated in Section 5.1. Hence, this structure, as designed for wind, safely withstands the blast load.

Figure 5-16, Figure 5-17, Figure 5-18 and Figure 5-19 show the response of the different elements that either start to yield or completely fail. Figure 5-20 shows the deflection of the second floor beam at midspan. Figure 5-21 shows a key elevation locating these elements. Figure 5-16 shows that the first floor compressed diagonal fails in compression. After this diagonal loses all of its strength, the other elements remain elastic or start to yield without considerable ductility. Hence, the permanent deformation

in the overall structure is small. Even though other diagonals yield, only one diagonal fails completely because the others are not exposed to as high of a ductility demand. In other terms, the maximum load and deformation that they experience lands somewhere along the strain hardening slope in the plastic region of their axial hinges.

Note that in Figure 5-16 and Figure 5-17 First Floor denotes the diagonal that spans from the first (ground) floor up to the second floor. Similarly, Second Floor denotes the diagonal that spans from the second to the third floor, and third floor denotes the diagonal spanning from the third floor up to the roof, as shown in Figure 5-21.

Figure 5-18 and Figure 5-20 refer to the beam in the second floor, as shown in Figure 5-14 or Figure 5-21. Note that positive is indicative of upward deflection and negative is downward in Figure 5-20.

Figure 5-19 shows the flexural strength in Column 2. The peak bending moment is 262 kip-ft, which would correspond to a stress of 35.8 ksi. The maximum compressive stress in the column is 10 ksi. The column was modeled without any hinges for simplicity, but it can be seen that the column remains elastic.
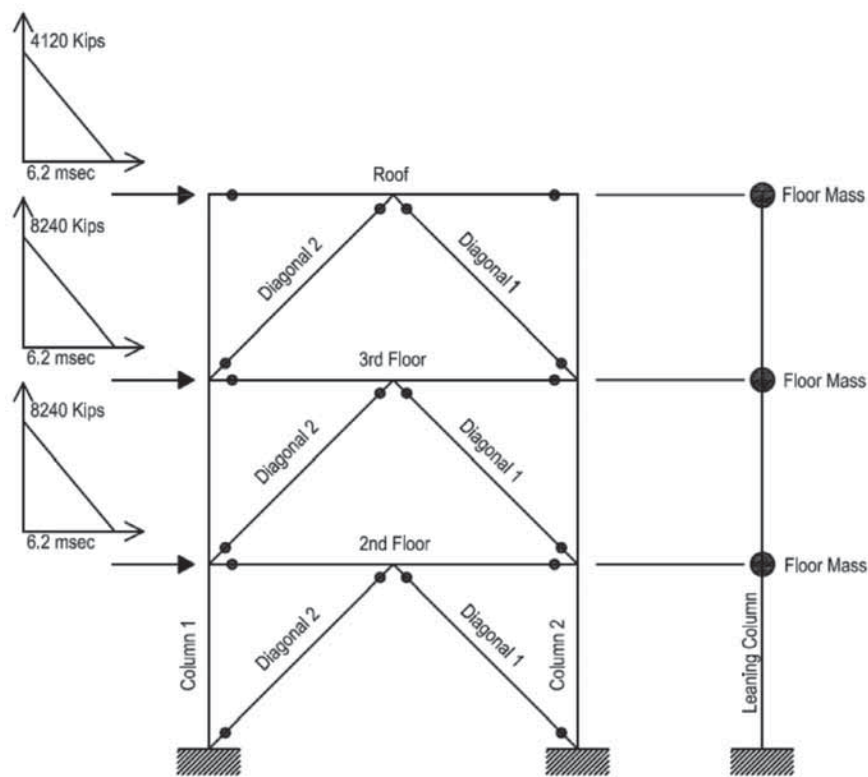

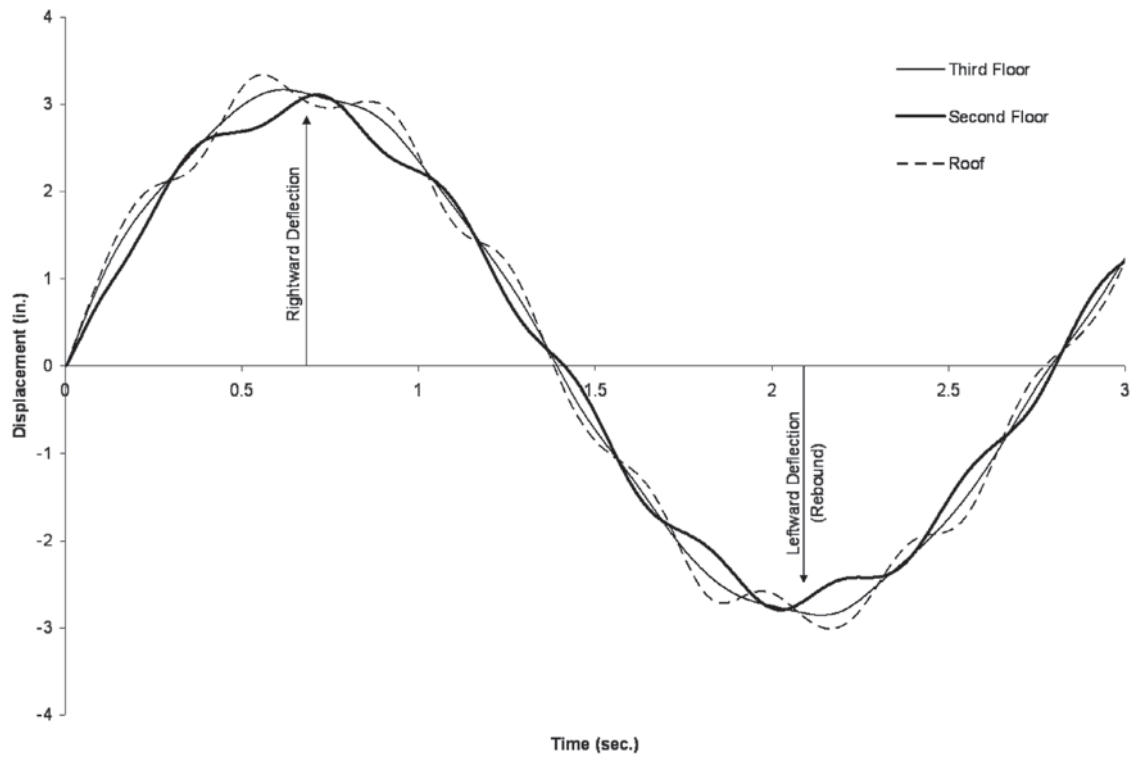*Fig. 5-14. Time-history of blast loading.*
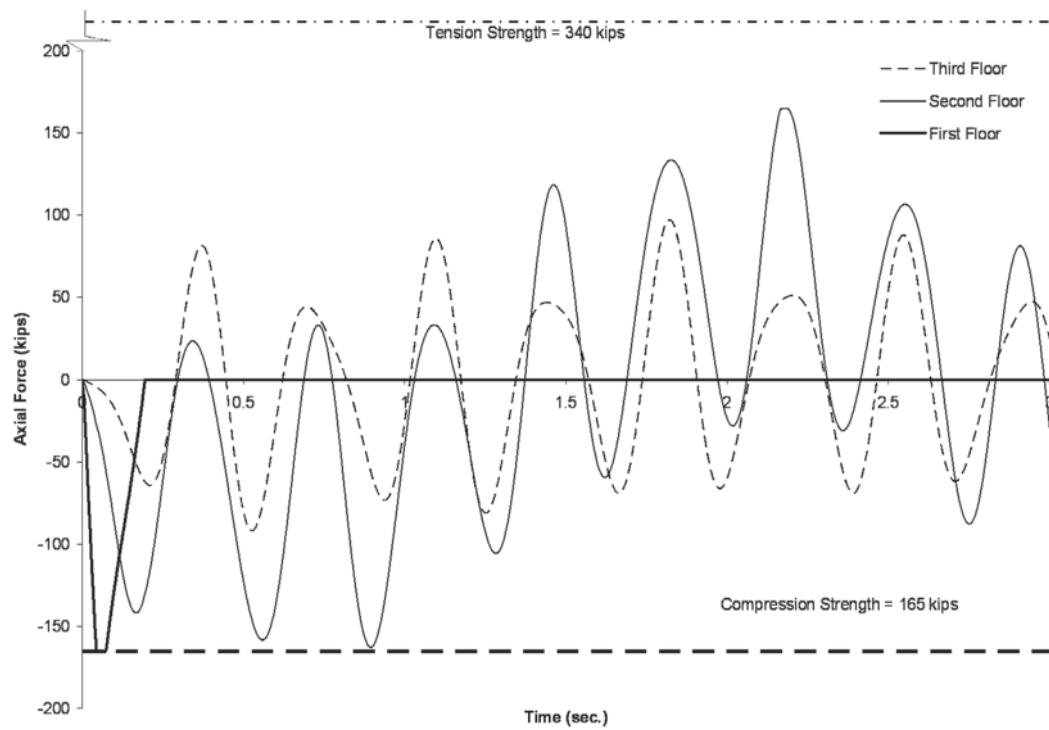
Fig. 5-15. Blast displacement.

Fig. 5-16. Force at Diagonal 1.
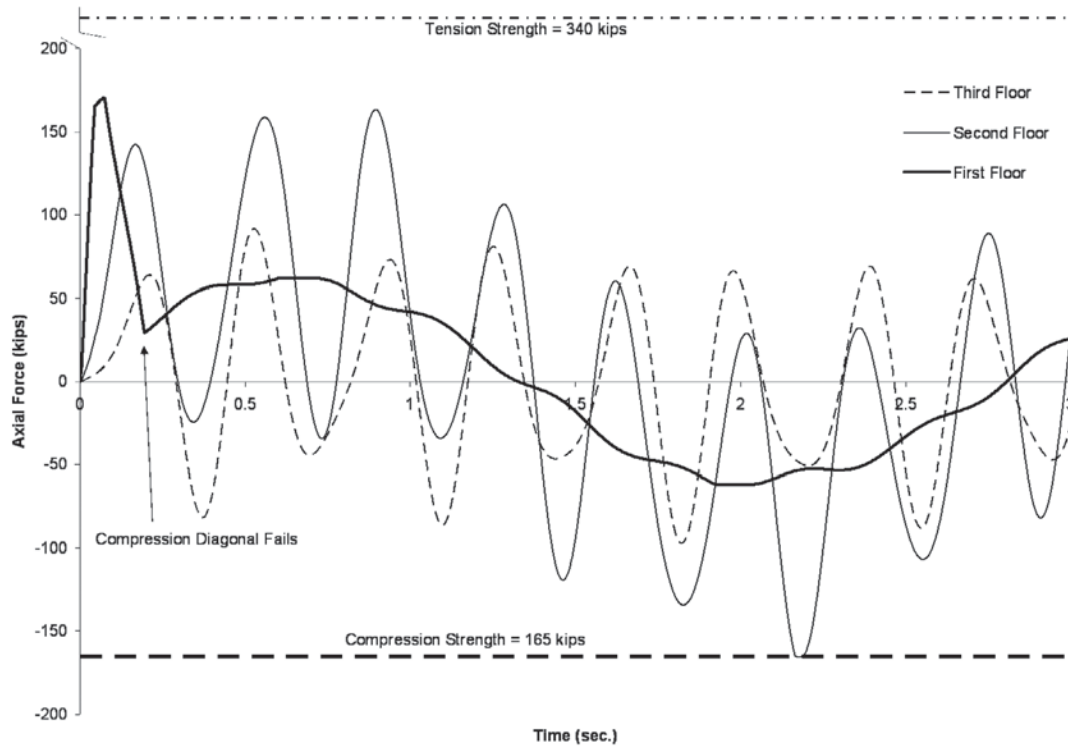
Fig. 5-17. Force at Diagonal 2.
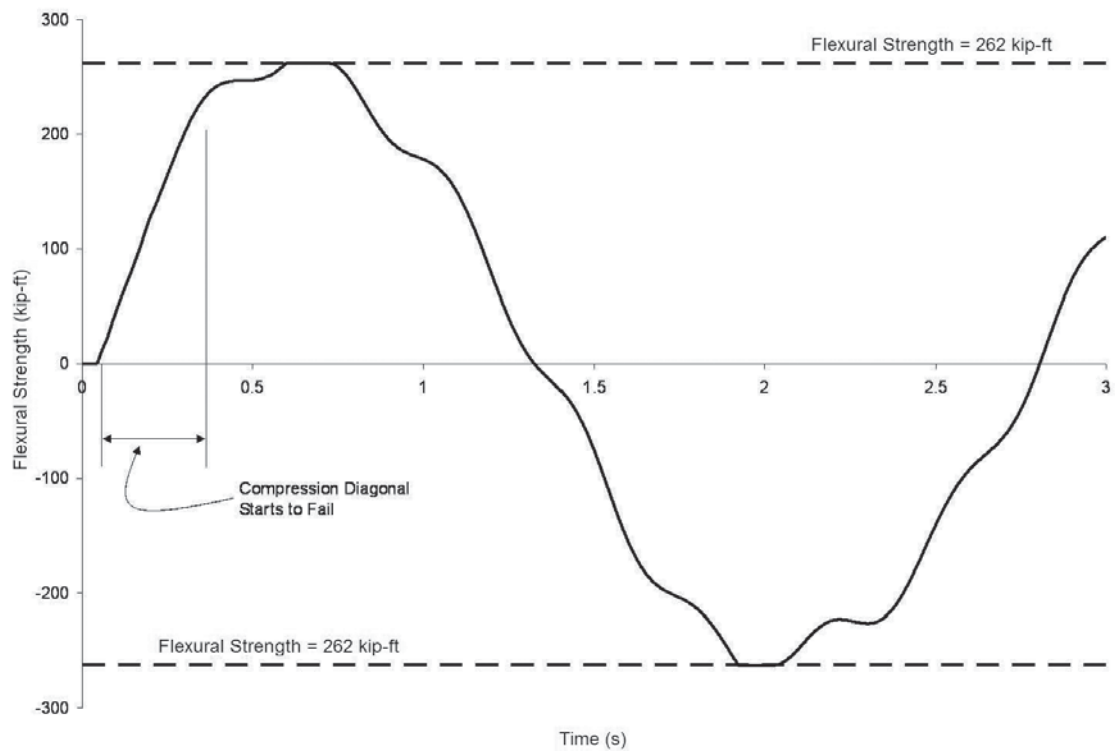
Fig. 5-18. Flexural strength of beam at second floor.
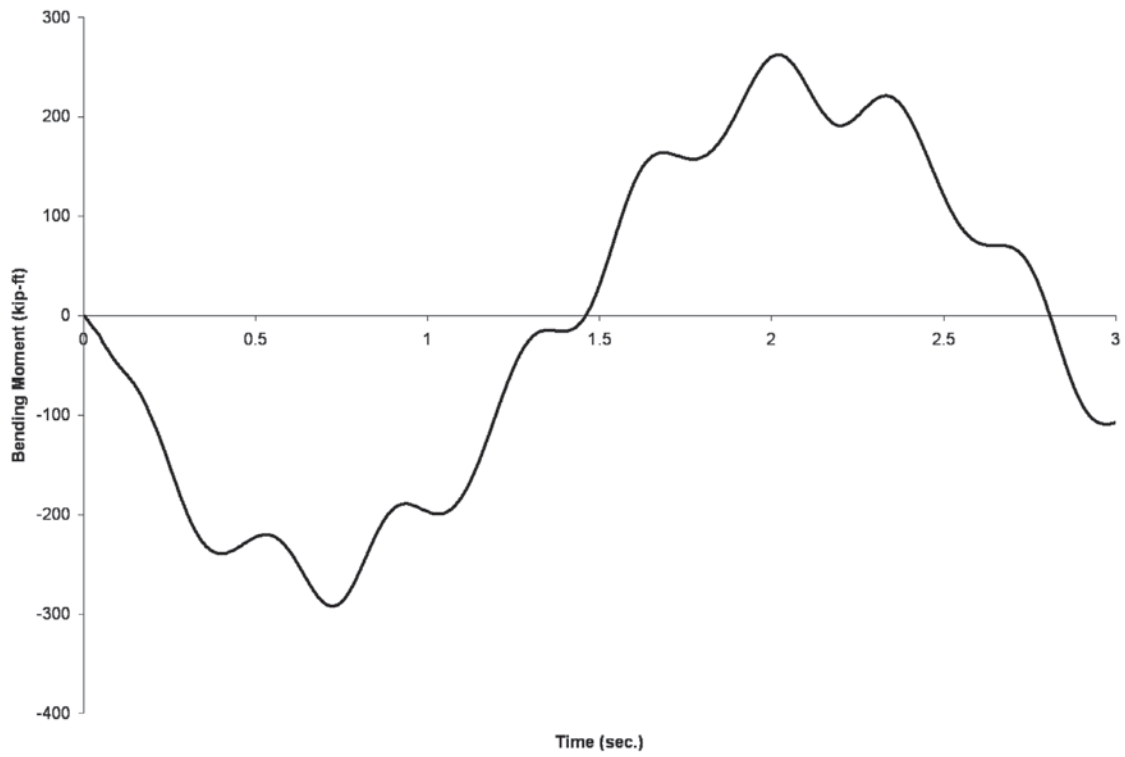
Fig. 5-19. Column 2 flexural strength.
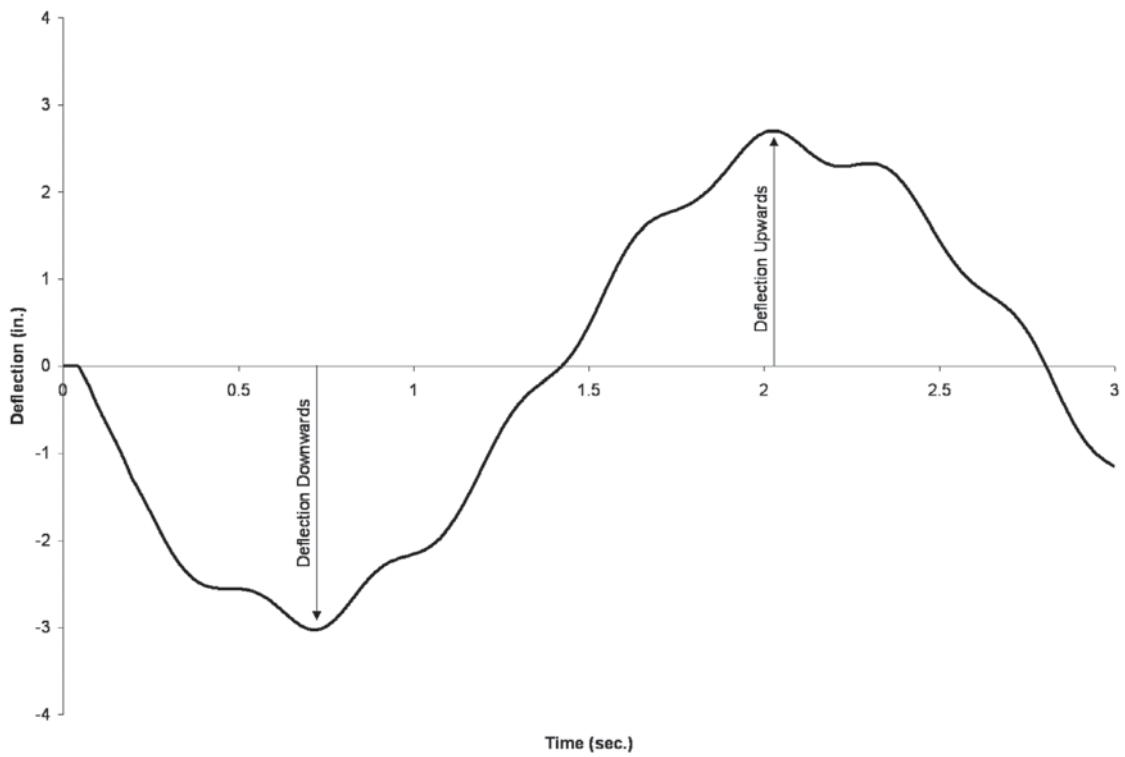
Fig. 5-20. Second floor midspan beam deflection.
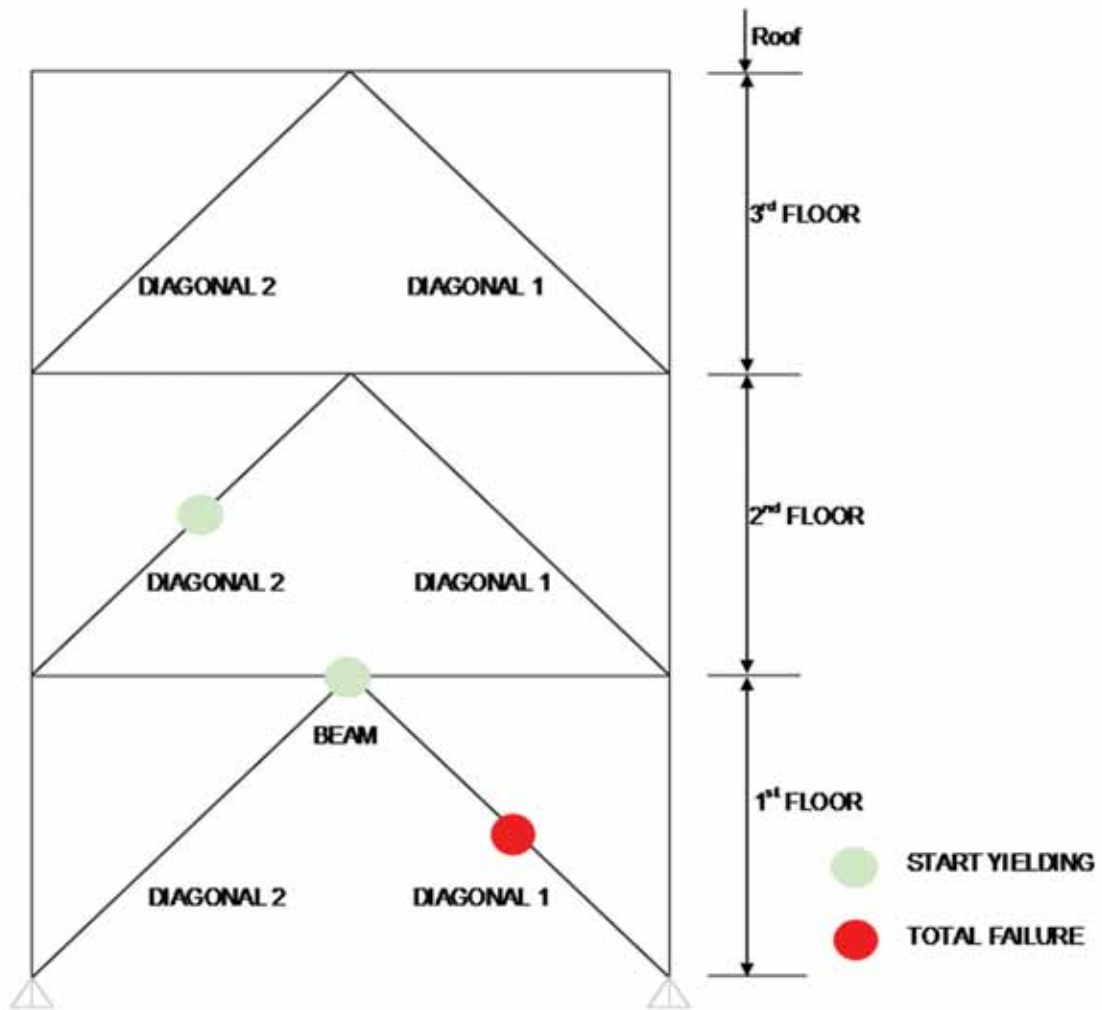
Fig. 5-21. Element response.

Chapter 6
Blast Resistant Analysis and Design of Structural Members

The purpose of this chapter is to define the structural properties used for nonlinear dynamic models, to understand the analysis results, and to classify or design the structural element for the desired criteria. Failure modes will be explained to determine the mechanism of collapse for the structural element. Deformation criteria will be established to classify the response of the element. The primary failure modes used to design structural elements are breaching, tension-compression, bending, shear, and axial-bending interaction. The secondary modes of failure such as brittle failure caused by local stress concentrations, welding, low temperatures, etc. are beyond the scope of this guide.

Member failure is defined through support rotation and ductility ratio. This definition is intended for the single degree of freedom systems (SDOF) and simplified multiple degree of freedom systems (MDOF). Strain based failure criteria may also be justified if strains are calculated using finite element methods that characterize the material properties, the details of construction, and many of the possible failure mechanisms. As used in this guide, ductility is defined as the ratio between the maximum deflection and the maximum elastic deflection. This parameter is smaller than one if the behavior is elastic and larger than one if the behavior is plastic.

The blast design of several building elements is exemplified in this chapter. The examples follow the load path from the façade to the lateral load resisting system. Examples include the design of a façade girt, façade column, perimeter beam, and some elements of the lateral load resisting systems designed in Chapter 5.

This chapter does not consider the energy dissipated along the load path and assumes that the elements are absorbing all of the energy, which is a conservative assumption. The designer should give attention to the reactions and the connections along the load path from one member to another as these will be required to transfer the full energy of the system. It will be shown that on the order of 80% of the energy from a blast load can be dissipated along the load path.

Blast mitigation design should be integrated with the overall structural design, not left to some later stage in design, as it may increase the stiffness or the mass of the structure which would affect the response of the structure to other loads.

Various programming tools or commercial software can be used to model and analyze the structures used as examples in this chapter. Table 4-2 shows a list of some of this software.

6.1 MATERIAL PROPERTIES OF STEEL FOR BLAST DESIGN

6.1.1 Strength Increase Factor (SIF)

For steel grades of 50 ksi or less, the average yield stress of steels currently produced is approximately 10% larger than the stress specified by ASTM; therefore, for blast design the specified minimum yield stress should be multiplied by a strength increase factor, *SIF*, of 1.10. For higher grades this average is smaller than 5%; therefore, no factor is used on those grades. Ultimate strength is not factored in any case.

6.1.2 Dynamic Increase Factor (DIF)

Steel mechanical properties vary with the time rate of strain. As compared with the static values normally used in design, the properties vary for dynamic loading as follows:

- The yield point increases substantially.
- The ultimate tensile strength increases slightly.
- Modulus of elasticity does not vary and the elongation at rupture either remains constant or is slightly reduced.

The factor used to modify the static stress due to dynamic load is the dynamic increase factor, *DIF*. These factors are defined in *Design of Blast Resistant Buildings in Petrochemical Facilities* (ASCE, 2010b), UFC 3-340-02, and PDC TR-06-01 (USACE, 2008).

The values summarized in Table 6-1 are based on an average strain rate of 0.10 in./in./s which is characteristic of low pressure explosions. These values are appropriate for most conventional explosive load environments. Higher values of strain rate give larger values of *DIF*. UFC 3-340-02 provides values of *DIF* for different average strain rates.

6.1.3 Dynamic Design Stress

Based on the expected ductility ratio and/or the damage allowed in the structural element, different dynamic yield points are defined by UFC 3-340-02. If the ductility ratio is smaller than or equal to 10, the dynamic design stress is:

Table 6-1. Dynamic Increase Factors (DIF) for Structural Steel and Aluminum			
	DIF (Low Pressure)		
ASTM Material Specification	Yield Stress		Ultimate Strength
	Bending/Shear	Tension/Compression	
A36 (36 ksi)	1.29	1.19	1.10
A588 (50 ksi)	1.19	1.12	1.05
A514 (90–100 ksi)	1.09	1.05	1.00
A446/A653 (40 ksi)	1.10	1.10	1.00
A572 (42–65 ksi)	1.19	1.10	1.00
A992 (50–65 ksi)	1.19	1.10	1.00
Stainless Steel Type 304/ AMS5501	1.18	1.15	1.00
Aluminum, 6061-T6/ AMS4113	1.02	1.00	1.00

$$f_{ds} = f_{dy} = SIF(DIF)F_y \qquad (6\text{-}1)$$

If the ductility ratio is greater than 10, the dynamic design stress is:

$$f_{ds} = f_{dy} + \frac{f_{du} - f_{dy}}{4} \qquad (6\text{-}2)$$

where

$$f_{du} = DIF(F_u) \qquad (6\text{-}3)$$

The dynamic design stress for shear is:

$$f_{dv} = 0.55 f_{ds} \qquad (6\text{-}4)$$

UFC 3-340-02 Figure 5-4 defines the blast criteria and the structural properties used in Figure 6-1. This figure depicts how the dynamic design stresses relate to the deformation (shown on the bottom line of the figure). The design section modulus is also dependent on the deformation in the member as well, and will be discussed in Section 6.3.5.
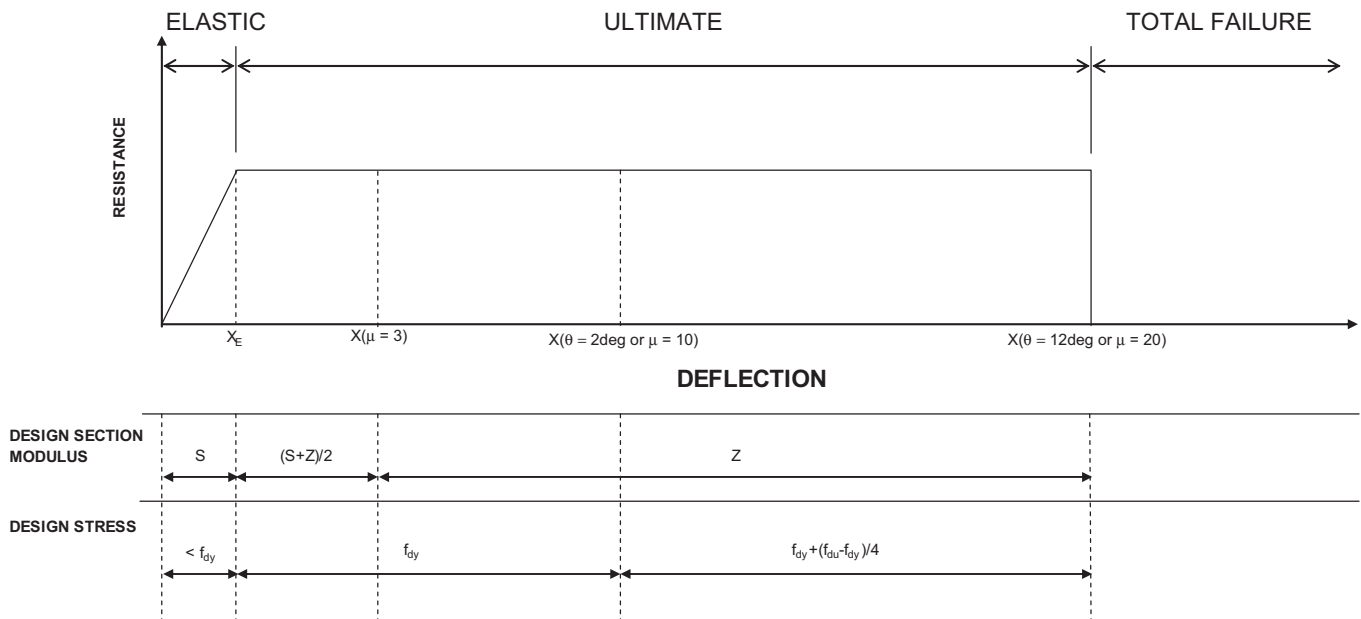
Fig. 6-1. UFC 3-340-02 criteria (DOD, 2008).

For typical design, unless governed by more detailed requirements, such as ASCE (2010b), UFC 3-340-02, or other established criteria discussed in Chapter 3, a simplified value may be used as follows:

$$f_{ds} = 1.30F_y \qquad (6\text{-}5)$$

$$f_{du} = 1.05F_u \qquad (6\text{-}6)$$

6.2 DESIGN CRITERIA FOR BLAST DESIGN

Due to the nature of blast loading, plastic design is required and is measured by support rotations and ductility. Different codes can be used to define the strength of the elements but no safety factor should be used in those calculations. Local and global stability should be guaranteed in those elements where plasticity must be achieved and ductility criteria must be used. Design and failure criteria are based on the results of explosive tests conducted by the U.S. government and reported in publications like UFC 3-340-02, and the *Protective Construction Design Manual* (AFESC, 1989).

The designer should determine, at the beginning of the project, the acceptance criteria to be used based on the level of protection desired for the building. Most projects have predefined criteria that must be used.

6.2.1 Load Combinations

In the absence of other governing criteria, the following load combination should be used:

$$1.0D + 0.25L + 1.0B \qquad (6\text{-}7)$$

where
D = dead load
L = live load
B = blast load

6.2.2 Ultimate Strength

Strength Factor

According to Section 6.1, the material properties for steel are increased for blast design based on the high strain rate produced by blast loading. Also, independent of the method used for design, any material or safety factor should be removed. Thus, for load and resistance factor design the resistance factor used in blast design is $\phi = 1.00$ and for allowable strength design the safety factor used in blast design is $\Omega = 1.00$. Thus, the design strength is taken equal to the nominal strength, without reduction.

Local Buckling

Blast design is based on the ultimate strength of the elements and the ductility of the system. Structural members subject to blast loads should be capable of undergoing plastic deformation. To allow hinges to form in the elements, sections must be compact in accordance with criteria in Appendix 1 of the AISC *Specification for Structural Steel Buildings* (AISC, 2010a), hereafter referred to as the AISC *Specification*, as this is an inelastic analysis and design procedure. The dynamic design stress, f_{ds}, should be used in place of the specified minimum yield stress, F_y, in the calculation of the limiting slenderness to establish the local buckling criteria.

Flexural and Lateral-Torsional Buckling

Flexural members should be sufficiently braced to permit plastic hinge formation. For these elements, lateral bracing as specified by the AISC *Specification* should be sufficient to remove lateral-torsional buckling as the controlling limit state. For elements designed to remain elastic, such as columns, transfer elements, etc., AISC *Specification* criteria should be applied in a way that ensures the stability of the member under the blast load combination based on the dynamic design stress neglecting any strength factor.

6.2.3 Deformation Criteria

Support Rotation

Support rotation is defined as the tangent angle at the support formed by the maximum beam deflection. In the plastic range, this value, neglecting the elastic deformation, can be related to the plastic hinge rotation. Note that if the hinge is not formed at the center of the beam, the support rotations are different on each side and the maximum rotation should be considered as shown in Figure 6-2.

Ductility

Ductility, μ, as used in blast design is defined as the ratio between the maximum displacement, Δ_m, and the elastic displacement, Δ_{el}, as follows:

$$\mu = \frac{\Delta_m}{\Delta_{el}} \qquad (6\text{-}8)$$

where the type of displacement is based on the element being considered. For example, an axially loaded element will be defined by its elongation, while an element in bending will be defined by rotation and/or deflection.

Deformation Response Range

Design of Blast Resistant Buildings in Petrochemical Facilities (ASCE, 2010b) classifies the deformation range in three different damaged stages: low, medium and high response

Table 6-2. Response Criteria for Structural Steel (NYCBC, 2008)		
Element	Maximum μ	Maximum θ, degrees
Open web steel joists[1]	2	6
Steel beams	20	10
Steel columns	5	6
[1] Response ratio (ductility) controlled by downward loading and rotation controlled by upward loading		

Table 6-3. *Design of Blast Resistant Buildings in Petrochemical Facilities,* Response Criteria, Low Response (ASCE, 2010b)		
Element	Maximum μ	Maximum θ, degrees
Beams, girts, purlins	3	2
Frame members	1.5	1
Cold-formed panels	1.75	1.25
Open-web joists	1	1
Plates	5	3

as a function of the damage in the building. UFC 3-340-02 also classifies the response as a function of the protection provided by the structural elements. This guide uses a low level of protection that implies a high response because the intent is to provide a design that avoids imminent collapse but allows substantial damage.

For different structural elements, this guide follows the response criteria shown in Table 6-2, which conforms to Table 1626.9.3 of the New York City (NYC) Building Code (NYCBC, 2008). The rotation criteria in Table 6-2 refer to support rotations. The criteria are defined for the behavior of a single element. These criteria apply to the design of

members, as the connections between members may have different criteria. The ductility limits are linked to a given mode of response. A flexural ductility is different from shear or tension.

There are several other sources for response criteria in addition to the NYC Building Code. It is up to the designer to determine which criteria are most applicable and should be used. Tables from UFC 3-340-02, *Design of Blast Resistant Buildings in Petrochemical Facilities* (ASCE, 2010b), and FEMA 356 (FEMA, 2000b) are included in this guide as Table 6-3, Table 6-4 and Table 6-5. The 2010 edition of *Design of Blast Resistant Buildings in Petrochemical*
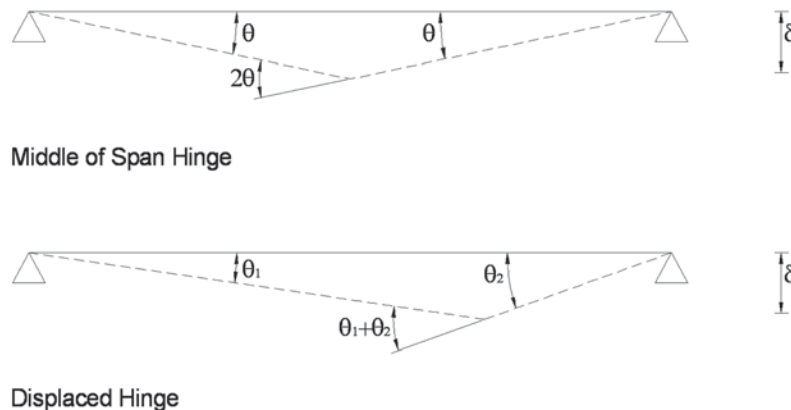
Fig. 6-2. Relationship of hinge rotation to support rotation.

Table 6-4. UFC 3-340-02 Response Criteria (DOD, 2008)			
Element		**Deformation Type**	**Maximum Deformation**
Beams, purlins, spandrels or girts	—	θ μ	12° 20
Frame structures	—	δ θ	H/25 2°
Cold-formed steel floor and wall panels	Without tension-membrane action	θ μ	1.25° 1.75
	With tension-membrane action	θ μ	4° 6
Open-web joists	—	θ μ	2° 4
Plates	—	θ μ	12° 20
θ = rotation μ = ductility δ = deflection			

Table 6-5. FEMA 356 Tension Response Criteria (FEMA, 2000b)					
	Acceptance Criteria				
	Plastic Deformation				
	IO	**Primary Members**		**Secondary Members**	
Element		**LS**	**CP**	**LS**	**CP**
Braces in tension	$0.25\Delta_T$	$7\Delta_T$	$9\Delta_T$	$11\Delta_T$	$13\Delta_T$
CP = collapse prevention LS = life safety IO = immediate occupancy					

Facilities (ASCE, 2010b) also has medium response and high response criteria in addition to the low response criteria included in Table 6-3. It is recommended that these sources be consulted for more information in determining design criteria.

In Table 6-5, Δ_T refers to the axial deformation at expected yielding load. It is important to note that FEMA is the only reference to have criteria for a tension member. This guide will therefore use these criteria for tension elements. Because this guide is concerned with a low level of security and prevention of collapse, it is recommended that the collapse prevention (CP) values be used. For information on distinguishing between primary and secondary members, see the discussion in FEMA 356 (FEMA, 2000b). FEMA 356 also includes acceptance criteria for other element types.

To help put these criteria in perspective, examine the values for a beam with a 30-ft-long span that starts to yield at midspan when the deflection is 4 in. A support rotation of 10°, as indicated in Table 6-2 as the maximum rotation for steel beams, implies a deflection of:

$$(15.0 \text{ ft})(12 \text{ in./ft})(\tan 10°) = 31.7 \text{ in.}$$

A ductility of 1 implies a deflection of 4 in. Thus, a ductility of 20, again taken from Table 6-2, would require a deflection of 80 in. Obviously, this level of ductility is not achievable and the support rotation controls. These, and values for the other criteria sources, are tabulated in Table 6-6.

Other criteria exist, such as U.S. Army Corps of Engineers Protective Design Center (USACE PDC) criteria, which are more restrictive and are usually used in commercial and governmental buildings. In Chapter 5, the maximum lateral displacement was limited to H/25 and a maximum plastic rotation of 2° was imposed to the overall behavior of the lateral system.

6.3 FAILURE MODES

6.3.1 Breaching

For blast loads in contact (or in very close proximity) to an element, the element will be breached before responding in a flexural manner due to the high pressure produced by the

Table 6-6. Example Deformation Response		
Criteria	**μ-controlled**	**θ-controlled**
NYCBC	20(4.00 in.) = 80.0 in.	(15.0 ft)(12 in./ft)(tan 10°) = 31.7 in.
ASCE	3(4.00 in.) = 12.0 in.	(15.0 ft)(12 in./ft)(tan 2°) = 6.29 in.
UFC	20(4.00 in.) = 80.0 in.	(15.0 ft)(12 in./ft)(tan 12°) = 38.3 in.

explosion. If the scaled distance as defined in Chapter 2 is below 2, it is possible for the element to breach before the overall response of the structural element starts.

For very close charges, temperature and the shock wave are important, in addition to the airblast. An explosion in direct contact, with a wall will interact directly with it and will induce a shock wave inside the wall. The speed and magnitude of the shock waves can cause the wall to crack internally. For example, when the shock wave reaches the opposite face of a concrete wall, a section of concrete may scab or separate from the wall due to the energy of the shock wave exceeding the tensile strength of the material.

For the preliminary design of the slab thickness, this Design Guide uses an experimental graphic found in UFC 3-340-02 and shown in Figure 6-3. The input for this graph is the thickness (T, feet), the stand-off (R, feet) and the charge (W, equivalent pounds of TNT). Depending on the performance requirements, the slab may be designed to allow a local breach in the bay closest to the blast, yet withstand the blast in adjacent bays. Typically, the stand-off and charge weight is specified in the data provided by the blast consultant. Other breaching curves can be found in UFC 3-340-01 (DOD, 2002), however, this document is export controlled and not available to the public.

6.3.2 Tension

According to AISC *Specification* Section D2, the available strength for elements under tension based on yielding of the member on the gross section is defined by:

$$\phi P_n = \phi F_y A_g \qquad (6\text{-}9)$$

where
A_g = gross area of the element
F_y = specified minimum yield stress of the material
ϕ = resistance factor, 0.90

Available strength due to the limit state of tension rupture through the net section should also be checked using AISC *Specification* Section D2, as applicable.

For blast loading:
F_y = f_{ds}, the dynamic design stress defined in Equations 6-1 and 6-2 (or Equation 6-5)
F_u = f_{du}, the dynamic design stress defined in Equation 6-3 (or Equation 6-6)
ϕ = 1.00, the resistance factor defined in Section 6.2.2.1

Axial hinge properties for these elements are elastic-plastic. If necessary, for computational stability, a hardening slope of 0.1% can be used in the plastic area. Examples of these hinges will be shown later in this chapter.

6.3.3 Compression

The available strength of compression elements, based on AISC *Specification* Chapter E is governed by the following equation:

$$\phi P_n = \phi F_{cr} A_g \qquad (6\text{-}10)$$

where
A_g = gross area of the element
F_{cr} = critical stress
ϕ = 0.90

For blast loading:
F_{cr} = critical stress determined in accordance with AISC *Specification* Chapter E substituting f_{ds} for F_y
ϕ = 1.00, the resistance factor defined in Section 6.2.2.1

For a tension-compression hinge, the recommendations of FEMA 356 (FEMA, 2000b) can be used, if no other proper criteria are defined.

6.3.4 Shear

For I-shapes it is assumed that flexure is carried primarily by the flanges while shear is carried primarily by the web. Thus, moment-shear interaction is neglected. The available strength of elements in shear, based on AISC *Specification* Chapter G, is governed by the following equation:

$$\phi V_n = \phi f_v A_w \qquad (6\text{-}11)$$

where
A_w = area of the web
f_v = $0.6 F_y$
ϕ = 1.00 for most W-shapes

For blast loading:
A_w = area of the web. Note that in UFC 3-340-02, A_w is defined as only the area between the flange plates. However, in normal design practice the AISC *Specification* definition of A_w equal to the overall

depth times the web thickness is used. This guide uses the AISC definition.

f_v = f_{dv} = dynamic design stress for shear ($f_v = 0.55f_{ds}$ from Section 6.1.3)

ϕ = 1.00 = resistance factor defined in Section 6.2.2

Connection strength is, in most cases, more critical than the shear strength of the beam.

6.3.5 Flexure

Based on the plastic response allowed for blast design, a plastic hinge will be allowed to form in the structural element. The assumption that the plastic hinge is concentrated at a section will be taken as adequate for practical purposes, even though deflection values may not be accurate.

The definition of plastic moment is a function of the ductility ratio expected in the structural element, as was shown in Figure 6-1. Based on Figure 6-4(a), if the ductility ratio is smaller than 3, the full plastic moment cannot be developed by the section. Thus, an average between the elastic and plastic section modulus is used when $1 < \mu < 3$ [Figure 6-4(b) and Figure 6-5]. The available flexural strength is:

$$\phi M_n = \phi M'_p = \phi f_{ds}\left(\frac{S+Z}{2}\right) \qquad (6\text{-}12)$$

where

S = elastic section modulus

Z = plastic section modulus

ϕ = 1.00

If the ductility ratio expected is larger than 3, the full plastic moment can be developed (Figure 6-4(c)). Thus, the available flexural strength is:

$$\phi M_n = \phi M_p = \phi f_{ds} Z \qquad (6\text{-}13)$$
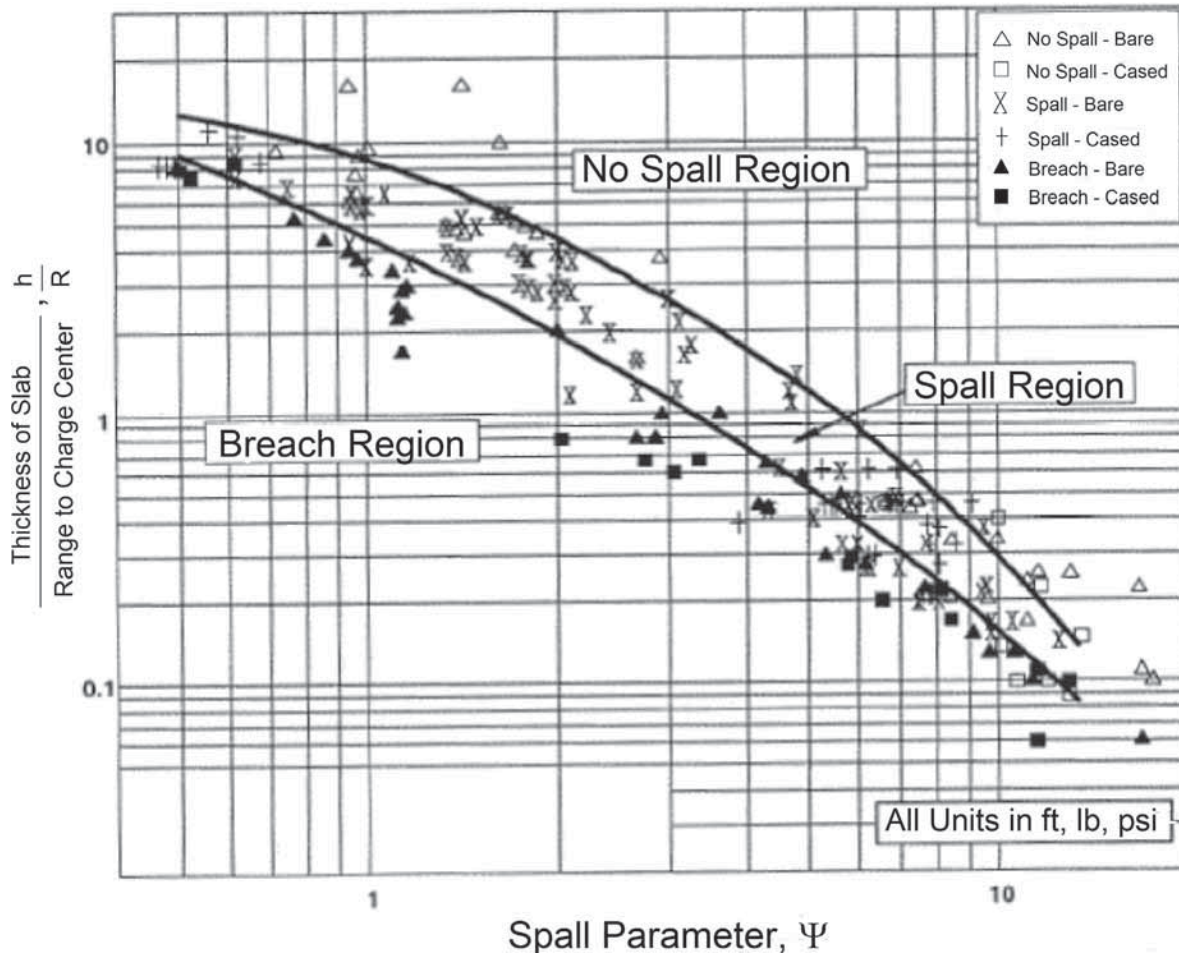
Fig. 6-3. UFC 3-340-02 breach chart (DOD, 2008).

For hand calculations, the behavior of the section is assumed elastic-perfectly plastic. For hand calculations in this guide, the plastic flexural strength of the section is given by Equation 6-13. To avoid computational instabilities, the hinge properties used for computer calculations should include plastic hardening, where the yield moment is defined by Equation 6-12 and the ultimate moment is defined by Equation 6-13 as recommended in UFC 3-340-02.

Provisions for lateral bracing are also given in UFC 3-340-02, although they are not discussed here.

6.3.6 Combined Forces

Provisions for combined axial force and flexure are presented in AISC *Specification* Chapter H. The strength and resistance factors defined previously are used in the appropriate interaction equations. If the designer wants to design an element to behave plastically, the member must be braced sufficiently in order to develop the full plastic moment. To dissipate the maximum energy, plastic design is recommended for all members (with the exception of columns and transfer beams which should remain elastic).

In the three panels:

(a) $\mu \leq 1$
$$\sigma = \frac{M}{S}$$

(b) $1 < \mu < 3$
$$\sigma = \frac{M}{\left(\dfrac{S+Z}{2}\right)}$$

(c) $\mu \geq 3$
$$\sigma = \frac{M}{Z}$$
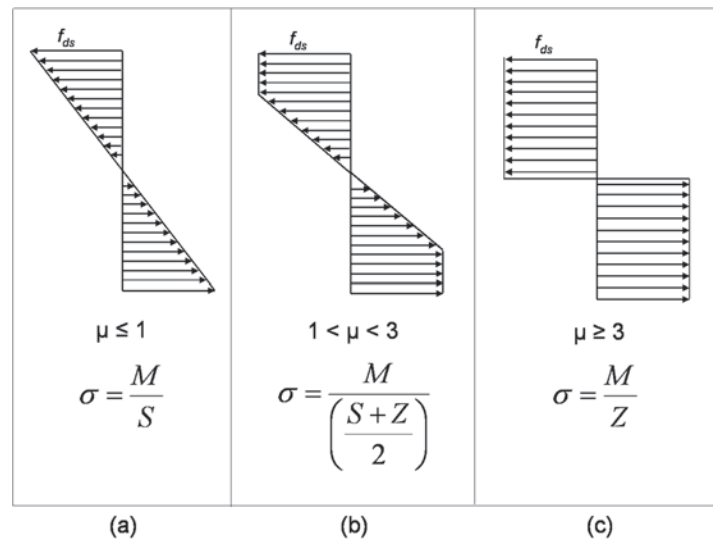
Fig. 6-4. Design section modulus (DOD, 2008).

Design moment for beams with moderate ductility ($\mu \leq 3$)

$$M_p = M_1 = f_{ds}\left(\frac{S+Z}{2}\right)$$

Design moment for beams with large ductility ($\mu > 3$)

$$M_p = M_2 = f_{ds}Z$$
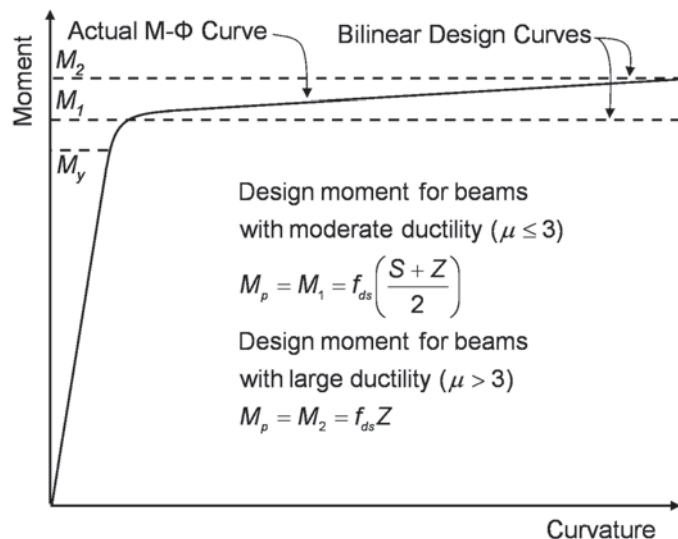
Fig. 6-5. Design moment for beams with moderate ductility (DOD, 2008).

6.4 DESIGN EXAMPLES

Example 6.1—Design of Structural Elements Subject to Indirect Blast Loading

Given:

In this example, the structural elements analyzed in the examples of Chapter 5 are checked for strength, including blast loading as necessary. Specifically, the following elements are designed:

(a) The tension rod used in Example 5.1

(b) The diagonal braces used in Example 5.2

(c) Columns from Example 5.1.

(d) The second floor beam from Example 5.2

The elastic-plastic behavior for each element used in Chapter 5 is defined in the following. The elements designed in this section all carry blast load, but are not subject to direct pressure from the blast. Example 6.2 will examine the effects of elements directly subject to blast pressure. The criteria used in this example to define the strength of the elements is based on UFC 3-340-02, unless otherwise noted. For element design, assume that there is no energy dissipation along the load path. A more accurate and less conservative procedure is to use the effect of the dynamic reactions of one member on another member along the load path.

When using member reactions to load adjacent members, natural frequencies should be compared. If the natural frequencies are close, a simultaneous solution is required to account for the interaction between the two members. If the period of the primary element (i.e., beam) is at least twice the period of the secondary element (i.e., girder), they can be treated as individual single degree of freedom (SDOF) structures on unyielding supports. If not, a multiple degree of freedom (MDOF) solution of the same system is required similar to what was discussed in Section 4.5.

The tension rods are ASTM A572 Grade 50 steel, the W-shapes are ASTM A992 steel, and the HSS shapes are ASTM A500 Grade C.

Solution:

From Table 2-4 of the AISC *Steel Construction Manual* (AISC, 2011a), hereafter referred to as the AISC *Manual*, the material properties are:

ASTM A572 Grade 50
$F_y = 50$ ksi
$F_u = 65$ ksi

ASTM A992
$F_y = 50$ ksi
$F_u = 65$ ksi

ASTM A500 Grade C
$F_y = 50$ ksi
$F_u = 62$ ksi

From AISC *Manual* Table 1-1 and Table 1-12, the geometric properties are:

HSS6×6×¼
$A_g = 5.24$ in.^{2}
$r = 2.34$ in.

W12×53
$A_g = 15.6$ in.^{2}
$r_y = 2.48$ in.

W12×35
$I_x = 285$ in.^{2}
$S_x = 45.6$ in.^{3}
$Z_x = 51.2$ in.^{3}

(a) Tension Rod of Example 5.1

The tension rod used in Example 5.1 is checked and the tension behavior is defined. The 38-ft-long rod is ¾ in. in diameter. Because the rod is upset, use the full cross-sectional area.

For a ductility ratio $\mu \leq 10$, the dynamic design stress for tension, as defined in Equation 6-1, is:

$$\begin{aligned} f_{ds} &= f_{dy} \\ &= (SIF)(DIF)F_y \\ &= 1.10(1.10)(50 \text{ ksi}) \\ &= 60.5 \text{ ksi} \end{aligned}$$

(6-1)

For a ductility ratio $\mu > 10$, the dynamic design stress, defined in Equation 6-2, is:

$$\begin{aligned} f_{ds} &= f_{dy} + \left(\frac{f_{du} - f_{dy}}{4} \right) \\ &= 60.5 \text{ ksi} + \left[\frac{1.05(65 \text{ ksi}) - 60.5 \text{ ksi}}{4} \right] \\ &= 62.4 \text{ ksi} \end{aligned}$$

(6-2)

where

$$f_{du} = 1.05 F_u \text{ from Equation 6-6}$$

Comparing these dynamic design stresses to the simplified value given by Equation 6-5:

$$\begin{aligned} f_{ds} &= f_{dy} \\ &= 1.30 F_y \\ &= 1.30(50 \text{ ksi}) \\ &= 65.0 \text{ ksi} \end{aligned}$$

(6-5)

Note that the simplified value is slightly less conservative. The remainder of the calculations throughout this chapter will utilize the simplified expression of Equation 6-5.

The dynamic design shear stress defined in Equation 6-4, for a ductility ratio $\mu = 10$, is:

$$\begin{aligned} f_{dv} &= 0.55 f_{ds} \\ &= 0.55(65 \text{ ksi}) \\ &= 35.8 \text{ ksi} \end{aligned}$$

(6-4)

The available tensile strength of the rod is determined from Equation 6-9, as follows:

$$\phi P_n = \phi F_y A_g$$

(6-9)

For blast loading:

$$\phi P_n = \phi f_{ds} A_g$$

$$= 1.00(65.0 \text{ ksi})\left[\pi\left(\frac{\frac{3}{4} \text{ in.}}{2}\right)^2\right]$$

$$= 28.7 \text{ kips}$$

The hinge properties used in Example 5.1 for this rod follows the elastic-plastic curve shown in Figure 6-6. A slight slope is included in the plastic region for computational convergence purposes.

The maximum horizontal displacement obtained in Example 5.1, Figure 5-8, is 4.24 in. This is less than the horizontal deflection limit of $H/25 = 7.20$ in. for frame structures. The maximum rotation at the base of the column for this displacement is:

$$\alpha = \tan^{-1}\left(\frac{\Delta}{H}\right)$$

$$= \tan^{-1}\left[\frac{4.24 \text{ in.}}{(15.0 \text{ ft})(12 \text{ in./ft})}\right]$$

$$= 1.34° < 2°$$

For small displacement formulation, the elongation in the rod can be determined. First, the angle of the diagonal is determined as:
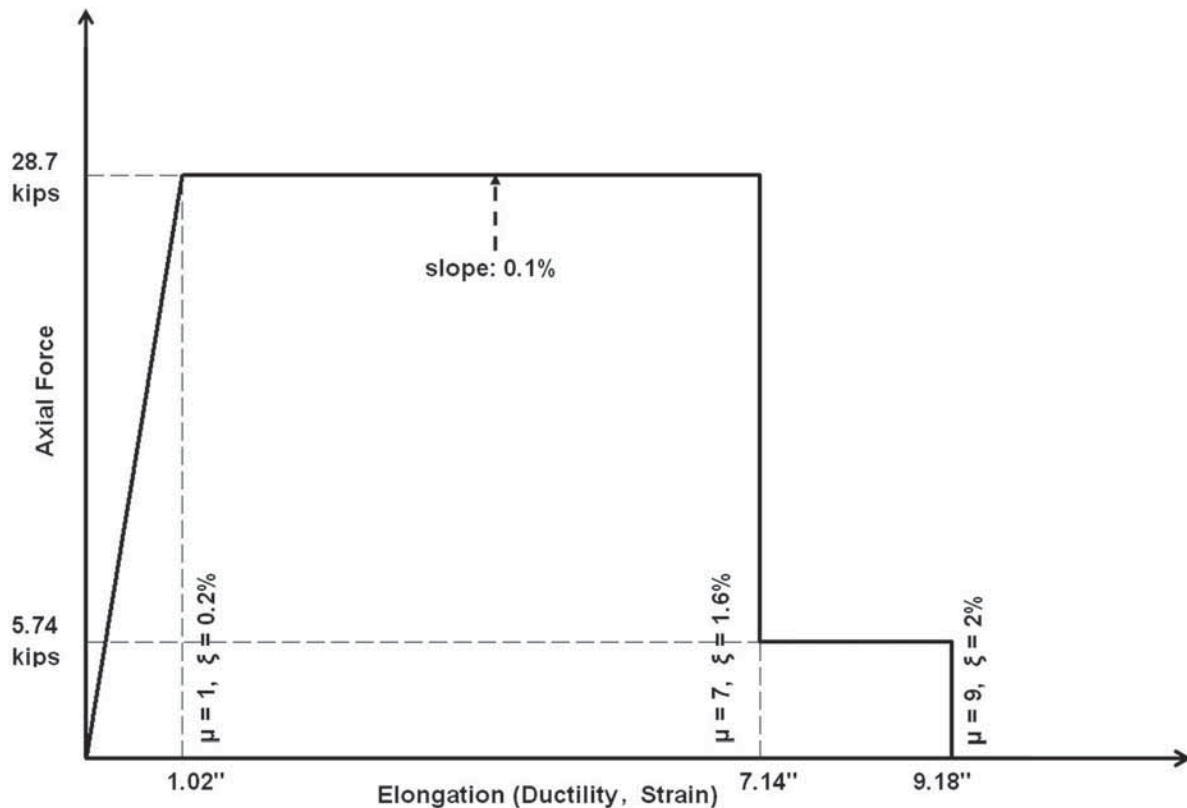
Fig. 6-6. Tension hinge properties.

$$\theta = \tan^{-1}\left(\frac{H}{L}\right)$$

$$= \tan^{-1}\left(\frac{15.0 \text{ ft}}{35.0 \text{ ft}}\right)$$

$$= 23.2°$$

Then, the elongation, assuming the top of the column moves horizontally is:

$$\Delta L = \Delta \cos\theta$$

$$= \left(4.24 \text{ in.}\right)\left(\cos 23.2°\right)$$

$$= 3.90 \text{ in.}$$

Thus, the elastic displacement of the 38-ft-long rod is:

$$\Delta_{el} = \frac{f_{ds} L}{E}$$

$$= \frac{\left(65.0 \text{ ksi}\right)\left(38.0 \text{ ft}\right)\left(12 \text{ in./ft}\right)}{29,000 \text{ ksi}}$$

$$= 1.02 \text{ in.}$$

Therefore, the ductility demand in the rod is:

$$\mu = \frac{3.86 \text{ in.}}{1.02 \text{ in.}}$$

$$= 3.78$$

This is the same value as the one obtained for the whole lateral system in Example 5.1. From Table 6-5, the allowable deformation is $9\Delta_T$. This is analogous to a response ratio of $\mu = 9$. With a ductility of 3.78, the demand is less than the capacity and therefore acceptable.

(b) Diagonal Brace of Example 5.2

The diagonal brace used in Example 5.2 is checked and the tension-compression behavior is defined in the following. The brace is a 17-ft-long HSS6×6×¼.

UFC 3-340-02 defines a maximum slenderness for compression elements as:

$$C_c = \sqrt{\frac{2\pi^2 E}{f_{ds}}}$$

$$= \sqrt{\frac{2\pi^2\left(29,000 \text{ ksi}\right)}{65.0 \text{ ksi}}}$$

$$= 93.8$$

This can be compared to the AISC *Specification* Section E3 limit for inelastic behavior of:

$$\frac{KL}{r} \le 4.71\sqrt{\frac{E}{F_y}}$$

For blast loading, $F_y = f_{ds} = 65.0$ ksi and $\phi = 1.00$, and the limit is:

$$4.71\sqrt{\frac{29,000 \text{ ksi}}{65.0 \text{ ksi}}} = 99.5$$

Note that this limit is significantly less than the suggested maximum slenderness of 200 given in the User Note in Section E2 of the AISC *Specification*. Assuming $K = 1.0$, the slenderness of this element is:

$$\frac{KL}{r} = \frac{1.0(17.0 \text{ ft})(12 \text{ in./ft})}{2.34 \text{ in.}}$$
$$= 87.2 < 93.8$$

The buckling stress is determined from AISC *Specification* Section E3 as:

$$F_e = \frac{\pi^2 E}{(KL/r)^2} \qquad\qquad (Spec. \text{ Eq. E3-4})$$
$$= \frac{\pi^2(29,000 \text{ ksi})}{(87.2)^2}$$
$$= 37.6 \text{ ksi}$$

The critical stress is:

$$F_{cr} = \left(0.658^{\frac{F_y}{F_e}}\right) F_y \qquad\qquad (Spec. \text{ Eq. E3-2})$$

For blast loading, $F_y = f_{ds} = 65.0$ ksi, and the critical stress is:

$$F_{cr} = \left(0.658^{\frac{f_{ds}}{F_e}}\right) f_{ds}$$
$$= \left(0.658^{\frac{65.0 \text{ ksi}}{37.6 \text{ ksi}}}\right)(65.0 \text{ ksi})$$
$$= 31.5 \text{ ksi}$$

Note that the buckling stress used here corresponds to the AISC *Specification*. This differs from UFC 3-340-02 which uses a buckling stress corresponding to the 1989 *Specification* (AISC, 1989).

Hence, for blast loading, with $\phi = 1.00$, the available compressive strength of the diagonal brace is:

$$\phi P_n = \phi F_{cr} A_g \qquad\qquad (6\text{-}10)$$
$$= 1.00(31.5 \text{ ksi})(5.24 \text{ in.}^2)$$
$$= 165 \text{ kips}$$

The available tensile yielding strength of the diagonal brace, from AISC *Specification* Section D2, is:

$$\phi P_n = \phi F_y A_g \qquad\qquad (6\text{-}9)$$

Table 6-7. Tension-Compression Hinge Parameters			
Loading	a	b	c
T	$11\Delta_T$	$14\Delta_T$	$0.8P_n$
C	$0.5\Delta_c$	$4.1\Delta_c$	$0.3F_{cr}$

For blast loading, $F_y = f_{ds} = 65.0$ ksi and $\phi = 1.00$, and the available tensile strength is:

$$\phi P_n = \phi f_{ds} A_g$$
$$= 1.00(65.0 \text{ ksi})(5.24 \text{ in.}^2)$$
$$= 341 \text{ kips}$$

With these tensile and compressive capacities, the tension-compression hinge properties used in Example 5.2 are derived as put forth in Figure 6-7, Table 5-6 and Table 5-7 of FEMA 356 (FEMA, 2000b). These hinge properties are used to model plastic hinges in the braces to allow for a nonlinear plastic analysis of the structure, as shown in Chapter 5.

From Table 5-7 of FEMA 356, the HSS section has the modeling parameters shown in Table 6-7 for tension and compression. Δ_T refers to the axial deformation at expected tensile yielding load, and Δ_c is the axial deformation at expected buckling load. Based on $E = 29,000$ ksi, its relationship to stress and strain, i.e., $\varepsilon = \sigma/E$ and the definition of strain, i.e., $\varepsilon = \Delta_L/L$, the values of Δ_T and Δ_c can be determined. Setting these two equations for ε equal to each other and solving for Δ_L results in:

$$\Delta_L = \frac{\sigma L}{E}$$

For tension:

$$\Delta_T = \frac{\sigma L}{E}$$
$$= \frac{(65.0 \text{ ksi})(17.0 \text{ ft})(12 \text{ in./ft})}{29,000 \text{ ksi}}$$
$$= 0.457 \text{ in.}$$
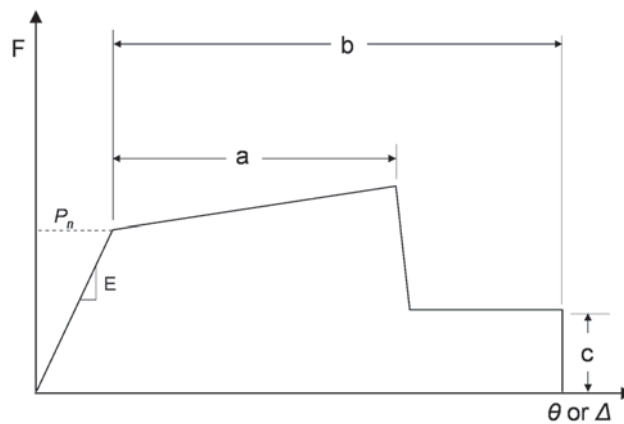
Fig. 6-7. FEMA 356 hinge parameters (FEMA, 2000b).

For compression:

$$\Delta_c = \frac{\sigma L}{E}$$

$$= \frac{(31.5 \text{ ksi})(17.0 \text{ ft})(12 \text{ in./ft})}{29,000 \text{ ksi}}$$

$$= 0.222$$

Using the allowable strain-hardening slope of 1.5% of the elastic slope for tension produces a maximum stress of approximately 1.15 of the yield stress (Fell et al., 2006). For compression, to avoid computational instabilities, use a 0.1% hardening slope. With this information, the hinge is compiled as Figure 6-8.

Results from Section 5.3, Example 5.2, indicate that only one diagonal at the first floor fails in compression while the others only started yielding. The structure remains stable despite the failure of one brace in compression due to its redundancy.

(c) Columns of Example 5.1

Columns 1 and 2 used in Example 5.1 are checked and designed to remain elastic. The column section used is a W12×53 with an effective length, $KL = 15$ ft.

For compression elements, the maximum slenderness and buckling load are checked. The UFC 3-340-02 maximum slenderness described previously is calculated to be:

$$C_c = \sqrt{\frac{2\pi^2 E}{f_{ds}}}$$

$$= \sqrt{\frac{2\pi^2 (29,000 \text{ ksi})}{65.0 \text{ ksi}}}$$

$$= 93.8$$
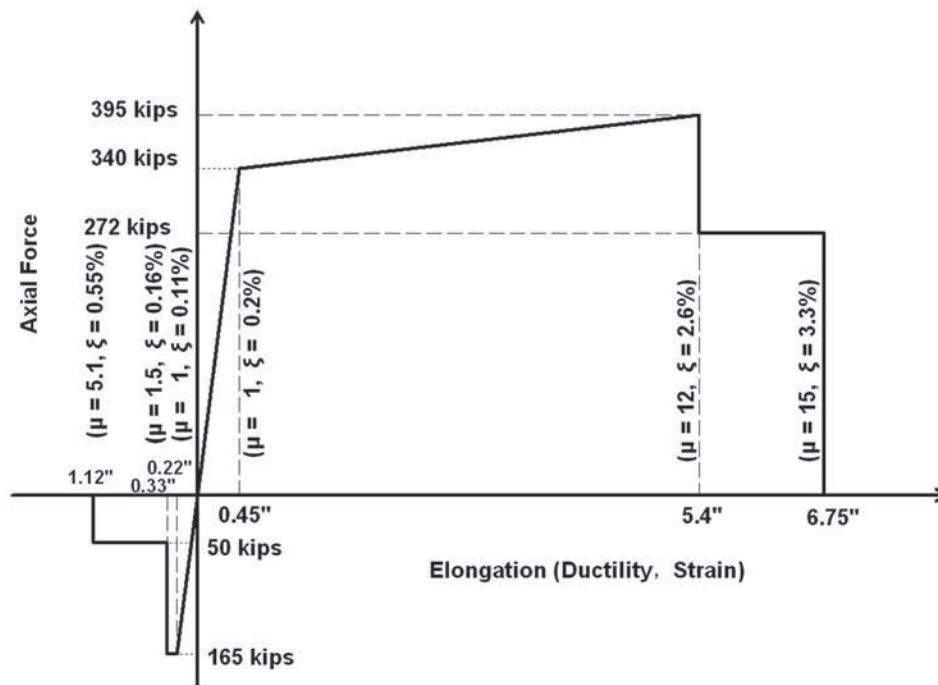
Fig. 6-8. Tension-compression hinge properties.

This can be compared to the AISC *Specification* Section E3 limit for inelastic behavior:

$$\frac{KL}{r} \leq 4.71\sqrt{\frac{E}{F_y}}$$

As determined previously, for blast loading, $F_y = f_{ds} = 65.0$ ksi, and the limit becomes:

$$4.71\sqrt{\frac{E}{f_{ds}}} = 4.71\sqrt{\frac{29{,}000 \text{ ksi}}{65.0 \text{ ksi}}}$$

$$= 99.5$$

Assuming $K = 1.0$, the slenderness of the W12×53 is:

$$\frac{KL}{r_y} = \frac{1.0(15.0 \text{ ft})(12 \text{ in./ft})}{2.48 \text{ in.}}$$

$$= 72.6 < 93.8$$

The buckling stress is defined in Equation 6-14 and for this case is:

$$F_e = \frac{\pi^2 E}{(KL/r)^2}$$
$$= \frac{\pi^2(29{,}000 \text{ ksi})}{(72.6 \text{ in.})^2}$$
$$= 54.3 \text{ ksi}$$

(*Spec.* Eq. E3-4)

The critical stress is:

$$F_{cr} = \left(0.658^{\frac{F_y}{F_e}}\right)F_y$$

(*Spec.* Eq. E3-2)

For blast loading, $F_y = f_{ds} = 65.0$ ksi, and the critical stress is:

$$F_{cr} = \left(0.658^{\frac{f_{ds}}{F_e}}\right)f_{ds}$$
$$= \left(0.658^{\frac{65.0 \text{ ksi}}{54.3 \text{ ksi}}}\right)65.0 \text{ ksi}$$
$$= 39.4 \text{ ksi}$$

For blast loading, $\phi = 1.00$, and the available compressive strength is:

$$\phi P_n = \phi A_g F_{cr}$$
$$= 1.00(15.6 \text{ in.}^2)(39.4 \text{ ksi})$$
$$= 615 \text{ kips}$$

The available tensile yielding strength of the W12×53 columns from AISC *Specification* Section D2 is:

$$\phi P_n = \phi F_y A_g$$

For blast loading, $F_y = f_{ds} = 65.0$ ksi and $\phi = 1.00$, and the available tensile strength is:

$$\phi P_n = \phi f_{ds} A_g$$
$$= 1.00(65.0 \text{ ksi})(15.6 \text{ in.}^2)$$
$$= 1,010 \text{ kips}$$

The maximum axial compressive load in Column 1 due to the blast load is 11.5 kips, as shown in Figure 5-10. Considering a 17.5 ft by 12.5 ft tributary area, a dead load of 50 psf, a live load of 30 psf, and the load combination given by Equation 6-7, the total column load is:

$$P_u = 1.0D + 0.25L + 1.0B$$
$$= 1.0(17.5 \text{ ft})(12.5 \text{ ft})(0.050 \text{ ksf}) + 0.25(17.5 \text{ ft})(12.5 \text{ ft})(0.030 \text{ ksf}) + 1.0(11.5 \text{ kips})$$
$$= 24.1 \text{ kips} < \phi P_n$$

The maximum axial compressive load in Column 2 due to the blast load is 11.5 kips, also shown in Figure 5-10. Considering a 35 ft × 12.5 ft tributary area, the total axial compressive load for this column is:

$$P_u = 1.0D + 0.25L + 1.0B$$
$$= 1.0(35 \text{ ft})(12.5 \text{ ft})(0.050 \text{ ksf}) + 0.25(35 \text{ ft})(12.5 \text{ ft})(0.030 \text{ ksf}) + 1.0(11.5 \text{ kips})$$
$$= 36.7 \text{ kips} < \phi P_n$$

The maximum compression is 24.1 kips in Column 1 and 36.7 kips in Column 2. These are significantly below the buckling load of the column ($\phi P_n = 615$ kips). The maximum stresses in the columns are 1.5 ksi and 2.4 ksi, respectively, therefore, the columns remain elastic.

(d) Second Floor Beam of Example 5.2

The second floor beam in Example 5.2, which is part of the braced frame, is checked next and its behavior is determined. The W12×35 beam has a length, $L = 24$ ft. It is modeled as a simply supported beam with a concentrated load at midspan where the braces meet.

For a starting point, it is initially assumed that the element has a ductility ratio smaller than 3. From Section 6.3.5 it is seen that for ductility ratios smaller than 3, the elastic-plastic flexural strength is given by:

$$M_p' = f_{ds} \left(\frac{S+Z}{2} \right) \tag{6-12}$$
$$= \left(\frac{65.0 \text{ ksi}}{12 \text{ in./ft}} \right) \left(\frac{45.6 \text{ in.}^3 + 51.2 \text{ in.}^3}{2} \right)$$
$$= 262 \text{ kip-ft}$$

where f_{ds} was determined previously as 65.0 ksi for blast loading using the simplified Equation 6-5.

From AISC *Manual* Table 3-23, the elastic deflection for this moment due to the concentrated load at midspan is:

$$\Delta = \frac{M'_p L^2}{12EI}$$

$$= \frac{(262 \text{ kip-ft})(12 \text{ in./ft})(24 \text{ ft})^2 (12 \text{ in./ft})^2}{12(29,000 \text{ ksi})(285 \text{ in.}^4)}$$

$$= 2.63 \text{ in.}$$

This deflection gives an elastic rotation of:

$$\theta = \tan^{-1}\left(\frac{\Delta}{L/2}\right)$$

$$= \tan^{-1}\left[\frac{2.63 \text{ in.}}{(24 \text{ ft})(12 \text{ in./ft})/2}\right]$$

$$= 1.05°$$

Note that the hinge rotation is double this support rotation (see Figure 6-2). These parameters define an elastic-perfectly plastic moment-rotation curve. Since many programs have convergence problems with a perfectly plastic zone, a sloped line should be introduced in this plastic region. This slope shown in Figure 6-9 is based on f_{ds} determined from Figure 6-1 and Equation 6-2 for ductility greater than 10. Therefore, the dynamic design stress is:

$$f_{ds} = f_{dy} + \frac{f_{du} - f_{dy}}{4} \tag{6-2}$$

where

$$f_{dy} = SIF(DIF)F_y \tag{6-1}$$
$$= 1.10(1.19)(50 \text{ ksi})$$
$$= 65.5 \text{ ksi}$$

$$f_{du} = DIF(F_u) \tag{6-3}$$
$$= 1.19(65 \text{ ksi})$$
$$= 77.4 \text{ ksi}$$

and

$$f_{ds} = 65.5 \text{ ksi} + \frac{77.4 \text{ ksi} - 65.5 \text{ ksi}}{4}$$

$$= 68.5 \text{ ksi}$$

The ultimate bending moment is:

$$M_{ult} = f_{ds} Z_x$$

$$= \frac{(68.5 \text{ ksi})(51.2 \text{ in.}^3)}{12}$$

$$= 292 \text{ kip-ft}$$

The maximum rotation, determined from Table 6-2 is:

$$\theta_{ult} = \min\left(10°, \ 20 \ \theta\right)$$

$$= \min\left(10°, \ 21°\right)$$

$$= 10°$$

Again, note that hinge rotation is double this support rotation. The moment-rotation diagram for the beam hinge is given in Figure 6-9.

Figure 5-20 shows the time-history deflection at midspan for the second-floor beam. The maximum deflection results in the first cycle with a value of 3 in. For this deflection the ductility is smaller than the maximum value defined in Table 6-2 for beams:

$$\mu = \frac{3.00 \text{ in.}}{2.63 \text{ in.}}$$

$$= 1.14 < 20$$

Note, also, that the ductility ratio is smaller than 3, indicating that the initial assumption was valid. If, conversely, the ratio was larger than 3 this process would have to be repeated with the correct M_p.

Example 6.2—Design of Structural Elements Subject to Direct Blast Loading: Façade Girt and Column

Given:

In the previous examples, the element behaviors were defined and included in the structural models used in Examples 5.1 and 5.2. The results from these examples were used in this chapter to check the adequacy of the members to support the loads defined in Chapter 5. These particular elements were not directly exposed to blast loads. In this example, the elements are designed and analyzed based on the blast load applied directly to them. Elements designed in Example 5.1 are simplified into an SDOF model and will be redesigned according to the requirements defined in this chapter. All steel is ASTM A992 material. Specifically, the following elements are designed:

(a) Façade Girt Design: Design an 8-in.-deep section. This element has been designed for wind as a MC8×20 of ASTM A992 material, with a deflection limitation of $L/260$.
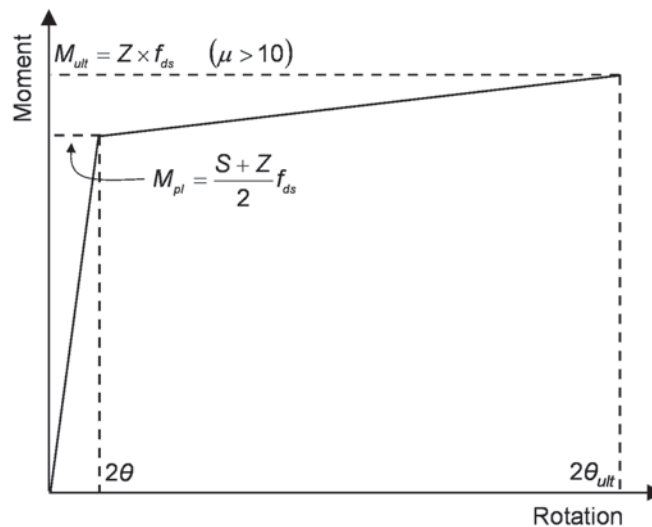
Fig. 6-9. Beam hinge moment-rotation curve.

(b) Façade Column Design: This element has been designed for wind as a W12×53 of ASTM A992 material, with a deflection limitation of $L/240$.

An introduction to the MDOF-to-SDOF simplification method was presented in Chapter 4. Figure 6-10 provides an overview of this method.

Note that the sample procedure equations given in Figure 6-10 are based on a simply supported beam with load and mass uniformly distributed. Equations for other boundary conditions were defined in Chapter 4. The same transformation as shown in Figure 6-10 can be performed by multiplying only the mass by the load-mass factor (Biggs, 1964). Figure 6-11 summarizes the SDOF solution.

$$M_{SDOF} = MK_{LM} = M\frac{K_M}{K_L} \tag{6-14}$$

This can be seen by starting from the simple force equilibrium equation, and applying the transformation shown in Figure 6-10. The simple force equilibrium equations are:

$$F = ku + M\ddot{u} \tag{6-15}$$

$$K_L F = kK_L u + MK_M \ddot{u} \tag{6-16}$$

This can then be simplified to show:

$$F = ku + M\frac{K_M}{K_L}\ddot{u} \tag{6-17}$$

The K_{LM} approach is simpler because it only uses one transformation factor and is standard practice in blast analysis/design. Here, the load factor, K_L, and the mass factor, K_M, are used because they have a more physical interpretation.

Equivalent SDOF Procedure
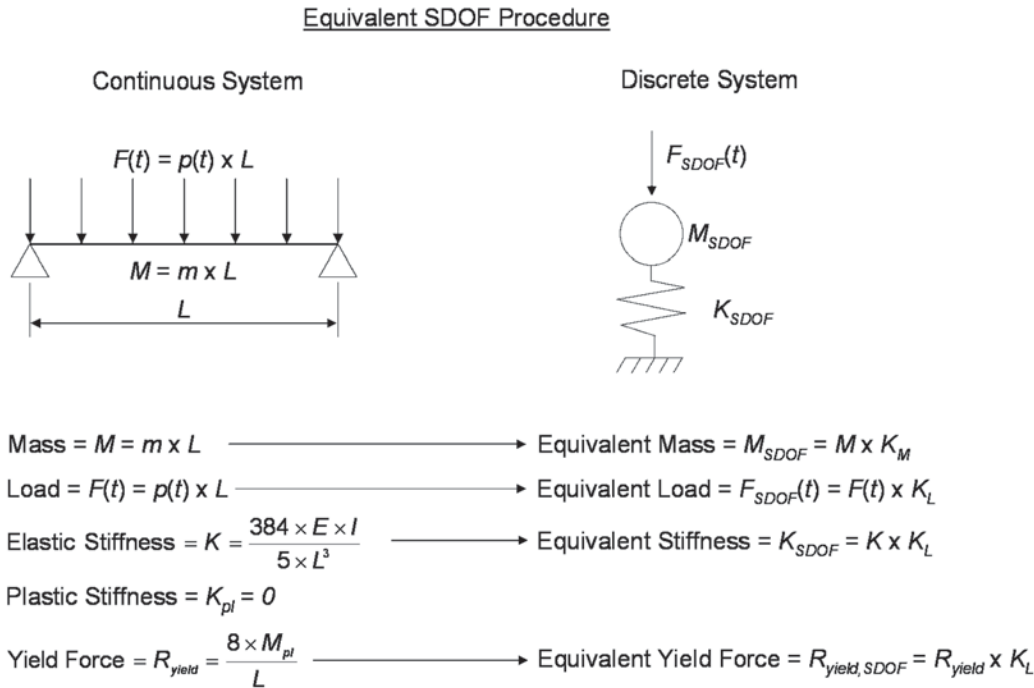
Fig. 6-10. MDOF-to-SDOF simplification.

Solution:

From AISC *Manual* Table 2-4, the material properties are:

    ASTM A992
    $F_y = 50$ ksi
    $F_u = 65$ ksi

(a) Façade Girt Design

The girt shown in Figure 6-12 is designed to support the blast load calculated in Chapter 2. The blast deflection criteria given in Table 6-2 shows that the ductility should be less than 20 and the support rotation should be less than 10°. As a preliminary design, the support rotation criterion is used because it does not assume the knowledge of the actual section used. Rigid-perfectly plastic behavior is assumed and the element is assumed sufficiently braced against lateral-torsional buckling.
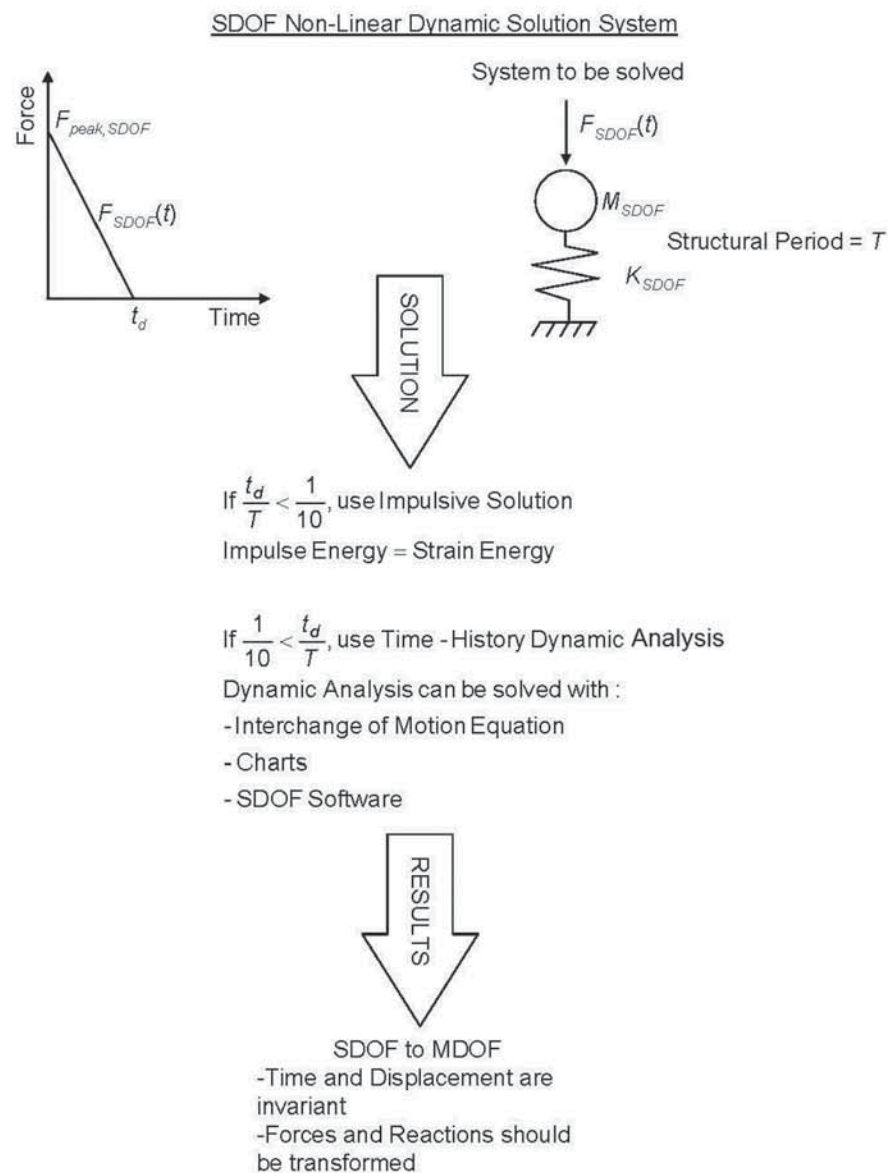
Fig. 6-11. SDOF solution.

For this rotation criterion, the maximum deflection allowed is:

$$\Delta_{max} = \left[\frac{(25.0 \text{ ft})(12 \text{ in./ft})}{2}\right]\sin 10°$$

$$= 26.0 \text{ in.}$$

The connection should be detailed for this high rotational capacity. Connection design will be discussed in Chapter 7.

In this example, the process shown in Figure 6-10 and Figure 6-11 will be followed. Begin by converting the mass and load from the MDOF system to an equivalent SDOF system that is easy to solve. Within this equivalent SDOF system, find the necessary yield force from the total energy and maximum deflection in the system. Next, convert this yield force back to the MDOF system and find the maximum moment. With this moment, design a section with the required plastic section modulus using the AISC *Specification*.

The self-weight of the façade is 40 psf. Therefore, the weight of the façade supported by the system is:

$$w = (40.0 \text{ psf})(25.0 \text{ ft})(5.00 \text{ ft})/(1{,}000 \text{ lb/kip})$$

$$= 5.00 \text{ kips}$$

The self-weight is important for the calculation of the mass involved in the movement of the system. The girt is included in the dynamic and modal calculations; however, it provides only lateral resistance to the wind loading and supports only its own weight.

From Example 2.1, the blast lasts for a duration of 6.19 ms and peaks at a pressure of 79.5 psi. The load associated with this blast pressure spread about the tributary area of the girt is given as:

$$F_{peak} = (79.5 \text{ psi})(144 \text{ in.}^2/\text{ft}^2)(5.00 \text{ ft})(25.0 \text{ ft})/(1{,}000 \text{ lb/kip})$$

$$= 1{,}430 \text{ kips}$$

Based on the SDOF simplification used for mass and loads uniformly distributed in the plastic range, the load and the stiffness are multiplied by the load factor, $K_L = 0.50$, and the mass is multiplied by the mass factor, $K_M = 0.33$, as found in Table 4-1. Therefore, the load and mass parameters used in the discrete system are:
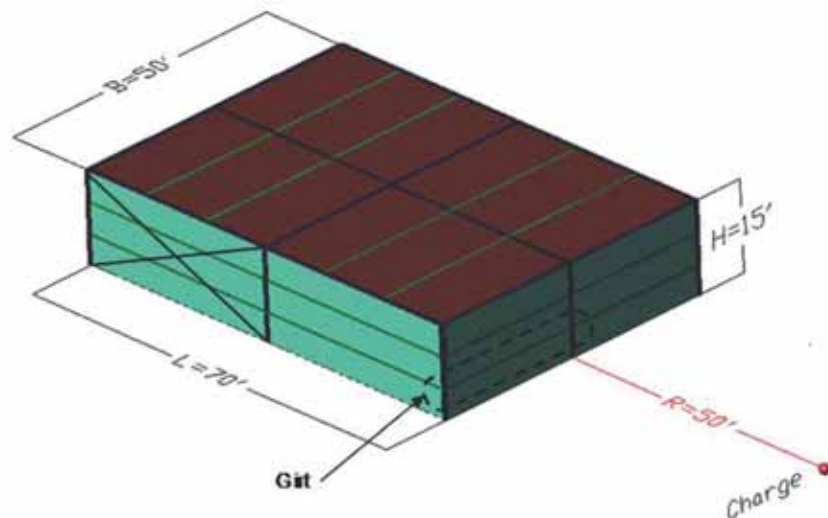
Fig. 6-12. Façade girt location.

$F_{peak,SDOF} = K_L F_{peak}$

$\qquad = 0.50\,(1,430 \text{ kips})$

$\qquad = 715 \text{ kips}$

$w_{SDOF} = K_M w$

$\qquad = 0.33\,(5.00 \text{ kips})$

$\qquad = 1.65 \text{ kips}$

The equivalent impulse due to the 6.19 ms blast in this SDOF system is determined from Equation 5-12 as follows:

$$I_{SDOF} = \frac{F_{peak,SDOF}\, t_d}{2}$$

$$\qquad = \frac{(715 \text{ kips})(6.19 \times 10^{-3} \text{ s})}{2}$$

$$\qquad = 2.21 \text{ kip-s}$$

The total energy produced by the blast load in the SDOF system is determined from Equation 5-3:

$$W_{P,SDOF} = \frac{I_{SDOF}^2}{2m_{SDOF}}$$

$$\qquad = \frac{(2.21 \text{ kip-s})^2}{2\left(\dfrac{1.65 \text{ kips}}{386 \text{ in./s}^2}\right)}$$

$$\qquad = 571 \text{ kip-in.}$$

To limit the maximum displacement (determined previously) to comply with the support rotation criteria, the SDOF yield force is:

$$R_{yield,SDOF} = \frac{W_{P,SDOF}}{\Delta_{max}}$$

$$\qquad = \frac{571 \text{ kip-in.}}{26.0 \text{ in.}}$$

$$\qquad = 22.0 \text{ kips}$$

The yield force for the continuous system is:

$$R_{yield} = \frac{R_{yield,SDOF}}{K_L}$$

$$\qquad = \frac{22.0 \text{ kips}}{0.50}$$

$$\qquad = 44.0 \text{ kips}$$

The maximum moment can be found using the equation for the maximum resistance given in Table 4-1:

$$M_p = \frac{R_{yield} L}{8}$$

$$= \frac{(44.0 \text{ kips})(25.0 \text{ ft})}{8}$$

$$= 138 \text{ kip-ft}$$

Assuming the full plastic moment is developed, the minimum plastic section modulus can be determined from Equation 6-13, with $f_{ds} = 1.30 F_y$, as follows:

$$Z_{min} = \frac{M_p}{f_{ds}}$$

$$= \frac{(138 \text{ kip-ft})(12 \text{ in./ft})}{1.30(50 \text{ ksi})}$$

$$= 25.5 \text{ in.}^3$$

Based on this preliminary design, there is no MC8 strong enough to support the blast. There are several possible modifications to improve the behavior of the system: increase the excited mass, increase the strength-stiffness of the system, or decrease the blast load by integrating a variable blast pressure that is a function of the distance to the charge along the girt. In this example, increase the steel section to an ASTM A992 W8×28.

For the W8×28, from AISC *Manual* Table 1-1, the geometric properties are:
d = 8.06 in.
t_w = 0.285 in.
Z_x = 27.2 in.
I_x = 98.0 in.^{4}

The plastic moment is:

$$M_p = f_{ds} Z \tag{6-13}$$

$$= \frac{1.30(50 \text{ ksi})(27.2 \text{ in.}^3)}{12 \text{ in./ft}}$$

$$= 147 \text{ kip-ft}$$

From AISC *Manual* Table 3-23, using the equation for maximum deflection for a uniformly distributed load on a simply supported beam, the elastic displacement is:

$$\Delta_{el} = \frac{5}{48} \frac{M_{pl} L^2}{EI}$$

$$= \frac{5}{48} \left[\frac{(147 \text{ kip-ft})(12 \text{ in./ft})(25.0 \text{ ft})^2 (12 \text{ in./ft})^2}{(29{,}000 \text{ ksi})(98.0 \text{ in.}^4)} \right]$$

$$= 5.82 \text{ in.}$$

The strength parameters to use in the dynamic calculation are determined in the following. From Table 4-1, the maximum resistance is:

$$R_{yield} = \frac{8M_p}{L}$$
$$= \frac{8(147 \text{ kip-ft})}{25.0 \text{ ft}}$$
$$= 47.0 \text{ kips}$$

Using the load factor, K_L, from Table 4-1, the SDOF yield force is:

$$R_{yield,SDOF} = K_L R_{yield}$$
$$= 0.50(47.0 \text{ kips})$$
$$= 23.5 \text{ kips}$$

Solving for K in Equation 5-16, the required structure stiffness is:

$$K = \frac{R_{yield}}{\Delta_{el}}$$
$$= \frac{47.0 \text{ kips}}{5.82 \text{ in.}}$$
$$= 8.08 \text{ kip/in.}$$

Using the load factor, K_L, from Table 4-1, the SDOF stiffness is:

$$K_{SDOF} = K_L K$$
$$= 0.50(8.08 \text{ kip/in.})$$
$$= 4.04 \text{ kip/in.}$$

The mass and load do not change from the previous calculations.

The period of the system, based on the SDOF mass determined previously, is:

$$T = 2\pi\sqrt{\frac{m_{SDOF}}{K_{SDOF}}}$$
$$= 2\pi\sqrt{\frac{1.65 \text{ kips}}{(386 \text{ in./s}^2)(4.04 \text{ kip/in.})}}$$
$$= 0.204 \text{ s}$$

The structural period (0.204 s) is more than 10 times longer than the load duration (0.00619 s), hence the assumption of impulsive load is correct.

Figure 6-13 shows the displacement computed using SDOF software. As can be seen from this plot, no damping was introduced into the system. The maximum deflection is 28.4 in. > 26.0 in., hence the rotation criterion is not met by a slight margin. The elastic displacement for this beam is 5.82 in., therefore the ductility ratio for this system is:

$$\mu = \frac{28.4 \text{ in.}}{5.82 \text{ in.}}$$
$$= 4.88 < 20$$

The maximum reaction occurs at the time of the maximum displacement. In the response from an impulse load, the maximum response occurs when the load is zero (i.e., after the load has finished). For a longer blast duration, the reaction is a combination of the direct load and the capacity of the resisting element. See Biggs (1964) for more information. Table 4-1 gives the following expression for the dynamic reaction:

$$V = 0.38R_{yield} + 0.12F$$
$$= 0.38(47.0 \text{ kips}) + 0.12(0 \text{ kips})$$
$$= 18.2 \text{ kips}$$

where
F = load applied at the time of maximum response

The dynamic available shear strength, from Equation 6-11, is:

$$\phi V_n = \phi f_{dv} A_w$$

where
$$f_{dv} = 0.55 f_{ds} \tag{6-4}$$
$$= 0.55(SIF)(DIF)f_{ds}$$
$$A_w = dt_w$$
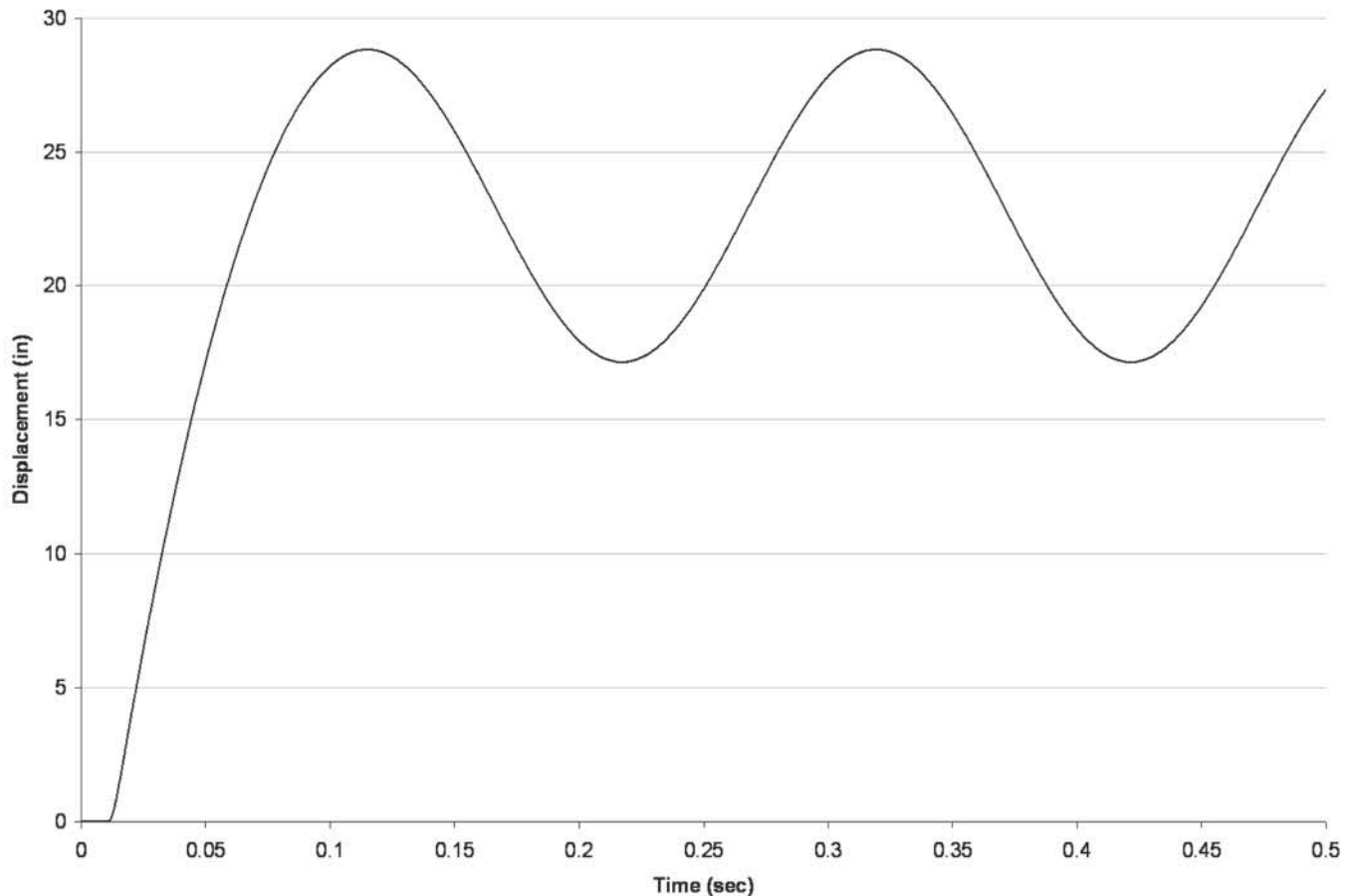
Fig. 6-13. SDOF displacement for façade girt in Example 6.2— determined by computer modeling.

Therefore:

$$\phi V_n = \phi f_{dv} A_w$$
$$= 1.00(0.55)(1.10)(1.19)(50 \text{ ksi})(8.06 \text{ in. })(0.285 \text{ in.})$$
$$= 82.7 \text{ kips} > 18.2 \text{ kips}$$

Hence, the section can support the shear. The connection should be designed for this capacity.

(b) Façade Column Design

The column shown in Figure 6-14 is designed to support the blast load calculated in Chapter 2. From AISC *Manual* Table 1-1, the geometric properties of the W12×53 are:

W12×53
A = 15.6 in.
I_x = 425 in.^{4}
S_x = 70.6 in.^{3}
r_x = 5.23 in.
r_y = 2.48 in.
r_{ts} = 2.79 in.
h_o = 11.5 in.
J = 1.58 in.^{4}

As mentioned in Section 6.3.6, columns are designed to remain elastic; therefore, the maximum flexural strength should not be reached. For the preliminary design, the column will be designed without axial compression. For the final design, combined axial compression and bending strength will be checked to determine the adequacy of this element.

For preliminary design, the girt is assumed infinitely rigid and all of the blast pressure is absorbed by the column; this is the same assumption used in Chapter 5. This being highly conservative, a more accurate approach would be to design for the girt reactions.
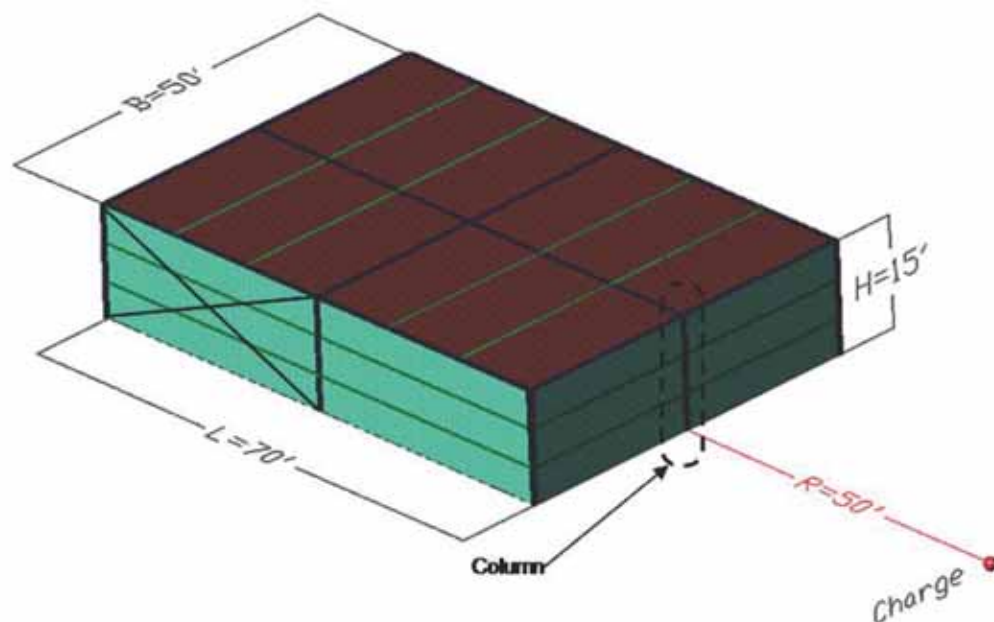
Fig. 6-14. Column location.

The self-weight of the façade is 40 psf. Therefore, the weight of the façade supported by the system is:

$$w = \frac{(40.0 \text{ psf})(25.0 \text{ ft})(15.0 \text{ ft})}{1,000 \text{ lb/kip}}$$

$$= 15.0 \text{ kips}$$

From Example 2.1, the blast lasts for a duration of 6.19 ms and peaks at a pressure of 79.5 psi. The load associated with this blast pressure spread about the tributary area of the column is given as:

$$F_{peak} = \frac{(79.5 \text{ psi})(144 \text{ in.}^2/\text{ft}^2)(15.0 \text{ ft})(25.0 \text{ ft})}{1,000 \text{ lb/kip}}$$

$$= 4,290 \text{ kips}$$

Following a similar procedure to the girt design example previously solved, convert the MDOF system to an equivalent SDOF system to solve. Based on the SDOF simplification used for mass and loads uniformly distributed in the plastic range, the load and the stiffness are multiplied by the load factor, $K_L = 0.50$, and the mass is multiplied by the mass factor, $K_M = 0.33$, as found in Table 4-1. Therefore, the load and mass parameters used in the discrete system are:

$$F_{peak,SDOF} = 0.50(4,290 \text{ kips})$$

$$= 2,150 \text{ kips}$$

$$w_{SDOF} = 0.33(15.0 \text{ kips})$$

$$= 4.95 \text{ kips}$$

The equivalent impulse due to the 6.19 ms blast in this SDOF system is determined from Equation 5-12 as follows:

$$I_{SDOF} = \frac{F_{peak,SDOF} \, t_d}{2}$$

$$= \frac{(2,150 \text{ kips})(6.19 \times 10^{-3} \text{ s})}{2}$$

$$= 6.65 \text{ kip-s}$$

The total energy produced by the blast load in the SDOF system is determined from Equation 5-3:

$$W_{P,SDOF} = \frac{I_{SDOF}^2}{2m_{SDOF}}$$

$$= \frac{(6.65 \text{ kip-s})^2}{2\left(\dfrac{4.95 \text{ kips}}{386 \text{ in./s}^2}\right)}$$

$$= 1,720 \text{ kip-in.}$$

For the W12×53, assuming a uniformly distributed load, the following properties define the structural behavior:

$$M_p = f_{ds} Z \tag{6-13}$$

$$= \frac{1.3(50 \text{ ksi})(77.9 \text{ in.}^3)}{12 \text{ in./ft}}$$

$$= 422 \text{ kip-ft}$$

From AISC *Manual* Table 3-23, using the equation for maximum deflection for a uniformly distributed load on a simply supported beam, the elastic displacement is:

$$\Delta_{el} = \frac{5}{48} \frac{M_p L^2}{EI}$$

$$= \frac{5}{48} \left[\frac{(422 \text{ kip-ft})(12 \text{ in./ft})(15 \text{ ft})^2 (12 \text{ in.})^2}{(29{,}000 \text{ ksi})(425 \text{ in.}^4)} \right]$$

$$= 1.39 \text{ in.}$$

The strength parameters to use in the dynamic calculation are determined in the following. From Table 4-1, the maximum resistance is:

$$R_{yield} = \frac{8M_{pl}}{L}$$

$$= \frac{8(422 \text{ kip-ft})}{15.0 \text{ ft}}$$

$$= 225 \text{ kips}$$

Using the load factor, K_L, from Table 4-1, the SDOF yield force is:

$$R_{yield,SDOF} = K_L R_{yield}$$

$$= 0.50(225 \text{ kips})$$

$$= 113 \text{ kips}$$

Solving for K in Equation 5-16, the required structure stiffness is:

$$K = \frac{R_{yield}}{\Delta_{el}}$$

$$= \frac{225 \text{ kips}}{1.39 \text{ in.}}$$

$$= 162 \text{ kip/in.}$$

Using the load factor, K_L, from Table 4-1, the SDOF stiffness is:

$$K_{SDOF} = K_L K$$

$$= 0.50(162 \text{ kip/in.})$$

$$= 81.0 \text{ kip/in.}$$

The period of the system is:

$$T = 2\pi \sqrt{\frac{m_{SDOF}}{K_{SDOF}}}$$

$$= 2\pi \sqrt{\frac{4.95 \text{ kips}}{(386 \text{ in./s}^2)(81.0 \text{ kip/s})}}$$

$$= 0.0791 \text{ s}$$

The column period (0.0791 s) is more than 10 times the load duration (0.00619 s), hence the assumption of impulsive load is correct. The period of the column is smaller than half of the beam period [0.0791 s < (0.204 s)/2 = 0.102 s]; therefore, the system is uncoupled and can be modeled separately.

Assuming elastic behavior, the maximum elastic energy that can be adsorbed by the SDOF system is given by the following, which can be derived from Equation 5-8 and Equation 5-16:

$$
\begin{aligned}
W_{S,el,max} &= \frac{R_{yield,SDOF}^2}{2K_{SDOF}} \\
&= \frac{(113 \text{ kips})^2}{2(81.0 \text{ kip/in.})} \\
&= 78.8 \text{ kip-in.} < 1{,}720 \text{ kip-in.}
\end{aligned}
$$

The maximum elastic energy is smaller than the energy induced by the impulse. Therefore, this element will achieve plastic behavior. As stated earlier, the intent is for columns to remain elastic. For the tributary blast load directly applied to the column, there is not an economical solution for this column to remain elastic. But the preliminary assumption of rigid behavior of the girt is highly conservative; the maximum load that this element is carrying comes from the reaction in the girt, not the blast pressure on the tributary area of the column. Assuming this reaction is static, the system to solve is defined in Figure 6-15, where the 23.5-kip end reactions from the girt are shown, calculated as half of R_{yield}. Note that this is different than the dynamic end reaction of 18.2 kips. The 23.5-kip load is used for redundancy and to be conservative.

The maximum bending moment for this configuration is:

$$
\begin{aligned}
M_B &= 2(23.5 \text{ kips})(15.0 \text{ ft}/3) \\
&= 235 \text{ kip-ft}
\end{aligned}
$$

The factored or required flexural strength is $1.0 M_B = 1.0(2{,}820 \text{ kip-in.}) = 2{,}820 \text{ kip-in.}$

The axial load on the column, based on a roof dead load of 30 psf, is:

$$
\begin{aligned}
P_D &= (30.0 \text{ psf})\left(\frac{50 \text{ ft}}{2}\right)\left(\frac{70 \text{ ft}}{4}\right)\Big/1{,}000 \text{ lb/kip} \\
&= 13.1 \text{ kips}
\end{aligned}
$$

The factored or required compressive strength is $1.0 P_D = 1.0(13.1 \text{ kips}) = 13.1 \text{ kips}$ based on Equation 6-7.

Next, the axial compressive and flexural available strength of this element are determined and checked using the combined compression and flexure interaction equations. For buckling about the weak axis, the column is assumed not to be braced by the girts. The buckling length is $K_y L = 1.0(15.0 \text{ ft}) = 15.0 \text{ ft}$, therefore, the slenderness is:

$$
\begin{aligned}
\frac{K_y L}{r_y} &= \frac{(15.0 \text{ ft})(12 \text{ in./ft})}{2.48 \text{ in.}} \\
&= 72.6
\end{aligned}
$$

For buckling about the strong axis, the column is also unbraced. The buckling length is $K_x L = 1.0(15.0 \text{ ft}) = 15.0 \text{ ft}$; therefore, the slenderness is:

$$
\begin{aligned}
\frac{K_x L}{r_x} &= \frac{(15.0 \text{ ft})(12 \text{ in./ft})}{5.23 \text{ in.}} \\
&= 34.4
\end{aligned}
$$

Because the weak axis slenderness ratio is larger, the available compressive strength will be based on that ratio.

Based on UFC 3-340-02, the maximum slenderness permitted for this element is:

$$C_c = \sqrt{\frac{2\pi^2 E}{f_{ds}}}$$

$$= \sqrt{\frac{2\pi^2 (29{,}000 \text{ ksi})}{1.3(50 \text{ ksi})}}$$

$$= 93.8$$

This compares to the AISC *Specification* limit for inelastic behavior of:

$$\frac{KL}{r} < 4.71\sqrt{\frac{E}{F_y}}$$

With $F_y = f_{ds} = 1.3(50 \text{ ksi}) = 65 \text{ ksi}$:

$$4.71\sqrt{\frac{29{,}000 \text{ ksi}}{65 \text{ ksi}}} = 99.5$$
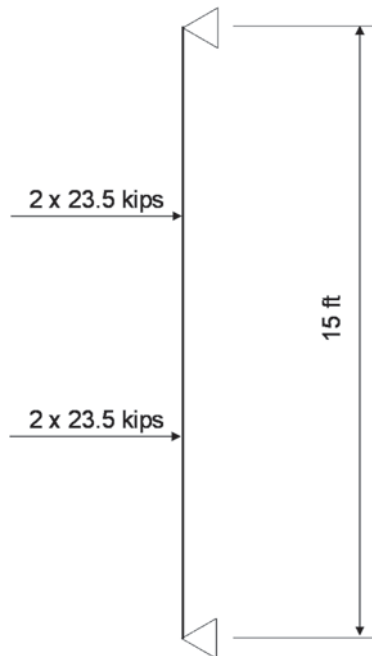
Fig. 6-15. Equivalent static reaction system.

Note that this is significantly lower than the value of 200 recommended in the AISC *Specification* Section E2 User Note. The buckling and critical stresses are determined from AISC *Specification* Section E3. The weak axis buckling stress is:

$$F_e = \frac{\pi^2 E}{(KL/r)^2}$$ (*Spec.* Eq. E3-4)

$$= \frac{\pi^2 (29{,}000 \text{ ksi})}{(72.6 \text{ in.})^2}$$

$$= 54.3 \text{ ksi}$$

Because $KL/r_y = 72.6 < 99.5$, the critical stress is:

$$F_{cr} = \left(0.658^{\frac{F_y}{F_e}}\right) F_y$$ (*Spec.* Eq. E3-2)

From Equation 6-5, $F_y = f_{ds} = 1.30(50 \text{ ksi}) = 65 \text{ ksi}$, and the critical stress is:

$$F_{cr} = \left(0.658^{\frac{65 \text{ ksi}}{54.3 \text{ ksi}}}\right)(65 \text{ ksi})$$

$$= 39.4 \text{ ksi}$$

The available compressive strength is:

$$\phi P_n = \phi F_{cr} A_g$$ (6-10)

$$= 1.00(39.4 \text{ ksi})(15.6 \text{ in.}^2)$$

$$= 615 \text{ kips}$$

The available tensile strength of the section is:

$$\phi P_n = \phi F_y A_g$$ (6-9)

For blast loading, with $F_y = f_{ds}$:

$$\phi P_n = 1.00(65 \text{ ksi})(15.6 \text{ in.}^2)$$

$$= 1{,}010 \text{ kips}$$

Determine the available flexural strength, assuming that this beam is laterally unsupported because the girts cannot carry any axial load after the blast. Therefore, the unbraced flexural strength is determined as follows from AISC *Specification* Section F2, with $F_y = f_{ds}$:

$$L_p = 1.76r_y \sqrt{\frac{E}{f_{ds}}} \qquad \text{(from \textit{Spec} Eq. F2-5)}$$

$$= 1.76(2.48 \text{ in.})\left(1/12 \text{ in./ft}\right)\sqrt{\frac{29,000 \text{ ksi}}{65 \text{ ksi}}}$$

$$= 7.68 \text{ ft}$$

$$L_r = 1.95r_{ts} \frac{E}{0.7f_{ds}} \sqrt{\frac{Jc}{S_x h_o} + \sqrt{\left(\frac{Jc}{S_x h_o}\right)^2 + 6.76\left(\frac{0.7f_{ds}}{E}\right)^2}} \qquad \text{(from \textit{Spec} Eq. F2-6)}$$

$$= \left\{ \begin{array}{l} 1.95(2.79 \text{ in.})\left[\dfrac{29,000 \text{ ksi}}{0.7(65 \text{ ksi})}\right] \\[4mm] \times \sqrt{\dfrac{\left(1.58 \text{ in.}^4\right)1.00}{\left(70.6 \text{ in.}^3\right)(11.5 \text{ in.})} + \sqrt{\left[\dfrac{\left(1.58 \text{ in.}^4\right)1.00}{\left(70.6 \text{ in.}^3\right)(11.5 \text{ in.})}\right]^2 + 6.76\left[\dfrac{0.7(65 \text{ ksi})}{29,000 \text{ ksi}}\right]^2}} \\[4mm] \times \left(1/12 \text{ in./ft}\right) \end{array} \right\}$$

$$= 23.2 \text{ ft}$$

The unbraced length of the column, $L_b = 15$ ft, falls between L_p and L_r. Therefore, the available flexural strength is given by:

$$\phi M_n = \phi C_b \left[M_p - \left(M_p - 0.7f_{ds}S_x\right)\left(\frac{L_b - L_p}{L_r - L_p}\right)\right] \leq \phi M_p \qquad \text{(from \textit{Spec}. Eq. F2-2)}$$

$$= 1.00(1.0)\left\{ 422 \text{ kip-ft} - \left[422 \text{ kip-ft} - 0.7(65 \text{ ksi})\left(70.6 \text{ in.}^3\right)\left(\frac{1}{12 \text{ in./ft}}\right)\right]\left(\frac{15.0 \text{ ft} - 7.68 \text{ ft}}{23.2 \text{ ft} - 7.68 \text{ ft}}\right)\right\}$$

$$\leq 1.00(422 \text{ kip-ft})$$

$$= 349 \text{ kip-ft} \leq 422 \text{ kip-ft}$$

where C_b is assumed to be 1.0.

Because $\dfrac{P_r}{P_c} = \dfrac{13.1 \text{ kips}}{615 \text{ kips}} = 0.02 < 0.2$, use AISC *Specification* Equation H1-1b to check the interaction of combined flexure and axial compression:

$$\frac{P_r}{2P_c} + \left(\frac{M_{rx}}{M_{cx}}\right) = \frac{13.1 \text{ kips}}{2(615 \text{ kips})} + \left(\frac{235 \text{ kip-ft}}{349 \text{ kip-ft}}\right)$$

$$= 0.684 \leq 1.0 \quad \textbf{o.k.}$$

We can compare the moment from the girt reactions to the maximum moment if subjected to full blast pressure as an indication of the energy dissipated by the façade. The maximum moment in the column due to the girt reactions was found above to be 235 kip-ft. Determine the moment due to the full blast pressure, as follows. The natural period of the column is:

$$T = 2\pi \sqrt{\frac{m_e}{K}} \qquad (5\text{-}10)$$

$$= 2\pi \sqrt{\frac{15.0 \text{ kips}}{\left(386 \text{ in./s}^2\right)162 \text{ kip/in.}}}$$

$$= 0.0973 \text{ s}$$

Therefore the dynamic reduction factor is:

$$k_{DRF} = \frac{\pi}{T/t_d} \tag{5-15}$$

$$= \frac{\pi}{0.0973 \text{ s}/6.19 \times 10^{-3} \text{ in.}}$$

$$= 0.200$$

The equivalent linear load on the column is:

$$q_{eq} = k_{DRF}\left(\text{Peak Pressure}\right)\left(\text{Tributary Width}\right)$$

$$= 0.200\left[\frac{\left(79.5 \text{ psi}\right)\left(144 \text{ in.}^2/\text{ft}^2\right)}{1,000 \text{ lb/kip}}\right]\left(25 \text{ ft}\right)$$

$$= 57.2 \text{ kip/ft}$$

The maximum moment due to this linear load is then:

$$M_{max} = \frac{q_{eq}L^2}{8}$$

$$= \frac{\left(57.2 \text{ kip/ft}\right)\left(15.0 \text{ ft}\right)^2}{8}$$

$$= 1,610 \text{ kip-ft}$$

The moment from the girt reactions is:

$$\left(\frac{235 \text{ kip-ft}}{1,610 \text{ kip-ft}}\right) = 14.6\%$$

Therefore, the girts absorb approximately 85% of the blast energy.

Example 6.3—Design of Structural Elements Subject to Direct Blast Loading: Composite Roof Beam

Given:

The composite beam shown in Figure 6-16 will be designed for the roof blast load defined in Figure 6-17. Note that this analysis is not based on the previous building. The structure consists of a 25-ft-long composite beam, consisting of a W14×22 with a 5½-in.-thick slab with a 3-in. metal deck. The beams are spaced at 6 ft on-center. The steel material is ASTM A992 and the concrete is normal weight with a specified compressive strength of 3 ksi. For blast design, the strength of concrete in compression is multiplied by 1.12 (dynamic increase factor from UFC 3-340-02). The composite beam is assumed to be fully braced at both flanges.

As shown in Figure 6-16, the effective flange width is 6 ft. There is 2.5 in. of concrete above the metal deck. The center of this concrete area is 11 in. from the center of the steel beam.

Solution:

From AISC *Manual* Table 2-4, the material properties are:

ASTM A992
F_y = 50 ksi
F_u = 65 ksi

From AISC *Manual* Table 1-1, the geometric properties of a W14×22 are:

W14×22
$A = 6.49$ in.^{2}
$d = 13.7$ in.
$t_w = 0.230$ in.
$h/t_w = 53.3$
$I_x = 199$ in.^{4}
$Z_x = 33.2$ in.^{3}

The composite section properties, based on the blast strength for the concrete and the steel and AISC *Specification* Chapter I, are determined in the following.

To find the moment of inertia of the composite section, first transform the section into a uniform material of steel. The modulus of elasticity of the concrete is:

$$E_c = 57,000\sqrt{f_c'}$$
$$= 57,000\sqrt{3,000 \text{ psi}}\left(\frac{1 \text{ ksi}}{1,000 \text{ psi}}\right)$$
$$= 3,120 \text{ ksi}$$

Therefore:

$$n = \frac{E_s}{E_c}$$
$$= \frac{29,000 \text{ ksi}}{3,120 \text{ ksi}}$$
$$= 9.29$$

From this, the 6 ft width of the composite section becomes $\dfrac{(6.00 \text{ ft})(12 \text{ in./ft})}{9.29} = 7.75$ in. in the transformed uniform section.

The elastic neutral axis of the composite section is found by taking the first moments of area about the top of the concrete deck as follows:
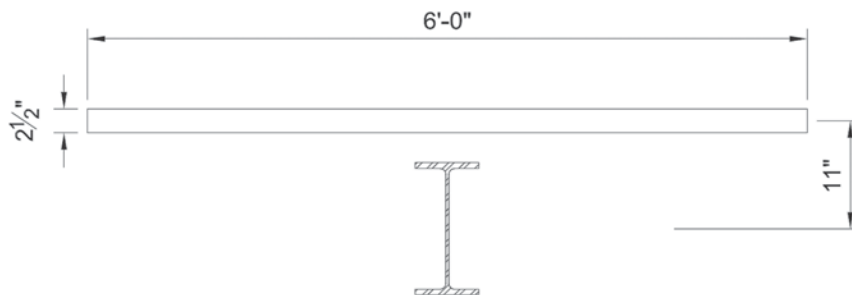
Fig. 6-16. Composite beam section

$$\bar{y} = \frac{\sum A_i y_i}{\sum A_i}$$

$$= \frac{(7.75 \text{ in.})(2.50 \text{ in.})\left(\dfrac{2.50 \text{ in.}}{2}\right) + \left(6.49 \text{ in.}^2\right)\left(\dfrac{2.50 \text{ in.}}{2} + 11.0 \text{ in.}\right)}{(7.75 \text{ in.})(2.50 \text{ in.}) + 6.49 \text{ in.}^2}$$

$$= 4.01 \text{ in.}$$

where $\bar{y}$ is the distance to the elastic neutral axis from the top of the concrete deck. Then, taking the second moments of area about the elastic neutral axis:

$$I_{conc} = \frac{(7.75 \text{ in.})(2.50 \text{ in.})^3}{12} + (7.75 \text{ in.})(2.50 \text{ in.})\left(4.01 \text{ in.} - \frac{2.50 \text{ in.}}{2}\right)^2$$

$$= 158 \text{ in.}^4$$
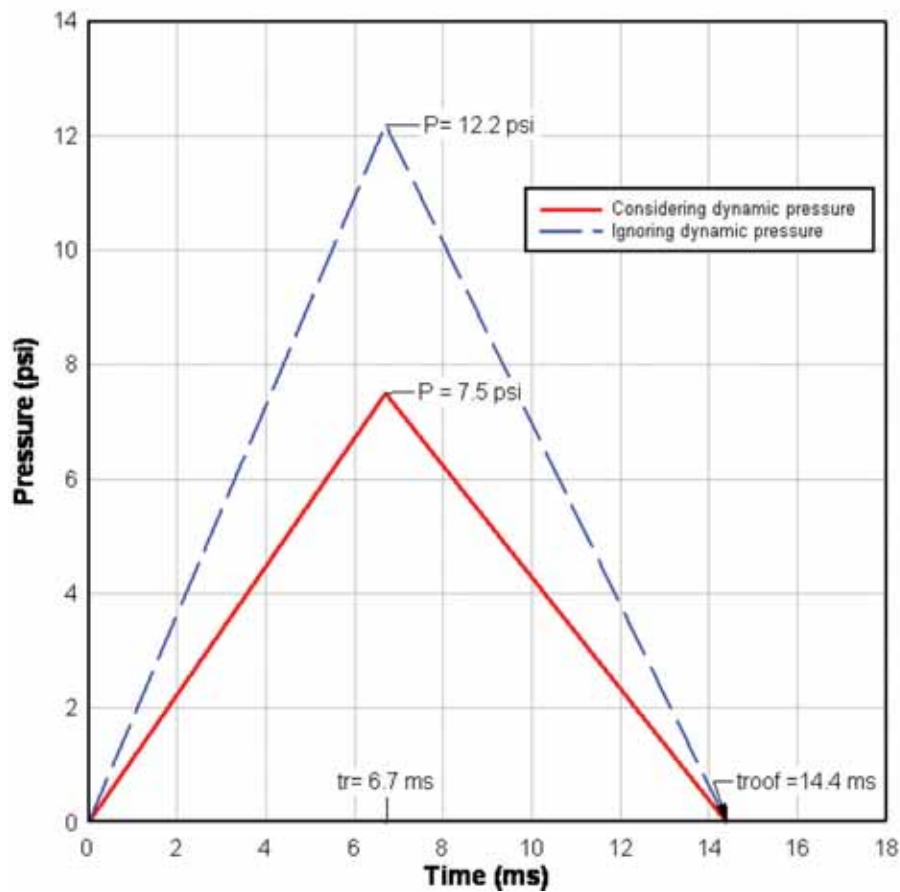
Fig. 6-17. Roof blast load.

$$I_{steel} = 199 \text{ in.}^3 + \left(6.49 \text{ in.}^2\right)\left(11.0 \text{ in.} + \frac{2.50 \text{ in.}}{2} - 4.01 \text{ in.}\right)^2$$

$$= 640 \text{ in.}^4$$

Therefore, $I_{tr} = 798 \text{ in.}^4$

Determine the available flexural strength

Determine from AISC *Specification* Section I3.2a whether the available flexural strength is based on the plastic stress distribution on the composite section or the superposition of elastic stresses for the limit state of yielding. For a W14×22:

$$\frac{h}{t_w} = 53.3 \le 3.76\sqrt{\frac{E}{f_{ds}}}$$

$$3.76\sqrt{\frac{E}{f_{ds}}} = 3.76\sqrt{\frac{29,000 \text{ ksi}}{1.3\left(50 \text{ ksi}\right)}}$$

$$= 79.4$$

Therefore, because $h/t_w = 53.3 < 79.4$, the available flexural strength is determined from the plastic stress distribution on the composite section, and $M_n = M_p$. To find M_p, the concrete compression area is first found by force balance using the dynamic strength of concrete, $f'_{dc} = 1.12(3.00 \text{ ksi}) = 3.36 \text{ ksi}$ and $f_{ds} = 1.30(50 \text{ ksi}) = 65 \text{ ksi}$ from Equation 6-5. The depth of the compression block is:

$$a = \frac{A_s f_{ds}}{0.85 f'_{dc} b_{eff}}$$

$$= \frac{\left(6.49 \text{ in.}^2\right)\left(65 \text{ ksi}\right)}{0.85\left(3.36 \text{ ksi}\right)\left(6.00 \text{ ft}\right)\left(12 \text{ in./ft}\right)}$$

$$= 2.05 \text{ in.}$$

Therefore:

$$M_p = A_s f_{ds}\left(\frac{d}{2} + t - \frac{a}{2}\right)$$

$$= \left(6.49 \text{ in.}^2\right)\left(65 \text{ ksi}\right)\left(\frac{13.7 \text{ in.}}{2} + 5.50 \text{ in.} - \frac{2.05 \text{ in.}}{2}\right)\left(\frac{1 \text{ ft}}{12 \text{ in.}}\right)$$

$$= 398 \text{ kip-ft}$$

And the available flexural strength is:

$$\phi M_n = 1.00(398 \text{ kip-ft})$$
$$= 398 \text{ kip-ft}$$

During the rebound, there is no composite action; however, the bottom flange is assumed to be fully braced. Thus, in the upward direction, the available flexural strength of the steel (using $Z_x = 33.2 \text{ in.}^3$ for the bare steel) is determined as follows, using Equation 6-5 for f_{dy}:

$$\phi M_{p,steel} = \phi Z f_{dy}$$

$$= 1.00\left[\frac{\left(33.2 \text{ in.}^3\right)\left(1.30\right)\left(50 \text{ ksi}\right)}{12 \text{ in./ft}}\right]$$

$$= 180 \text{ kip-ft}$$

The load used for this example is shown in Figure 6-17.

The existing dead load from the concrete and deck is 60 psf, hence the total dead load on the beam is:

$$w = \frac{(60.0 \text{ psf})(25.0 \text{ ft})(6.00 \text{ ft})}{1,000 \text{ lb/kip}}$$
$$= 9.00 \text{ kips}$$

The peak load for the 12.2 psi peak blast pressure is:

$$F_{peak} = \frac{(12.2 \text{ psi})(144 \text{ in.}^2/\text{ft}^2)}{1,000 \text{ lb/kip}}(6.00 \text{ ft})(25.0 \text{ ft})$$
$$= 264 \text{ kips}$$

Based on the SDOF simplification used for mass and loads uniformly distributed in the plastic range, the load and the stiffness are multiplied by the load factor, $K_L = 0.50$, and the mass is multiplied by the mass factor, $K_M = 0.33$, as found in Table 4-1. Therefore, the parameters used in the discrete system are determined as defined in Figure 6-9. The equivalent load is:

$$F_{peak,SDOF} = (264 \text{ kips})(0.50)$$
$$= 132 \text{ kips}$$

The equivalent weight is:

$$w_{SDOF} = (9.00 \text{ kips})(0.33)$$
$$= 2.97 \text{ kips}$$

From AISC *Manual* Table 3-23, the maximum elastic deflection for a uniformly distributed load is:

$$\Delta_{el} = \frac{5M_p L^2}{48EI_{tr}}$$
$$= \frac{5(398 \text{ kip-ft})(12 \text{ in./ft})(25 \text{ ft})^2 (12 \text{ in./ft})^2}{48(29,000 \text{ ksi})(798 \text{ in.}^4)}$$
$$= 1.93 \text{ in.}$$

From Table 4-1, the maximum resistance to use in the dynamic calculation is:

$$R_{yield} = \frac{8M_p}{L}$$
$$= \frac{8(398 \text{ kip-ft})}{25 \text{ ft}}$$
$$= 127 \text{ kips}$$

For the design of this beam, the existing dead load is applied simultaneously with the blast load and will reduce the beam strength.

$$R_{yield,reduced} = 127 \text{ kips} - 9.00 \text{ kips}$$
$$= 118 \text{ kips}$$

From Table 4-1 and Figure 6-9, for the SDOF system, the equivalent load is:

$$R_{yield,SDOF} = (118 \text{ kips})(0.50)$$
$$= 59.0 \text{ kips}$$

The stiffness is:

$$K = \frac{R_{yield}}{\Delta_{el}}$$
$$= \frac{127 \text{ kips}}{1.93 \text{ in.}}$$
$$= 65.8 \text{ kip/in.}$$

The SDOF stiffness is:

$$K_{SDOF} = (65.8 \text{ kip/in.})(0.50)$$
$$= 32.9 \text{ kip/in.}$$

From Equation 5-10, the period of the structure is:

$$T = 2\pi \sqrt{\frac{m_{SDOF}}{K_{SDOF}}}$$
$$= 2\pi \sqrt{\frac{w_{SDOF}}{gK_{SDOF}}}$$
$$= 2\pi \sqrt{\frac{2.97 \text{ kips}}{(386 \text{ in./s}^2)(32.9 \text{ kip/in.})}}$$
$$= 0.0961 \text{ s}$$

For this example, the beam period is less than 10 times the load duration, 0.0961 s < 10(0.0144 s) = 0.144 s; therefore, the impulse formulation cannot be used. For the rebound in the upward direction, where $M_{p,steel}$ was determined previously, the force is determined from the expression in Table 4-1:

$$R_{yield,steel} = \frac{8M_{p,steel}}{L}$$
$$= \frac{8(180 \text{ kip-ft})}{25 \text{ ft}}$$
$$= 57.6 \text{ kips}$$

Again, the dead load is applied simultaneously with the blast load and therefore, for the rebound, the available strength is increased.

$$R_{yield,steel} = 57.6 \text{ kips} + 9.00 \text{ kips}$$
$$= 66.6 \text{ kips}$$

The elastic deflection for the noncomposite steel beam is:

$$\Delta_{el,steel} = \frac{5M_{p,steel}L^2}{48EI_{steel}}$$

$$= \frac{5(180 \text{ kip-ft})(12 \text{ in./ft})(25 \text{ ft})^2 (12 \text{ in./ft})^2}{48(29,000 \text{ ksi})(199 \text{ in.}^4)}$$

$$= 3.51 \text{ in.}$$

The maximum negative force is:

$$R_{Rebound,SDOF} = (66.6 \text{ kips})(0.50)$$

$$= 33.3 \text{ kips}$$

Therefore, the elastic stiffness at the rebound is:

$$K_{Rebound,SDOF} = \frac{R_{Rebound,SDOF}}{\Delta_{el,steel}}$$

$$= \frac{33.3 \text{ kips}}{3.51 \text{ in.}}$$

$$= 9.49 \text{ kip/in.}$$

From Equation 5-10, the period at the rebound is:

$$T = 2\pi \sqrt{\frac{m_{SDOF}}{K_{Rebound,SDOF}}}$$

$$= 2\pi \sqrt{\frac{2.97 \text{ kips}}{(386 \text{ in./s}^2)(9.49 \text{ kip/in.})}}$$

$$= 0.179 \text{ s}$$

For the rebound, the beam period is greater than 10 times the load duration, 0.179 s > 10(0.0144 s) = 0.144 s; therefore, the impulse formulation can be used for the rebound response.

Graphical Solution

This system can be solved graphically using the approach presented in Chapter 4. Using Figure 4-4, the dynamic amplification factor is obtained based on the ratio between the structural period and the load duration:

$$\frac{T}{t_d} = \frac{0.0961 \text{ s}}{0.0144 \text{ s}}$$

$$= 6.67$$

From Figure 4-4, the dynamic load factor, *DLF*, is found to be 0.4. Dynamic load applied to the beam is:

$$F_{eq} = DLF\left(F_{peak}\right)$$

$$= 0.4(264 \text{ kips})$$

$$= 106 \text{ kips}$$

This is less than the strength of the beam, $R_{yield,reduced} = 118$ kips, hence the system remains elastic in the first cycle.

Because no damping is considered and the system remains elastic in the first cycle, the rebound in the second cycle needs to absorb the total energy developed by the impulse. This energy procedure results in the following strain energy, where the impulse, I, is determined from Equation 4-1:

$$W_{Impulse,SDOF} = \frac{I_{SDOF}^2}{2m_{SDOF}} \qquad \text{(from Eq. 5-7)}$$

$$= \frac{\left[\dfrac{(132 \text{ kips})(0.0144 \text{ s})}{2}\right]^2}{2\left(\dfrac{2.97 \text{ kips}}{386 \text{ in./s}^2}\right)}$$

$$= 58.7 \text{ kip-in.}$$

The plastic displacement due to the rebound is determined as follows, where $W_{Rebound,el,max}$ is determined from Equation 5-8:

$$\Delta_{Rebound,pl} = \frac{\left(W_{Impulse,SDOF} + W_{Rebound,el,max}\right)}{R_{Rebound,SDOF}} \qquad \text{(from Eq. 5-9)}$$

$$= \frac{1}{33.3 \text{ kips}}\left[58.7 \text{ kip/in.} + \frac{(9.49 \text{ kip/in.})(3.51 \text{ in.})^2}{2}\right]$$

$$= 3.52 \text{ in.}$$

Therefore, the ductility obtained at the rebound is:

$$\mu = \frac{3.52 \text{ in.}}{3.51 \text{ in.}}$$
$$= 1.00 < 20$$

which is acceptable.

Computer Calculations

As an alternative, a software program may be used to evaluate the composite beam for blast loading, using an SDOF simplification. The parameters for the load used in the analysis were previously calculated:

$w_{SDOF} = 2.97 \text{ kips}$ $\qquad$ $F_{peak,SDOF} = 132 \text{ kips}$

The load applied follows the time history shown in Figure 6-17. The yield force and stiffness were obtained previously as:

$R_{yield,SDOF} = 59.0 \text{ kips}$ $\qquad$ $K_{SDOF} = 32.9 \text{ kip/in.}$

And the rebound properties are:

$R_{Rebound,SDOF} = 33.3 \text{ kips}$ $\qquad$ $K_{Rebound,SDOF} = 9.49 \text{ kip/in.}$

For this particular example, SAP2000 was used. However, any of the software packages or programming tools mentioned in Chapter 4 would suffice. To solve, an SDOF model was constructed of two tension-only elements with the appropriate stiffness, as shown in Figure 6-18. Plastic hinges according to FEMA 356 (FEMA, 2000b) are introduced in both elements to account for any plastic behavior. These are derived in the same manner as those used in previous examples and in the modeling of Chapter 5. The mass and peak blast forces were both applied to the node at which the tension elements connect.

In order to account for the nonlinearity of the system and to get accurate deflections, the dead load should be included in the time-history analysis. Using nonlinear direct integration time-history analysis, the maximum displacement (see Figure 6-19) is:

$$\Delta_{SDOF} = 1.98 \text{ in.} \qquad \Delta_{SDOF,Rebound} = 2.87 \text{ in.}$$

Note that these values include the deflection from the dead load.

Hence, the ductility is:

$$
\begin{aligned}
\mu &= \frac{\Delta_{max}}{\Delta_{el}} \\
&= \frac{1.98 \text{ in.}}{1.93 \text{ in.}} \\
&= 1.03
\end{aligned}
$$

For the rebound, the ductility is:

$$
\begin{aligned}
\mu &= \frac{2.87 \text{ in.}}{3.51 \text{ in.}} \\
&= 0.818
\end{aligned}
$$

Note that, as the composite action is not utilized in the rebound, the beam is much more flexible in this direction. As a result, the beam deflects considerably more upwards (during the rebound) than it does downwards.

For the SDOF solution, the element just starts to yield as a composite beam but not during the rebound. Figure 6-20 shows the force resultant from the SDOF system. Note that this plot, again, includes the dead load.

The maximum shear force corresponds to the maximum end reaction. Using the equation from Table 4-1 again, with $F = 0$ at the time of maximum response, we get:

$$
\begin{aligned}
V &= 0.38 R_{yield} + 0.12F \\
&= 0.38 (127 \text{ kips}) + 0.12 (0 \text{ kips}) \\
&= 48.3 \text{ kips}
\end{aligned}
$$

The available shear strength for blast loading is determined in accordance with Section 6.3.4:

$$
\begin{aligned}
\phi V_n &= \phi f_{dv} A_w \\
&= 1.00 \left[0.55 (1.30)(50 \text{ ksi}) \right] (13.7 \text{ in.})(0.230 \text{ in.}) \\
&= 113 \text{ kips} > 48.3 \text{ kips}
\end{aligned}
$$

where
f_{dv} = dynamic design stress for shear defined in Section 6.1.3
A_w = area of the web

Hence, the section can support the shear. The connection should be designed for this available strength.
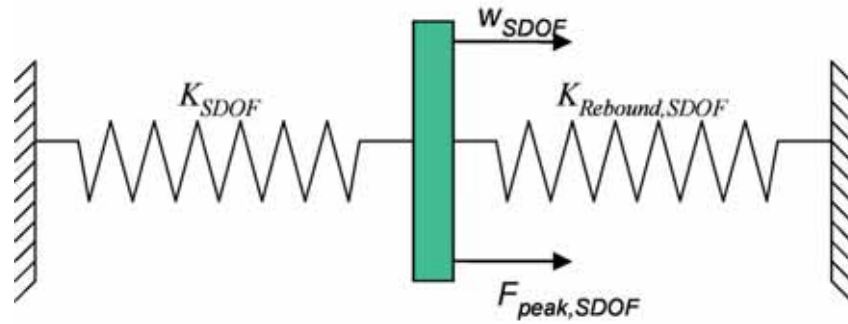
Fig. 6-18. SDOF model.
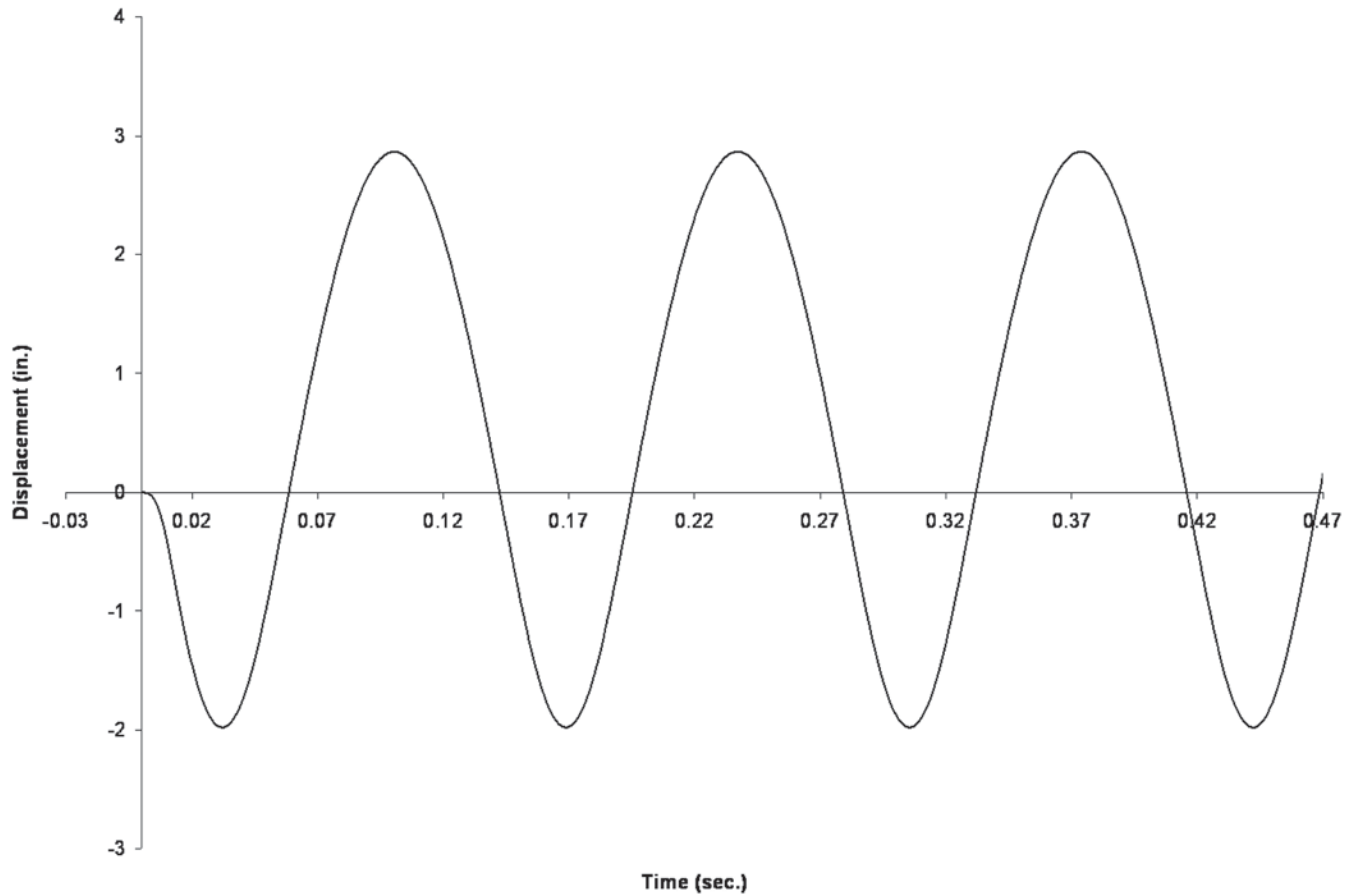
Fig. 6-19. SDOF displacement (including dead load).
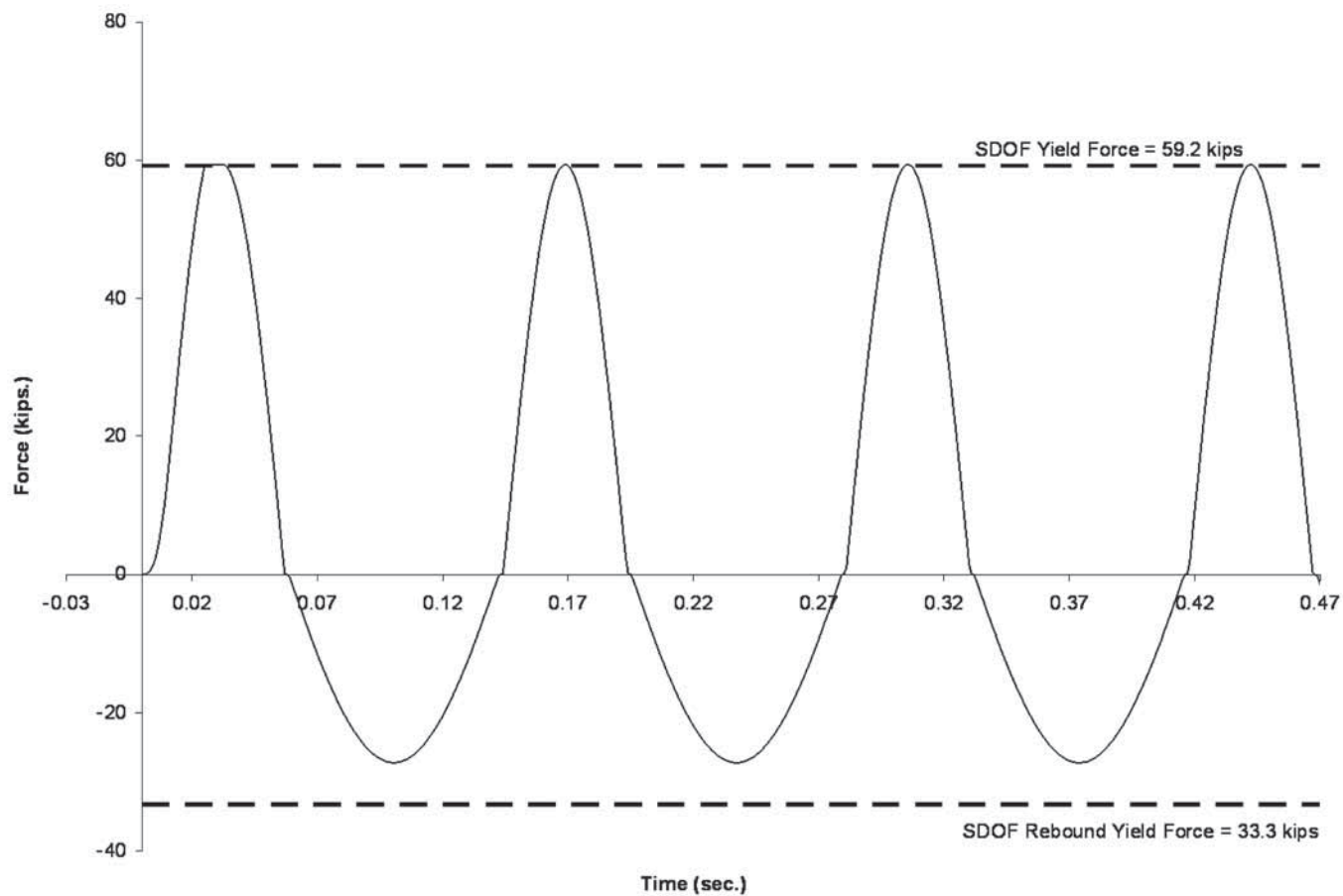
Fig. 6-20. SDOF force (including dead load).

Chapter 7
Design of Connections for Blast Resistant Structures

This chapter discusses the design of connections for blast resistant buildings, including general considerations and design procedures.

General connection design to transfer forces between members of the structural system is introduced in this chapter. Other considerations, like direct blast acting on large connection plates, are beyond the scope of this Design Guide and a finite element analysis should be used to determine the response of these connections.

7.1   GENERAL CONSIDERATIONS

Failure in steel structures often initiates at the connections of members, as opposed to the members themselves. There are a number of reasons for this, including:

- The design of many members is controlled by considerations other than strength, including deflection, vibration control and architectural requirements. Such members are often substantially stronger than required to resist the design forces. Connections, however, are typically designed based only on considerations of strength and therefore, often have little overstrength or reserve capacity to match the overstrength of the members.

- Connections are often controlled by sudden modes of failure such as tensile rupture at bolt holes or block shear rupture. These brittle modes of failure preclude redistribution of forces and the mobilization of ductile behavior.

- Connections tend to be of limited size and therefore, even when exhibiting ductile behavior, can only accommodate limited plastic deformation before reaching their ultimate capacities.

It is important in the design of blast resistant structures, particularly those expected to be loaded into their inelastic range of behavior, that sudden failure modes be avoided so that the plastic response of the structure can be mobilized. It is also important to remember that blast loading may also result in load reversal, sometimes in the form of rebound. Connections should be designed with equal strength under load reversal unless the following apply:

1. Member strength is limited in one direction of load application, by consideration of buckling as will occur for braces in compression and flexural members with one flange braced and the other unbraced.

2. A nonlinear dynamic analysis is performed to determine the maximum connection loads in both positive and negative loading applications.

Design of connections should, as a minimum, comply in all respects with the requirements of Chapter J of the AISC *Specification*, except as specifically modified herein.

7.2   DESIGN RESPONSIBILITY

Design of connections for structural elements intended to resist blast forces should be completed by the engineer of record. The design considerations associated with design of connections for blast resistant construction are beyond those normally considered by fabricators when selecting standard connections from the AISC *Steel Construction Manual* (AISC, 2011a).

7.3   CONNECTION DUCTILITY

In the previous chapters of this Design Guide, it has been emphasized that resistance to blast effects requires ductile behavior which can be assured through plastic design. FEMA 350 (FEMA, 2000a) provides valuable information on the available ductility and rotation capacity for several common types of steel connections.

7.4   CONNECTION STRENGTH

Connections should be designed to develop the full plastic capacity of the supported members, so that the plastic response of the structure can be mobilized in resisting blast-induced stresses. It should be noted that the dynamic plastic capacity of an element, loaded briefly by impulsive loading, is often greater than the static plastic capacity. When nonlinear dynamic analysis of structures and structural elements under blast loading is performed, the connections should be designed for the peak forces obtained from the analysis.

7.4.1   Required Strength

The required strength of connections should be determined according to the load combination discussed in Section 6.2.1:

$$R_u = 1.0D + 0.25L + 1.0B \tag{6-7}$$

where
- B = blast load
- D = dead load
- L = live load

Note that when this combination is used, live load reductions

otherwise permitted by ASCE/SEI 7 (ASCE, 2010a) should not be taken.

7.4.2 Available Strength

The available strength of connections, ϕR_n, should be determined using the LRFD method in accordance with the AISC *Specification*, as modified herein. When computing the available strength of connections, ϕR_n, the value of the resistance factor, ϕ, may be taken as unity. This is a conceptual departure from the AISC *Specification*, in which different failure modes and member types have varying resistance factors based on a reliability analysis. In this guide, all failure modes and member types are treated uniformly with regard to the resistance factor. The specified minimum yield stress and ultimate tensile strength of the connection material, as well as bolt and weld strength, may be increased to account for the dynamic increase factor, *DIF*, noted in Section 6.1.2. Note that strength increase factors, *SIF,* discussed in Section 6.1.1, permitted for the design of members, are not used in the design of connections as an additional means of assuring that connections will be capable of developing the strength of the member.

For typical connection design, unless governed by more detailed requirements such as DOD (2008) or other established criteria discussed in Chapter 3, a simplified value may be used:

$$f_{ds} = 1.20F_y \qquad (7\text{-}1)$$

$$f_{du} = 1.05F_u \qquad (7\text{-}2)$$

This is in accordance with the simplified values of Chapter 6 (Equations 6-5 and 6-6), where $f_{ds} = 1.30F_y$ and $f_{du} = 1.05F_u$. Removing the effect of *SIF* from Section 6.1.1 of 1.10 on F_y and 1.00 on F_u results in Equations 7-1 and 7-2.

7.5 BOLTED CONNECTIONS

7.5.1 Shear Connections

High-strength bolted connections in shear should be proportioned such that bolt bearing is the controlling limit state. Bolts may be pretensioned as required for slip-critical connections and must be pretensioned when required by AISC *Specification* Section J1; however, slip resistance should not be relied upon.

The size of fasteners and connected elements should be selected such that connection strength is controlled by bearing of the bolt against the connected elements rather than shearing of the bolts. Except for connections employing long-slotted holes, with the slot oriented perpendicular to the direction of applied force, bearing strength may be determined using Equation J3-6b of the AISC *Specification*, assuming deformation at service load is not a design

consideration. Block shear rupture should not be a controlling limit state.

For shear connections of flexural members with simple spans, consideration should be given to the use of short-slotted holes perpendicular to the line of force transfer to facilitate development of large connection rotations under load.

7.5.2 Tension Connections

In general, tensile strength of connections should be controlled by yielding of the connected elements rather than by the tensile strength of the bolts or tensile rupture of the connected parts.

7.6 WELDED CONNECTIONS

7.6.1 Filler Metals

As required by the AISC *Seismic Provisions for Structural Steel Buildings* (AISC, 2010b), weld filler metals should be rated for a minimum Charpy V-notch toughness of 20 ft-lb at 0 °F. Additionally, filler metals should have a toughness of 40 ft-lb at a temperature not less than 20 °F above the lowest anticipated service temperature.

7.6.2 Quality Assurance

Visual inspection should be provided for all welds designed to resist blast loading. Complete-joint-penetration groove welds should be subjected to 100% ultrasonic testing or radiographic testing. Acceptance criteria for flaws in complete-joint-penetration groove welds subjected to ultrasonic testing following the procedures contained in AWS D1.1, Clause 6, Part F (Ultrasonic Testing (UT) of Groove Welds) (AWS, 2010) should be in accordance with AWS D1.1, Table 6.2 (UT Acceptance-Rejection Criteria, Statically Loaded Nontubular Connections). A suitable alternative is to treat the groove welds as part of a dynamically loaded structure and use Table 6.3 (UT Acceptance-Rejection Criteria, Cyclically Loaded Nontubular Connections) or use the procedures of Annex S (UT Examination of Welds by Alternative Techniques). Acceptance criteria for these latter two methods are to be in accordance with AWS D1.1 Table S.1 (Acceptance-Rejection Criteria), cyclically loaded structures (weld class D) (AWS, 2010).

7.6.3 Tension Applications

Single-sided fillet welds and single-sided partial-joint-penetration groove welds should not be used in tension applications. Backing should be removed from all complete-joint-penetration groove welds in tension applications, with the root pass of the weld backgouged and repaired in accordance with AWS D1.1 requirements (AWS, 2010) or in

accordance with the AISC *Seismic Provisions for Structural Steel Buildings* (AISC, 2010b). Backing bars can remain where their presence is not detrimental to the performance of the connection. An example of this is at the top flange weld in many moment connections that are prequalified per AISC *Prequalified Connections for Special and Intermediate Steel Moment Frames for Seismic Applications* (AISC, 2010c).

T-joints in which material thicker than 12 in. will be subjected to through-thickness tension should be ultrasonically tested for lamellar tearing subsequent to welding.

7.6.4 Flexural Applications

Single-sided fillet welds and single-sided partial-joint-penetration groove welds should not be used in applications where significant flexural tensile stresses will be developed in the weld.

7.7 BRACING AND MOMENT-RESISTING CONNECTIONS

In addition to the modifications required for available strength discussed previously, bracing and moment-resisting connections should be designed in accordance with the AISC *Seismic Design Manual* (AISC, 2012).

Moment-resisting connections should be of a type that provides sufficient strength and ductility to meet the demand. Where the design concept requires the development of a plastic hinge, connections prequalified in accordance with AISC *Seismic Provisions* Chapter K are recommended.

Chapter 8
Resistance to Progressive Collapse

This chapter provides engineering guidance for analysis and design of structures to resist progressive collapse. The current state of the art for progressive collapse design in the United States and Europe is presented, followed by new proposals for step-by-step procedures. Analysis examples are provided at the end of the chapter for each of the proposed solution procedures. Given that progressive collapse is driven in large part by the self-weight of the structure, steel structures, with their relatively light weight, can be particularly well suited for design against progressive collapse. Recommendations are provided to the engineer for designing redundant, progressive collapse resistant systems.

8.1   OVERVIEW

8.1.1   Progressive Collapse Definition

Although there is no single, uniform definition of progressive collapse in the structural engineering design community, the American Society of Civil Engineers standard ASCE/SEI 7-10 (ASCE, 2010a) Section C1.4 defines "progressive collapse" as "the spread of an initial local failure from element to element, resulting eventually in the collapse of an entire structure or a disproportionately large part of it."

8.1.2   Brief Explanation of the
Design/Analysis Problem

Once a structural member has failed, its load is distributed to the surrounding members. If the surrounding members can support this additional load, then any further failure is arrested. If the surrounding members cannot carry this additional load, failure can extend vertically or horizontally as the surrounding members also fail. Once the cause of failure (fire, blast, impact, etc.) has dissipated, the loading is predominately due to gravity. The failure typically extends vertically through the structure until the failing members reach the ground or a portion of the structure is strong and ductile enough to arrest the collapse. If the failure reaches an area of the structure with stiffness discontinuity, it may redirect the failure propagation horizontally across the structure further extending the collapse.

As a design problem, progressive collapse is particularly challenging. It is difficult to identify the load case to be examined. Typical design is normally limited to linear behavior of the elements and associated structural response, whereas progressive collapse is highly nonlinear in both material response and geometric formulation. Finally, dynamic effects play a large role in progressive collapse response.

All of these factors must be considered when formulating parameters for a progressive collapse design problem.

8.1.3   Basic Concepts

The following terminology and concepts are consistently used when discussing progressive collapse:

Load Path: The intended gravity load path utilized in structural design. In most steel construction, the load path flows from the slab, to the beams, to the girders, to the columns, to the footings, and to the soil.

Element Collapse: The failure of any element such that it can no longer support vertical load.

Local Collapse: A collapse limited to a single bay on a single floor. Larger collapse areas could be considered a progressive collapse, or a disproportionate collapse. Various guidelines or standards may describe local collapse differently.

Alternate Load Path: Any redundant load path available to the gravity load. The alternate load path is provided by designing into the structure the ability to bridge across potential key element failures.

Key Element: Any element for which failure would result in more than a local collapse. In the load path described above, a failure of the slab, beams, or girders normally results in a failure localized to that bay. A failure of the column may result in the collapse of an entire bay along with the corresponding bay in any other floor supported by the column. The large area of collapse categorizes the column as a key element. Other key elements may be trusses, transfer girders, etc.

Specific Local Resistance: A design methodology that attempts to protect individual key elements from collapse by increasing the element strength. This is accomplished by designing the element for specific additional applied loads that are meant to simulate accidental loading.

Threat-Independent Approach: A design approach that does not assume any specific abnormal load on the structure. It may not be feasible to rationally examine all potential sources of collapse initiation. Instead of assuming a load, individual columns or key elements are removed as a "load initiator." The goal of using a threat-independent approach is not to prevent collapse from a specific threat, but to control and contain the spread of damage once localized damage or collapse has occurred. The strategy places a premium

on well-designed structural continuity, post-event capacity, ductility, and robustness as compared with the use of a specific load for the design of key elements.

8.2 ANALYSIS AND DESIGN CODES AND GUIDELINES

8.2.1 Introduction

In response to terrorist attacks on U.S. facilities, both domestic and abroad, several U.S. Government agencies, including the General Services Administration (GSA) and the Department of Defense (DOD), have developed independent security criteria to be used in the design of each of these agency's unique facilities. In Europe, progressive collapse design is not limited to government facilities; rather, it is addressed for all buildings in the British Code and Eurocode. Current U.S. codes and standards vary in their treatment of progressive collapse. The International Building Code (ICC, 2012) mentions progressive collapse. ACI 318 (ACI, 2011) has prescriptive detailing requirements for structural integrity for concrete structures. ASCE/SEI 7-05 (ASCE, 2005) requires that "buildings and other structures shall be designed to sustain local damage with the structural system as a whole remaining stable and not being damaged to an extent disproportionate to the original local damage." ASCE/SEI 7-10 (ASCE, 2010a) and certain local building codes also contain requirements for structural integrity against progressive collapse.

In contrast to dedicated progressive collapse standards, which provide instructions for progressive collapse analysis and design, the guidance provided in most of the existing codes is vague in defining the key issues that must be addressed in performing a progressive collapse analysis and design. The key issues are:

- Providing a quantifiable definition of progressive collapse
- Presenting a specific analysis approach and procedure to be used in the assessment of progressive collapse potential
- Providing guidance as to what analysis scenarios should be considered
- Providing design procedures to mitigate progressive collapse potential

The lack of guidance provided by the existing building codes has resulted in conflicting interpretations as to how one should approach progressive collapse design and/or analysis.

8.2.2 U.S. General Services Administration Guidelines

The U.S. General Services Administration (GSA) provides facilities to federal agencies. To minimize the amount of interpretation required by the engineer/analyst when working on government facilities, the GSA developed a comprehensive, threat-independent guideline for the consideration of progressive collapse—*Progressive Collapse Analysis and Design Guidelines for New Federal Office Buildings and Major Modernization Projects*, issued in November 2000. These guidelines were the first of their kind to provide an explicit process that any structural engineer could use to evaluate the progressive collapse potential of a multi-story facility. The original guidelines focused primarily on reinforced concrete structures. The GSA subsequently identified the need to update the original guidelines to address the progressive collapse potential of steel frame structures. As a result, the GSA guidelines were revised and re-released in June 2003 (USGSA, 2003).

Design Approach

The GSA guidelines take an alternate-load-path approach to threat-independent scenarios. There are no prescriptive requirements or specific element design forces within this standard. Although a threat-independent approach is utilized, the GSA guidelines allow the engineer to limit the number of column locations which must be considered for removal. Within this framework, only exterior columns and areas affected by uncontrolled pedestrian space, underground parking, or atypical structural features need be considered. Each location should be considered in an independent analysis (i.e., only one vertical support element is removed during the analysis, etc.).

When using the guidelines, an established analysis technique should be selected. Techniques that can be applied in the determination of the potential for progressive collapse consist of a combination of the following:

- Linear or nonlinear analysis
- Static or dynamic analysis
- Two-dimensional or three-dimensional analysis

A three-dimensional, linear-static analysis procedure is preferred by the GSA. More sophisticated analysis techniques (e.g., nonlinear, dynamic procedures) are permitted. However, caution must be exercised due to potential numerical convergence problems that may be encountered during execution of the analysis; sensitivities to assumptions for boundary conditions, geometry and material models; and other complications due to the size of the structure.

Loading

Downward loading required in the GSA guidelines for assessing progressive collapse potential consists of the estimated dead load, potential live load, and potential increases caused by the dynamics of the problem.

For static analysis, the recommended downward loading of the structure is:

$$Load = 2(D + 0.25L) \qquad (8\text{-}1)$$

where
   D = dead load
   L = live load

In this load combination, the live load is reduced to 25% of the design load to account for the difference between the actual live load present in a building and the design load used. The factor of 2 is used to approximate dynamic amplification of the load when a support is instantaneously removed.

For dynamic analysis, the load factor of 2 is removed from the load combination.

Linear Static Procedure

The procedure presented in the GSA guidelines recommends a linear static analysis. This procedure approximates dynamic effects when used in conjunction with the load combination specified in Equation 8-1. It approximates nonlinear material properties and element ductility through the use of demand-to-capacity ratios (*DCR*). *DCR* for the primary and secondary structural components are determined as:

$$DCR = \frac{Q_{UD}}{Q_{CE}} \qquad (8\text{-}2)$$

where
  Q_{UD} = acting force (demand) determined in the component and/or connection/joint (moment, axial force, shear, and possible combined forces)
  Q_{CE} = expected ultimate, unfactored capacity of the component and/or connection/joint (moment, axial force, shear and possible combined forces)

The linear static analysis procedure consists of removing a vertical support from the structure with the appropriate load applied, and then determining which members or connections exceed the acceptance criteria. For members that exceed the allowable *DCR* values in flexure, the ends of the member are released and replaced with moments applied to the joint equal to the member capacity, which approximate the plastic portion of the element response. This process is continued until no allowable *DCR* values are exceeded. Allowable *DCR* values are provided in the GSA guidelines for various structural forces and connection types.

If alternate load paths are available for effectively redistributing loads that were originally supported by the removed structural element, the structure has a low potential for progressive collapse. Conversely, if alternate load paths are not available for effectively redistributing loads that were originally supported by the removed structural element, the structure has a high potential for progressive collapse. The extent of allowable collapse is defined in the GSA guidelines.

The acceptance criteria for nonlinear analysis differ from the linear analysis acceptance criteria. Nonlinear acceptance criteria are based upon the ductility and rotation limits of specific components rather than *DCR* values. A table providing nonlinear acceptance criteria is also provided in the GSA guidelines. It should be noted that the use of a linear procedure, as provided for in the GSA guidelines, is not intended for and not capable of predicting the detailed response or damage state that a building may experience when subjected to the instantaneous removal of a primary vertical element. However, a linear procedure, albeit a simplified methodology, may, with proper judgment, be used for determining the potential for progressive collapse (i.e., a high or low potential for progressive collapse), provided the acceptance criteria accounts for the uncertainties in behavior in the form of appropriate demand-to-capacity ratios.

8.2.3 Department of Defense Criteria

The Department of Defense (DOD) currently requires that all new and existing buildings of three stories or more be designed to avoid progressive collapse. These design requirements can be found in Unified Facilities Criteria 4-023-03, *Design of Buildings to Resist Progressive Collapse* (DOD, 2010).

While there are some similarities to the GSA progressive collapse design guidelines, this Unified Facilities Criteria (UFC) was developed independently due to the uniqueness of the types of structures in the DOD building inventory and the difference between civilian and military approaches to protection levels. In addition to reinforced concrete and structural steel, this UFC also addresses masonry, wood, and cold-formed steel construction.

Design Approach

The DOD progressive collapse design requirements are threat independent. They incorporate both direct and indirect design approaches and, in overall philosophy, draw heavily upon the existing British design requirements. Both approaches are defined within the context of the load and resistance factor design (LRFD) philosophy. This enables the use of existing, material-specific LRFD design codes and should facilitate the transfer of some or all of the requirements to the civilian design community.

In indirect design, resistance to progressive collapse is considered implicitly "through the provision of minimum levels of strength, continuity and ductility." This design methodology uses "tie forces" and establishes ductility requirements. Direct design resistance to progressive collapse uses alternate load paths.

Structural progressive collapse design is correlated to building occupancies similar to those presented in ASCE/SEI 7-10 (ASCE, 2010a) and IBC 2006 (ICC, 2006). At the lower levels of protection, either indirect design (tie forces)

or direct design (alternate load path) is employed. For higher levels of protection, the alternate load path method is required in addition to the tie forces. Additional ductility requirements are specified for higher levels of protection.

Tie Forces

In the tie-force approach, the building is mechanically tied together to enhance continuity and ductility and to develop alternate load paths. Tie forces are typically provided by the existing structural elements and connections that are designed using conventional design procedures to carry the standard loads imposed upon the structure.

Depending upon the construction type, there are several horizontal ties that must be provided: internal, peripheral, and ties to edge columns, corner columns and walls. Vertical ties are required in columns and load-bearing walls. Figure 8-1 illustrates these ties for typical frame construction. Note that these tie forces are not synonymous with "reinforcement ties" as defined for reinforced concrete design.

Alternate Load Path

The alternate load path method is used when a vertical structural element cannot provide the required tie strength or for structures that require medium or high levels of protection. There are three allowable analytical formulations:

- Linear Static: The geometric formulation is based on small deformations and the material is treated as linear elastic, with the exception of discrete hinges that may be inserted. The full load is applied at one time to the structure from which a vertical load-bearing element has been removed.

- Nonlinear Static: The material and geometry are treated as nonlinear. A load history from zero load to the full factored load is applied to the structure with a vertical load-bearing element removed.

- Nonlinear Dynamic: The material and geometry are treated as nonlinear. A dynamic analysis is performed by instantaneously removing a vertical load-bearing
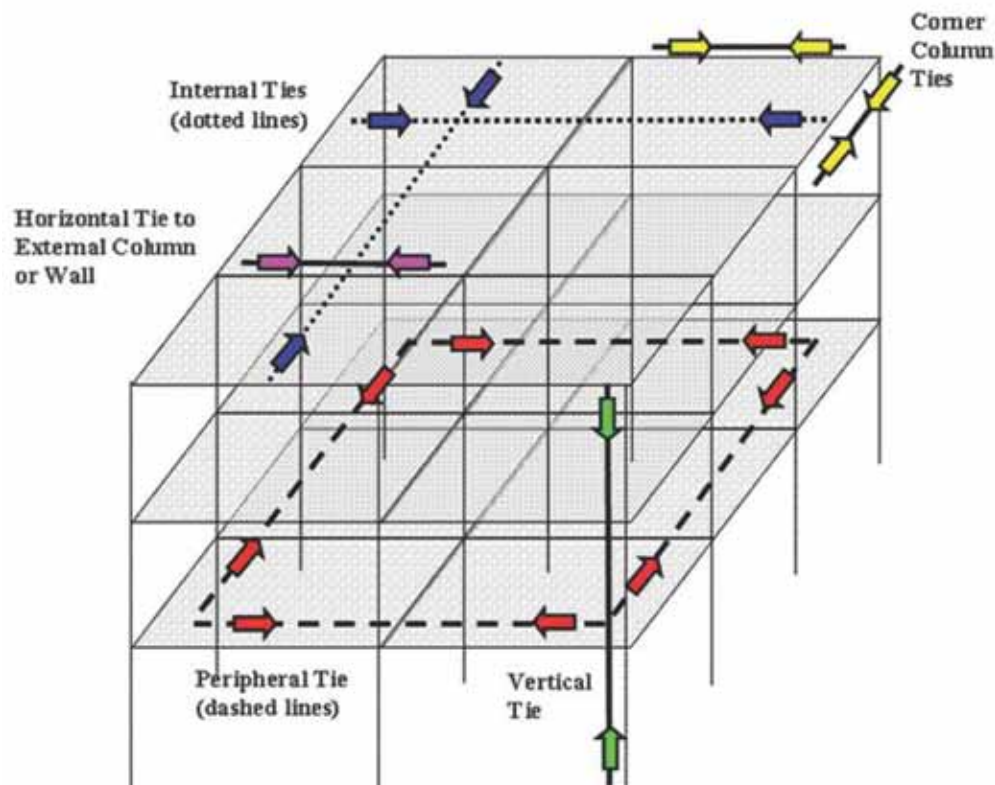
Note: The required External Column, External Wall, and Corner Column tie forces may be provided partly or wholly by the same elements that are used to meet the Peripheral or Internal tie requirement.

Fig. 8-1. Schematic of tie forces in a frame structure.

element from the fully loaded structure and analyzing the resulting motion.

The alternate load path method follows the LRFD philosophy by employing load combinations for extreme loading and resistance factors to define design strengths. While different loads are used for the static and dynamic analyses, both load combinations are based on ASCE/SEI 7-10, Section 2.5, Load Combinations for Extraordinary Events (ASCE, 2010a):

$$Load = (0.9 \text{ or } 1.2) D + A_k + 0.5L + 0.2S \quad \text{(ASCE/SEI 7 Eq. 2.5-1)}$$

where
A_k = load or load effect resulting from extraordinary event A
D = dead load
L = live load
S = snow load

For the removal of a wall or column on the external envelope of a building, the damage limits in an earlier edition of UFC 4-023-03 required that the predicted collapsed area of the floor directly above the removed element be less than the smaller of 750 ft^2 (70 m^2) or 15% of the total area of that floor, and the floor directly beneath the removed element should not fail. In addition, any collapse must not extend beyond the influence area for the removed element. Updated criteria in DOD (2010) allow no damage to the floor.

The acceptability criteria for the structural elements and connections in the alternate load path method consist of strength requirements and deformation limits. The moments, axial forces and shears that are calculated for the elements and connections in each alternate load path analysis are the required strengths based on the factored load combination. These required strengths must be compared to the design strengths of each element and connection. In addition, the deflection and rotations that are calculated in the alternate load path model must be compared against the deformation limits that are specific to each material type. If any structural element or connection violates an acceptability criterion (strength or deformation), modifications must be made to the structure before it is reanalyzed, as discussed in detail in UFC 4-023-03 (DOD, 2010).

Additional Ductility Requirements

According to the UFC 4-023-03 (DOD, 2005), for medium and high levels of protection for structures, all perimeter ground floor columns and load-bearing walls must be designed such that the lateral uniform load, which defines the shear capacity, is greater than the load associated with the flexural capacity including compression membrane effects where appropriate. This requirement reduces the possibility that a ground floor perimeter wall or column will fail in a brittle failure mode (shear) when subjected to lateral load. This requires the engineer to harden or upgrade the ground floor columns or walls which would be the likely locations of the largest blast loads or vehicle impact. In the UFC 4-023-03 (DOD, 2010), Additional Ductility Requirements have been replaced with Enhanced Local Resistance, which is required for Occupancy Categories III and IV.

8.2.4 British Standards

British Standards (BSI, 1997; BSI, 2000; BSI, 2005a; BSI, 2005b) require consideration of progressive collapse for all buildings taller than four stories and provide three different methods for avoiding disproportionate collapse: tying, bridging and key elements.

The first design option, tying, is intended to provide effective horizontal and vertical ties to increase structural continuity and increase the level of redundancy. BSI (2000) requires all buildings to be effectively tied together at each principal floor level. From BSI (2000), Section 2.4.5.3, all the ties and their end connections should be designed to resist the following factored tensile forces:

For internal ties

$$0.5(1.4g_k + 1.6q_k) s_t L \geq 17 \text{ kips (75 kN)}$$

For edge ties

$$0.25(1.4g_k + 1.6q_k) s_t L \geq 17 \text{ kips (75 kN)}$$

where
g_k = specified dead load per unit area of the floor or roof
q_k = specified imposed load (live load) per unit area of the floor or roof
s_t = mean transverse spacing of the ties
L = span

BSI (2000) considers "ties" to include steel members and their connections, steel bar reinforcement anchored to the steel frame, and steel mesh reinforcement in a composite slab with profiled steel sheeting—or any combination of the three. Compliance with these standards in the U.K. usually requires little or no extra costs. Where tying is not feasible, it is recommended that the structure be able to bridge over the loss of an untied member and the area of collapse be limited and localized. This is usually achieved by removing each untied element, one at a time, and checking that on its removal the area of the structure at risk of collapse is limited to the smaller of 15% of the story area or 750 ft^2 (70 m^2).

BSI (2000) Section 2 also gives the following load combination:

$$Load = D + \frac{1}{3}L + \frac{1}{3}W \quad \text{(8-4)}$$

where
    W = wind load

In these checks for notional removal of members, only one-third of the ordinary wind load and one-third of the ordinary imposed load are included, together with the dead load. In the case of buildings used predominantly for storage, or where the imposed load is of a permanent nature, the full imposed load should be used.

Finally, if it is not possible to bridge over the removed member, this member should be designed as a protected or key element. Key elements are designed to be capable of sustaining additional loads derived from a pressure of 5 psi (34 kN/m^2) applied to the surface of the structural member in any direction.

In 2010, the British Standards discussed in this section were replaced by the following Eurocode documents and UK Eurocode amendments:

> *Eurocode 3: Design of Steel Structures, General Rules and Rules for Buildings*, EN 1993-1-1:2005 (CEN, 2005a)

> *Eurocode 3: Design of Steel Structures, Plated Structural Elements*, EN 1993-1-5:2006 (CEN, 2006b)

> *Eurocode 3: Design of Steel Structures, Material Toughness and Through-Thickness Properties*, EN 1993-1-10:2005 (CEN, 2005b)

> *Eurocode 3: Design of Steel Structures, Piling,* EN 1993-5:2007 (CEN, 2007a)

> *Eurocode 3: Design of Steel Structures, Crane Supporting Structures*, EN 1993-6:2007 (CEN, 2007b)

> *Eurocode 3: Design of Steel Structures, Design of Joints*, EN 1993-1-8:2005 (CEN, 2005c)

> *Eurocode 2: Design of Concrete Structures, General Rules and Rules for Buildings*, EN 1992-1-1:2004 (CEN, 2004)

> *Recommendations for the Design of Masonry Structures to EN 1996-1-1 and EN 1996-2*, PD 6697:2010 (CEN, 2010)

> *Eurocode 6: Design of Masonry Structures, General Rules for Reinforced and Unreinforced Masonry Structures*, EN 1996-1-1:2005 (CEN, 2005d)

> *Eurocode 6: Design of Masonry Structures, Simplified Calculation Methods for Unreinforced Masonry Structures*, EN 1996-3:2006 (CEN, 2006c)

> *Eurocode 6: Design of Masonry Structures, Design Considerations, Selection of Materials and Execution of Masonry*, EN 1996-2:2006 (CEN, 2006d)

8.2.5 Eurocode

Eurocode 1: Actions on Structures, General Actions, Accidental Actions, EN 1991-1-7:2006 (CEN, 2006a) includes progressive collapse requirements that are based upon and similar to those in the British Standard.

8.3 ANALYTICAL APPROACHES TO PROGRESSIVE COLLAPSE

Several existing standards discussed previously address progressive collapse design. This chapter is intended to provide guidance for the analysis of steel structures for resistance to progressive collapse beyond what is provided in the current codes and government standards. This section proposes the use of nonlinear pushover analysis (energy balance method) as a tool to address progressive collapse analysis and design. This section also discusses nonlinear dynamic analysis, an approach adopted in the latest editions of the GSA and UFC progressive collapse guidelines.

8.3.1 Analysis Concepts

Selection of Collapse Phase for Analysis/Design

For the purpose of analysis and design, a collapse progression can be separated into three phases: the initiating event, the local collapse, and the progression. In terms of blast design, after the explosion the load from the blast pressure travels through the load path to the lateral system. If an element along the load path does not possess the required strength and ductility, there will be an initial element failure; this is the first phase, or initiating event. After this initial element failure, the elements surrounding the failed member become overstressed due to the redistribution of the load that was previously in the failed element. If these elements are not able to sustain the newly added load, there will be a local collapse, or the second phase. Finally, after the local collapse, the collapse will progress to surrounding elements, perhaps indefinitely. Any of these phases could be addressed in a progressive collapse resistant design. However, this chapter of the Design Guide focuses on the second phase, as the previous seven chapters demonstrate that steel structures can also be designed to be quite effective at resisting an initiating event due to blast. The intent here is to eliminate the local collapse, not prevent the initiating event.

The first phase is the initial element failure. Typically, this is assumed to be the failure of a column or other key element. Designing for this phase of the collapse requires knowledge of the applied load. This phase was dealt with in Chapters 5, 6 and 7. Due to the numerous potential sources of element overload (blast, impact, fire, etc.), the scale of the unknown load may vary substantially. For this reason, a threat-independent approach is usually preferred, which assumes initial failure and attempts to arrest the collapse in

another phase. The second phase is the collapse of the structure immediately affected by the element failure. To arrest the collapse in this phase, the affected area must be able to bridge across the failure. The third phase is the progression of the collapse outside the immediate failure zone. However, as the collapse region grows, the energy required to arrest the collapse grows. For example, the calculations in Figure 8-2 and Figure 8-3 show that it is exceedingly difficult to arrest the collapse once one floor falls on the floor below. Although typical design problems use a dynamic amplification of 2 as shown in Figure 8-2, a mass falling from any height will result in amplification factors larger than 2 as shown in Figure 8-3.

For a system that is permitted to yield, the dynamic amplification is much less than for a system that remains elastic. However, for the same assumptions described in Figure 8-3, a plastic hinge still requires an axial yield strength of 4.6mg to absorb the energy of the falling mass, as shown in Figure 8-4, where m is the mass of the structure and g is the acceleration due to gravity. This is much larger than a typical design force. These simplistic analyses do not account for more complicated scenarios like yielding, rupture, falling

---

External Energy from Mass Falling

$$E_{EXT} = mg(\delta + h) + mg\delta$$
$$E_{EXT} = 2mg\delta + mgh$$

Internal Energy is Area Under P-δ Curve for Spring
For Linear-Elastic Spring:

$$E_{EXT} = E_{INT}$$
$$2mg\delta + mgh = \tfrac{1}{2}k\delta^2$$
$$\tfrac{1}{2}k\delta^2 - 2mg\delta - mgh = 0$$
$$\delta = \frac{2mg + \sqrt{(2mg)^2 + 4\left(\tfrac{k}{2}\right)(mgh)}}{k}$$

If $h = 0$:

$$\delta = \frac{4mg}{k}$$
$$P = 4mg$$

2 masses produce 4mg, therefore Dynamic Amplification = 2
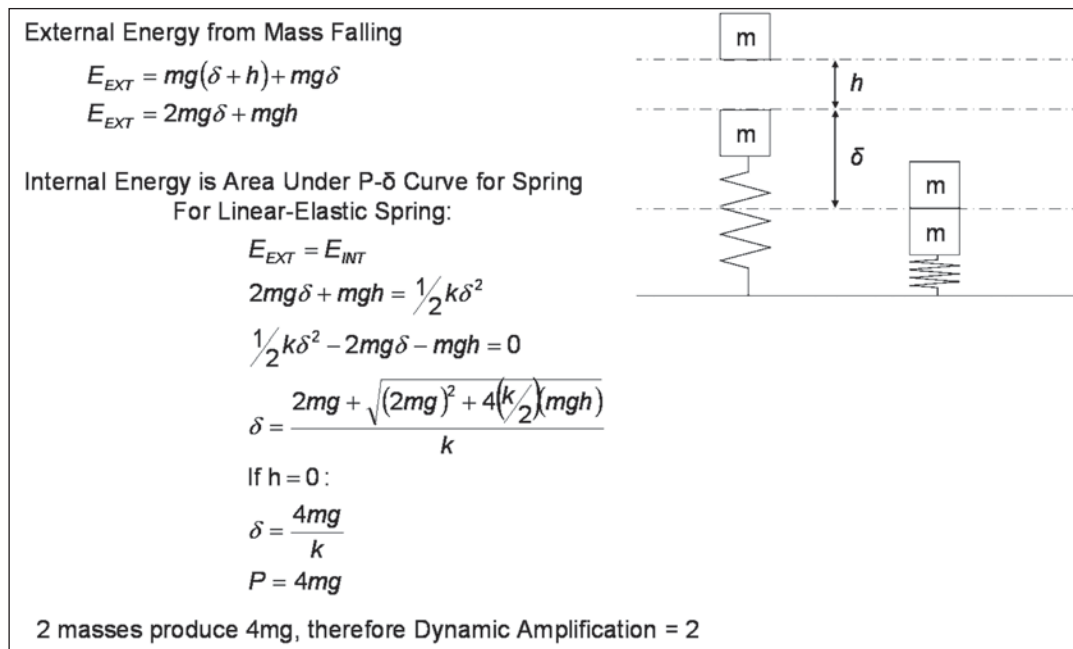
Fig. 8-2. Dynamic effects of falling mass (h=0).

More realistic assumption of h:

Assume the story height is half of the bay length, $h = 0.5L$.

Assume the beam was designed for deflection, $\delta_{Design} = \dfrac{L}{240} = \dfrac{mg}{k}$

Solve for story height:

$$h = 120 \times \frac{mg}{k}$$

Solve for δ:

$$\delta = \frac{2mg + \sqrt{244m^2g^2}}{k}$$
$$\delta = 17.6\frac{mg}{k}$$
$$P = 17.6mg$$

2 masses produce 17.6 mg, therefore Dynamic Amplification = 8.8
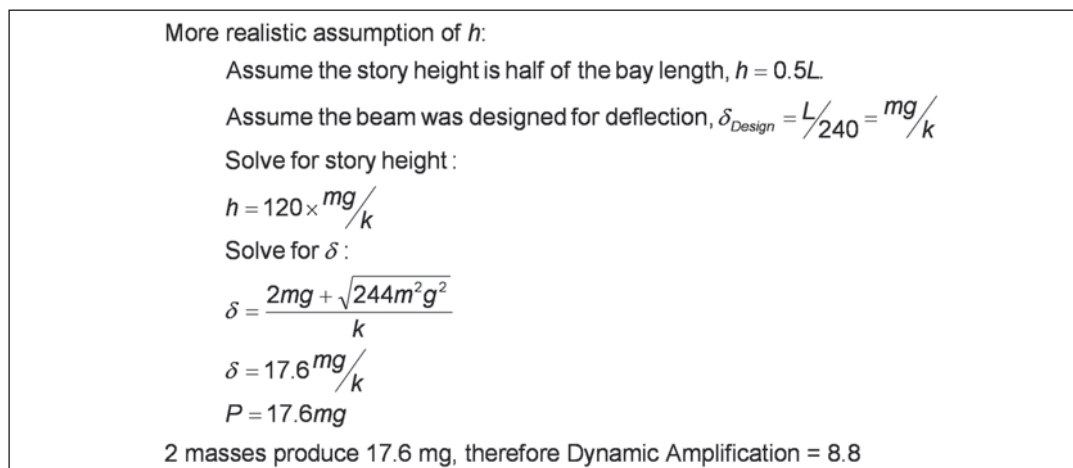
Fig. 8-3. Dynamic effects of falling mass (assume story height).

debris, etc., but do provide a general sense of the relative behaviors.

The following procedures and recommendations are directed at eliminating local collapse, which, if unchecked, leads to a progressive collapse. This allows for a threat independent methodology without forces that are unreasonably large for design.

Selection of Analysis Approach

To produce representative results, any progressive collapse analysis methodology must deal with both the dynamic nature of the loading and the nonlinear nature of the resistance. The GSA guidelines (USGSA, 2003) present a simple linear elastic static analysis procedure that approximates these through the use of load amplification factors and demand-to-capacity ratios. However, these are approximations which can be improved upon with the more accurate analytical methods currently available. Another more accurate, yet still relatively simple, option is to use the principle of conservation of energy to account for the dynamic effects as shown in Figure 8-2. A third, potentially more accurate, yet relatively complex, option is the use of a nonlinear dynamic analysis

---

Internal Energy is Area Under P-δ Curve for Spring

<u>For a Rigid-Plastic Spring</u>

$$E_{EXT} = E_{INT}$$

$$2mg\delta + mgh = P_y\delta$$

$$P_y = \frac{2mg\delta + mgh}{\delta}$$

Best case: h=0

$$P_y = 2mg$$

The system must have twice the design load to arrest the collapse.

For a more realistic assumption of h:

$$h = 0.5L$$

Assume the spring designed for deflection:

$$\delta_{Design} = L/240 = h/120 = mg/k$$

$$h = 120 \cdot mg/k$$

Assume the spring ductility:

$$\delta_{Ult} = 10 \cdot \delta_y = 10 \cdot P_y/k$$

Solve for required strength:

$$P_y = \frac{2mg(10 \cdot P_y/k) + mg(120 \cdot mg/k)}{10 \cdot P_y/k}$$

$$P_y = 4.6 \cdot mg$$

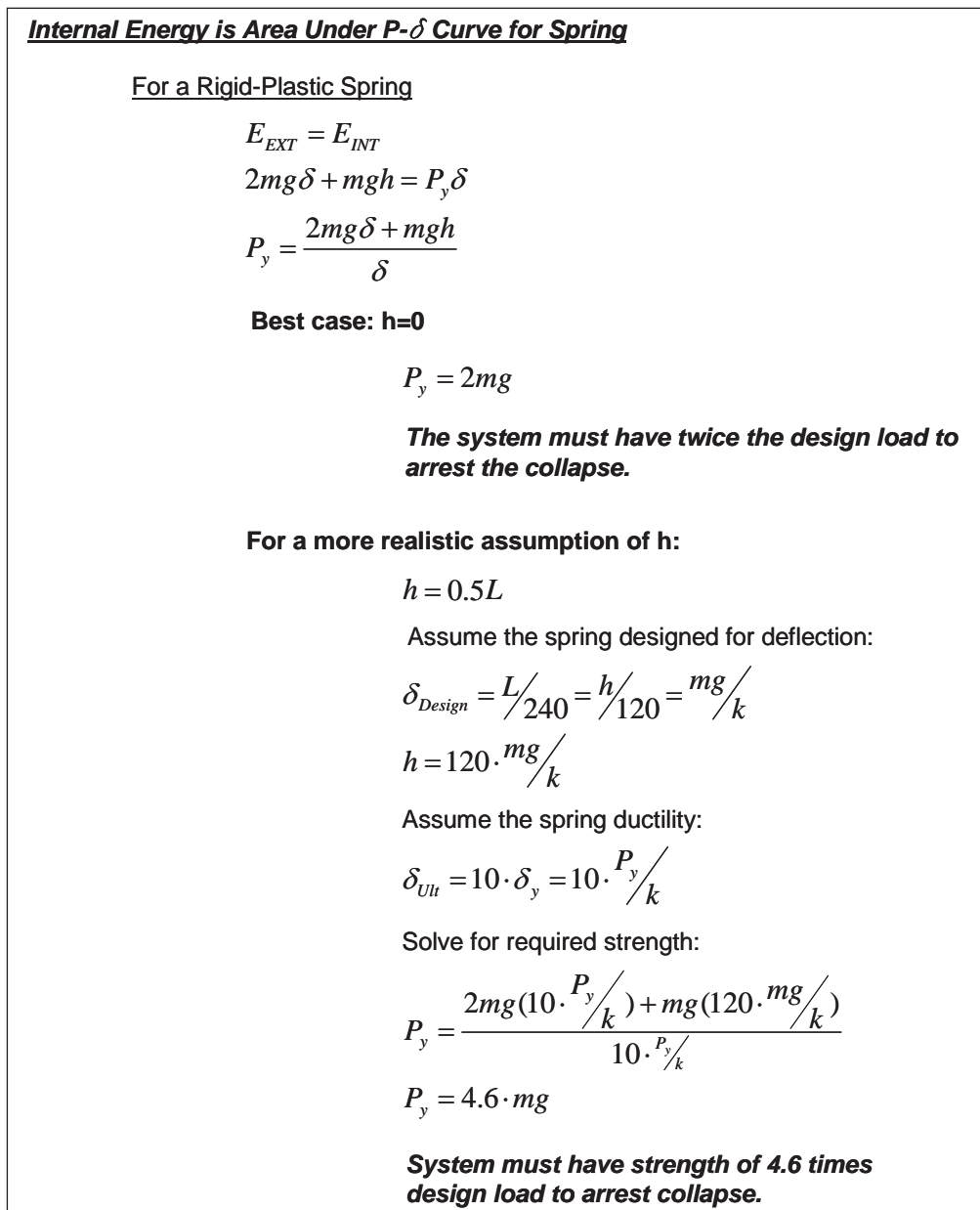**System must have strength of 4.6 times design load to arrest collapse.**

Fig. 8-4. Required yield strength of plastic hinge.

to be discussed in Section 8.3.3. As mentioned previously, the latest editions of both the GSA and UFC progressive collapse guidelines allow for nonlinear dynamic analysis methods. The GSA guidelines also provide corresponding acceptance criteria. The accuracy of any method used will be limited by uncertainty in the actual material properties present, as well as the necessary idealization of member and connection behavior.

For a linear static system, the deflection calculated by balancing the work for a mass falling from zero height is twice the static deformation for the same load. This is the same amplification factor that is used for many dynamic load analyses. However, this "amplification" is a transient effect; it is not necessary for the structure to have capacity to withstand twice the static load, only that it be able to accommodate the larger deflection. For a yielding system, the resistive force function is a nonlinear function of the displacement, and must be calculated with a nonlinear pushover analysis.

Structural Behavior

Because there are different approaches to modeling and analyzing progressive collapse, it is important for the engineer to identify the structural behavior modes to be examined before beginning the study. This behavior should be kept in mind while making modeling decisions and while analyzing results. If a collapse is to be arrested by the floor system, the alternate load path can be provided by several possible modes of behavior. The possible modes of behavior generally available in steel-framed structures are flexural action in the steel framing, flexural action in the composite steel beam-concrete slab system, catenary action in the steel framing, membrane action in the slab, or a combination of the above. Arching action in the composite system may also be initially present.

When using the steel framing to provide the alternate load path, the connection types are important. If the framing includes moment connections, their bending strength can be used to arrest the collapse. If it includes shear connections, catenary action will be required and the connections designed for axial load. This means that nonlinear geometry must be included in the analysis, and the system must allow for large displacements.

To develop catenary action, tension forces are transferred from the beams connected to the failed column to the rest of the structure. The forces may be transferred via the shear studs in a composite slab to the concrete slab, which then develops a compression ring or may be transferred to the rest of the structure via the connections at the end of the beams. Depending on how the bays are built, both mechanisms can work simultaneously. Consideration of axial force through the steel beam shear connections and development of concrete reinforcement at bay edges is essential for the catenary action to be developed.

When using the metal deck and slab to provide the alternate load path, the bay sizes are critical. Whereas a typical slab construction may be adequate for smaller bays, the thickness and reinforcing of the slab may need to be increased for larger bays. The slab will use membrane action to arrest the collapse, so nonlinear geometry will be required in the analysis. Corner and perimeter bays, due to their geometry, cannot develop the membrane action that an interior bay develops; hence other engineering approaches are necessary to account for the partial loss of membrane action.

The amount of damping present in progressive collapse analyses is not well known. Seismic analyses use 5% critical damping; seismic events have multiple oscillations and accelerations less than gravity. Progressive collapse events have fewer oscillations and accelerations equal to gravity. Energy analysis methods ignore damping and are conservative, while nonlinear time-history analysis methods incorporate damping and are more exact. Some engineers believe the 5% critical damping is conservative when used in progressive collapse analyses and use a 1% to 3% critical damping. Other values can be used at the discretion of the engineer. Nevertheless, due to the noncyclic character of the loading event, the damping does not influence the behavior of the system. It is the inelastic energy absorption of the connections in combination with the threshold capacity of the system (members and connections) that defines the outcome of the alternate load path analysis.

8.3.2 Nonlinear Static Pushover Analysis: Energy Balance Approach

The energy balance approach to progressive collapse analysis is advantageous in that it provides a means to account for nonlinear dynamic effects through the use of the pushover analysis. The energy method assumes a conservative system and does not account for assumed building damping (viscous or modal). This is a good approximation because little energy is lost through classical damping up to the maximum displacement. If the elements resisting progressive collapse undergo nonlinear deformations, the amount of energy that could have been dissipated through damping would be marginal in comparison. The energy method captures only the modal behavior proportional to the loading and does not describe the behavior of a collapse that excites several modes. For key element removal, the pushover basis is a reasonable approach.

Modeling

To utilize the energy balance approach, a numerical model of the building must be created which can accommodate nonlinear pushover analyses. To model the initiating event, a single support or key element is removed from the model. Nonlinear material properties are necessary to capture the

post-yield behavior and load redistribution of the system. Default FEMA 356 (FEMA, 2000b) hinges are one option to approximate nonlinear section behavior. Other section behavior models can be used, but they must capture the linear, plastic and plastic limit regions of the section behavior.

Appropriate hinge properties for the various connections or materials (i.e., composite beams), is a topic which requires further research. Unless the hinge properties used are reliably known, the sensitivity of analysis results to hinge uncertainty should be explored and any solution bracketed within likely bounds. If catenary or membrane action is expected to contribute, nonlinear geometry (large displacement) solution methods are required. Both axial and rotational nonlinear deformations of the connections are important for catenary action.

Loading

The design load combination should be the expected load:

$$Load = D + 0.25L \qquad (8\text{-}5)$$

where
  D = dead and superimposed dead load
  L = live load

This load combination is intended to represent the actual load on the system, as opposed to the more conservative loads used for typical design. For certain occupancies, such as storage, the 0.25 factor on the live load should be adjusted to reflect the actual expected load.

Procedure

Discretion is left to the engineer to determine what structural behavior is desired (i.e., elastic or plastic frame analysis,

steel catenaries and slab diaphragm, or slab membrane, etc). Once the model has been created and loaded, the analysis procedure is as follows and as shown in Figure 8-5 and Figure 8-6:

1. Load the entire structure with the design load prescribed in Equation 8-5. Compute the reaction, P_{Design}, of the key element to be removed.

2. Remove the column or key element for the current study and replace it with a load equal and opposite to the element force removed; typically, the axial force, P_{Design}.

3. Apply a point load to the model opposite to the reaction applied in Step 2 (P_{Push}). This load will serve as the reference load pattern for a static pushover analysis.

4. Perform the pushover analysis for the increasing point load.

5. Calculate the external work of the system as the product of the applied load and the resulting displacement. Calculate the internal work of the system as the area under the force versus displacement pushover curve.

$$W_{EXT} = \int_{0}^{\Delta} P_{Design}\, d\Delta = P_{Design}\,\Delta \qquad (8\text{-}6)$$

$$W_{INT} = \int_{0}^{\delta} P_{Push}(\delta)d\delta \qquad (8\text{-}7)$$
$$= \text{area under pushover curve}$$

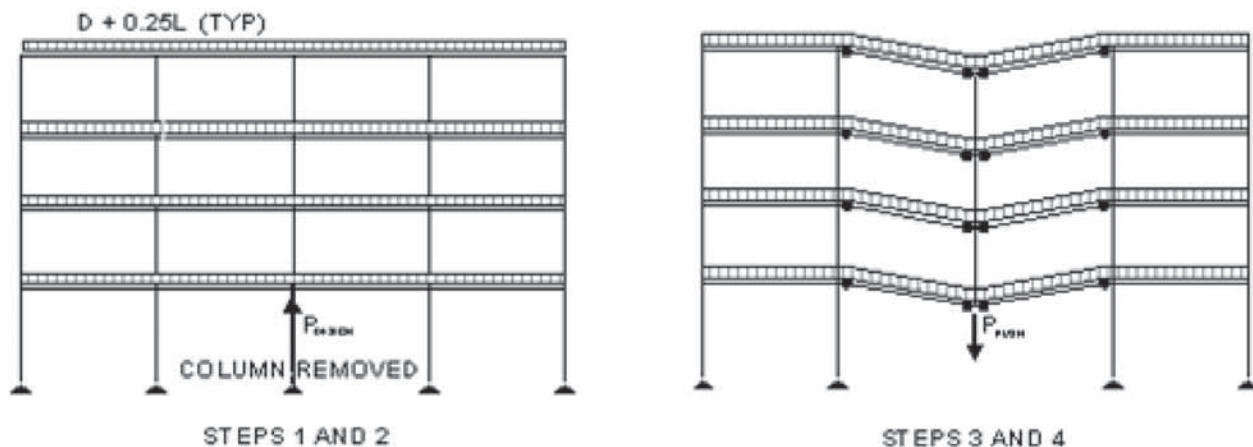6. Plot the capacity curve with the applied load.

Fig. 8-5. Frame example of energy balance procedure.

$$\text{Capacity}(\Delta) = \frac{W_{INT}(\Delta)}{\Delta} \qquad (8\text{-}8)$$

The external work is the sum of the potential and kinetic energy. At the point of the maximum displacement, just before there is an elastic reversal, the kinetic energy is zero.

Acceptability Criterion

The ability of the system to arrest a progressive collapse can be seen in either the work plot or the capacity curve plot. If the system has sufficient post-yield ductility to dissipate the energy from the falling floor, there will be a point where the external work done on the system will equal the internal work done by the system. This can be seen as the intersection point between the internal and external work shown in Step 5 of Figure 8-6 or in the intersection between the capacity curve and the applied load shown in Step 6 of Figure 8-6. Conversely, if the system fails through brittle fracture or strength degradation before achieving the balanced energy condition, the curves will not intersect, and the system is shown to lack resistance to progressive collapse.

It is also important to verify that the structure is detailed to accommodate the level of displacement calculated by the intersection of the design force and the capacity curve. Special attention should be paid to connections to avoid rupture and to bracing of flexural and axial members to avoid buckling.

8.3.3 Nonlinear Dynamic Analysis: Time-History Approach

The energy-balance approach deals explicitly with the non-linear material and geometric properties of the progressive collapse response and indirectly addresses the dynamic effects. Another analysis option is a nonlinear dynamic analysis. This approach is computationally intensive, but deals explicitly with the dynamic effects.
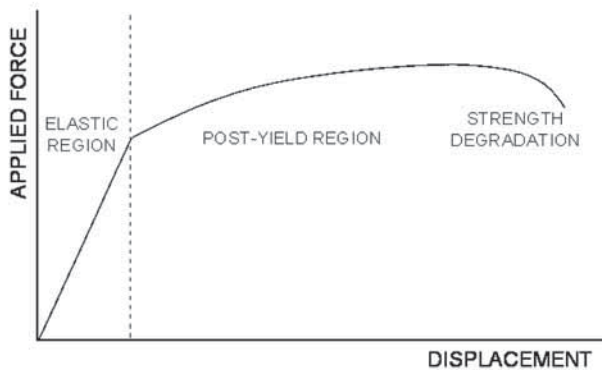
Step 4: Pushover Curve
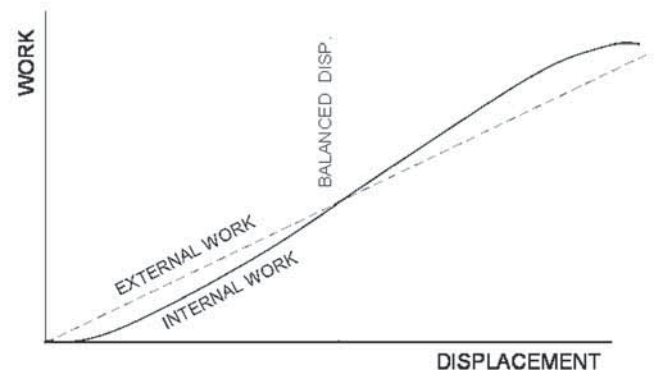
Step 5: Internal and External Work
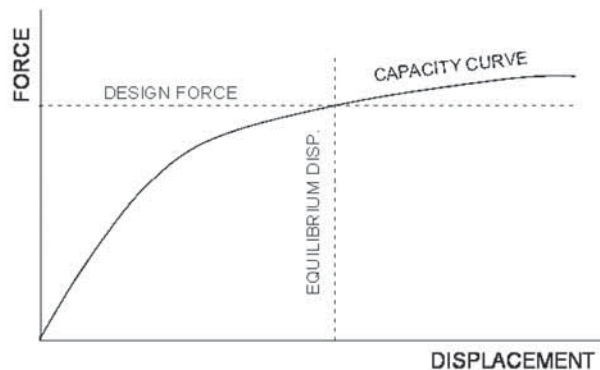
Step 6: Capacity Curve

Fig. 8-6. Typical energy balance results.

Modeling

The finite element modeling of the system is similar to that used in the energy-balance approach described in Section 8.3.2. For the dynamic analysis, however, the engineer should determine if hysteretic hinge elements are required. Unlike pushover analysis, it is likely there will be load reversal during the time-history response, which will require linear unloading of elements after they have yielded.

Loading

The loading for the dynamic analysis is similar to that used in the energy-balance approach described in Section 8.3.2. The design combination, P_{Design}, is $D + 0.25L$, as seen in Equation 8-5. The mass corresponding to the design load must also be applied to the model to achieve the correct dynamic response. The point load for time-history analysis, $P_{Load\ Function}$, must be time-dependent. To simulate

Fig. 8-7. Time-history modeling.

instantaneous loss of the supporting element, this load must ramp up from zero to P_{Design} within a time period equal to or less than $^1/_{10}$ the natural period of the response. For accuracy and calculation stability, a smaller time step may be required.

Procedure

As stated above, the engineer has the option to decide what structural behavior is modeled. Once the model has been created and loaded, the analysis procedure is as follows:

1. Load the entire structure, as shown in Figure 8-7, with the design load prescribed in Equation 8-5.

2. Remove the column or key element for the current study, and replace it with a load equal and opposite to the element force removed, typically, axial force, P_{Design} (see Figure 8-7).

3. Apply a point load to the model opposite to the reaction applied in Step 2 ($P_{Load\ Function}$) (see Figure 8-8). This load will serve as the reference load pattern for the time-dependent load function.

4. Perform the nonlinear dynamic time-history analysis.

5. Plot the structural response and responses of any critical elements.

6. Calculate the following key system parameters shown in Figure 8-9:

   Δ_{MAX}, maximum system displacement

   Δ_{PL}, permanent deformation of the system

   t_d, natural period of the system with the column removed

Verify that the loading function applied the load in a time less than or equal to $0.1t_d$. To be conservative, the natural period of the undamaged structure can be used. As the nonlinearity of the system's response increases, the difference between the maximum and final displacements decreases. To shorten
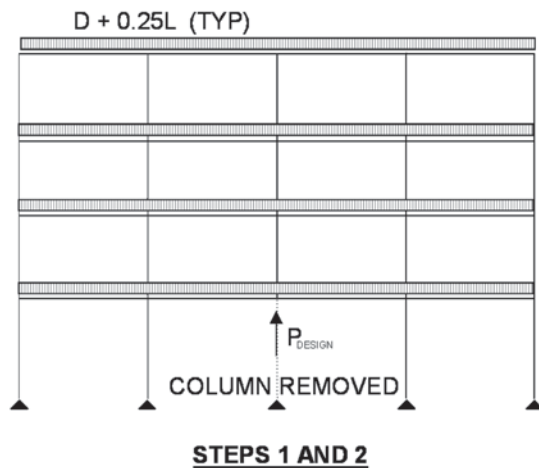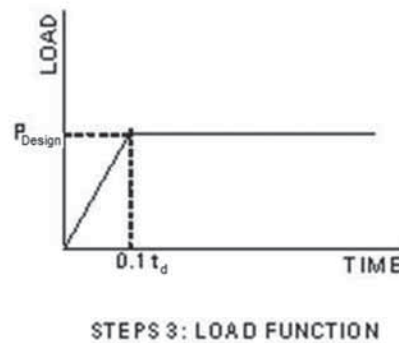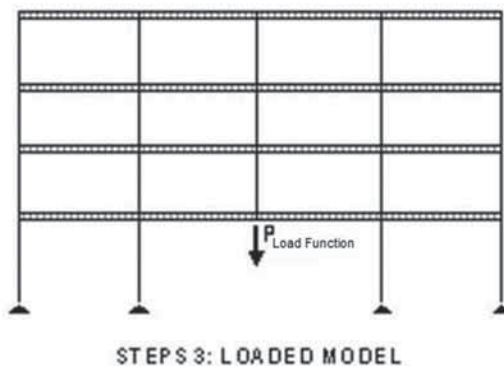

Fig. 8-8. Time-history loading.

the computer analysis, Δ_{PL} can be calculated by averaging Δ_{MAX} with the deflection at the first trough in Figure 8-9.

Acceptability Criteria

For the structural design to be considered adequate for arresting the collapse, it must meet two criteria:

1. The structure must be detailed to accommodate Δ_{MAX} for the structure and for each of the elements.

2. The analysis must run to completion without the structure becoming unstable. Care should be taken when interpreting the results of an incomplete analysis as this may be caused by a local or numerical instability which may be a modeling problem or by a structural instability which would indicate a collapse progression.

8.4 RECOMMENDATIONS

The following recommendations are grouped into prescriptive detailing, general design and analytical methods. The prescriptive detailing recommendations are applicable to all of the members of the structure and are intended to increase the toughness and redundancy without additional analysis. This is similar in concept to detailing requirements in high seismic zones. These requirements are applied to all designs, without regard to the actual forces. The benefit derived from prescriptive detailing has not been quantified. Future testing could quantify the benefit of these prescriptive detailing requirements. The general design recommendations should apply to the building as a whole and should make the engineer aware of the significance of bay size, key elements, column location, beam size, and metal deck slabs. The analytical design and analysis recommendations are applicable

to all key elements of a structure. They are based on a threat independent methodology and are focused on creating a quantifiable alternate load path in which each floor is capable of bridging across the failed key element in case of the loss of the key element. This bridging can be accomplished within the steel framing or within the concrete slab or with a combination of both. The benefit derived from the analysis and design is quantifiable.

8.4.1 Prescriptive Recommendations

In any structural design, there are means for increasing toughness and redundancy without additional analysis. When required, these recommendations are applied to all designs without regard to the actual forces.

Steel Detailing

There are currently two sets of building code requirements intended to address structural integrity—the New York City Building Code (NYCBC, 2008) and the International Building Code (ICC, 2012). The New York City Building Code requires all bolted connections to have a minimum of two bolts and that bolted connections of all columns, beams, braces, and other structural elements that are part of the lateral load resisting system be designed as bearing connections with pretensioned bolts or as slip-critical connections. All end connections of beams and girders must have a minimum available axial tensile strength equal to the larger of the provided vertical shear strength of the connections at either end, but not less than 10 kips. Elements and their connections that brace compression elements should have an available axial tensile strength of at least 2% of the required strength of the compression element being braced but not less than 10 kips.
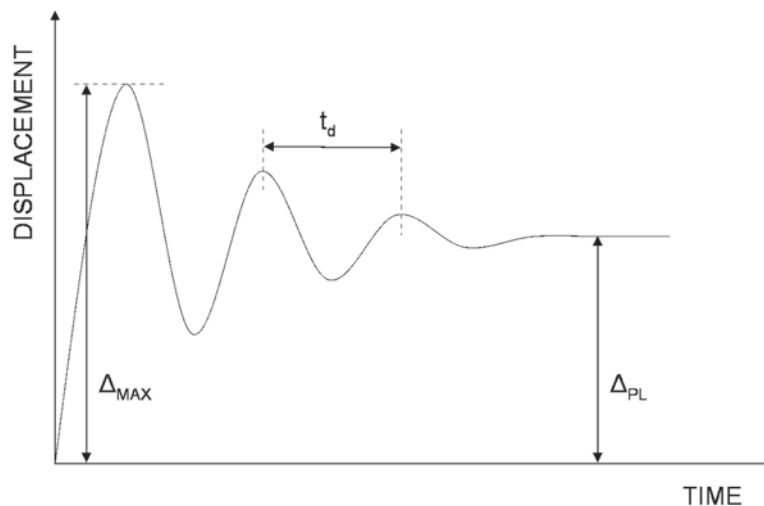

Fig. 8-9. Example time-history result.

If more than one element braces a compression element, the strength can be shared but all braces should have an available tensile strength equal to at least 1% of the column load, but not less than 10 kips. Column splices should have an available tensile strength at least equal to the largest design gravity load reaction applied to the column at any floor level located within four floors below the splice.

The 2012 International Building Code has provisions that require all beam connections to have a nominal tensile strength at least equal to ⅔ the required shear strength for the connection for design by LRFD, but not less than 10 kips. It also requires that column splices have a minimum design strength in tension to transfer the design dead and live load tributary to the column between the splice and the splice or base below.

In progressive collapse design, when considering catenary action, connections often have very high demand in both tension and rotation. As an example, the detail in Figure 8-10 uses a plate at the bottom of the beam in addition to a shear tab. If the shear tab fails due to rotation, the plate will provide axial capacity while allowing the beam to rotate around the point of connection of the plate. Engineers should be aware of the depth-to-span ratio of the beam when considering catenary action. Large beams can be designed elastically or through traditional plastic methods, while smaller beams must have connections with high rotational and axial deformation capacity.

Structural Slab Detailing

To improve the integrity of the structural slab, the following details should be considered:

- Welded wire fabric reinforcement in concrete slabs should be continuous over all supports and in all spans. The minimum area of continuous reinforcement should be 0.0015 times the total area of concrete. The mesh should have tension splices and be developed at discontinuous edges.
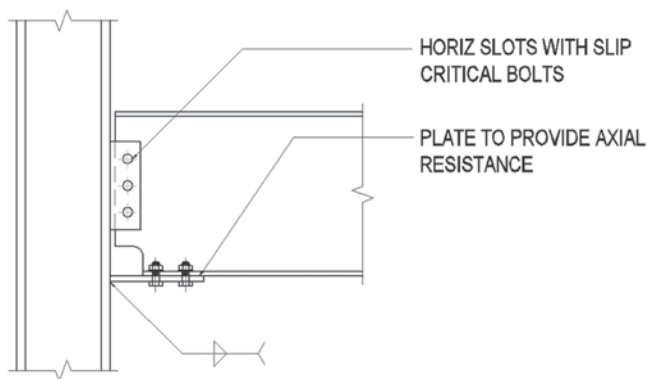

Fig. 8-10. Schematic beam connection detail.

- The connection of permanent metal decking to the steel should have, as a minimum, a 36/3 pattern. Side-lap connections should have a minimum strength equal to the strength of a button punch every 24 in. on center.

- Connections at the discontinuous edges of metal decking to supporting members should have a minimum connection strength equal to the strength of a ¾-in. puddle weld every 12 in. on center.

- Additional reinforcing bars should be placed in the metal deck slab to develop a minimum force per unit length of 50% of the tensile strength of the decking.

- Metal deck should be arranged such that the deck panels do not end at column lines, providing deck continuity at the probable location of maximum demand.

- Shear studs should not be less than ½ in. in diameter. Shear stud spacing should not be greater than one stud per foot averaged over the length of the beam.

8.4.2 General Design Recommendations

Bay Size

The capability of typical structures to bridge across a failed column is strongly correlated to the size of the bay; the larger the bay, the more prone the structure is to progressive collapse. As the size of the bay increases, steel sizes increase but the slab typically does not. This generates a slab that is not proportional to the bay size. As the slab is an important part of the resistance due to action of the compression ring and the tension reinforcing, the relationship of the slab thickness and reinforcing to the column spacing should be considered. Therefore, special attention should be given to structures with bays in excess of 30 ft or with irregularly sized bays.

Key Elements

The engineer must determine which structural elements would cause extensive collapse if lost. These are referred to as key elements. Key elements include major columns, transfer girders or trusses, and structural elements that brace key elements and whose failure would result in failure of the key element. Elements that brace secondary elements need not be considered key elements. If key elements are present in a structure, the structure should be designed to account for their potential loss one at a time, by the alternate load path method. Alternatively, the key elements should be strengthened to resist specific threat-dependent loads. By adding sufficient redundancy, the removal of elements will not lead to a global collapse. Hence, the element is no longer a key element. The goal of the engineer should be to increase the

redundancy of structures by providing alternate load paths. Where alternate load paths cannot be provided, key elements should be designed for specific local resistance using threat-dependent loads. If specific threat dependent loads are unknown, the following specific local loads may be used:

- Each key compression element should be designed for a concentrated load equal to 2% of its axial load but not less than 15 kips, applied at mid-length in any direction, perpendicular to its longitudinal axis. For large columns, this provision can be considerable but it has been part of the New York City Building Code for decades. This load should be applied in combination with the full dead load and 25% of the live load in the column.

- Each bending element should be designed for a combination of the principal applied moments and an additional moment equal to 10% of the principal applied moment applied in the perpendicular plane. By reducing the buckling tendency, this provision adds stability to the element.

- Connections of each tension element should be designed to develop the smaller of the ultimate tensile capacity of the member or three times the force in the member.

- All structural elements should be designed for a reversal of load equal to 10% of the design load.

Column Location

The engineer should individually consider the corner columns, the perimeter columns and the interior columns. Corner columns are made redundant by the steel members framing into them. Perimeter columns with framing only on three sides are made redundant by the steel framing and slab. Interior columns are made redundant by the steel floor framing alone, the metal deck slab alone, or by a combination of both.

Beam Size

To develop catenary action and dissipate a large amount of energy, the beams should be capable of reaching their plastic strength. The larger the beam, the larger the connection required to produce the beam plasticity. Therefore, the smallest possible beam size which meets all serviceability and strength requirements, along with connections capable of developing the tension capacity of the beam, should be considered.

Metal Deck/Concrete Slab

If catenary action develops, significant anchoring forces are resisted primarily by a compression ring forming in the slab, as will be demonstrated in Section 8.5.4. Additionally, the slab has three components in place to resist tensile stresses, which will be explored in Section 8.5.5. Significant tensile strength is available through the wire mesh reinforcing, the steel beams that are attached to the concrete through the shear studs, and the metal deck that is made effectively continuous through bars placed in the slab.

8.4.3 Analytical Design Recommendations

To minimize the impact of the unknowns inherent in the accidental loading assumptions in progressive collapse analysis, a threat-independent methodology should be considered. For each key element assumed to be removed, an alternate load path should be provided in which each floor is capable of bridging across the failed key element. This bridging can be accomplished within the steel framing or within the concrete slab or through a combination of the two.

The analytical approach should deal explicitly with nonlinear material properties and large displacements. It is advantageous to address the dynamic effects with an analysis that is more accurate than simply applying dynamic amplification factors. The energy balance method described in Section 8.3.2 or the nonlinear dynamic analysis method described in Section 8.3.3 are recommended.

8.5   DESIGN EXAMPLE

Example 8.1—Analysis of Structural System with Removal of an Interior Column

This section presents the analyses of typical composite concrete slab and steel beam/girder floor systems with an interior column removed. It considers bay sizes of 24 ft by 24 ft (Model A) and 36 ft by 36 ft (Model B). There are several available modes of structural behavior that may be considered, including catenary action in the steel framing, flexural action in the steel framing, flexural action in the composite steel-concrete slab system, membrane action in the slab, or a combination thereof. There are also different analytical procedures available, including the linear elastic static procedure presented in the GSA documents, the energy balance approach discussed in Section 8.3.2, and the nonlinear dynamic approach. The examples presented here illustrate the use of a small subset of the possible behaviors and methods. The following three analyses are performed for each structural system and are designated as Parts (a), (b) and (c) of this example:

(a) Steel Pushover Approach

(b) Reinforced Slab Solution

(c) Steel Nonlinear Dynamic Approach

Part (a), the steel pushover approach, considers catenary action in the steel framing alone. Assuming large displacements, the pushover and capacity curves are computed using the energy balance approach. The results from the energy balance analysis are then compared to the results of a time-history analysis of the same structural system. The concept of catenary action of the steel members is then explored and through a parametric study it is shown that the smaller a steel member is, the larger the deflection and the less demand on the connection. The idea that the slab can develop membrane action and the presence of a compression ring is also discussed. Using the energy balance method, this example demonstrates that when the steel beams are treated as cables in tension, a solution can be found, although significant tension forces develop. The connections required to resist these axial forces may likely have significant flexural capacity. Consideration of the flexural as well as axial capacity of the framing connections, along with the use of composite behavior with the concrete in the slab, will lead to a more economical design. This is left for the reader to explore.

In Part (b), the purpose of the reinforced slab solution is to present a rational and economical method to design for collapse prevention by considering membrane action in the slab. Based on the testing of slabs, an energy balance method is used to analyze the membrane strength of a slab. The pushover curve for the tensile membrane capacity of the slab is computed based on the simplified iterative method reported by Mitchell and Cook (1984). The reinforcement in the slab is assumed to be continuous in order to develop the membrane capacity. For many projects, the slab membrane solution may be the simplest and most economical method available.

Part (c) uses the steel nonlinear dynamic approach and explores the results using a highly detailed computer model that incorporates nonlinear material properties and large displacements. The gravity load is applied and then the center column is removed. This method includes all structural components and is time intensive. In the end, the observed deflection is similar to the results from the steel pushover and slab membrane approaches demonstrated in Parts (a) and (b).

Given:

Figure 8-11 gives the geometry of a floor system with a 24-ft by 24-ft bay size (Model A). The composite floor consists of a 5½-in. composite slab consisting of 3-in. metal deck and 2½-in. normal weight concrete. The wire mesh is 6×6 W1.4×W1.4 WWF (F_y = 60 ksi) and the metal deck is 20 gage (F_y = 33 ksi) with the ribs perpendicular to the beams. The composite beams are ASTM A992 W12×19 spaced 8 ft on center, with (24) ¾-in.-diameter steel headed stud anchors. The beam shear connections consist of a ¾-in.-thick ASTM A36 single plate with three ¾-in.-diameter ASTM A325 bolts. The composite girders are ASTM A992 W16×31, with (27) ¾-in.-diameter steel headed stud anchors. The girder shear connections consist of a ¼-in.-thick ASTM A36 single plate with four ¾-in.-diameter ASTM A325 bolts. The specified compressive strength of the concrete is 3.5 ksi, and the modulus of elasticity is:

$$E_c = \left(145 \text{ lb/ft}^3\right)^{1.5} \left(33\sqrt{3,500 \text{ psi}}\right)/1,000 \text{ lb/kip}$$
$$= 3,410 \text{ ksi}$$

The floor framing and slab are continuous on all sides of the framing plan shown. The floor system will be analyzed for the removal of the center column. At collapse initiation, the uniform service load is 87.5 psf (dead load = 50 psf, sustained dead load = 25 psf, 25% of live load = 12.5 psf).

For the 36-ft by 36-ft floor system (Model B), the geometry, distributed loading (87.5 psf), and materials are equivalent to those of the 24-ft by 24-ft model; however, the bays are 36-ft square, with 12-ft spacing between beams. There is also more reinforcement and the girders, beams shear studs, and connections are slightly more robust. The wire mesh is 6×6 W2.9×W2.9 WWF (F_y = 60 ksi). The composite beams are ASTM A992 W12×50 spaced 12 ft on center, with (36) 1-in.-diameter steel headed stud anchors. The beam shear connections consist of a ¼-in.-thick ASTM A36 single plate with (3) ¾-in.-diameter ASTM A325 bolts. The composite girders are ASTM A992 W18×97, with (42) 1-in.-diameter steel headed stud anchors. The girder shear connections consist of a ¼-in.-thick ASTM A36 single plate with four ¾-in.-diameter ASTM A325 bolts.

The slab mode is based on its reinforcement. Model A uses 6×6 W1.4×W1.4 WWF, which provides 0.028 in.^{2}/ft. Model B has 6×6 W2.9×W2.9 WWF, which provides 0.058 in.^{2}/ft. The yield strain for both models is:

$$\varepsilon_{yield} = \frac{60 \text{ ksi}}{29{,}000 \text{ ksi}}$$
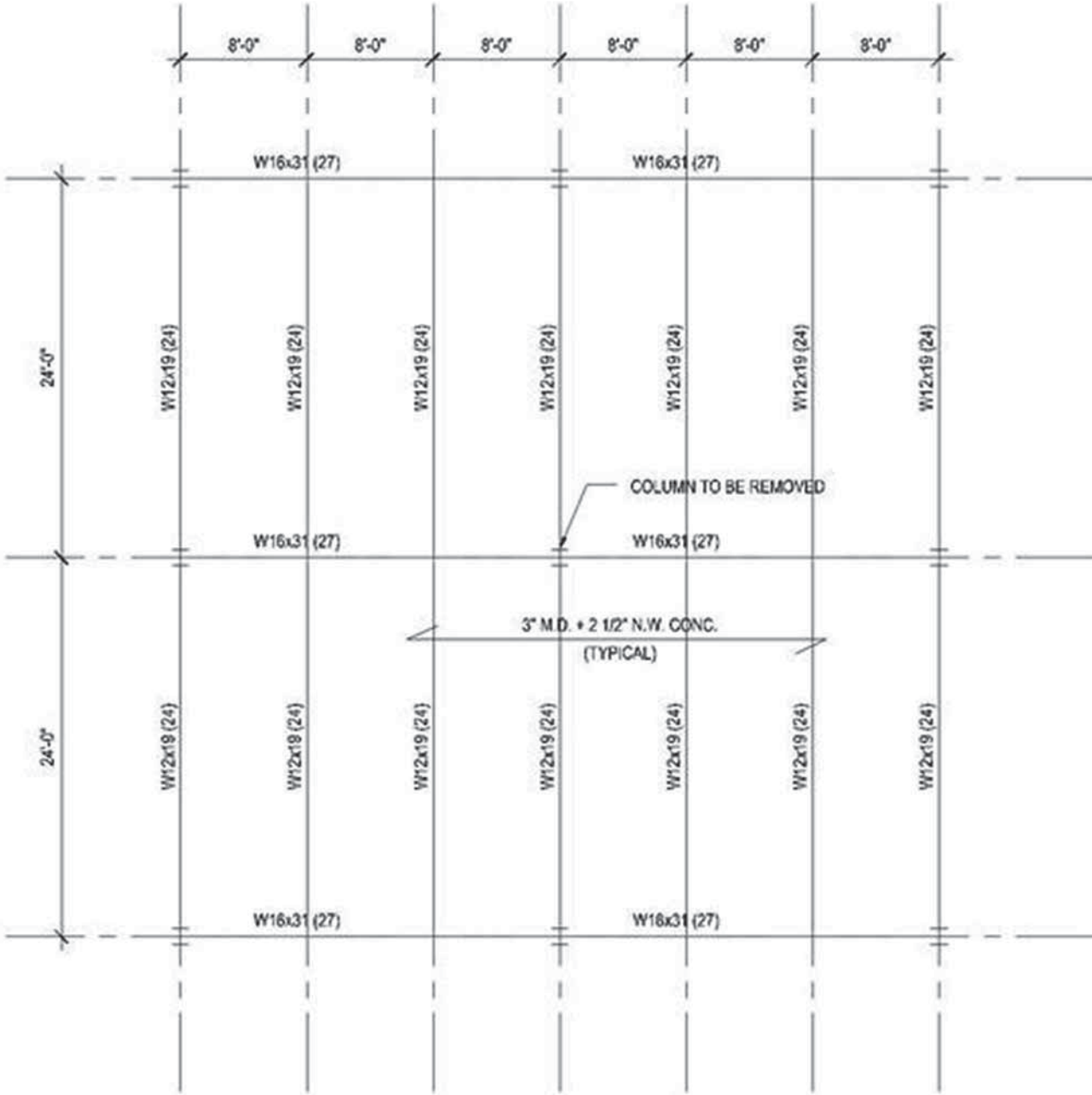$$= 0.00207$$

Fig. 8-11. Test composite floor system (Model A)

The elongation of typical wire sizes is on the order of 7% [*Manual of Standard Practice—Structural Welded Wire Reinforcement*, Wire Reinforcement Institute, page 9, Table 3(b) and Table 3(c) (WRI, 2010)]. This corresponds to a ductility of 35, which is well beyond the range of deflection considered in this example. The material behavior model for these calculations is elastic perfectly-plastic. The effective span length, after removal of the column, for the elements in Model A are $L_x = L_y = 2(24 \text{ ft}) = 48.0$ ft. The effective span length, after removal of the column, for the elements in Model B are $L_x = L_y = 2(36 \text{ ft}) = 72.0$ ft.

Solution:

From AISC *Steel Construction Manual* (AISC, 2011a), Table 2-4, the material properties are:

ASTM A36
$F_y = 36$ ksi
$F_u = 58$ ksi

ASTM A992
$F_y = 50$ ksi
$F_u = 65$ ksi

From AISC *Manual* Table 1-1, the geometric properties are:

W12×19
$A_g = 5.57$ in.^{2}

W16×31
$A_g = 9.13$ in.^{2}

W12×50
$A_g = 14.6$ in.^{2}

W18×97
$A_g = 28.5$ in.^{2}

Nonlinear geometry and nonlinear material properties are necessary to capture load redistribution for the vertical collapse progression scenarios. To look at the axial forces developed through catenary action in the beams, large displacements must be considered. Nonlinear material properties are included for all failure scenarios. Discrete plastic hinges are used in the steel frame elements to model these effects based on FEMA 356 (FEMA, 2000b). The axial hinges are simply a modeling concept that allows the beams to yield axially. For this example, the only hinge modeled is the axial tensile yielding capacity of the beams. Figure 8-12 shows this generic hinge property. From AISC *Specification* Section D2(a), with $\phi = 1.00$, the available axial tensile yielding strength is:

For Model A

W12×19
$\phi P_n = \phi F_y A_g$

$\quad = 1.00(50 \text{ ksi})(5.57 \text{ in.}^2)$

$\quad = 279$ kips

W16×31
$\phi P_n = \phi F_y A_g$

$\quad = 1.00(50 \text{ ksi})(9.13 \text{ in.}^2)$

$\quad = 457$ kips

For Model B

W12×50
$\phi P_n = \phi F_y A_g$

$\quad = 1.00(50 \text{ ksi})(14.6 \text{ in.}^2)$

$\quad = 730$ kips

W18×97

$$\phi P_n = \phi F_y A_g$$

$$= 1.00(50 \text{ ksi})(28.5 \text{ in.}^2)$$

$$= 1{,}430 \text{ kips}$$

(a) Steel Pushover Approach

For the purposes of this example, only the steel beams are modeled. For Model A (Figure 8-13), the beams framing into the W16×31 and their hinge properties are included. For Model B (Figure 8-14), the beams framing into the W18×97 and their hinge properties are included. For both models, the tensile yield strength of these elements is included as a hinge property in the center of the span as discussed previously.

The connections are designed to carry the full gravity load. All of the elements are assumed pinned at the boundaries; hence their reactions must be distributed through the compression ring that is formed in the slab surrounding the collapse. It is initially assumed that the compression ring is effectively rigid and provides sufficient anchorage. After computing the pushover and capacity curves for both models, the assumption of rigid anchorage provided by the compression in the perimeter of the slab is checked.

Both Models A and B assume rigid supports to guarantee sufficient horizontal restraint. The anchorage is provided by the concrete compression ring in the slab, allowing the beams to develop the necessary tensile forces for catenary action. The tension forces are transferred to the rest of the structure via the connections at the supports and to the concrete through the steel headed stud anchors present in the composite beams. A simplified model of the compression in the slab that enables the beams to develop catenary forces is presented later. Catenary behavior will be observed for large displacements.

Both Models A and B assume that the beam sections develop their yield strengths in tension. The engineer should ensure that the axial deformation capacity of a connection is not exceeded before the required catenary strength is developed. The tie-force method outlined in the UFC requires connections to be capable of rotating 0.2 rad (11.4°). Possible localized connection failure
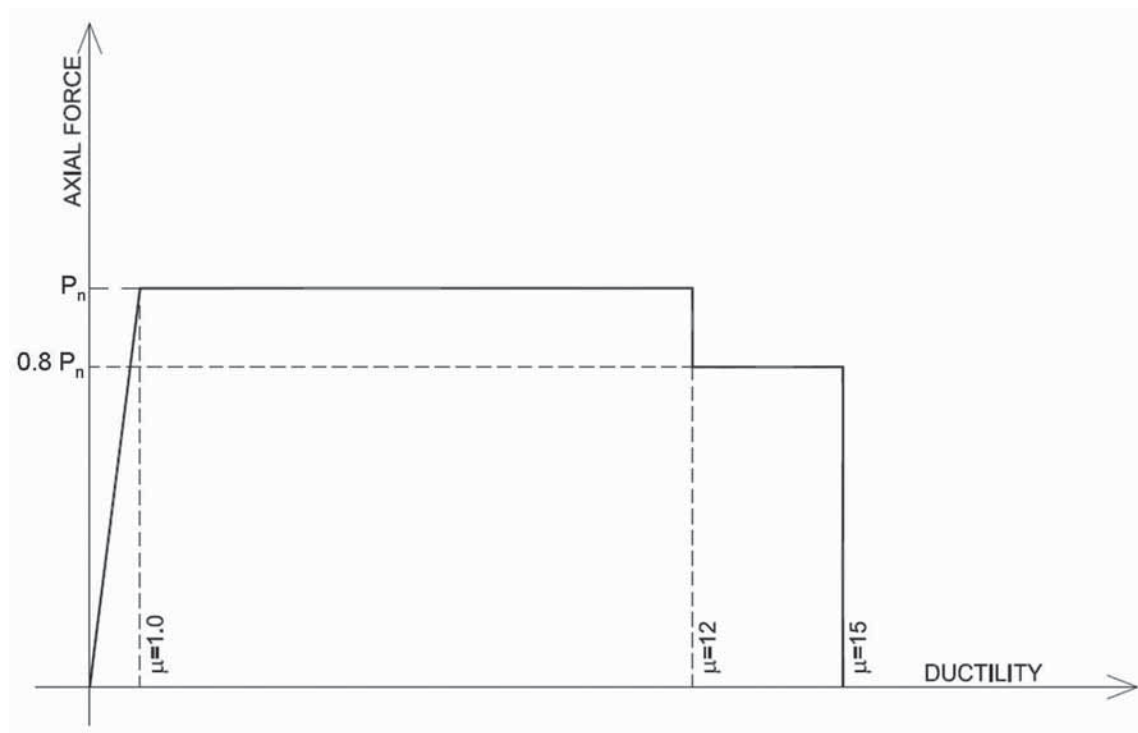

Fig. 8-12. Generic hinge diagram.

mechanisms are failure of the studs, tearing of the web of the beam, tearing of the column web, and/or tearing of the single plate. Localized yielding at the connections is also likely.

To prevent tear out of the single plate, designing the connection to allow up to an inch of deformation in the connection is desirable. For this deformation and the corresponding rotation, the edge distance may need to be increased beyond what would normally be used. Increasing the edge distance may enhance the strength in tension and the rotation capacity of the connection.

In this example, analysis of both models neglects the strength of the reinforced concrete and relies exclusively on the strength provided by the steel beams. Therefore, these examples are a simplification of the actual behavior and give an indication to the engineer of the strength and redundancy of the structure.

Procedure

The procedure to obtain the pushover curve for this structure is based on the following assumptions:
  • The structure is symmetric; no horizontal displacement is expected at the center node.
  • The beams act as truss elements; no bending deflection is assumed. Therefore, the deflection between the girder and the beam is directly related.
  • The material behavior of the structure is elastic perfectly-plastic.
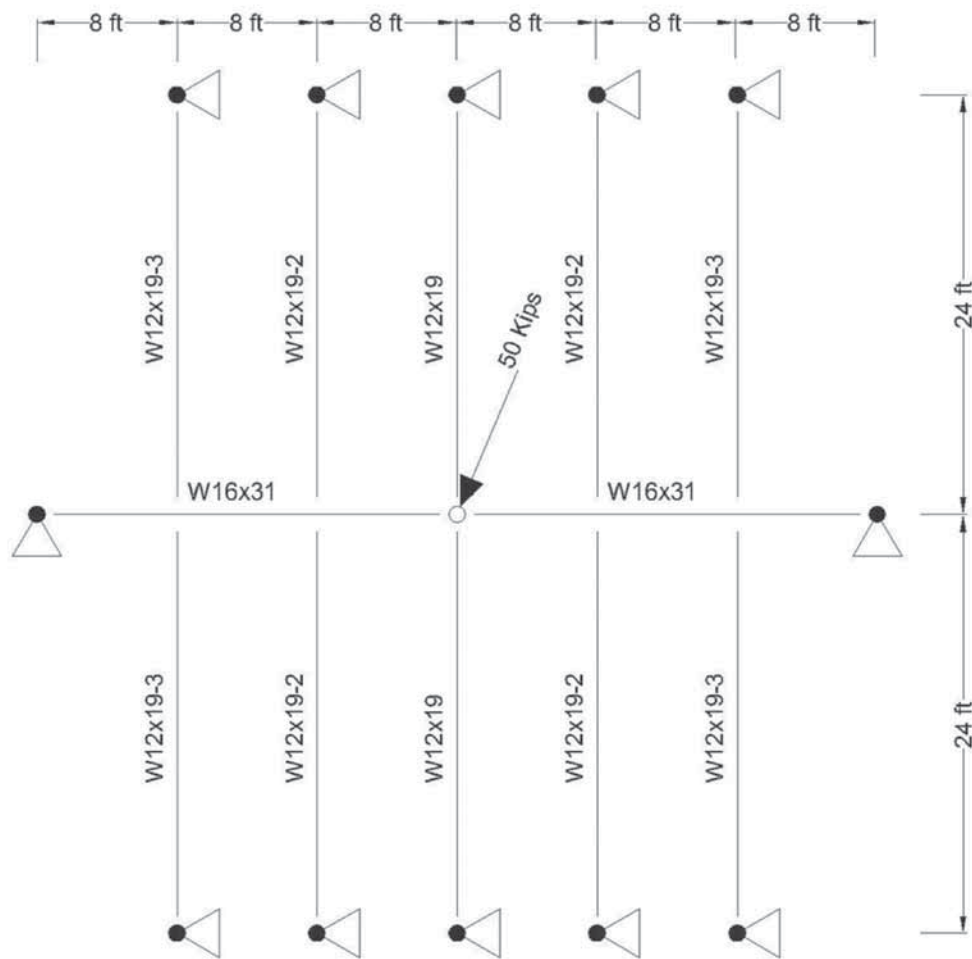
Fig. 8-13. Model A.

The procedure for two beams framing into one single node is indeterminate with nonlinear large displacements and material properties are included. For both Models A and B, this particular problem includes the three beams framing into the girder and the girder itself. The procedure to obtain the pushover and capacity curves is outlined in the following and shown in Figure 8-15:

1. Impose a vertical deflection, Δ.

2. Compute the angle, θ, of the element for this vertical deflection as:

$$\theta = \tan^{-1}\left(\frac{\Delta}{L}\right) \qquad (8\text{-}9)$$

3. For this rotation, the actual length of the beam is:

$$L+\Delta L = \frac{\Delta}{\sin\theta} \qquad (8\text{-}10)$$

4. And the increment in length can be computed as:

Fig. 8-14. Model B.

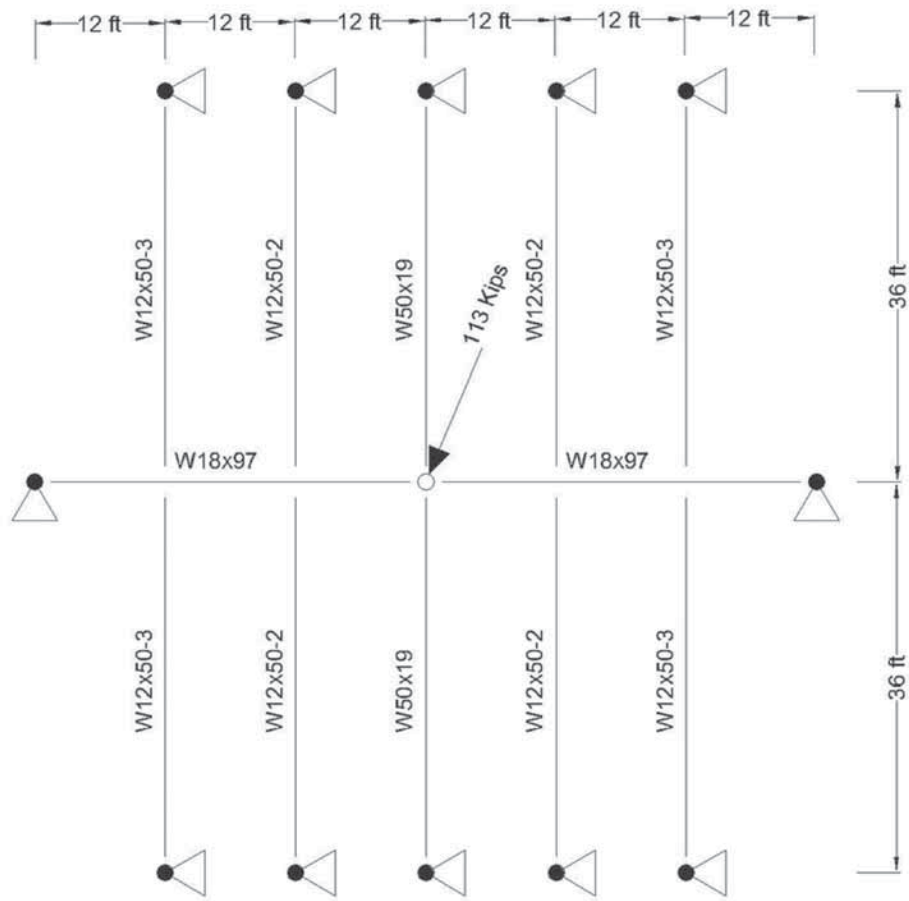$$\Delta L = \frac{\Delta}{\sin \theta} - L \qquad (8\text{-}11)$$

5. Hence the axial load in the beam is:

$$N = \frac{EA}{L} \Delta L \leq AF_y \qquad (8\text{-}12)$$

6. And the vertical force associated with the vertical deflection for only one beam is:

$$F = N \sin \theta \qquad (8\text{-}13)$$

The pushover curve for one beam can be plotted as F versus Δ. For more beams framing into the same node, the forces for each one can be added. For beams framing into the girder, the vertical deflection is associated with the control displacement, Δ. For this problem there are two beams framing into the girder and the vertical displacement associated with each beam is $\frac{2}{3}\Delta$ and $\frac{1}{3}\Delta$ as shown in Figure 8-16. The sum of the vertical forces from the two beams framing into the girder and the vertical force from the girder give the total vertical force. This approach assumes that the deflections along the girder vary linearly with the distance to the point of maximum deflection. If the bending deformation of the girder is included, the solution is more accurate. When bending is not considered, as in this example, the result is conservative.

Capacity Curve

The theory presented in the previous section and Section 8.3.2 is used to compute the pushover and capacity curves for both models. Figure 8-17 and Figure 8-19 show the pushover curve and the capacity curve for Model A and Model B, respectively, and Figure 8-18 and Figure 8-20 show the tensile force for Model A and Model B, respectively. The area below the pushover curve is the energy that the structure can absorb. The area below the pushover curve divided by the corresponding displacement yields the capacity curve of the structure.
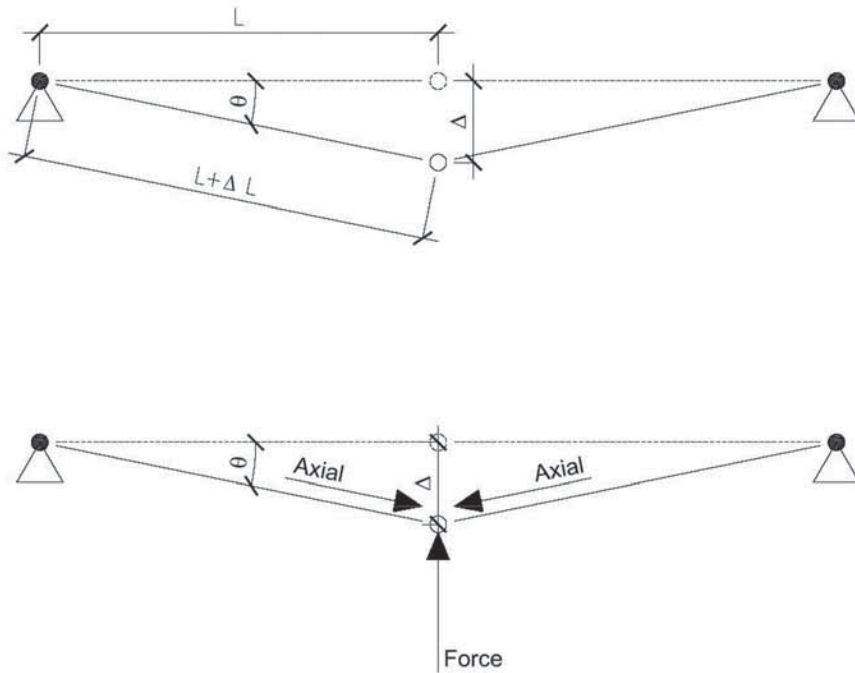

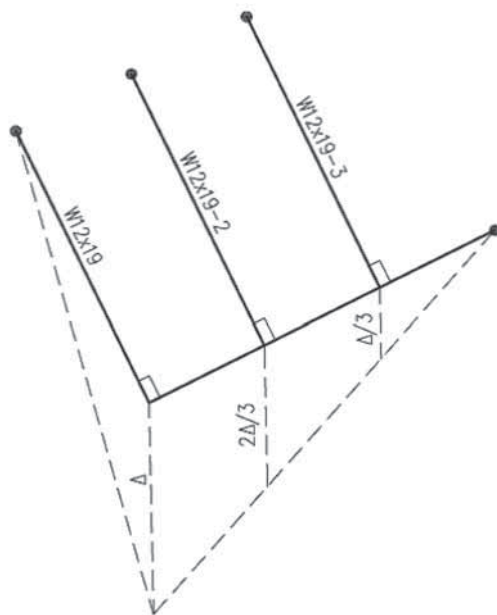*Fig. 8-15. Procedure for obtaining pushover and capacity curves.*

Fig. 8-16. Linear displacement (neglecting bending of girder).
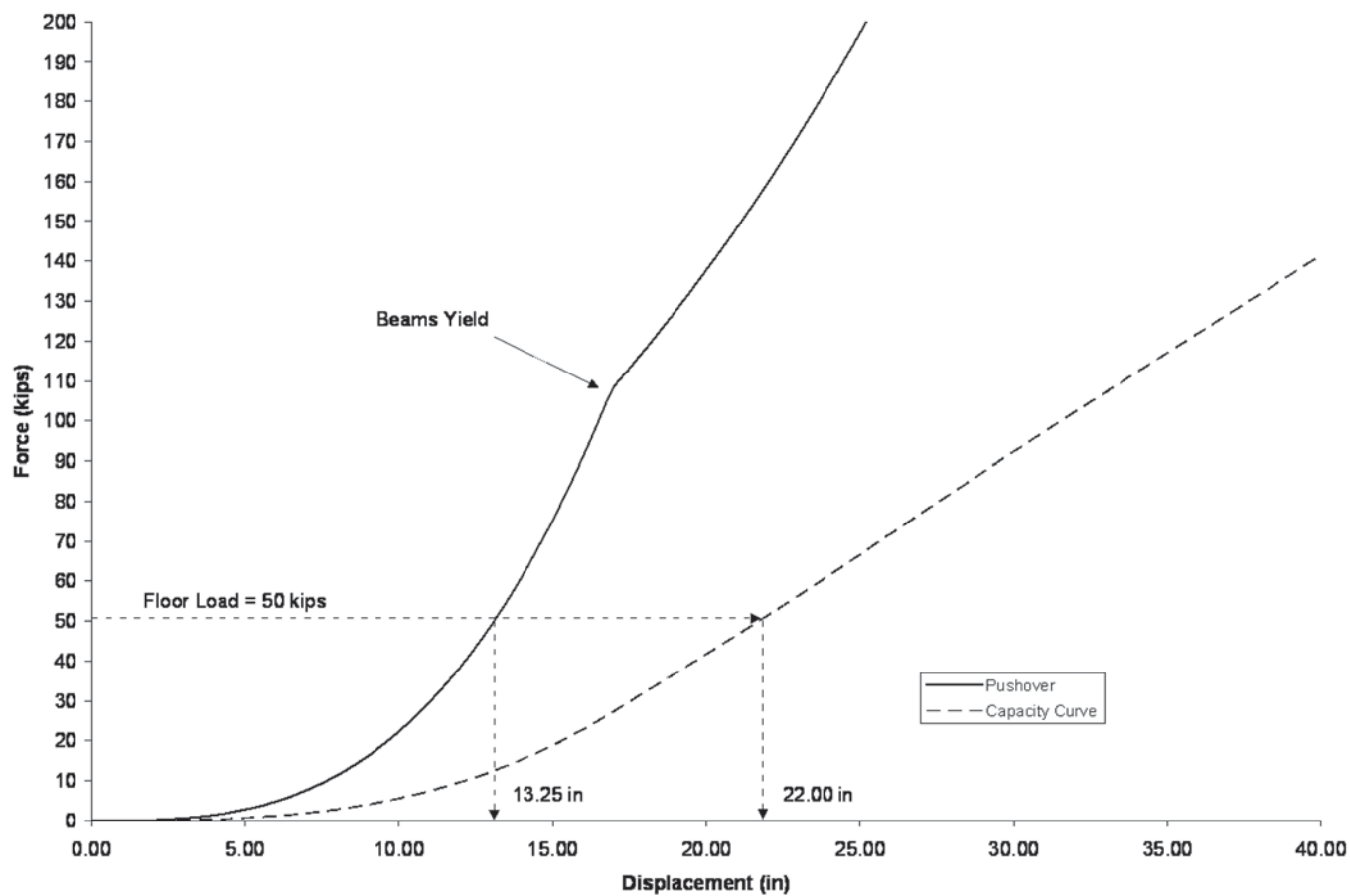

Fig. 8-17. Pushover curve, capacity curve and load for Model A.

For Model A, Figure 8-17 shows that for the 50-kip load, the vertical deflection is 22.0 in. when an energy balance is reached. Figure 8-18 shows the axial force in the beams versus the vertical deflection of the system. For the maximum deflection obtained, the two girders and two beams framing into the removed column have yielded, and will develop tensile forces of 457 kips and 279 kips, respectively. At the maximum deflection, the connections should be able to develop a rotation of 4.4° (0.077 rad) based on Equation 8-9. The four beams represented by W12×19-2 in Figure 8-13 are subjected to a tension force of 205 kips, a deflection of 14.7 in., and hence the connection for these elements should be designed to rotate 2.9° (0.051 rad). The four beams represented by W12×19-3 are subjected to a tension force of 50 kips, a deflection of 7.33 in., and must be able to rotate 1.5° (0.026 rad).

For Model B, Figure 8-19 shows that the vertical deflection is 29.4 in. when an energy balance is reached. Figure 8-19 shows the axial force in the beams versus the vertical deflection of the system. For the maximum deflection, the two girders and two beams framing into the removed column have yielded. The axial force of the beams is transferred into the compression ring of the slab through the shear stud connections. The girder will develop 1,430 kips, while the beams framing into the central node will develop 730 kips. At the maximum deflection, these connections should be able to tolerate a rotation of 3.9° (0.068 rad). The four beams represented by W12×50-2 are subjected to a tension force of 435 kips, and the connection for these elements should be designed to rotate 2.6° (0.045 rad). The four beams represented by W12×50-3 are subjected to a tension force of 110 kips, and must be able to rotate at least 1.3° (0.023 rad).

The observed rotations are all below the rotation limits outlined in Chapter 6. Table 6-2 sets the rotation limit of the steel beams and girders at 10°. Model A shows rotations of 4.4° (0.077 rad), 2.9° (0.051 rad), and 1.5° (0.026 rad), which are all well under the allowable rotation. Similarly, the beams in Model B are observed to rotate 3.9° (0.068 rad), 2.6° (0.045 rad), and 1.3° (0.023 rad) and remain below the limits presented in Chapter 6 for member design. It is important to recognize that the connections must have the capacity for this rotation as well. From FEMA 356 (FEMA, 2000b), the rotational capacity of a single-plate connection
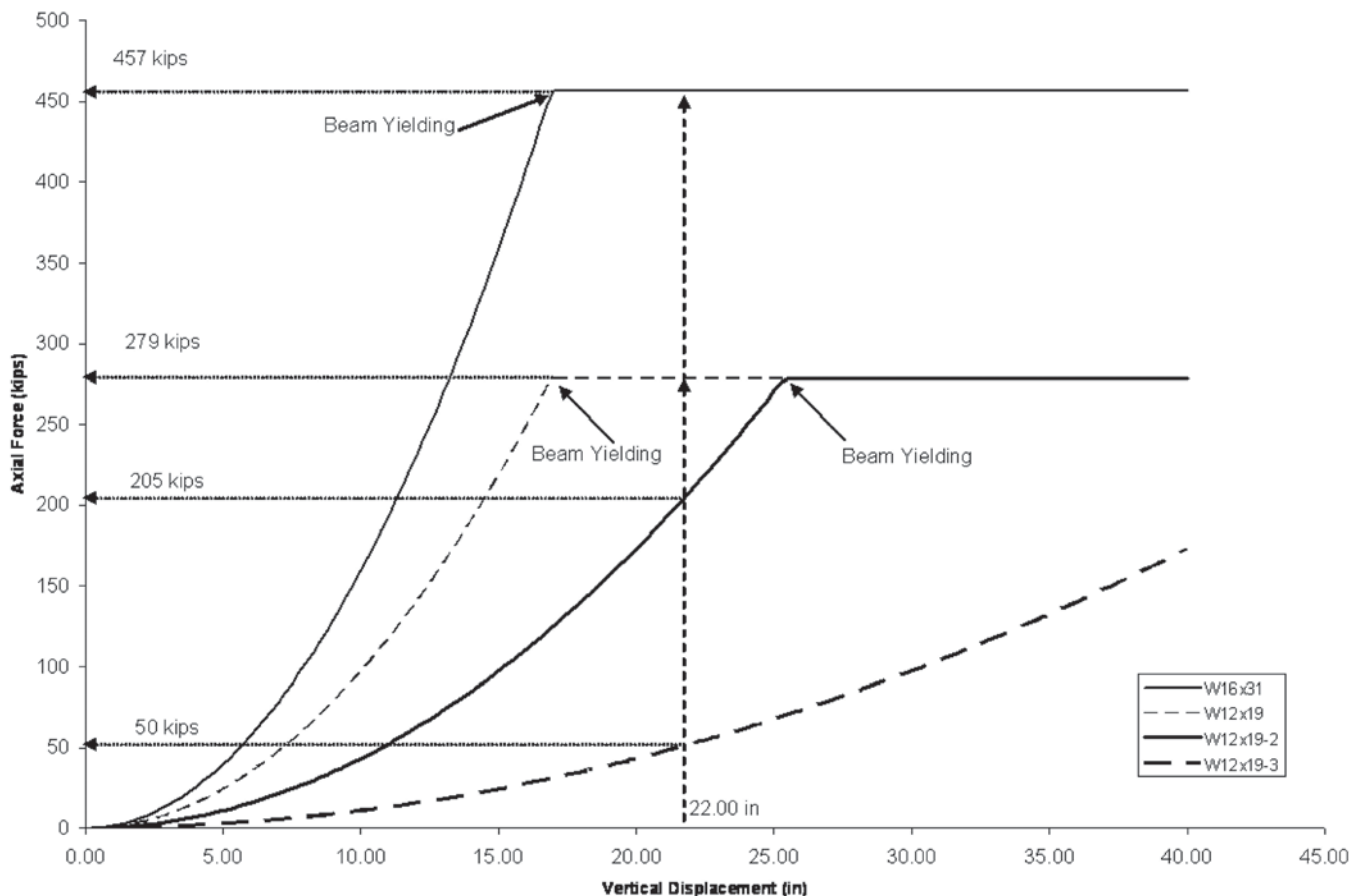

Fig. 8-18. Beam tensile force for Model A.

can be found as $\theta = 0.15 - 0.0036d_{bg}$, where d_{bg} is the depth of the bolt group. Therefore, assuming a 3-in. spacing between bolts, the rotational capacities for the W16×31 and W12×19 are 6.7° (0.12 rad) and 7.4° (0.13 rad), respectively.

Parametric Study

A parametric study of Model A is presented in this section. The area of the elements is varied from 0.5 to 2 times the initial area. The element capacities remain proportional to the element areas. All other parameters in the system remain constant. The pushover and capacity curves for each case have been determined. The results are shown in Figure 8-21. Note that the behavior of this system is nonlinear for each load due to geometric and material nonlinearities. Therefore, twice the deflection does not result in twice the force.

As beam size is increased, vertical deflection decreases. The whole assembly has to absorb the same amount of energy, but with a larger beam the connections must be able to carry more of the load because the beam absorbs less energy in bending. As beam size decreases, vertical deflection increases and thereby the axial force in the beams and connections is reduced. However, the larger the deflection the more longitudinal and rotational ductility must be absorbed by the beams and connections.

Table 8-1 shows the axial load in the different elements in Model A. Note that the stiffer the system, the bigger the axial load needed to be supported by the connection. These values are higher than the axial capacity from a regular shear connection which would require significant strengthening. A more economical approach may be to account for the tensile strength developed in the slab reinforcing, which will be checked in part (b) of this example. Based on this parametric study, elements with greater axial stiffness result in smaller vertical deflections, greater axial force, and smaller ductility demand in the connection. The resulting connection is strong and expensive. To reduce the cost of the connection, the engineer should consider using as small a member as possible.
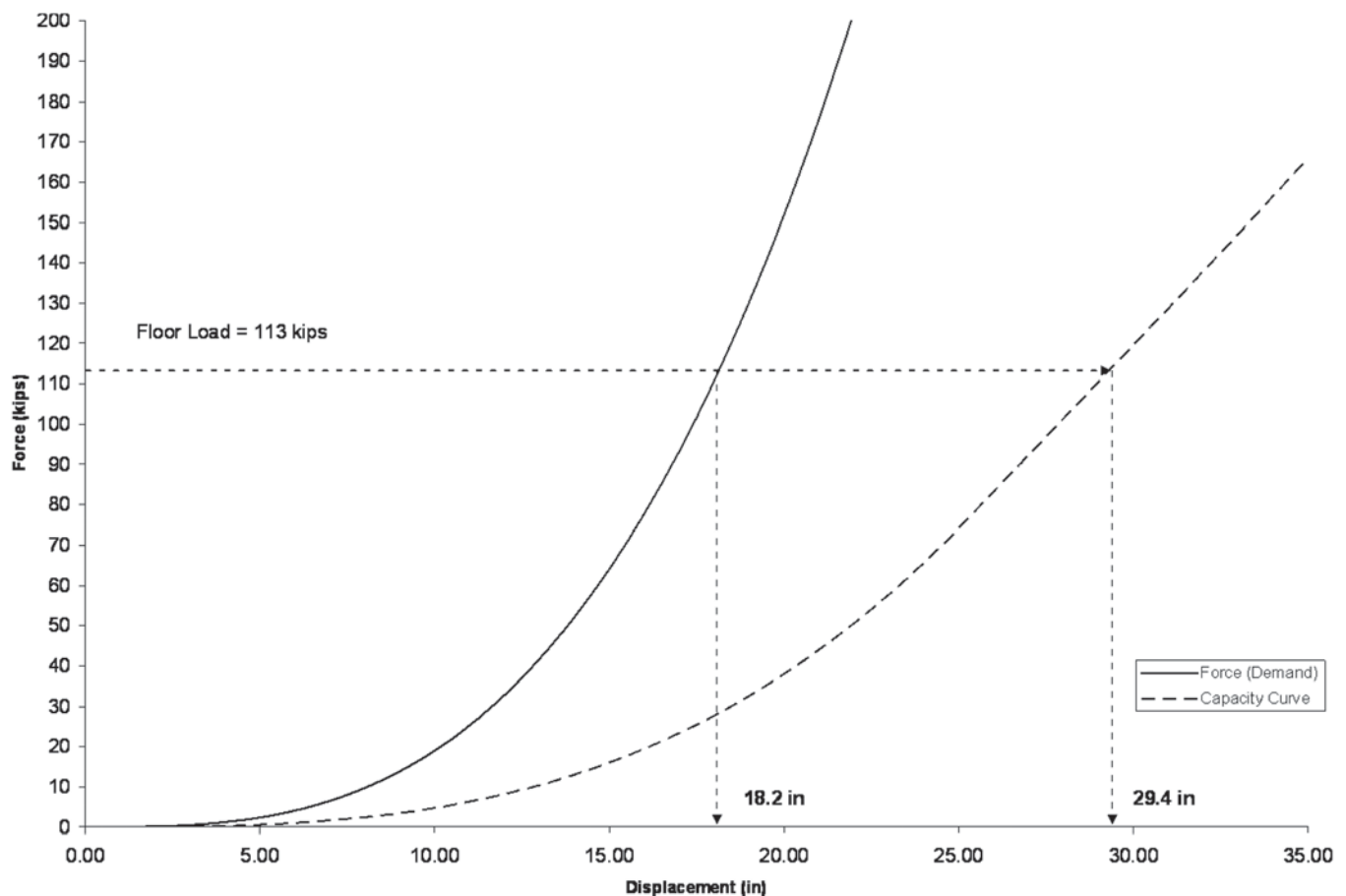
Fig. 8-19. Pushover curve, capacity curve and load for Model B.

Table 8-1.	Axial Load/Connection Capacity for Parametric Study of Model A					
	2A		**A**		**0.5A**	
Location	**N**	**N$_{yield}$**	**N**	**N$_{yield}$**	**N**	**N$_{yield}$**
W16	867	912	456	456	228	228
W12	530	558	279	279	140	140
W12-2	235	558	205	279	140	140
W12-3	59	558	50	279	54	140

Nonlinear Dynamic Comparison: Time-History Approach

Model A (24-ft by 24-ft bays) is analyzed using a nonlinear dynamic approach and the results are compared to the deflections calculated by the pushover method. For this analysis the load of the column is applied as a step load. The mass of the system is uniformly applied over the W12×19 beams. No damping is used. The boundary conditions are as follows:

- Pin supports at the base of the columns

- Horizontal restraints at the top of the columns

- Torsional restraint at the top of the center column to stabilize the top portion of the column when the lower portion is removed

Fig. 8-20. Beam tensile force for Model B.

- Horizontal restraints along the south and west sides of the slab to model the continuity of the floor system on at least two sides. The horizontal restraints are placed where the beams or girders on the adjacent spans would be.
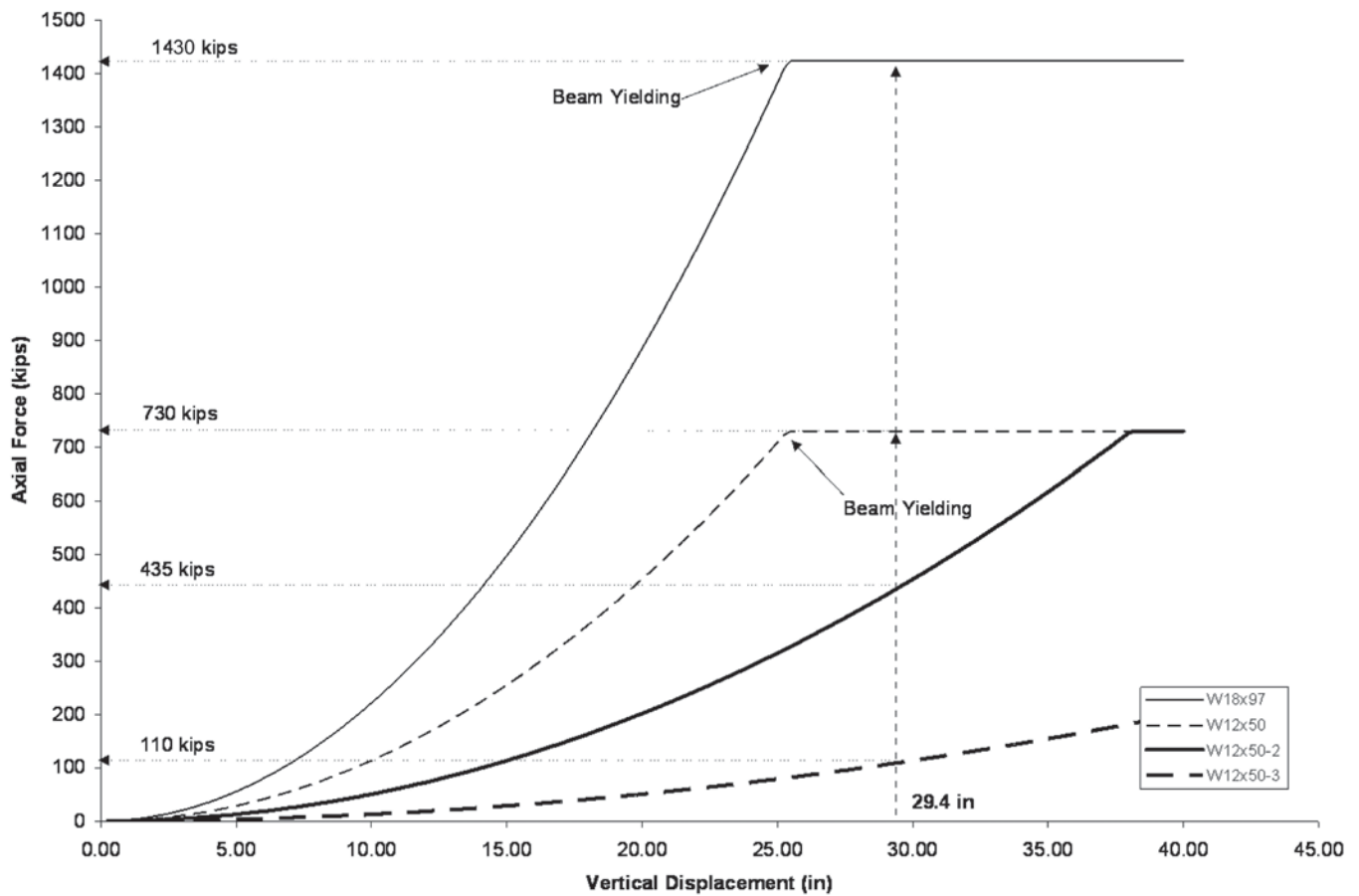
Figure 8-22 presents the vertical deflection versus time results from the time-history analysis. For Model A, the maximum deflection is 22.5 in. Comparing the nonlinear dynamic approach (time-history method) to the nonlinear static approach (energy balance/steel pushover method), it is seen that both methods produce similar results. The energy balance method gives a maximum deflection of 22.0 in. (Figure 8-17). Based on the time-history analysis, the W16×31 and W12×19-1 framed to the removed column have yielded (Figure 8-23). Beam W12×19-2 has a tensile force of 227 kips and beam W12×19-3 has a tensile force of 59 kips (Figure 8-23). These axial forces are slightly higher than those calculated by way of the energy balance method (Figure 8-18). It is important to note that the nonlinear dynamic approach is substantially more time consuming and complex than the simplified pushover method. In both models the axial forces in the beams and girders are substantial at large deflections. Connections sufficient to develop these axial forces, while exhibiting the necessary rotational ductility, would be necessary.

Compression Ring

The boundary conditions modeled in these problems assume pinned connections at the edge of the collapsed span. This assumption requires that the reaction be distributed to the slab using continuity in the reinforcement or compression in the slab (Figure 8-24). For composite floor systems with sufficient horizontal restraint (i.e., interior bays) this is a reasonable assumption. Based on testing by Allam et al. (2000), simply supported slabs will self-equilibrate at large deflections through tension in the central regions and a compression ring along the perimeter zones. The amount of catenary action to resist collapse is dependent on the stiffness of the anchorage. The following examples will verify that the compression ring induced in the slab provides sufficient anchorage. For a more accurate assessment, a finite element analysis or other comparable analysis could be used.
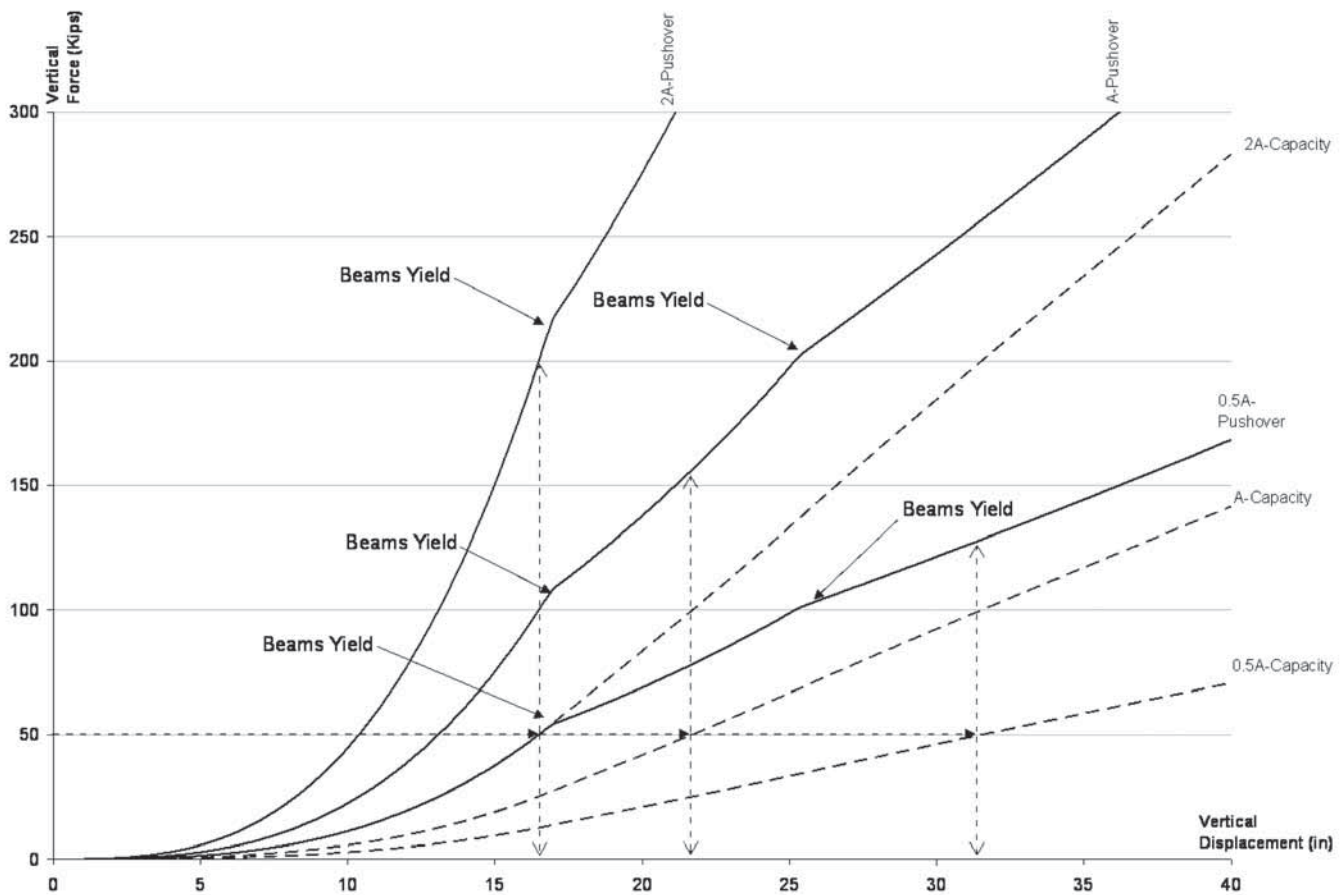
Fig. 8-21. Pushover and capacity curves for parametric study.

The following outlines a simplified procedure to estimate the strength of the compression ring for the idealized system depicted in Figure 8-24 and geometry shown in Figure 8-25. It is recommended that the engineer make similar calculations or use finite element methods to check that the assumption of anchorage due to the compression ring is valid. Although generally a small effect, flexibility/deformation of the compression ring can affect the results by increasing the vertical deflection. The following calculations include consideration of slippage in the steel-concrete interface through the steel headed stud anchors.

To find the deflection in the compression ring, use the maximum tensile force (available tensile yield strength) from Model A determined previously:

$$F_{Compression} = F_{Tensile} \cos 45°$$
$$= (457 \text{ kips})(0.707)$$
$$= 323 \text{ kips}$$

Determine the width, w, of the idealized compression ring:

$$w = \frac{F_{Comp}}{0.85 f_{conc} t}$$
$$= \frac{323 \text{ kips}}{0.85(3.5 \text{ ksi})(2.50 \text{ in.})}$$
$$= 43.4 \text{ in.}$$
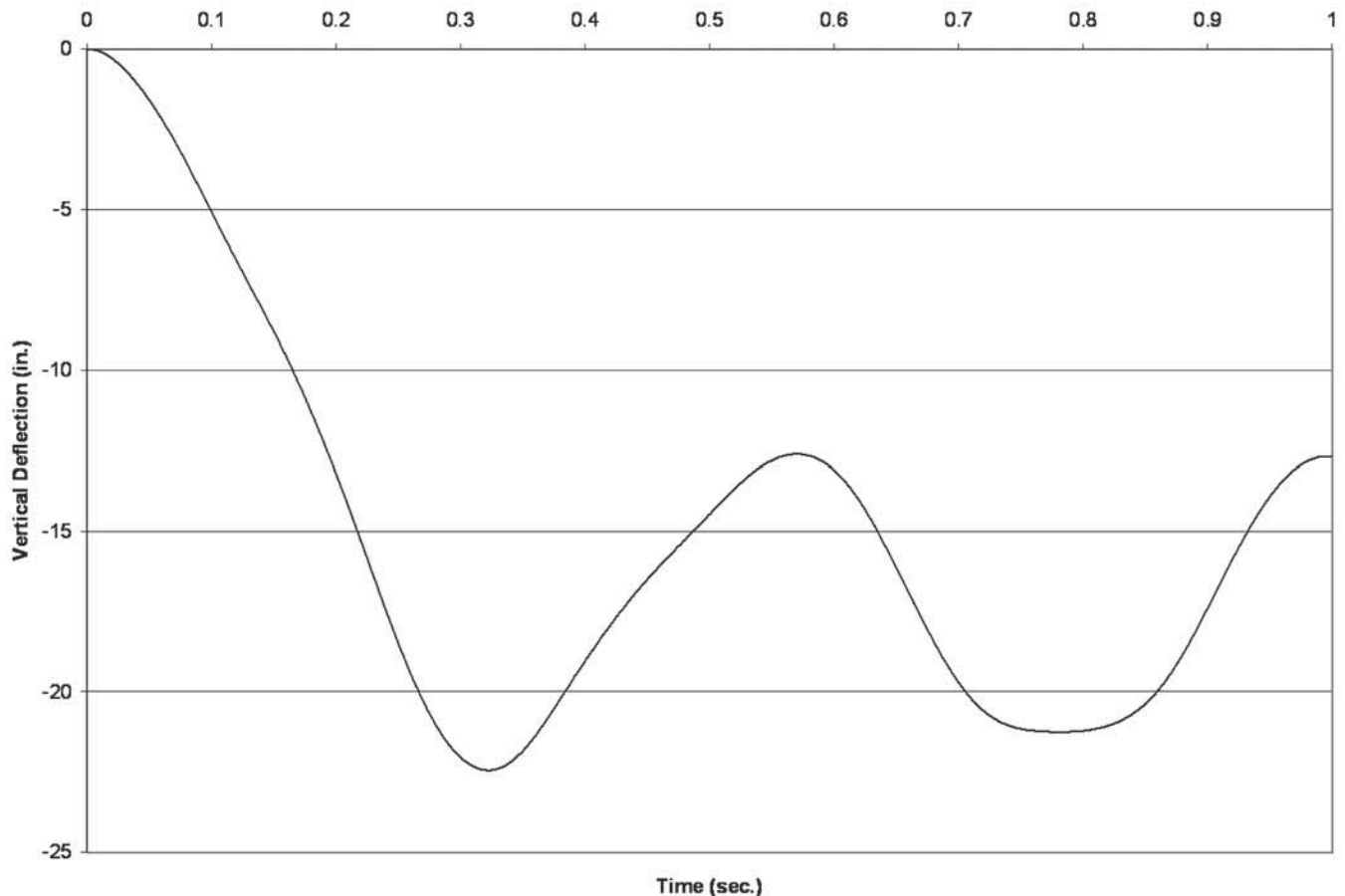
Fig. 8-22. Vertical deflection—Model A.

where

   t = thickness of the slab

   f_{conc} = specified compressive strength of the concrete

The strut length of the compression ring is:

$$
\begin{aligned}
L_{Strut} &= L_{Beam}/\sin 45° - w \\
&= \left[24.0 \text{ ft} (12 \text{ in./ft})\right]/0.707 - 43.4 \text{ in.} \\
&= 364 \text{ in.}
\end{aligned}
$$

The compressive force causes axial deformation in the compression ring which results in a radial displacement at the perimeter beam-column joints (Figure 8-26):
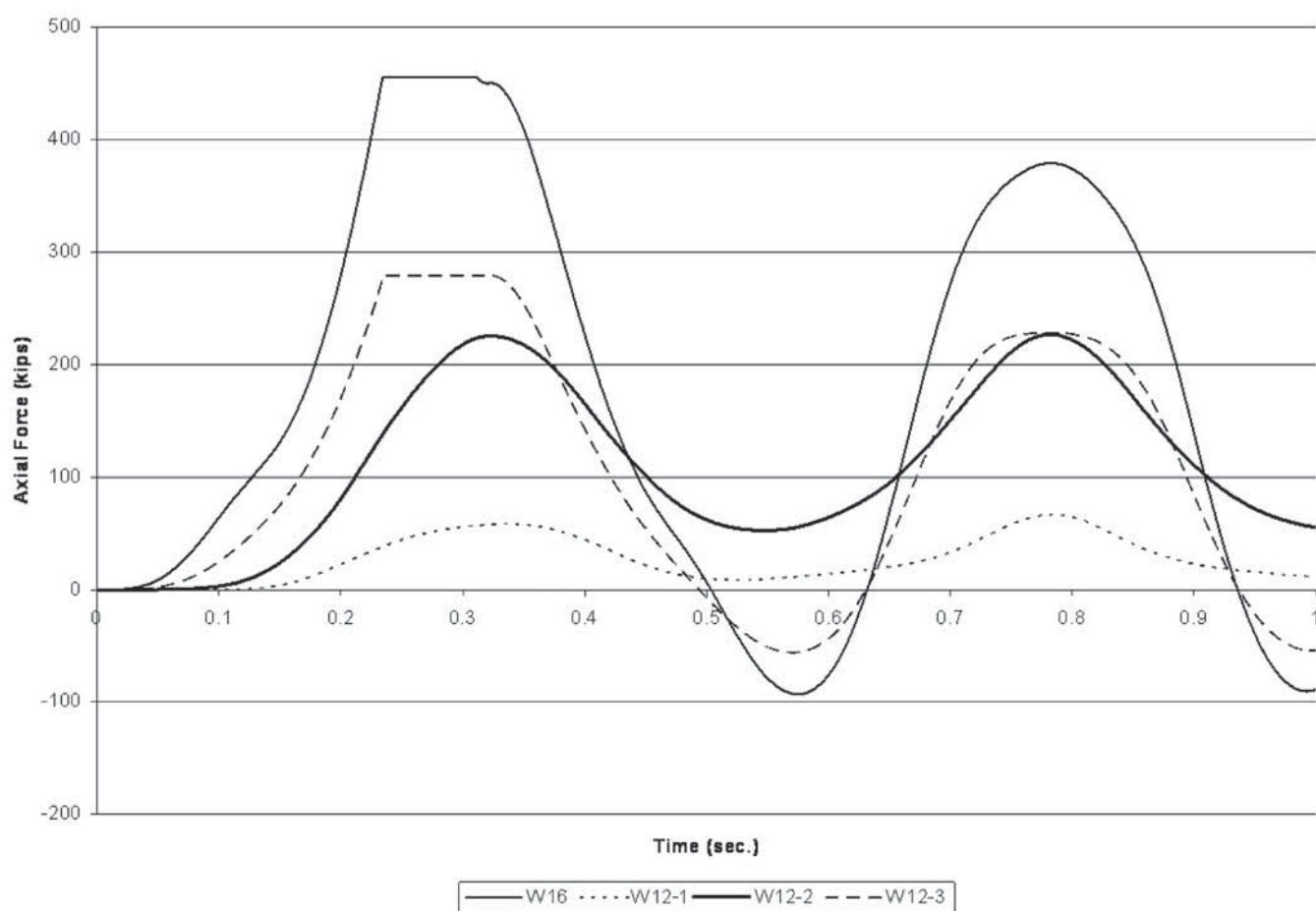
Fig. 8-23. Axial load in the beams for Model A.

$$\Delta_r = \sqrt{2}\left(\frac{\delta_{axial}}{2}\right)$$

$$= \sqrt{2}\left(\frac{F_c L_{strut}}{2E_c A}\right)$$

$$= (1.41)\left[\frac{(323 \text{ kips})(364 \text{ in.})}{2(3,410 \text{ ksi})(43.4 \text{ in.})(2.5 \text{ in.})}\right]$$

$$= 0.224 \text{ in.}$$

To check the slippage of the steel headed stud anchors and the capacity of each stud, refer to Grant et al. (1977) and Easterling et al. (1993). According to Easterling et al. (1993), the nominal strength of each steel headed stud anchor is 24 kips and the slippage is ⅛ in. To develop the full strength of the beam, 19 shear studs are required. Because the design is conservatively using more than one steel headed stud anchor per foot (27 studs on the girder and 24 on the beam), the actual slip should be less than that calculated.

The total displacement due to the flexibility of the compression ring (0.224 in.) plus the slippage of the steel headed stud anchors (⅛ in.) is 0.349 in. Using the procedure discussed previously, the extended length of the beam in Model A due to the central vertical deflection of 22.0 in. is:
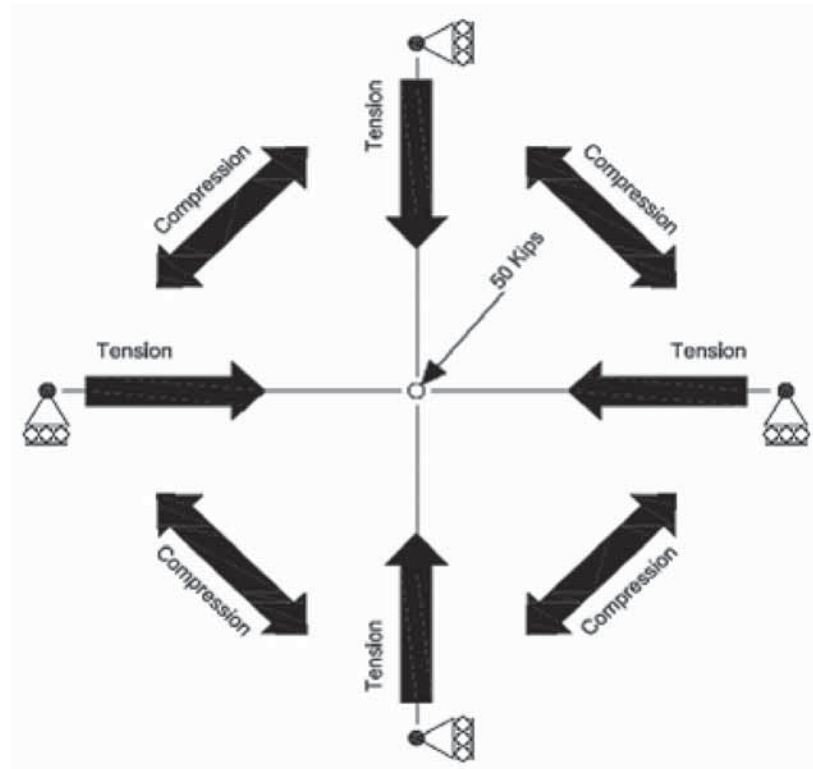
Fig. 8-24. Concrete compression ring.

$$L_e = \sqrt{L_o^2 + \Delta^2}$$
$$= \sqrt{(288 \text{ in.})^2 + (22.0 \text{ in.})^2}$$
$$= 289 \text{ in.}$$

Adding the 0.349 in. to the elongated length as shown in Figure 8-27, the total vertical deflection is:

$$\Delta_{TOT} = \sqrt{(L_e + 0.349)^2 - (288 \text{ in.})^2}$$
$$= \sqrt{(289 \text{ in.} + 0.349 \text{ in.})^2 - (288 \text{ in.})^2}$$
$$= 27.9 \text{ in.}$$

The resulting vertical deflection, Δ_{TOT}, is 20% greater than the calculated deflection, Δ, when complete anchorage was assumed. This derivation is conservative and the additional displacement is within an acceptable range.
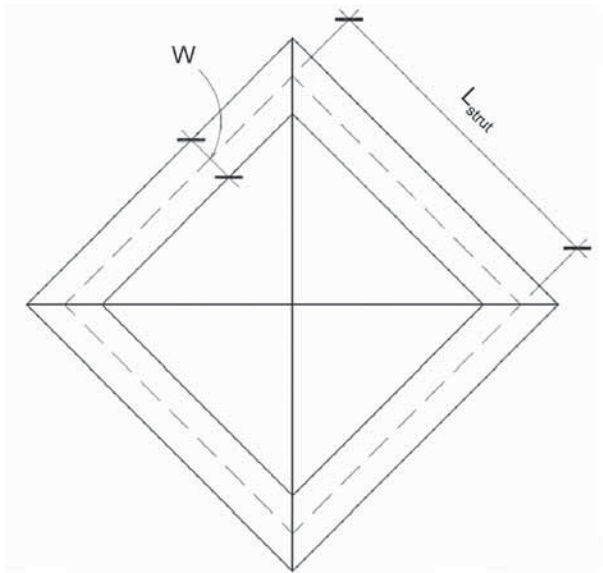
Fig. 8-25. Geometry of concrete compression ring.
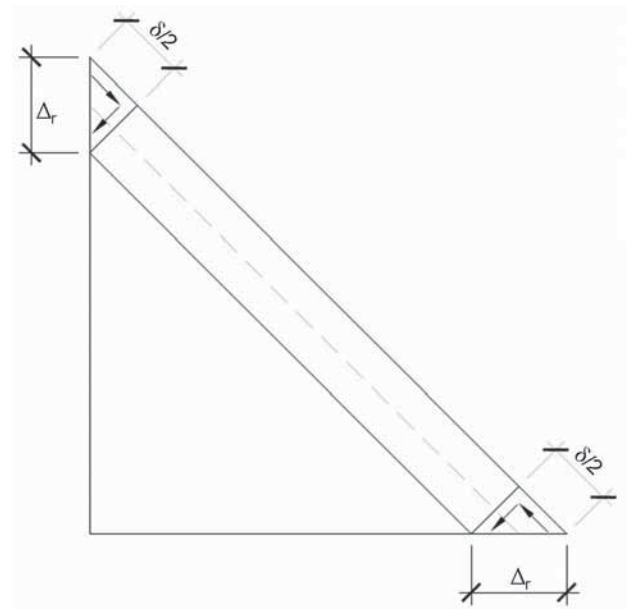
Fig. 8-26. Radial displacement, Δ, due to compressive deformation, δ.
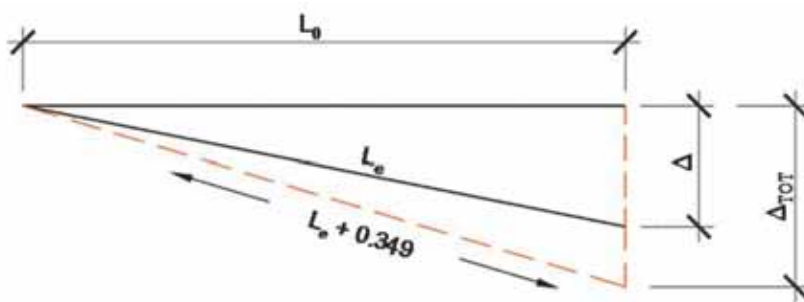
Fig. 8-27. Additional deflection due to anchorage flexibility and stud slippage.

When the same check is performed for Model B, the width of the compression ring is over half the bay width and the percent increase in vertical deflection is 16%. The deflected shape of the concrete slab forms a bowl, similar in many ways to an inverted dome. The width of the compression ring illustrated in the previous calculations is consistent with the known compressive stress region in domes. In an inverted dome, there are two types of stresses—compressive and tensile along the parallels and tensile stresses along the meridians. Near the base or support, the hoop stresses are compressive and become tensile lower in the inverted dome. In a half-dome spherical shell, the hoop stresses are tensile below 50° latitude and compressive above 50° latitude. In the bays, the area of concrete in the compression ring is substantial and the engineer should verify that there is enough compression capacity in the concrete and sufficient tension capacity in the reinforcement.

Conclusions

In this part of Example 8.1, the energy method was used to develop the pushover and capacity curves. The results were compared to the results of a time-history analysis and found to be similar. This example has explored the concept of catenary action of the steel beams and girders and has determined that the axial demand on the connections, in many instances, requires the development of the axial yield strength of the beams and girders. Without test data or complex analytical models, it is difficult to ascertain if the connection design is adequate. By design, connections that achieve the tension capacity of the steel member, while maintaining a level of longitudinal and rotational ductility, become ductile moment connections that resist bending behavior in addition to tensile forces. Increasing the shear tab thickness and/or directly welding the beam web to the column will also enhance the connection strength and ductility as shown by Khandelwal and El-Tawil (2007). Through a parametric study, the idea was introduced that smaller steel members increase the deflections and decrease the demands on the connections.

In addition, the idea was introduced that it is superior to rely on the concrete slab rather than to rely on the adjacent structural bays to provide the axial restraint for the catenary forces. The slab can develop a compression ring that produces the required beam restraint. The tension in the member can be transferred through the steel headed stud anchors to the concrete, creating a compression ring around the perimeter of the bay that contains the removed column. In this case, the connections do not develop the full tensile capacity of the member. However, because the transfer of the beam tensile force to the slab is critical, the spacing of the steel headed stud anchors should not exceed one stud anchor per foot of beam. A simplified method for checking the strength of the compression ring in the concrete was presented. If the concrete compression ring is not considered, perimeter connection forces become quite large.

When designing to resist progressive collapse, it would generally not be economical for the engineer to exclusively consider catenary action of the structural steel. In this example, cable action or catenary action in the steel beams redistributed vertical loads and assisted in reaching a new equilibrium. However, the axial forces necessary to redistribute the vertical loads are large. Inclusion of the flexural behavior of the steel connections, or of the composite steel-slab action at connections, will give a more economical design. Moment connections resist forces in bending, thus generating a plastic hinge mechanism that dissipates energy and resists the collapse of the structural bay. The analytical concepts introduced in this example are also valid for hinges in bending. If the engineer wants to use moment connections, the procedure will be similar, with replacement of the axial hinges with moment-rotation hinges. Further still, the engineer may take advantage of membrane action of the slab, considering the tensile strength of the steel reinforcing within the slab and the compression capacity of the concrete in the slab to achieve a more economical design. This will be further explored in Part b of this example.

(b) Reinforced Slab Solution

Mitchell and Cook (1984) reported on a simplified method to determine the tensile membrane response of slabs that have in-plane restraints at their edges. The method assumes that the membrane takes on a circular deformed shape and that concrete carries no tension. The complete load-deflection response can be predicted by using the following equations combined with the stress-strain relationship of the reinforcement:

$$w = \frac{2T_x \sin\sqrt{6\varepsilon_x}}{L_x} + \frac{2T_y \sin\sqrt{6\varepsilon_y}}{L_y} \tag{8-14}$$

where
$\quad w \quad$ = predicted distributed load

L_x, L_y = clear span in the long and short direction respectively (Note that these spans are calculated after removal of the column.)

T_x = force in the reinforcement in the x-direction corresponding to the strain, ε_x

T_y = force in the reinforcement in the y-direction corresponding to the strain, ε_y

ε_x = strain in the x-direction

ε_y = strain in the y-direction assumed to be equal to $\varepsilon_x \left(L_x^2 / L_y^2 \right)$

The resulting load-deflection relationship is a pushover curve because the equation was empirically derived from tests of slowly loaded slabs.

The relationship between the central deflection, the geometry of the panel, and the strain in the reinforcement is:

$$\delta = \frac{3L_x \varepsilon_x}{2\sin\sqrt{6\varepsilon_x}} \tag{8-15}$$

The complete load versus central deflection response can be obtained by using the following solution procedure:

1. Choose a value of ε_x.

2. Calculate ε_y.

3. Determine T_x and T_y corresponding to ε_x and ε_y using the stress-strain relationship.

4. Calculate the load, w.

5. Calculate the defection, δ.

See Table 8-2 for the calculations.

Model Results

The parameters used here are those defined in Part (a) of this example. Following the procedure derived from Mitchell and Cook (1984) from the previous section, the pushover curve and capacity curve are plotted and shown in Figure 8-28 for Model A and Figure 8-29 for Model B. The capacity curve is obtained by the same procedure utilized in Part (a) of this example.

Considering only the strength of the steel reinforcement in the slab, the total vertical deflection is 48.5 in. for Model A (wire mesh reinforcement 6×6-W1.4×W1.4 WWF which is the equivalent of No. 3 bars spaced at 48 in. on center) and 54.5 in. for Model B (wire mesh reinforcement 6×6-W2.9×W2.9 WWF which is approximately the equivalent of No. 3 bars spaced at 24 in. on center). The deflections calculated for Model A and Model B are equivalent to rotations of 9.6° and 7.2°, respectively.

Increasing the area of reinforcement reduces the deflection in the slab. For example, if the reinforcement in Model A is increased to 6×6-W2.9×W2.9 WWF, the deflection is reduced to 26.5 in. or 5.26°. Similarly, if the reinforcement in Model B is increased to 6×6-W5×W5 WWF, the deflection is reduced to 36.3 in. or 4.8°. Figure 8-28 and Figure 8-29 show the pushover and capacity curves for Model A reinforced with 0.028 in.^{2}/ft and Model B reinforced with 0.058 in.^{2}/ft, respectively. Table 8-3 shows the deflection and corresponding rotation for various areas of steel slab reinforcement for both models.

Conclusions

In this part of Example 8.1, it was shown that slab structures could develop secondary load carrying mechanisms and exhibit a degree of membrane action. The deflections in Model A and Model B for this formulation are within reason when considering only the strength of the slab reinforcement. The deflection calculations neglected any contribution of the steel in the metal deck. If continuity of the metal deck can be guaranteed, the capacity of the system increases. Additionally, only the tension capacity was checked because in compression there is concrete in addition to the reinforcing providing strength; thus, tension controls.

The performance of this system can be further improved by combining the capacity curve of the steel and the slab. Increasing the slab reinforcement reduces the impact of the collapse on the beam connections and reduces the rotation and axial load demand. In this example, the slab's resistance to collapse was investigated with respect to the individual bay. Horizontal restraint was not considered because the tests by Mitchell and Cook (1984) show that, with large deformations, the response of a simply supported slab is essentially the same as a fully restrained slab. This result is due to the ability of the slab to form its own in-plane edge

Table 8-2. Reinforced Slab Calculations

	X	Y	units
A_s	0.058	0.058	in²/ft
F_y	60	60	ksi
T_{yield}	3.48	3.48	kips/ft
ϵ	0.002	0.002	
L	72	72	ft
μ	15	15	
ϵ_{max}	0.08	0.08	

36'x36' Bay (Mitchell and Cook, 1984)

$\epsilon/\epsilon_{x,yield}$	ϵ_x	ϵ_y	T_x	T_y	δ	ω	F	W	Capacity
0.000001	2.07E-09	2.07E-09	0.00	0.00	0.0	2.15E-11	0	0.00	0.00
0.05	1.03E-04	1.03E-04	0.17	0.17	5.4	2.41E-04	1	3.34	0.62
0.1	2.07E-04	2.07E-04	0.35	0.35	7.6	6.81E-04	4	8.67	1.14
0.15	3.10E-04	3.10E-04	0.52	0.52	9.3	1.25E-03	6	17.24	1.85
0.2	4.14E-04	4.14E-04	0.70	0.70	10.8	1.93E-03	10	29.13	2.71
0.25	5.17E-04	5.17E-04	0.87	0.87	12.0	2.69E-03	14	44.36	3.68
0.3	6.21E-04	6.21E-04	1.04	1.04	13.2	3.54E-03	18	62.93	4.77
0.35	7.24E-04	7.24E-04	1.22	1.22	14.2	4.46E-03	23	84.86	5.96
0.4	8.28E-04	8.28E-04	1.39	1.39	15.2	5.44E-03	28	110.15	7.23
0.45	9.31E-04	9.31E-04	1.57	1.57	16.2	6.50E-03	34	138.80	8.59
0.5	1.03E-03	1.03E-03	1.74	1.74	17.0	7.61E-03	39	170.82	10.03
0.55	1.14E-03	1.14E-03	1.91	1.91	17.9	8.78E-03	45	206.21	11.54
0.6	1.24E-03	1.24E-03	2.09	2.09	18.7	1.00E-02	52	244.97	13.12
0.65	1.34E-03	1.34E-03	2.26	2.26	19.4	1.13E-02	58	287.10	14.78
0.7	1.45E-03	1.45E-03	2.44	2.44	20.2	1.26E-02	65	332.61	16.49
0.75	1.55E-03	1.55E-03	2.61	2.61	20.9	1.40E-02	72	381.49	18.28
0.8	1.66E-03	1.66E-03	2.78	2.78	21.6	1.54E-02	80	433.75	20.12
0.85	1.76E-03	1.76E-03	2.96	2.96	22.2	1.69E-02	87	489.40	22.02
0.9	1.86E-03	1.86E-03	3.13	3.13	22.9	1.84E-02	95	548.42	23.98
0.95	1.97E-03	1.97E-03	3.31	3.31	23.5	1.99E-02	103	610.83	25.99
1	2.07E-03	2.07E-03	3.48	3.48	24.1	2.15E-02	111	676.62	28.06
1.05	2.17E-03	2.17E-03	3.48	3.48	24.7	2.20E-02	114	744.09	30.11
1.1	2.28E-03	2.28E-03	3.48	3.48	25.3	2.25E-02	117	811.57	32.08
1.15	2.38E-03	2.38E-03	3.48	3.48	25.9	2.30E-02	119	879.07	33.98
1.2	2.48E-03	2.48E-03	3.48	3.48	26.4	2.35E-02	122	946.58	35.82
1.25	2.59E-03	2.59E-03	3.48	3.48	27.0	2.40E-02	125	1014.10	37.59
1.3	2.69E-03	2.69E-03	3.48	3.48	27.5	2.45E-02	127	1081.64	39.31
1.35	2.79E-03	2.79E-03	3.48	3.48	28.0	2.50E-02	129	1149.20	40.98
1.4	2.90E-03	2.90E-03	3.48	3.48	28.6	2.54E-02	132	1216.76	42.61
1.45	3.00E-03	3.00E-03	3.48	3.48	29.1	2.59E-02	134	1284.35	44.19
1.5	3.10E-03	3.10E-03	3.48	3.48	29.6	2.63E-02	136	1351.94	45.73
1.55	3.21E-03	3.21E-03	3.48	3.48	30.1	2.67E-02	139	1419.55	47.23
1.6	3.31E-03	3.31E-03	3.48	3.48	30.5	2.72E-02	141	1487.17	48.69
1.65	3.41E-03	3.41E-03	3.48	3.48	31.0	2.76E-02	143	1554.81	50.12
1.7	3.52E-03	3.52E-03	3.48	3.48	31.5	2.80E-02	145	1622.46	51.52
1.75	3.62E-03	3.62E-03	3.48	3.48	32.0	2.84E-02	147	1690.13	52.90
1.8	3.72E-03	3.72E-03	3.48	3.48	32.4	2.88E-02	149	1757.80	54.24
1.85	3.83E-03	3.83E-03	3.48	3.48	32.9	2.92E-02	151	1825.50	55.56
1.9	3.93E-03	3.93E-03	3.48	3.48	33.3	2.96E-02	153	1893.20	56.85
1.95	4.03E-03	4.03E-03	3.48	3.48	33.7	3.00E-02	155	1960.92	58.11
2	4.14E-03	4.14E-03	3.48	3.48	34.2	3.03E-02	157	2028.66	59.36
2.05	4.24E-03	4.24E-03	3.48	3.48	34.6	3.07E-02	159	2096.41	60.58
2.1	4.34E-03	4.34E-03	3.48	3.48	35.0	3.11E-02	161	2164.17	61.79
2.15	4.45E-03	4.45E-03	3.48	3.48	35.4	3.14E-02	163	2231.95	62.97
2.2	4.55E-03	4.55E-03	3.48	3.48	35.9	3.18E-02	165	2299.74	64.13
2.25	4.66E-03	4.66E-03	3.48	3.48	36.3	3.22E-02	167	2367.54	65.28
3.25	6.72E-03	6.72E-03	3.48	3.48	43.7	3.86E-02	200	3726.30	85.31
4.25	8.79E-03	8.79E-03	3.48	3.48	50.1	4.40E-02	228	5090.73	101.71
5.036	1.04E-02	1.04E-02	3.48	3.48	54.6	4.78E-02	248	6167.16	113.01
5.25	1.09E-02	1.09E-02	3.48	3.48	55.7	4.88E-02	253	6460.86	115.90
6.25	1.29E-02	1.29E-02	3.48	3.48	61.0	5.32E-02	276	7836.55	128.57
7.25	1.50E-02	1.50E-02	3.48	3.48	65.8	5.71E-02	296	9217.88	140.13
8.25	1.71E-02	1.71E-02	3.48	3.48	70.3	6.08E-02	315	10604.86	150.81
9.25	1.91E-02	1.91E-02	3.48	3.48	74.6	6.43E-02	333	11997.48	160.79
10.25	2.12E-02	2.12E-02	3.48	3.48	78.7	6.75E-02	350	13395.75	170.20
11.25	2.33E-02	2.33E-02	3.48	3.48	82.6	7.06E-02	366	14799.69	179.11
12.25	2.53E-02	2.53E-02	3.48	3.48	86.4	7.35E-02	381	16209.30	187.60
13.25	2.74E-02	2.74E-02	3.48	3.48	90.1	7.63E-02	395	17624.59	195.72
14.25	2.95E-02	2.95E-02	3.48	3.48	93.6	7.89E-02	409	19045.56	203.52
15.25	3.16E-02	3.16E-02	3.48	3.48	97.0	8.15E-02	422	20472.24	211.03
16.25	3.36E-02	3.36E-02	3.48	3.48	100.4	8.39E-02	435	21904.62	218.27
17.25	3.57E-02	3.57E-02	3.48	3.48	103.6	8.63E-02	447	23342.72	225.29
18.25	3.78E-02	3.78E-02	3.48	3.48	106.8	8.86E-02	459	24786.55	232.09

Energy Balance reached
--> Capacity of slab is
equal to gravity load

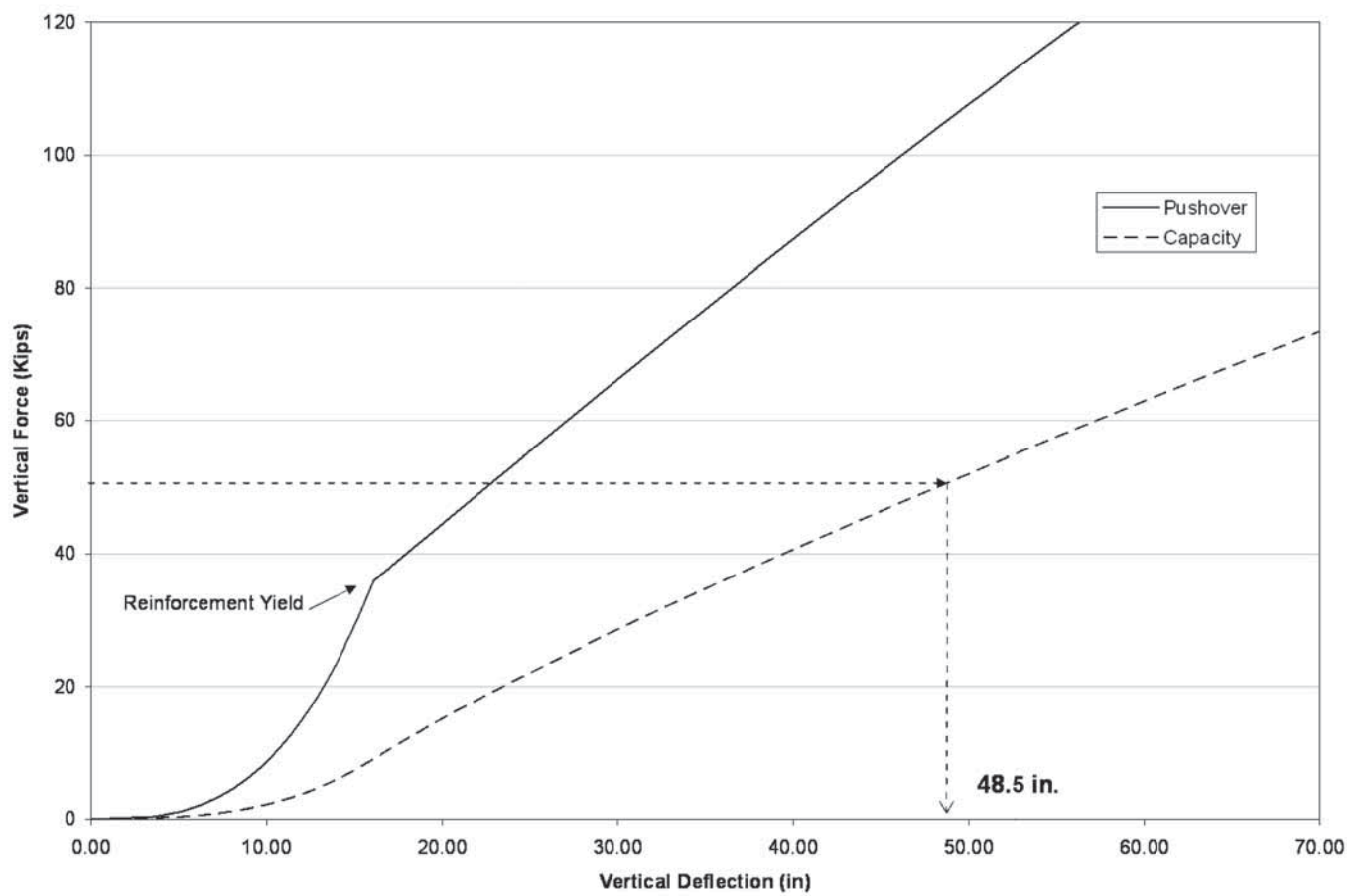| Table 8-3. Slab Reinforcement & Resulting Deflection/Rotation			
Bay Size, ft	Area of Steel Reinforcement, in.^{2}	Deflection, in.	Rotation, deg
24	0.028	48.5	9.56
	0.058	26.5	5.26
36	0.037	82.3	10.8
	0.058	54.5	7.19
	0.100	36.3	4.80

Fig. 8-28. Pushover and capacity curve for the slab for Model A.

restraint by forming a compression ring around its perimeter. Engineers should investigate the significance of these assumptions for their particular structure. Vertical support is provided by the steel beams and girders framing the perimeter of the failing bay, and the capacity of those supporting members should also be confirmed. Additionally, the bottom reinforcement should be anchored to the column to provide post punching shear resistance.

(c) Steel Nonlinear Dynamic Approach

In this part of Example 8.1, the composite floor system consists of the same components as described for Model A in the introduction to Example 8.1. The purpose of this example is to illustrate what occurs when all of the components of the composite steel floor system are accounted for.

Nonlinear Analysis Model

The model is intended to be used in the analysis of the composite floor system described above, when the middle column is removed. CSI Perform-Collapse (Computers & Structures, Inc.) is used to model the composite floor system with the modeling assumptions given in the following and shown in Figure 8-30. The analysis procedure is equally applicable to other software with nonlinear shell elements and dynamic analysis capabilities.

Boundary Conditions

The following boundary conditions are assumed:

- Pin supports at the base of the columns (Restraints = U_x, U_y and U_z).
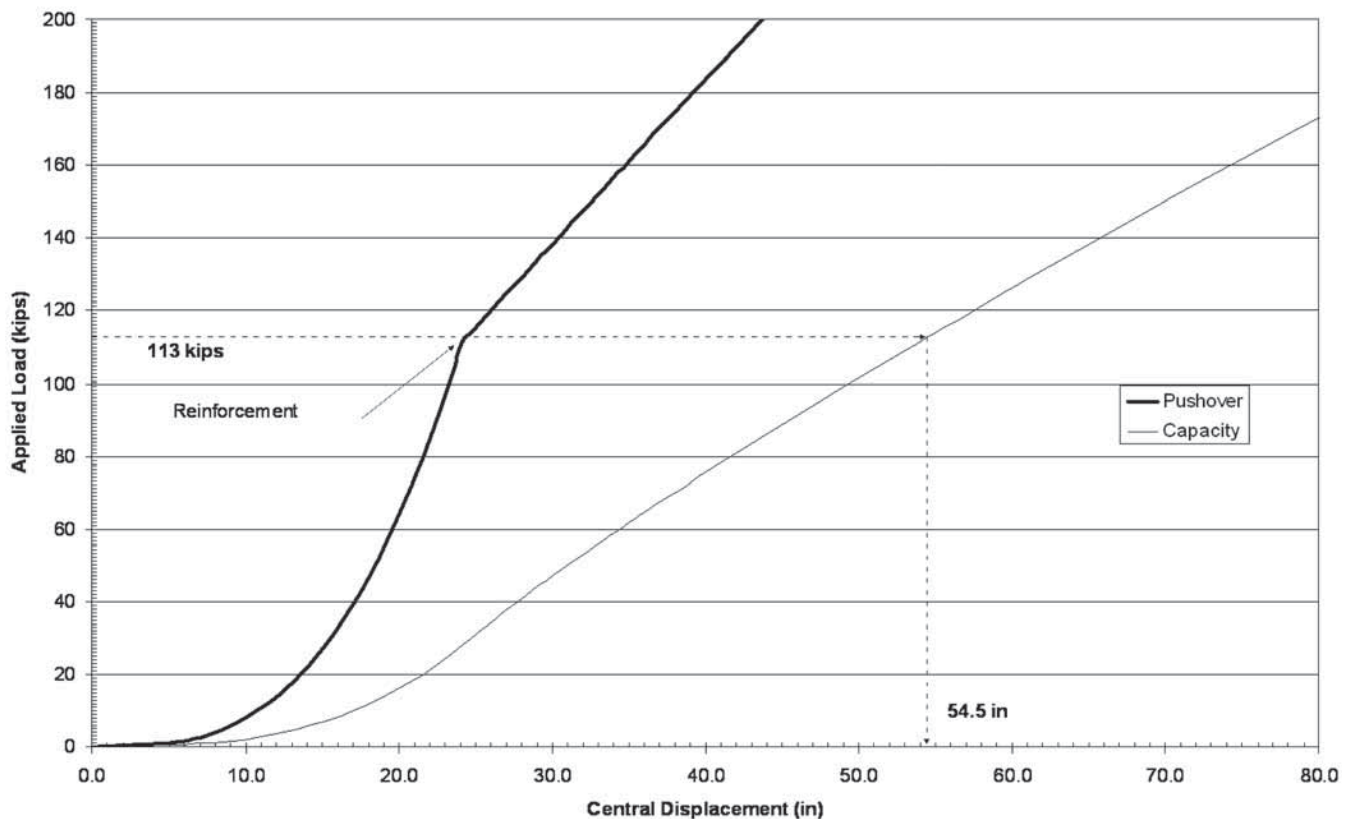- Horizontal restraints at the top of the columns (Restraints = U_x and U_y).

Fig. 8-29. Pushover and capacity curve for the slab for Model B.

- Torsional restraint at the top of the center column to stabilize the top portion of the column when the lower portion is removed (Restraint = R_z).

- Horizontal restraints along the south and the west sides of the slab to model the continuity of the floor system on at least two sides. The horizontal restraints are placed where the beams or girders on the adjacent spans would most likely be (Restraints = U_x or U_y).

Loads

The total service load of 87.5 psf is applied uniformly as point loads at the nodes of the shell elements.

Composite Floor Slab

The slab was modeled as five concrete layers, two wire mesh layers (one layer in each direction), and one deck layer, using nonlinear shell elements (2 ft by 3 ft). The slab layers are connected at the nodes. There is no bond slip between the steel and the concrete layers. The slab was modeled above the centroid of the steel beams and girders (top of slab elevation is 11.5 in. above the centroid of the beams and girders). The slab elements are not connected to the columns. They are only connected to the beams through the steel headed stud anchor elements.

The concrete slab was modeled with a constant thickness of 4.0 in. as five layers. The top and bottom layers are ½ in. thick and the other layers are 1 in. thick. The concrete material was modeled as an inelastic concrete material with brittle strength having the following material properties: concrete modulus, E_c = 3,410 ksi; specified compressive strength, f'_c = 3.5 ksi; and tensile strength, f_t = 0 ksi (no tensile strength). The concrete starts losing strength at a strain = 0.003 in./in., and it loses all of its compressive strength at a strain = 0.0035 in./in. This is illustrated in Figure 8-31.

The metal deck was modeled as a steel layer in the east-west direction (*x*-direction) with an effective thickness of 0.0508 in. It was placed 4.0 in. below the top of the concrete slab. The deck was assumed to have no strength in the perpendicular direction. The metal deck material was modeled as an inelastic steel material. The deck has a modulus of elasticity, E = 29,000 ksi, a specified minimum yield strength, F_y = 33 ksi, and a ductility ratio of 10. The stress-strain relationship for the metal deck is shown in Figure 8-32.

The wire mesh was modeled as two steel layers, one in the east-west direction (*x*-direction) and another in the north-south direction (*y*-direction) with an effective thickness of 0.00233 in. It was placed 1.0 in. below the top of the concrete slab. The wire mesh material was modeled as an inelastic steel material. The wire material has a modulus of elasticity, E = 29,000 ksi, a specified minimum yield strength, F_y = 60 ksi, and a ductility ratio of 10. The wire mesh stress-strain relationship is shown in Figure 8-33.
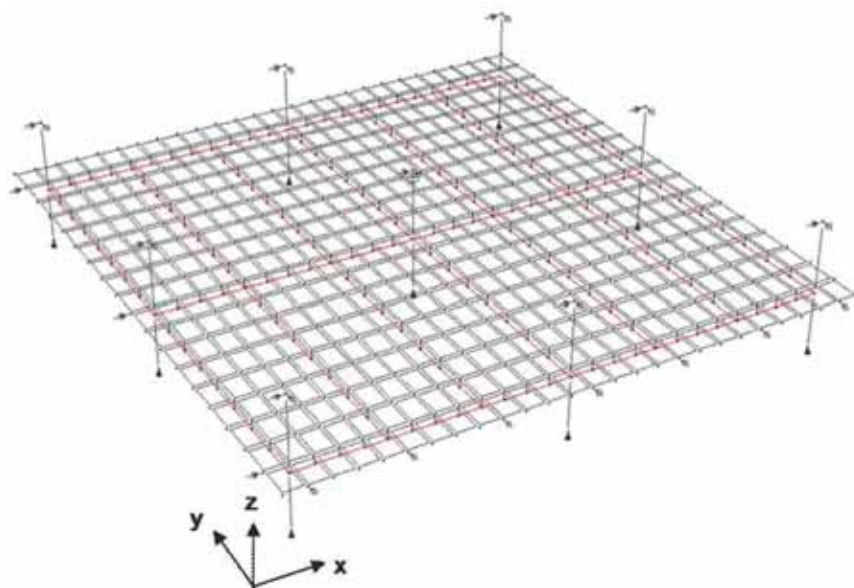

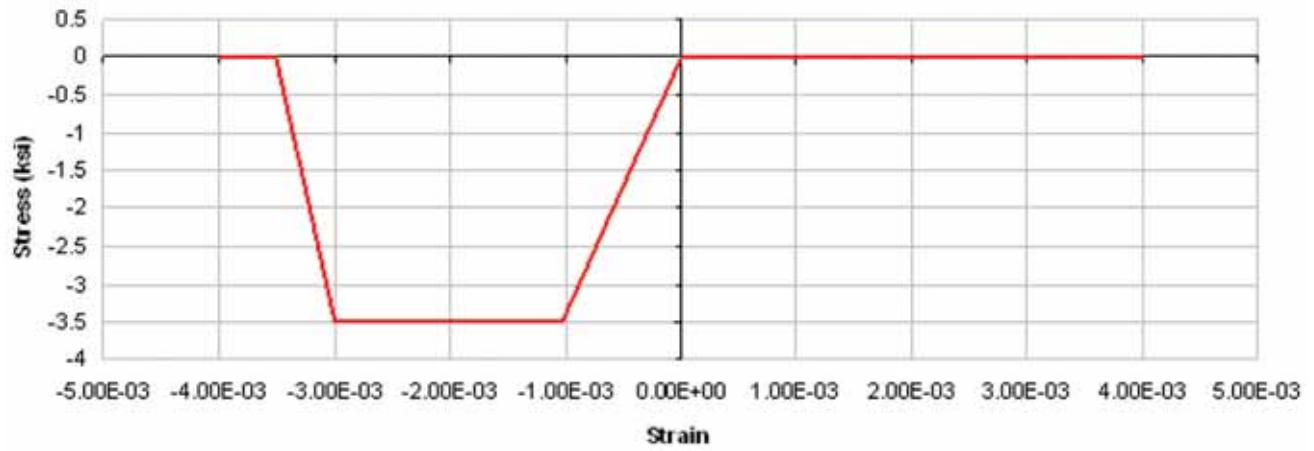*Fig. 8-30. CSI Perform-Collapse model for the composite floor system.*

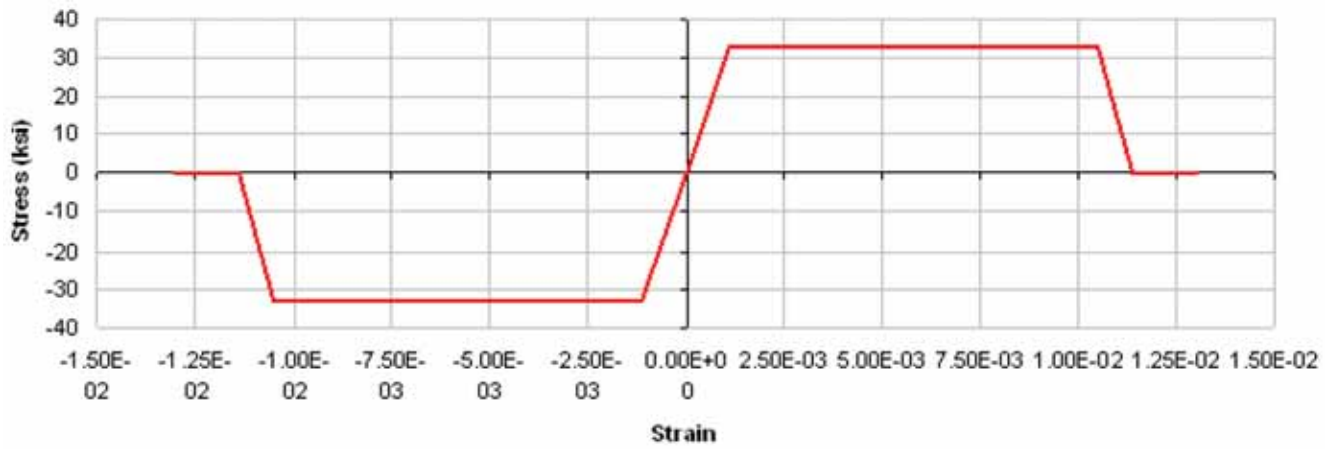*Fig. 8-31. Nonlinear concrete slab stress-strain relationship.*

Fig. 8-32. Nonlinear deck material stress-strain relationship.
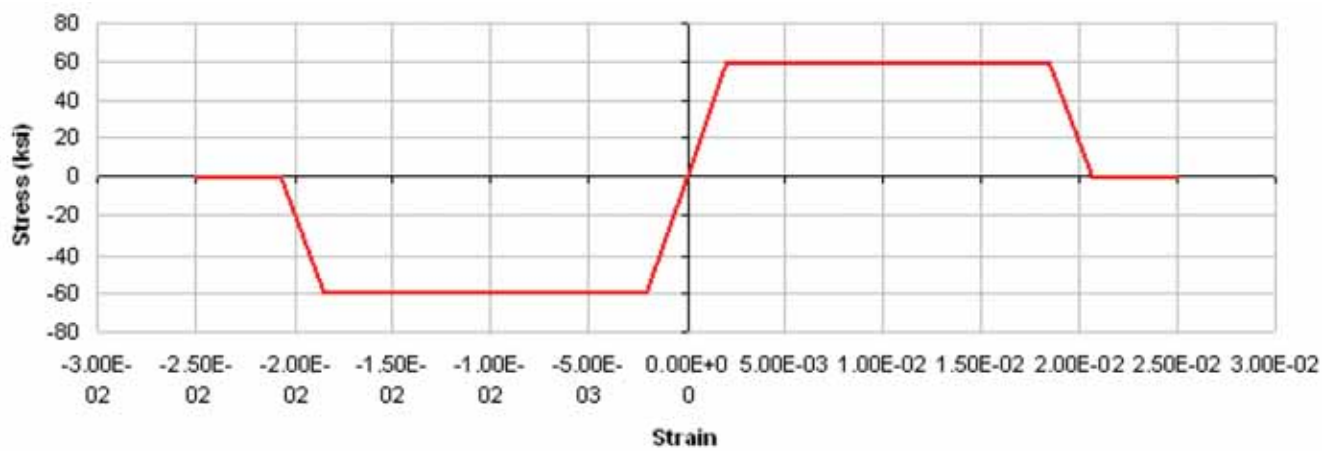

Fig. 8-33. Nonlinear wire mesh stress-strain relationship.

Columns

The columns were modeled as elastic steel columns that span from the mid-height of the lower floor to the mid-height of the upper floor. Each column consists of two elements. The first spans from the mid-height of the lower floor to the beam node and the other spans from the beam node to the mid-height of the upper floor. The column elements are ASTM A992 W14×193 sections.

Composite Beams

The composite beams were modeled as elastic steel beams with moment releases and nonlinear axial connections at the ends. The beams are ASTM A992 W12×19 sections.

Composite Girders

The composite girders were modeled as elastic steel beams with moment releases and nonlinear axial connections at the ends. The girders are ASTM A992 W16×31 sections with $F_y = 50$ ksi.

Beam and Girder Connections

The beam and girder connections were modeled as shear connections with moment releases and nonlinear axial capacity. Because the connections, during the cable action behavior, are primarily controlled by the axial force, they were modeled with nonlinear axial hinges. No shear hinges or interactions between the axial force and shear force were introduced at this point. The axial capacity of the beam end connections is controlled by the tear-out of the single plate. This failure mode was modeled using an inelastic fiber section. One fiber was used to model each ¾-in.-diameter bolt. An arbitrary area of 1.0 in.^{2} was used for each fiber. The fiber coordinates correspond to the bolt locations. An arbitrary length of 1.0 in. was used for the inelastic section of the beam, which represents the axial hinge at each end. From AISC *Specification* Section J3.10, with the dynamic increase factor applied, the available bearing strength of the single plate is determined as follows:

$$\phi R_n = \phi 1.5 l_c t \left(1.05 F_u\right) \le \phi 3.0 dt \left(1.05 F_u\right)$$
$$= 1.00 (1.5) \left[1.25 - \left(\text{\textonehalf} \text{in.}/2\right)\right] (\text{\textonequarter} \text{in.})(1.05)(58 \text{ ksi})$$
$$= 19.3 \text{ kips}$$
$$\phi 3.0 dt \left(1.05 F_u\right) = 1.00(3.0)(\text{¾ in.})(\text{¼ in.})(1.05)(58 \text{ ksi})$$
$$= 34.3 \text{ kips}$$
$$19.3 \text{ kips} \le 34.3 \text{ kips}$$

where the edge distance is 1.25 in. The bolt holes were assumed to be standard holes (¹³⁄₁₆ in.). Tearout is shown to control and the stress-strain relationship of the single-plate tear-out was assumed as shown in Figure 8-34.
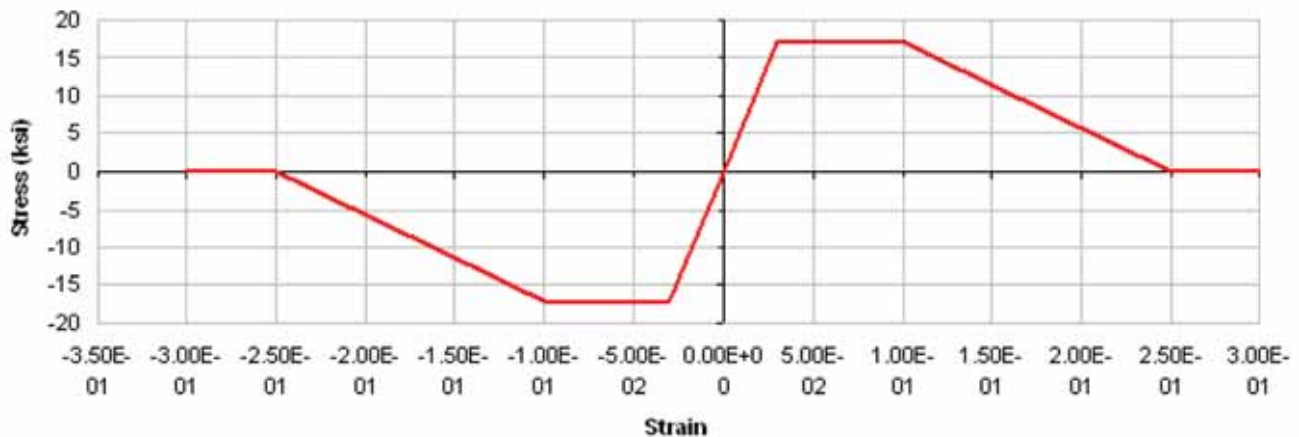

Fig. 8-34. Stress-strain relationship of single-plate tear-out.

Steel Headed Stud Anchors

The steel headed stud anchors were modeled using vertical beam elements that connect the slab nodes to the beams and girders. Shear hinges are used in the vertical elements to model the inelastic behavior of the stud anchors. The stud anchors of the beams and girders are lumped at the nodes. Depending on the number of stud anchors, each vertical element may represent more than one stud anchor. From AISC *Manual* Table 3-21, for deck perpendicular, assuming one stud per rib in the weak condition, the nominal horizontal shear strength of a single ¾-in.-diameter steel headed stud anchor is 17.2 kips. With $\phi = 1.00$ and the dynamic increase factor of 1.05, the available horizontal shear strength is 18.1 kips. In this model, each vertical element at the beam represents 1.14 stud anchors and each vertical element at the girder represents 2.45 stud anchors. The vertical elements were assigned the same cross sections as the beams or girders they connect to. The length of the vertical elements is 9.5 in. from the centroid of the beam to the centroid of the slab. The force-displacement relationship of the shear hinge in the stud elements at the beams and girders was assumed as shown in Figure 8-35 and Figure 8-36.

Metal Deck Splice

The deck is assumed to be continuous except at the center. A row of shell elements was modeled without the metal deck (concrete and wire mesh layers only) to represent a possible splice located at the center of the floor. The splice is assumed to be continuous as shown in Figure 8-37.
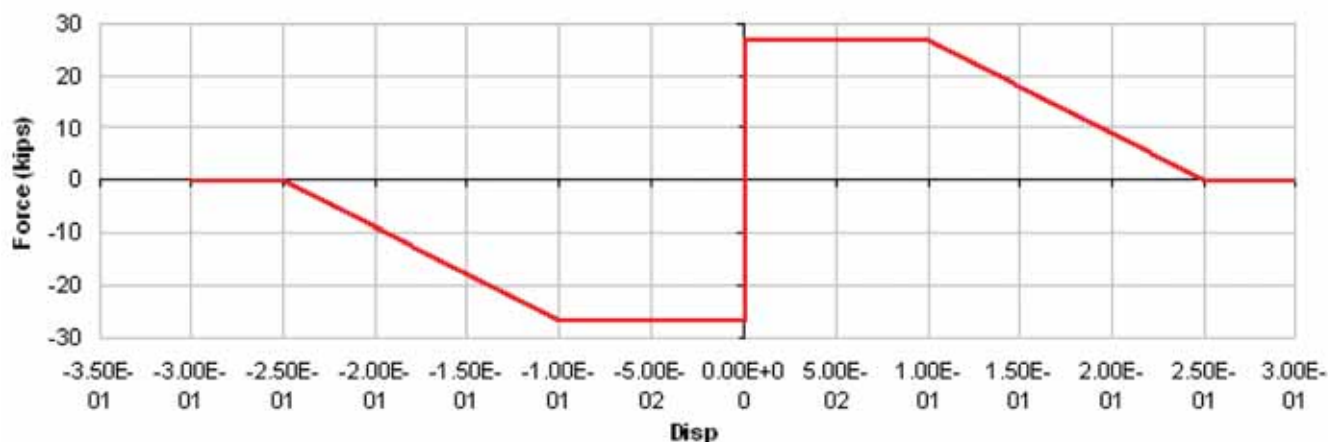

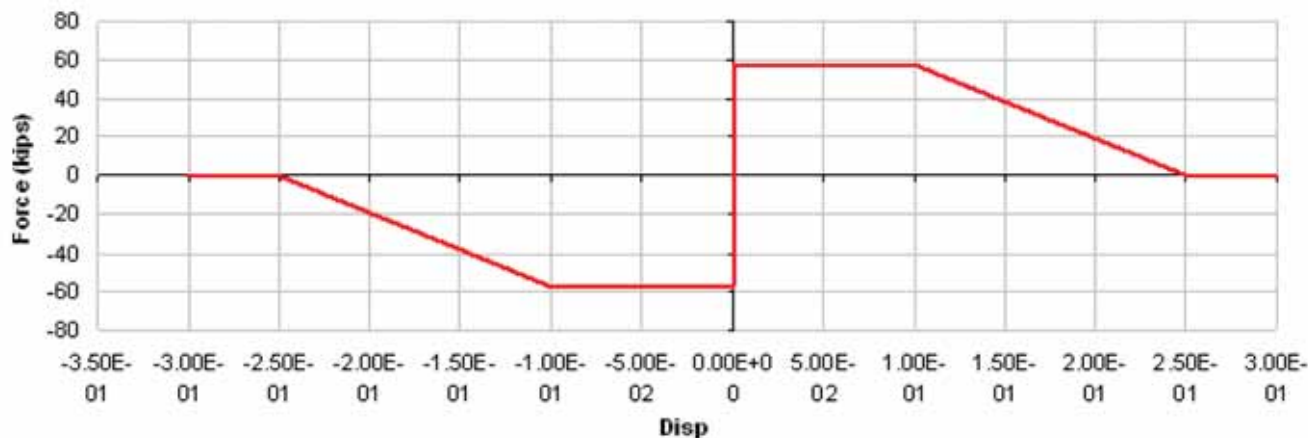*Fig. 8-35. Force-displacement relationship of stud anchor elements at beams.*

Fig. 8-36. Force-displacement of stud anchor elements at girders.

Analysis Results

The analysis was done in two phases. First, the gravity load was applied with the center column in place and the model was analyzed using nonlinear analysis with large displacements. Then the column was removed and the floor was analyzed using a static nonlinear analysis with large displacements. An impact factor of 3 was used in the column removal load case to force the analysis to proceed beyond the displacement of the full static load. The analysis kept running until an energy balance was reached at twice the static load.

Deformed Shape

The deformed shapes for both phases are shown in Figure 8-38 and Figure 8-39. The deformation increased almost linearly with the load during phase 1. During phase 2, the deformation at the center point, where the column was removed, kept increasing gradually with the load to 2.7 in., and then it increased suddenly from 2.7 in. at 42% of the load to 14.8 in. at 60% of the load. After the sudden increase, the deformation increased gradually again until it reached a maximum of 20 in. at the full static load. The deformation continued to increase gradually until an energy balance was reached at 200% of the static load and a deformation of 33.6 in. The pattern of displacement is shown in Figure 8-40.

Beam and Girder Connections

The sudden increase in the deflection of the floor system appears to be a result of the failure of the beam and girder connections. The axial capacity of the girder connection, shown in Figure 8-41, drops suddenly after reaching its capacity at 42% of the load (the same load step at which the sudden increase in deflection was observed).

Steel Layers in the Composite Slab

As expected, the deck behavior was linear for phase 1. The metal deck started yielding at the center in phase 2. Yielding was also observed in the wire mesh where the deck splice was modeled and at the shell elements where the slab was modeled without the metal deck as seen in Figure 8-42. It was observed that the load rapidly shifted to the slab at 42%; the same load step at which the beam and girder connections started failing. The steel layers of the slab kept yielding to a maximum strain that is 15.5 times their initial yield strain at the point of energy balance. The strain in the steel layers exceeded 10 times their yield strain (i.e., it exceeded the maximum assigned ductility in the steel layers) at 157% of the load as illustrated in Figure 8-43. This means that the steel layers of some slab elements at the center started breaking before the energy balance was reached. However, the overall floor system, with the assumed material ductility, seemed to have sufficient capacity to arrest the floor collapse.
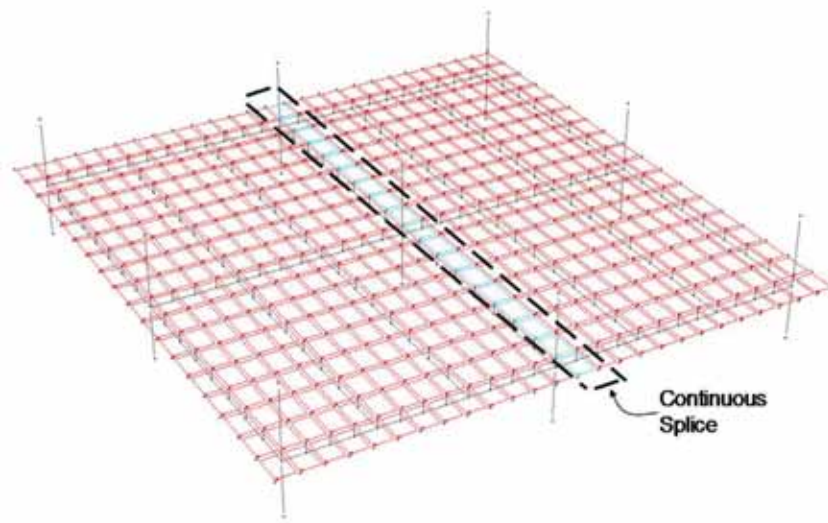

*Fig. 8-37. Metal deck is discontinued to model a possible splice.*

Conclusion

The following conclusions are drawn from this analysis:

- The removal of the center column is contained by the composite floor system. The floor does not collapse.

- Once the column is removed, the load is first resisted by coupled forces. At the center, where the column is removed, tension develops in the beam-to-girder connections and compression develops in the slab. At the perimeter columns, compression develops in the beam-to-girder connections and tension develops in the steel layers of the slab.

- Once the beam-to-girder connections at the center start failing, the load near the center shifts to the slab. The steel layers of the slab start yielding and a large deformation is observed.

- The bolted connections of the beams and girders failed progressively by tearing out the shear tab, starting with the bottom bolt and progressing up.
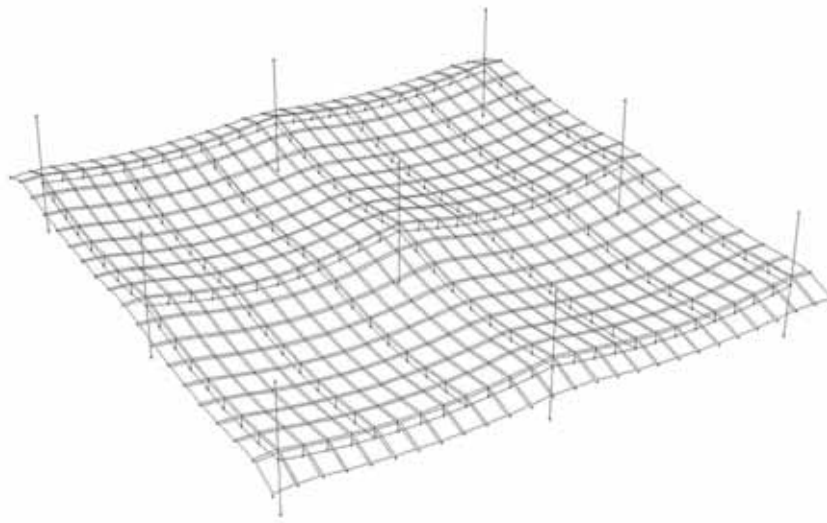
Fig. 8-38. Deformed shape for phase 1 (gravity load with column in place).
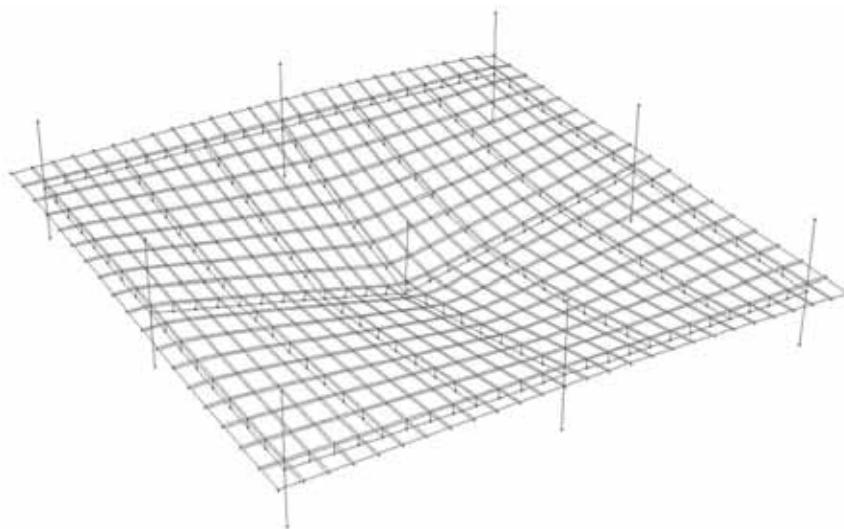
Fig. 8-39. Deformed shape for phase 2 (center column removed).

- Although the beams lost their axial continuity with the failure of the middle connections, they continued to play a significant role by working compositely with the slab.

- The wire mesh provided tensile continuity in the slab where the deck splice was modeled.

8.6 EXAMPLE SUMMARY

Based on the example presented in this chapter, the following conclusions can be drawn:

- The steel framing acting alone as tension members in catenary action can provide a solution but may not be reasonable due to the large connection and restraint forces required.

- Steel framing action in tension and bending, in concert with the concrete slab acting in compression, provides a reasonable solution. The steel headed stud anchors tie the two materials together.

- The concrete/metal deck slab, properly reinforced, can be designed as a membrane to span across the failing bay on its own. This method is simple and efficient.

- If a more sophisticated analysis is employed that incorporates the contribution of all the structural elements present—beams, studs, deck, concrete and reinforcement—the engineer may obtain a more economical design. The engineer does not need to resort to a full nonlinear dynamic analysis, but can utilize the nonlinear static pushover method coupled with the energy balance approach to compute the pushover and capacity curves. Additionally, the engineer should try to use the smallest steel beams possible thus creating more demand on the concrete and causing the stresses in the concrete to be significant. Progressive collapse is avoided if the initial collapse is prevented.

The examples discussed in this chapter are only applicable to the floors that are not directly affected by the blast that
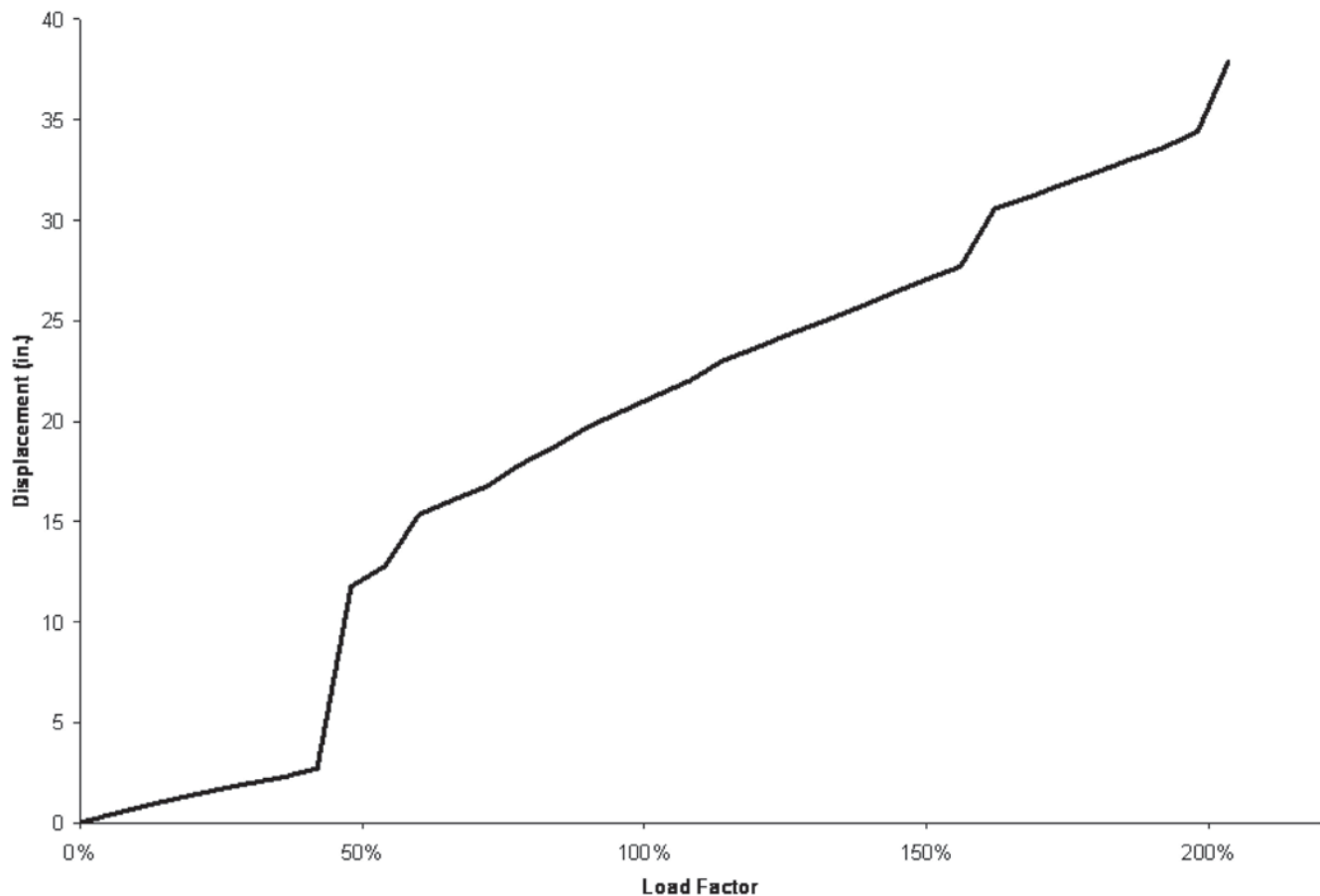

Fig. 8-40. Maximum deformation at the center (location of column removal).
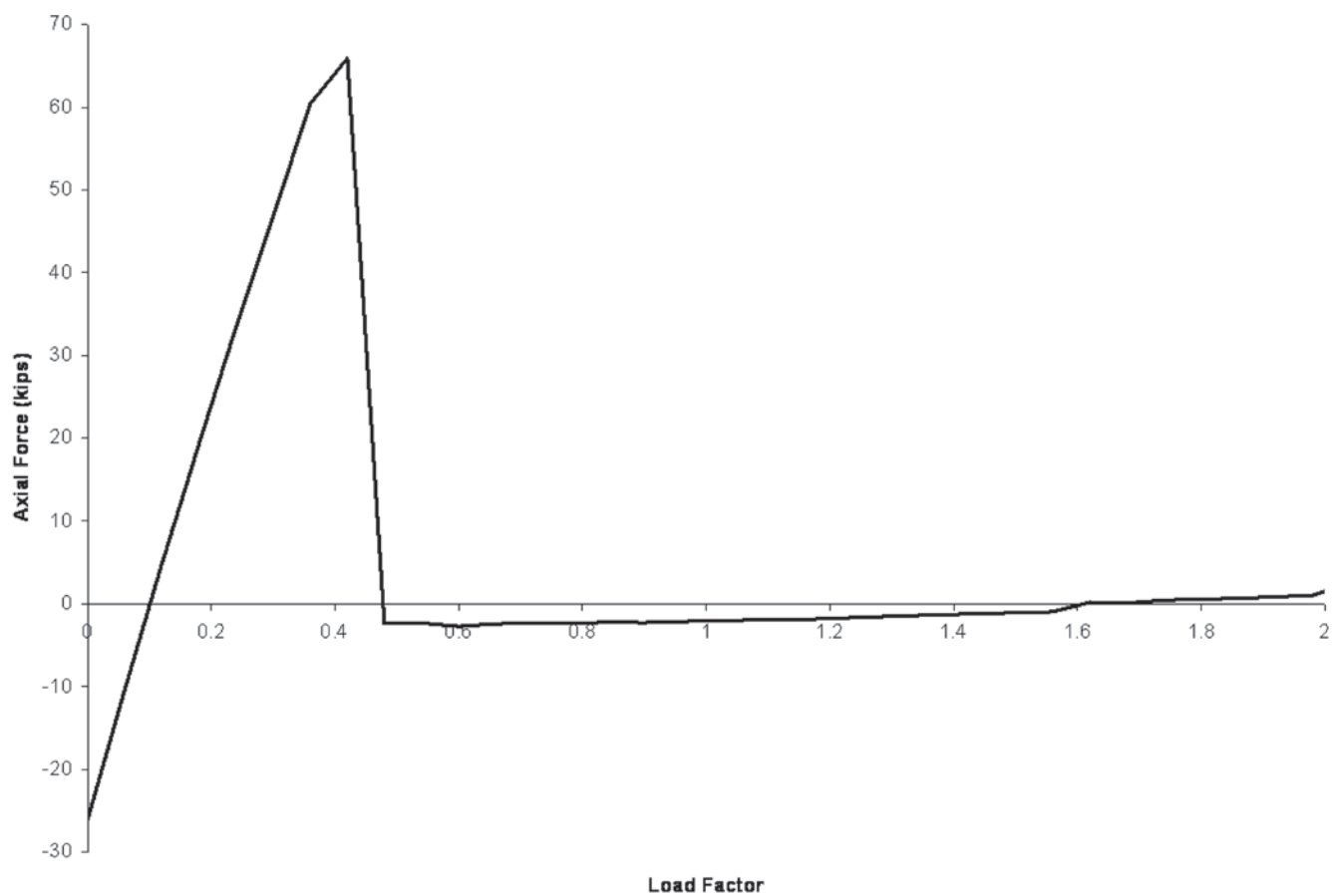
Fig. 8-41. Axial force in girder connection.
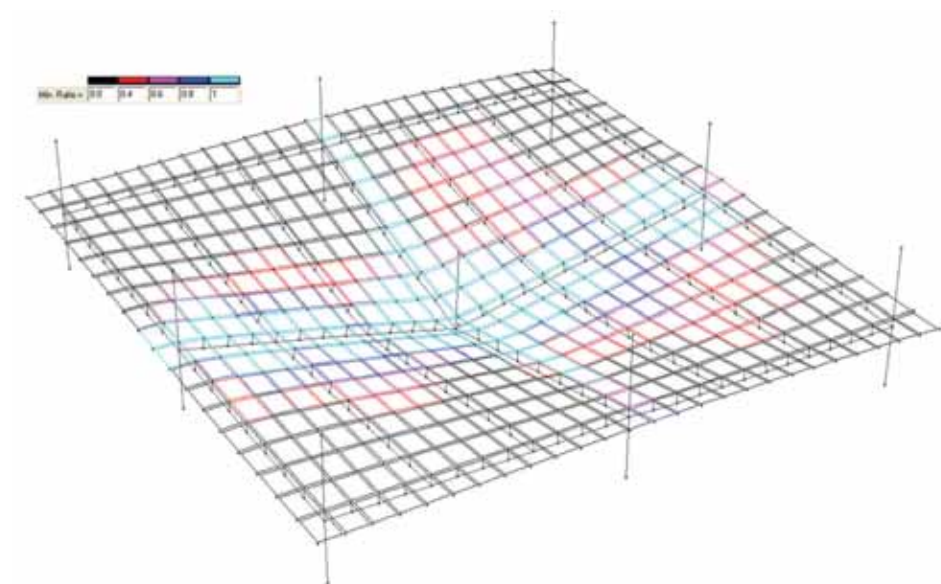
Fig. 8-42. Yielded steel layers at the energy balance stage (200% static load).

breaches the column. The floors that have not suffered damage will support themselves after the removal of the column preventing the failure of all the slabs that are supported by the column removed. The blast that breaches the column will produce uplift, damage the slab above the column, and limit the capability of this slab to subsequently develop membrane action. Corner and perimeter columns, due to their geometry, cannot develop the membrane action that an interior column develops; hence, other engineering approaches are necessary to account for the partial loss of membrane action.
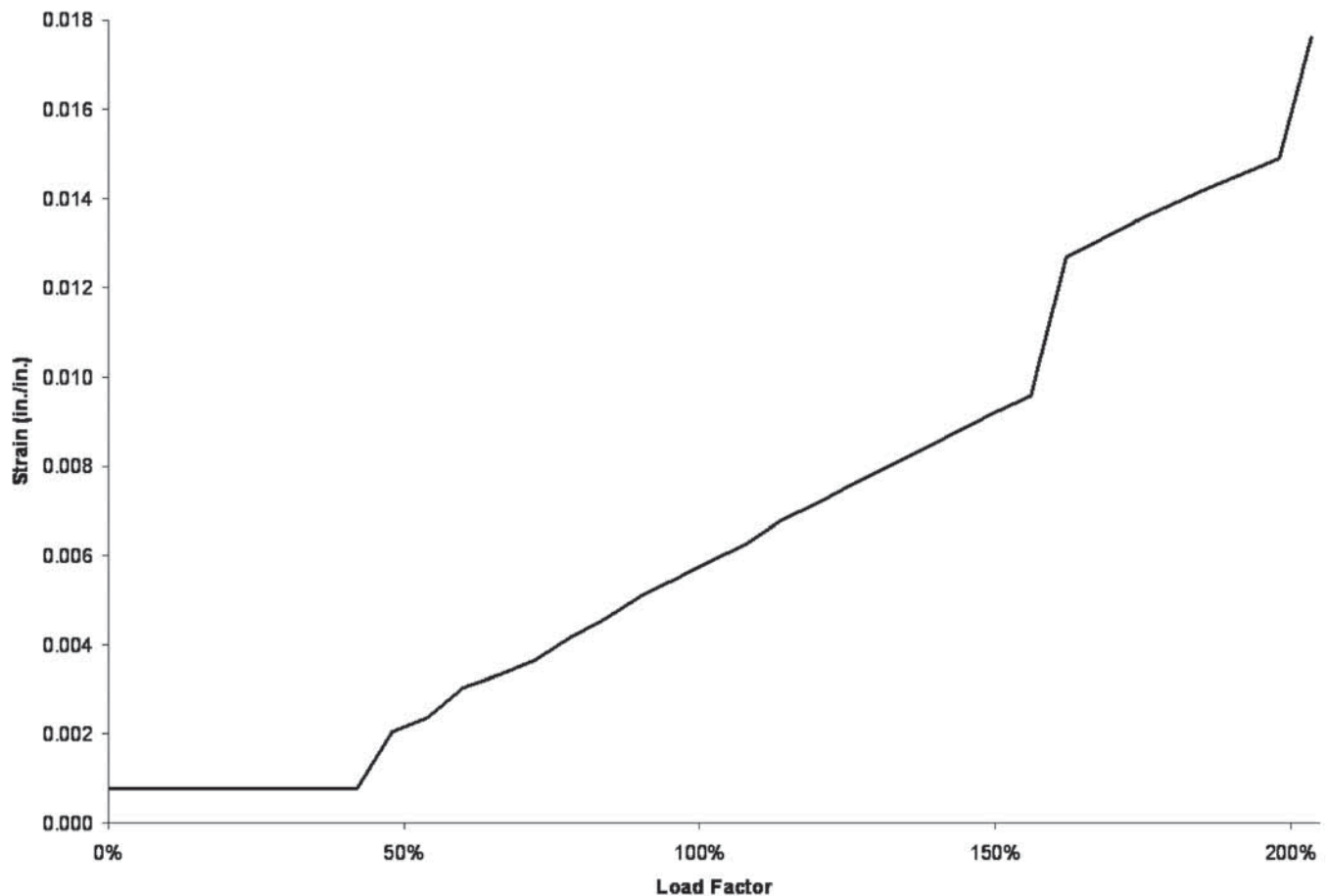
Fig. 8-43. Steel tension strain in composite slab: steel layers start yielding at 44% of the load.

SYMBOLS

(Note: ms = milliseconds)

A — Surface area exposed to the pressure wave, in.^{2}

A_g — Gross area of the element, in.^{2}

A_k — Load or load effect resulting from an extraordinary event A, kips

A_w — Area of the web, in.^{2}

B — Blast load, kips

C_r — Ratio of reflected pressure to free-field pressure

D — Dead load, kips

DCR — Demand-to-capacity ratios

DIF — Dynamic increase factor

DLF — Dynamic load factor

E_c — Modulus of elasticity of concrete, ksi

F_{cr} — Critical stress, ksi

F_{max} — Maximum resisting force the structure would experience if it were capable of remaining elastic, kips

F_{peak} — Peak blast load, kips

F_u — Specified minimum tensile strength, ksi

F_y — Specified minimum yield stress, ksi

F_{yield} — Force that would cause the structure to yield, kips

I — Impulse, psi-ms

I_r — Reflected impulse, psi-ms

I_{so} — Side-on impulse, psi-ms

K — Structure stiffness, kip/in.

K_L — Load factor

K_{LM} — Load mass factor

K_M — Mass factor

L — Span, in.

L — Live load, kips

M_p — Plastic moment, kip-in.

P — Pressure, psi

P_o — Atmospheric pressure; peak pressure, psi

P_r — Reflected pressure, psi

P_{so} — Free-field pressure, psi; side-on peak pressure, psi

Q_{UD} — Acting force (demand) determined in component or connection/joint (moment, axial force, shear, and possible combined forces)

Q_{CE} — Expected ultimate, unfactored capacity of the component and/or connection/joint (moment, axial force, shear and possible combined forces)

R — Stand-off distance, ft

R_{gpu} — Shear rupture capacity of the gusset plate underneath the weld, kip/in.

R_{gpy} — Shear yield capacity of the gusset plate underneath the weld, kip/in.

R_m — Maximum resistance, kips

R_{tu} — Tube rupture capacity under conventional shear, kip/in.

R_{tvu} — Shear rupture capacity of the tube underneath the weld, kip/in.

R_{tvy} — Shear yield capacity of the tube underneath the weld, kip/in.

R_{ty} — Tube yield capacity under conventional shear, kip/in.

R_w — Shear capacity of the weld material, kip/in.

S — Elastic section modulus, in.^{3}

S — Snow load, kips

SIF — Strength increase factor

SR — Strength ratio

T — Natural period of structure, s

T_x — Force in the reinforcement in the x-direction corresponding to the strain, ε_x, kips

T_y — Force in the reinforcement in the y-direction corresponding to the strain, ε_y, kips

U — Shock front velocity, ft/ms

V — Velocity of the system, ft/ms

W — TNT equivalent charge weight, lb

W_k — Kinetic energy, joule

W_P — Energy produced by the load pulse, joule

W_S — Strain energy absorbed by the system, joule

$W_{S,el}$ — Strain energy for linear elastic behavior, joule

Z	Plastic section modulus, in.^{3}	t_d	Load duration, ms
Z	Scaled distance, ft/lb$^{1/3}$	t_e	Load duration, ms
c	Viscous damping	t_r	Rise time to peak pressure, ms
c_c	Critical damping	u_s	Particle velocity, ft/ms
d_{bg}	Depth of the bolt group, in.	v_i	Initial velocity, ft/ms
f	Cyclic frequency, cycles per second	w	Distributed load, kips
f'_c	Minimum compressive strength of concrete, ksi	w_i	Weight per floor, kips
f_{conc}	Compressive strength of the concrete, ksi	x_{max}	Peak displacement, in.
f_i	Force per floor used to obtain the displacement per floor, kips	x_o	Arbitrary displacement, in.
		Δ	Displacement, in.
f'_{dc}	Dynamic strength of concrete, ksi	Δ_{PL}	Permanent deformation of the system, in.
f_{ds}	Dynamic design stress, ksi	Δ_T	Axial deformation at expected yielding load, in.
f_{dv}	Dynamic design stress for shear, ksi	Δ_c	Axial deformation at expected critical stress, in.
g	Acceleration due to gravity, 386 in./s^2	Δ_{el}	Elastic displacement, in.
g_k	Specified dead load for the floor or roof, kips	Δ_i	Displacement per floor, in.
k_{DRF}	Dynamic reduction factor for impulsive loads where $T > t_d$	Δ_m	Maximum displacement, in.
		Δ_{max}	Peak displacement, in.
m	Mass of the structure, lb	Δ_{yield}	Yield displacement, in.
m_e	Mass of the system, lb	ε_x	Strain in the x-direction
p_s	Density of air behind shock front, lb/ft^3	ε_y	Strain in the y-direction assumed to be equal to $\varepsilon_x \left(L_x^2 / L_y^2 \right)$
q_k	Specified imposed load (live load) for the floor or roof, kips		
q_o	Peak dynamic pressure, psi	μ	Ductility
s_t	Mean transverse spacing between ties, in.	ϕ	Resistance factor
t	Thickness of the slab, in.	ω	Undamped natural frequency, rad per unit of time
t_2	Time to peak pressure, ms	ω_d	Damped natural frequency for the structure, rad per unit of time
t_a	Time of arrival, ms		

REFERENCES

ACI (2011), *Building Code Requirements for the Structural Concrete and Commentary,* ACI 318-11, American Concrete Institute, Farmington Hills, MI.

AFESC (1989), *Protective Construction Design Manual*, ESL-TR-87-57, Prepared for Engineering Services Laboratory, Air Force Engineering and Services Center, Tyndall Air Force Base, FL.

AISC (1989), *Specification for Structural Steel Buildings—Allowable Stress Design and Plastic Design*, American Institute of Steel Construction, Chicago, IL.

AISC (2010a), *Specification for Structural Steel Buildings*, ANSI/AISC 360-10, American Institute of Steel Construction, Chicago, IL.

AISC (2010b), *Seismic Provisions for Structural Steel Buildings*, ANSI/AISC 341-10, American Institute of Steel Construction, Chicago, IL.

AISC (2010c), *Prequalified Connections for Special and Intermediate Steel Moment Frames for Seismic Applications*, ANSI/AISC 358-10, American Institute of Steel Construction, Chicago, IL.

AISC (2011a), *Steel Construction Manual*, 14th Ed., American Institute of Steel Construction, Chicago, IL.

AISC (2012), *Seismic Design Manual*, 2nd Ed., American Institute of Steel Construction, Chicago, IL.

Allam, A.M., Burgess, I.W. and Plank, R.J. (2000), "Simple Investigations of Tensile Membrane Action in Composite Slabs in Fire," Paper 03.02, *Proceedings of International Conference on Steel Structures of the 2000s*, Istanbul, pp. 327–332.

ASCE (1995), *Minimum Design Loads for Buildings and Other Structures,* ASCE 7-95, American Society of Civil Engineers, New York, NY.

ASCE (2005), *Minimum Design Loads for Buildings and Other Structures*, ASCE/SEI 7-05, American Society of Civil Engineers, New York, NY.

ASCE (2010a), *Minimum Design Loads for Buildings and Other Structures*, ASCE/SEI 7-10, American Society of Civil Engineers, New York, NY.

ASCE (2010b), *Design of Blast Resistant Buildings in Petrochemical Facilities*, American Society of Civil Engineers, New York, NY.

ASCE (2011), *Blast Protection of Buildings*, ASCE/SEI 59-11, American Society of Civil Engineers, New York, NY.

AWS (2010), *Structural Welding Code—Steel*, AWS D1.1/D1.1M, American Welding Society, Miami, FL.

Baker, W.E. (1983), *Explosion Hazards and Evaluation*, Elsevier Scientific Publishing Company, New York, NY.

Biggs, J.M. (1964), *Introduction to Structural Dynamics*, McGraw Hill, New York, NY.

BSI (1996), *Loading for Buildings: Code of Practice for Dead and Imposed Loads*, BS 6399-1, British Standards Institution, London.

BSI (1997), *Structural Use of Concrete—Part 1: Code of Practice for Design and Construction*, BS 8110-1, British Standards Institution, London.

BSI (2000), *Structural Use of Steelwork in Buildings—Part 1: Code of Practice for Design—Rolled and Welded Sections*, BS 5950-1, British Standards Institution, London.

BSI (2005a), *Code of Practice for the Use of Masonry—Part 1: Structural Use of Unreinforced Masonry,* BS 5628-1, British Standards Institution, London.

BSI (2005b), *Code of Practice for the Use of Masonry—Part 1: Structural Use of Reinforced and Prestressed Masonry*, BS 5628-2, British Standards Institution, London.

BSI (2010), *Recommendations for the Design of Masonry Structures to BS EN 1996-1-1 and BS EN 1996-2,* PD 6697:2010, British Standards Institution, London.

CEN (2004), *Eurocode 2: Design of Concrete Structures, General Rules and Rules for Buildings,* EN 1992-1-1:2004, Comité Européen de Normalisation, Brussels, Belgium.

CEN (2005a), *Eurocode 3: Design of Steel Structures, General Rules and Rules for Buildings,* EN 1993-1-1:2005, Comité Européen de Normalisation, Brussels, Belgium.

CEN (2005b), *Eurocode 3: Design of Steel Structures, Material Toughness and Through-Thickness Properties,* EN 1993-1-10:2005, Comité Européen de Normalisation, Brussels, Belgium.

CEN (2005c), *Eurocode 3: Design of Steel Structures, Design of Joints*, EN 1993-1-8:2005, Comité Européen de Normalisation, Brussels, Belgium.

CEN (2005d), *Eurocode 6: Design of Masonry Structures, General Rules for Reinforced and Unreinforced Masonry Structures,* EN 1996-1-1:2005, Comité Européen de Normalisation, Brussels, Belgium.

CEN (2006a), *Eurocode 1: Actions on Structures, General Actions, Accidental Actions*, EN 1991-1-7: 2006, Comité Européen de Normalisation, Brussels, Belgium.

CEN (2006b), *Eurocode 3: Design of Steel Structures, Plated Structural Elements,* EN 1993-1-5:2006, Comité Européen de Normalisation, Brussels, Belgium.

CEN (2006c), *Eurocode 6: Design of Masonry Structures, Simplified Calculation Methods for Unreinforced Masonry Structures,* EN 1996-3:2006, Comité Européen de Normalisation, Brussels, Belgium.

CEN (2006d), *Eurocode 6: Design of Masonry Structures, Design Considerations, Selection of Materials and Execution of Masonry,* EN 1996-2:2006, Comité Européen de Normalisation, Brussels, Belgium.

CEN (2007a), *Eurocode 3: Design of Steel Structures, Piling,* EN 1993-5:2007, Comité Européen de Normalisation, Brussels, Belgium.

CEN (2007b), *Eurocode 3: Design of Steel Structures, Crane Supporting Structures,* EN 1993-6:2007, Comité Européen de Normalisation, Brussels, Belgium.

Center for Chemical Process Safety (1994), *Guidelines for Evaluating the Characteristics of Vapor Cloud Explosions, Flash Fires, and BLEVEs*, American Institute of Chemical Engineers, New York, NY.

Center for Chemical Process Safety (2003), *Understanding Explosions*, American Institute of Chemical Engineers, New York, NY.

Chopra, A.K. (1980), *Earthquake Dynamics of Structures—A Primer*, Earthquake Engineering Research Institute, Oakland, CA.

Clough, R.W. and Penzien, J. (1993), *Dynamics of Structures*, 2nd Edition, McGraw-Hill, New York, NY.

DOD (2002), *Design and Analysis of Hardened Structures to Conventional Weapons Effects*, UFC 3-340-01, Department of Defense, Washington, DC.

DOD (2005), *Design of Buildings to Resist Progressive Collapse*, UFC 4-023-03, Department of Defense, Washington, DC.

DOD (2007), *Minimum Antiterrorism Standards for Buildings*, UFC 4-010-01, Department of Defense, Washington, DC.

DOD (2008), *Structures to Resist the Effects of Accidental Explosions*, UFC 3-340-02, Department of Defense, Washington, DC.

DOD (2010), *Design of Buildings to Resist Progressive Collapse*, UFC 4-023-03, Department of Defense, Washington, DC.

DOD (2012), *Minimum Antiterrorism Standards for Buildings*, UFC 4-010-01, Department of Defense, Washington, DC.

DOJ (1995), *Vulnerability Assessment of Federal Facilities*, U.S. Marshals Service, Department of Justice, Washington, DC.

Easterling, W.S., Gibbings, D.R. and Murray, T.M. (1993), "Strength of Shear Studs in Steel Deck on Composite Beams and Joists," *Engineering Journal*, AISC, Vol. 30, No. 2, 2nd Quarter, pp. 44–55.

Fell, B.V., Kanvinde, A.M., Deierlein, G.G., Myers, A.T. and Fu, X. (2006), "Buckling and Fracture of Concentric Braces Under Inelastic Cyclic Loading," *Steel Tips*, Structural Steel Educational Council.

FEMA (2000a), *Recommended Seismic Design Criteria for New Steel Moment-Frame Buildings*, FEMA 350, Federal Emergency Management Agency, Washington, DC

FEMA (2000b), *Prestandard and Commentary for the Seismic Rehabilitation of Buildings*, FEMA 356, Building Seismic Safety Council, Federal Emergency Management Agency, Washington, DC.

FEMA (2003a), *Reference Manual to Mitigate Potential Terrorist Attacks Against Buildings*, FEMA 426, Federal Emergency Management Agency, Washington, DC.

FEMA (2003b), *Primer for Design of Commercial Buildings to Mitigate Terrorist Attacks*, FEMA 427, Federal Emergency Management Agency, Washington, DC.

FEMA (2005), *Risk Assessment: A How-To Guide to Mitigate Potential Terrorist Attacks*, Risk Management Series, FEMA 452, Federal Emergency Management Agency, Washington, DC.

Grant, J.A., Fisher, J.W. and Slutter, R.G. (1977), "Composite Beams with Formed Steel Deck," *Engineering Journal*, AISC, Vol. 14, No. 1, 1st Quarter, pp. 24–43.

Hurty, W.C. and Rubenstein, M.F. (1964), *Dynamics of Structures*, Prentice-Hall.

ICC (2006), *International Building Code,* International Code Council, Washington DC.

ICC (2012), *International Building Code,* International Code Council, Washington DC.

ISC (2004), *Security Design Criteria for New Federal Office Buildings and Major Modernization Projects*, Interagency Security Committee, Washington, DC.

ISC (2008), *Facility Security Level Determinations*, Interagency Security Committee, Washington, DC.

ISC (2010), *Physical Security Criteria for Federal Facilities,* Interagency Security Committee, Washington, DC.

ISC (2012), *Design Basis Threat*, Interagency Security Committee, Washington, DC.

Khandelwal, K. and El-Tawil, S. (2007), "Collapse Behavior of Steel Special Moment Resisting Frame Connections," *Journal of Structural Engineering*, ASCE, Vol. 133, pp. 646–655.

Marchand, K.A. and Alfawakhiri, F. (2005), *Facts for Steel Buildings: Blast and Progressive Collapse*, American Institute of Steel Construction, April.

Mitchell, D. and Cook, W.D. (1984), "Preventing Progressive Collapse of Slab Structures," *Journal of Structural Engineering*, Vol. 110, No. 7, pp. 1,513–1,532.

Newmark, N.M. (1956), "An Engineering Approach to Blast Resistant Design," *ASCE Transactions*, Vol. 121, Paper 2786, American Society of Civil Engineers, New York, NY.

Norris, C.H., Hansen, R.J., Holley, M.J., Biggs, J.M., Namyet, S. and Minami, J.K. (1959), *Structural Design for Dynamic Loads*, McGraw-Hill.

NYCBC (2008), *Building Code of the City of New York,* New York City Building Code, New York, NY.

USACE (1957), *Design of Structures to Resist the Effects of Atomic Weapons*, Report No. EM 1110-345-415, U.S. Army Corps of Engineers, Washington, DC.

USACE (2008), PDC TR-06-01 Rev 1 *Methodology Manual for the Single-Degree-of-Freedom Blast Effects Design Spreadsheets,* U.S. Army Corps of Engineers, Washington, DC.

USGSA (1997), *GSA Security Criteria*, U.S. General Services Administration, Washington, D.C.

USGSA (2003), *Progressive Collapse Analysis and Design Guideline for New Federal Office Buildings and Major Modernization Projects*, U.S. General Services Administration, Washington, DC.

Wang, P.C. (1967), *Numerical and Matrix Methods in Structural Analysis*, John Wiley & Sons.

WRI (2010), *Manual of Standard Practice—Structural Welded Wire Reinforcement,* WWR-500, Wire Reinforcement Institute, Hartford, CT.